Analysis of subcellular protein targeting mechanisms in the single-cell C4 species *Bienertia sinuspersici*

Von der Naturwissenschaftlichen Fakultät der
Gottfried Wilhelm Leibniz Universität Hannover

Zur Erlangung des Grades
Doktorin der Naturwissenschaften
(Dr. rer. nat.)

genehmigte Dissertation
von
Diana Wimmer, M. Sc.

2017

Referent:	Dr. Sascha Offermann
Korreferent:	Prof. Dr. Hans-Peter Braun
Tag der Promotion:	28.04.2017

„Niemand ist fort, den man liebt, denn Liebe ist ewige Gegenwart.“

Stefan Zweig

in memoriam

Rut und Horst Wimmer

Parts of this work contributed to the following publications:

Wimmer D, Bohnhorst P, Shekhar V, Hwang I, Offermann S (2017)

Transit peptide elements mediate selective protein targeting to two different types of chloroplasts in the single-cell C4 species *Bienertia sinuspersici*

Scientific Research **7**: 41187

Erlinghaeuser M[1], Hagenau L[1], Wimmer D[1], Offermann S (2016)

Development, subcellular positioning and selective protein accumulation in the dimorphic chloroplasts of single-cell C4 species.

Current Opinion in Plant Biology **31**: 76–82. [1]equally contributed

Offermann S, Friso G, Doroshenk KA, Sun Q, Sharpe RM, Okita TW, Wimmer D, Edwards GE, van Wijk KJ *(*2015)

Developmental and subcellular organization of single-cell C4 photosynthesis in *Bienertia sinuspersici* determined by large-scale proteomics and cDNA assembly from 454 DNA sequencing.

Journal of Proteome Research **14**: 2090–2108.

Zusammenfassung

Der C4-Stoffwechsel bewirkt eine Verminderung der Photorespiration und ermöglicht dadurch eine besonders effektive Kohlenstofffixierung. In den meisten C4-Spezies findet die primäre und sekundäre Kohlenstofffixierung in unterschiedlich differenzierten Zellen statt, den Mesophyll- und den Bündelscheidenzellen. Im Gegensatz dazu führt die terrestrische *single-cell* C4 Spezies *Bienertia sinuspersici* eine einzigartige C4-Photosyntheseform innerhalb einzelner Chlorenchymazellen durch. Dabei finden die beiden Kohlenstofffixierungsschritte in unterschiedlichen Kompartimenten statt. Die primäre CO_2-Fixierung durch die Phospho*enol*pyruvat Carboxylase findet im Zytoplasma des peripheren Kompartiments statt. Der dazu notwendige primäre Akzeptor (Phospho*enol*pyruvat) wird spezifisch nur von den Chloroplasten des peripheren Kompartiments gebildet. Die finale CO_2 Fixierung mittels Ribulose-1,5-bisphosphat-Carboxylase/Oxigenase (RuBisCO) findet ausschließlich in den Chloroplasten des zentralen Kompartiments (C-Chloroplasten) statt. Die beiden Chloroplastentypen sind mit unterschiedlichen Proteinsets ausgestattet. Diese sind fast alle kernkodiert und müssen selektiv den richtigen Chloroplastentypen zugeführt werden. Die damit verbundenen Regulationsprozesse waren zu Beginn der vorliegenden Arbeit unbekannt. Es wurde spekuliert, dass das unterschiedliche Vorkommen der Proteine entweder auf selektiven Transportprozessen der entsprechenden Proteine oder der sie kodierenden mRNAs basiert, oder aber auf selektiven Proteindegradationsprozessen innerhalb der Chloroplasten.

Im ersten Schritt wurde die Proteinverteilung zwischen den beiden Chloroplastentypen mittels Massenspektroskopie untersucht. Weiterhin wurde der Einfluss der Proteinsequenz sowie des mRNA-Targetings auf die Selektivität analysiert. Dazu wurden GFP-Lokalisationsstudien mit den zuvor identifizierten differentiell akkumulierten Proteinen Pyruvat, Pi-Dikinase, Triosephosphatisomerase, Adenylatkinase und der kleinen Untereinheit von RuBisCO durchgeführt. Hierbei wurde gezeigt, dass die selektive Lokalisation der Proteine in den P-Chloroplasten vom Transitpeptid abhängig ist. Dies wurde jedoch nicht für die C-Chloroplasten beobachtet. Durch Mutagenese-Analysen wurde ein vier Aminosäure langes Motiv innerhalb des Transitpeptids identifiziert, welches für das selektive Targeting in die P-Chloroplasten verantwortlich ist. *Codon-swap*-Experimente sowie die Einführung einer artifiziellen Köder-mRNA zeigten, dass die mRNA keinen Einfluss auf die selektive Lokalisation der untersuchten Proteine besitzt. Weiterhin wurde ein transientes *Agrobakterium*-vermitteltes Transformationssystem in *B. sinuspersici* etabliert und die subzelluläre Lokalisation verschiedener Organellenmarker untersucht. Dabei wurde gezeigt, dass das periphere Kompartiment eine hohe Anzahl an Mitochondrien aufweist. Dies steht im Kontrast zu vorherigen Studien, welche die Mitochondrien nur im Zentralkompartiment nachwiesen.

Schlagworte: *single-cell* C4, Transitpeptide, *Agrobakterium*-vermittelte Transformation

Abstract

C4 photosynthesis suppresses photorespiration resulting in increased carbon fixation efficiency. The majority of C4 species separate primary and secondary carbon fixation reactions between two different cell types, the mesophyll and bundle sheath cells. In contrast, the terrestrial single-cell C4 species *Bienertia sinuspersici* performs a unique mode of C4 photosynthesis within individual chlorenchyma cells. The two steps of carbon fixation are separated into two different compartments. CO_2 is initially fixed by action of phospho*enol*pyruvate carboxylase within the cytoplasm of a peripheral compartment. The primary carbon acceptor required for this reaction (phospho*enol*pyruvate) is made exclusively in the chloroplasts of the peripheral compartment (P-chloroplasts). Final CO_2 fixation via ribulose-1,5-bisphosphate-carboxylase/-oxygenase (RuBisCO) occurs exclusively in the chloroplasts of the central compartment (C-chloroplasts). Both chloroplast types have a specialized protein composition which is required to fulfill their specialized functions in the C4 cycle. Since most of these chloroplast localized proteins are nuclear encoded, a sorting mechanism must exist which ensures partitioning into the correct chloroplast type. However, the required regulatory processes are currently unknown. It has been speculated previously that sorting could be based on either selective protein transport, selective mRNA transport or selective protein degradation.

In this thesis, protein distribution between the two chloroplast types was analyzed via mass spectroscopy. The importance of the protein sequence as well as the mRNA sequence on selective protein accumulation was then analyzed. This was achieved by GFP localization assays with the previously identified differential accumulating proteins pyruvate, Pi-dikinase, triosephosphate isomerase, adenylate kinase and the small subunit of RuBisCO. It was demonstrated that transit peptides mediate selective localization of P-chloroplast specific proteins. However, this was not the case for C-chloroplast targeted proteins. A four amino acid motif was identified which is responsible for selective protein targeting to the P-chloroplasts. Codon-swap experiments as well as implementing an artificial bait mRNA indicated that mRNA was not involved in selective localization of the proteins analyzed. Furthermore, a transient *Agrobacterium*-mediated transformation system was established which was used to analyze the subcellular localization of a variety of organelle markers. This demonstrated that mitochondria are also abundant in the peripheral compartment which is in contrast to previous studies which identified mitochondria mainly in the central compartment.

Keywords: single-cell C4, transit peptides, *Agrobacterium*-mediated transformation

Table of contents

Abbreviations 1

Section 1 - Analysis of subcellular protein targeting mechanisms in the single-cell C4 species *Bienertia sinuspersici*: An overview

1.1 Photorespiration and C4 photosynthesis 4

1.2 Single-cell C4 species 7

1.2.1 Cell biology and development

1.2.2 Biochemistry of single-cell C4 photosynthesis

1.3 How does differential accumulation of nuclear encoded proteins in the two different chloroplast types work? 12

1.4 Chloroplast import of nuclear encoded proteins 14

1.4.1 Transit peptide mediated import through the TOC-TIC complex

1.4.2 Integration of outer envelope proteins

1.4.3 mRNA targeting

1.4.4 Alternative protein import through the secretory pathway

1.5 Objectives of this thesis 20

1.6 References 22

Section 2 - Analysis of subcellular protein targeting mechanisms in the single-cell C4 species *Bienertia sinuspersici*: Publications

2.1 Developmental and subcellular organization of single-cell C4 photosynthesis in *Bienertia sinuspersici* determined by large-scale proteomics and cDNA assembly from 454 DNA sequencing **37**

2.2 Development, subcellular positioning and selective protein accumulation in the dimorphic chloroplasts of single-cell C4 species **57**

2.3 Transit peptide elements control differentiation of different chloroplasts within individual cells in the single-cell C4 species *Bienertia sinuspersici* **65**

2.4 Development of an *Agrobacterium*-mediated transformation protocol for the single-cell C4 species *Bienertia sinuspersici* enables high resolution in vivo protein localization analysis of subcellular compartmentation **88**

Appendix **122**

Curriculum Vitae

List of publications

Conference contributions

Danksagung

Abbreviation

1,3-BPGA	1,3-bisphosphoglycerate
2PG	2-phosphoglycolate
3-PGA	3-phosphoglyceric acid
aa	amino acid
ADP	adenosine diphosphate
AK	adenylate kinase
AKR2	ankyrin repeat-containing protein 2
Ala	alanine
AMP	adenosine monophosphate
Amyl-1	α-amylase I-1
ARD	ankyrin-repeat domain
Asp	aspartate
Asp-AT	aspartate aminotransferase
ATP	adenosine triphosphate
BASS	bile-acid sodium symporter
BSC	bundle sheath cells
BS-chloroplasts	bundle sheath chloroplasts
CAH1	carbonic anhydrase 1
CAM	crassulacean acid metabolism
CBB cycle	Calvin-Bensson-Bassham cycle
CC	central compartment
C-chloroplast	chloroplasts of the central compartment
CCM	carbon concentration mechanisms
DHAP	dihydroxyacetone phosphate
DNA	desoxyribonucleic acid
E-4-P	erythrose-4-phosphate
eIF4E	eukaryotic translation initiation factor 4E
ER	endoplasmic reticulum
F-1,6-BP	fructose-1,6-bisphosphate
F-6-P	fructose-6-phosphate
FBPase	1,6-fructose bisphosphatase

G	glycolate
G3P	glyceraldehyde-3-phosphate
G-3-P	glyceraldehyde-3-phosphate
GAP	GTPase-activating protein
GAPDH	glyceraldehyde phosphate dehydrogenase
GDP	guanosine diphosphate
GFP	green fluorescence protein
GTP	guanosine triphosphate
HPR1	hydroxypyruvate reductase
HSP70	heat shock protein 70
LHCII	light-harvesting complex II
M&M model	multi-selection and multi-order model
MA	malate
MC	mesophyll cells
M-chloroplasts	mesophyll chloroplasts
mRNA	messenger ribonucleic acid
MSD1	manganese superoxide dismutase 1
NAD-MDH	NAD malate dehydrogenase
NAD-ME	NAD-malic enzyme
NADPH	nicotinamide adenine dinucleotide phosphate
NADP-MDH	NADP-dependent malate dehydrogenase
NADP-ME	NADP-malic enzyme
OAA	oxaloacetate
OEM	outer envelope membrane
OEP7	outer envelope protein 7
OOP	organellar oligopeptidase
PA	pyruvate
PC	peripheral compartment
P-chloroplasts	peripheral chloroplasts
PEP	phosphoenolpyruvate
PEP-C	phosphoenolpyruvate carboxylase
PEPCK	phosphoenolpyruvate carboxykinase

PGK	phosphoglycerate kinase
PGP	phosphoglycolate phosphatase
PP	pyrophosphatase
PPDK	pyruvate, pi-dikinase
PPi	inorganic phosphate
PPT	phosphate/PEP translocator
PreP	presequence protease
R-5-P	ribose-5-phosphate
RCA	rubisco activase
RLSU	RuBisCO large subunit
RPE	ribulose phosphate epimerase
RSSU	RuBisCO small unit
Ru-5-P	ribulose-5-phosphate
RuBisCO	ribulose-1,5-bisphosphate-carboxylase/-oxygenase
RuBP	ribulose-1,5-bisphosphate
S-1,7-BP	sedoheptulose-1,7-bisphosphate
S-7-P	sedoheptulose-7-phosphate
SA	signal-anchored
SBPase	sedoheptulose-1,7-bisphosphatase
SCC4	single-cell C4
SFBA	fructose bisphosphate aldolase
SPP	stromal processing peptidase
TA	tail-anchored
TKL	transketolase
TMD	transmembrane domain
TOC-TIC complex	translocon of the outer (TOC) and inner membrane (TIC) complex
TP	transit peptide
TPI	triose phosphate isomerase
TPT	triose phosphate translocator
UTR	untranslated region
VDAC	voltage-dependent anion channel
X-5-P	xylulose-5-phosphate

Section 1 - Analysis of subcellular protein targeting mechanisms in the single-cell C4 species *Bienertia sinuspersici*: An overview

Chapter 1 gives an overview of photorespiration and C4 photosynthesis and, in particular, of a special C4 photosynthesis form, termed single-cell C4 photosynthesis (SCC4) focusing on the model species *Bienertia sinuspersici*. Furthermore, it takes a closer look at the two different cell compartments in Bienertia with distinct chloroplast types as well as potential variants of the sorting process of differentially located proteins in the chloroplasts.

1.1 Photorespiration and C4 photosynthesis

The first CO_2 fixation step in C3 plants takes place in the Calvin-Benson-Bassham (CBB) cycle in the chloroplast stroma to fix the energy supplied from the light reaction in storable molecules. The enzyme Ribulose-1,5-bisphosphate-carboxylase/-oxygenase (RuBisCO) catalyzes the first reaction step between CO_2 and ribulose-1,5-bisphosphate (RuBP) in the CBB cycle. The resulting six-carbon molecule disintegrates into two molecules of 3-phosphoglyceric acid (3-PGA). This three-carbon molecule (C3) is the first stable product in the CBB cycle. 3-PGA is then reduced during the CBB cycle under the consumption of adenosine triphosphate (ATP) and nicotinamide adenine dinucleotide phosphate (NADPH) into glyceraldehyde-3-phosphate (G3P) which is later (outside the CBB cycle) converted into glucose or sucrose (Bauwe et al., 2010).

RuBisCO has a high affinity to CO_2 but can also fix O_2 (Bowes et al., 1971). Because of this, the CO_2/O_2 ratio in the chloroplasts is important for an effective CO_2 fixation. Under natural conditions, the amount of O_2 is much higher in the stroma in comparison to CO_2. During the oxygenation of RuBP by RuBisCO, one molecule of the toxic 2-phosphoglycolate (2PG) is produced (Bauwe et al., 2010). For detoxification, 2PG is degraded in an energy consuming process involving peroxisomes, mitochondria and chloroplasts. Plants can lose 25 % previously fixed carbon during photorespiration (Sage, 2004). In warm, dry and saline environments, plants close the stomata to reduce water loss through transpiration (Chaves et al., 2009). Therefore, CO_2 concentration decreases rapidly in the chloroplasts and consequently, photorespiration increases.

Some plants developed carbon concentration mechanisms (CCM) to increase the CO_2 concentration around RuBisCO to avoid photorespiration. 50 years ago, Hatch and Slack (1966) described the most prominent form of CCM in terrestrial plants, termed C4 photosynthesis (Hatch and Slack, 1966). C4 photosynthesis evolved independently 61 times

in higher plants during evolution (Sage, 2016). The earliest event was 24–35 million years ago in grasses (Kellogg, 1999; Sage, 2004) as the atmospheric CO_2 level declined from 800 ppm to 400 ppm (Zhang et al., 2013). In dicots, the first C4 plants developed within the family Chenopodiaceae. Here, the initial event was 14-21 million years ago in Salsolea and 8-11 million years ago in Atriplex (Kadereit et al., 2003).

C4 plants separate the initial CO_2 fixation and the carbon refixation in the CBB cycle in two different cell types, the mesophyll cells (MC) and the bundle sheath cells (BSC). This special separation form of two cell types to perform C4-photosynthesis is referred to as Kranz anatomy (Haberlandt, 1904). Both cell types have different compositions of photosynthetic proteins, e.g. the first inorganic carbon fixing enzyme phospho*enol*pyruvate carboxylase (PEP-C) is highly abundant in the mesophyll cells, whereas RuBisCO and decarboxylases are highly abundant in the bundle sheath cells (Edwards et al., 1970; Berry et al., 1970). Furthermore, MC and BSC each have distinct chloroplasts types, the mesophyll chloroplasts (M-chloroplasts) and the bundle sheath chloroplasts (BS-chloroplasts). These chloroplasts have different roles in the C4 photosynthetic carbon fixation pathway (Majeran et al., 2005).

The mesophyll cells are responsible for the initial fixation of inorganic carbon in the cytoplasm. PEP-C catalyzes the carboxylation of phospho*enol*pyruvate (PEP) with bicarbonate. The resulting oxaloacetate (four-carbon molecule [C4]) is converted into malate or aspartate, respectively, and diffuses through the plasmodesmata into the BSC where the C4 molecule is decarboxylated and the CO_2 can be refixed in the CBB cycle. This increases the amount of CO_2 around RuBisCO and reduces the carbon loss by photorespiration. there are three different variations of the decarboxylation of the C4 molecule in the BSC which are dependent on the different C4 subtype (Figure 1) (Edwards et al., 1971; Hatch et al., 1975; Hatch and Kagawa, 1976; Ludwig, 2016).

(A) The NADP-malic enzyme (NADP-ME) subtype reduces oxaloacetate (OAA) in the M-chloroplasts to malate by the NADP-dependent malate dehydrogenase (NADP-MDH) which diffuses into the BSC. Here, malate is decarboxylated in the BS-chloroplasts by NADP-ME. The released CO_2 is fixed by RuBisCO and the remaining pyruvate (PA) diffuses back into the M-chloroplasts where it is regenerated by pyruvate, Pi-dikinase (PPDK) into PEP.

(B) The NAD-malic enzyme (NAD-ME) subtype transaminates OAA by an aspartate aminotransferase (Asp-AT) to aspartate (Asp) in the cytoplasm of the MC which is then transported into the mitochondria of the BSC. Asp is transaminated back to OAA, then reduced to malate and decarboxylated by NAD-ME. The released CO_2 diffuses into the chloroplasts and is fixed in the CBB cycle. Pyruvate from decarboxylation of malate is transported back into the cytoplasm and is converted to alanine (Ala). Ala diffuses back into the MC and is converted to pyruvate which is imported into the M-chloroplasts and regenerated to PEP.

(C) The phospho*enol*pyruvate carboxykinase (PEPCK) subtype uses a different way to concentrate CO_2 in the BS-chloroplasts. OAA is converted to malate in the M-chloroplasts and to aspartate in the cytoplasm. Both C4 molecules diffuse into the BSC. Here, malate is decarboxylated in the mitochondria by NAD-ME and the CO_2 diffuses into the BS-chloroplasts. The regeneration process of PEP is similar to the NAD-ME subtype. Additionally, aspartate is converted back to OAA and decarboxylated by PEPCK in the cytoplasm. The released CO_2 diffuses into the BS-chloroplasts and the remaining PEP diffuses back into the MC.

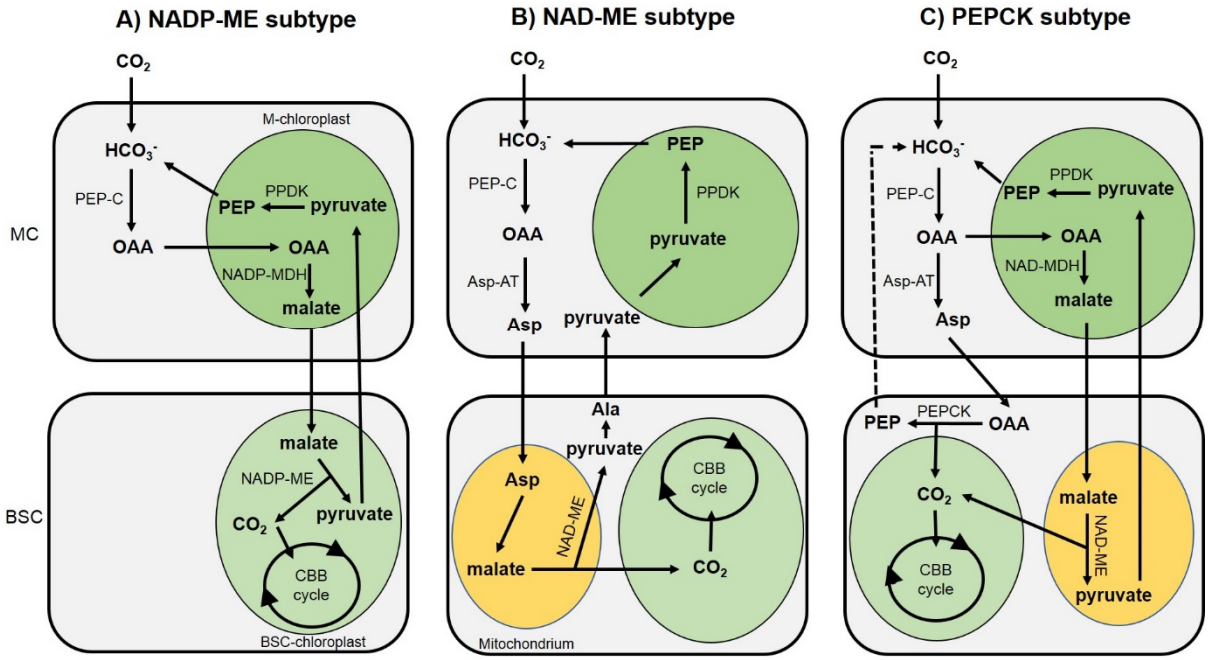

Figure 1: Different carbon fixation pathways in C4 plants. Adapted from (Ludwig, 2016)

Schematic overview of the three different C4 decarboxylation pathways: The NADP-malic enzyme (NADP-ME), the NAD-malic enzyme (NAD-ME) and the phospho*enol*pyruvate carboxykinase (PEPCK) subtype. MC – mesophyll cell; BSC – bundle sheath cell; CBB cycle – Calvin-Benson-Bassham cycle; **Abbreviations enzymes**: PEP-C - phospho*enol*pyruvate carboxylase; PPDK - pyruvate, Pi-dikinase; NADP-MDH - NADP-dependent malate dehydrogenase; Asp-AT – aspartate aminotransferase; **Abbreviations metabolites**: HCO_3^- - bicarbonate; OAA – ocaloacetate; PEP – phospho*enol*pyruvate; Asp – aspartate; Ala - alanine

The M- and BSC-chloroplasts are different in structure, size and shape dependent on the different subtypes (Rhoades and Carvalho, 1944). In maize and sorghum (NADP-ME subtype), M-chloroplasts have large, well developed and numerous grana. Photosystem II is highly abundant in M-chloroplasts and supplies NADPH. Conversely, BS-chloroplasts have poorly developed grana and less photosystem II (Andersen et al., 1972). The M-chloroplasts are randomly distributed along the plasma membrane and can reposition in response to light and/or stress. In contrast, BS-chloroplasts are located close to the vascular tissue (centripetal) or the MC (centrifugal) depending on the C4 subtype and are immobile (Yamada et al., 2009).

Both positional variants have physiological advantages for the plants. The centripetal position prevents a leakage of CO_2 in the MC, especially in plants without suberized lamella between MC and BS (Hattersley and Browning, 1981). In contrast, the centrifugal position enhance the metabolic exchange between both cell types (Maai et al., 2011).

1.2 Single-cell C4 species

In the year 2000, in the Central Asian region, the first terrestrial species *Suaeda aralocaspica* (Amaranthaceae) was discovered that shows typical features of C4 photosynthesis in one single chlorenchyma cell instead of Kranz anatomy (Freitag and Stichler, 2000). The leaf anatomy shows a similar structure to the previously described C4 salsoloid type that has a water storage parenchyma tissue and Kranz anatomy with distinctive peripheral layers of palisade and Kranz cells (Voznesenskaya et al., 1999; Voznesenskaya et al., 2001). However, *S. aralocaspica* has only one layer of palisade-shaped chlorenchyma between the hypodermal cells and the central water storage tissue and shows no Kranz anatomy. The main difference to other C4 salsoloid species is the coexistence of two different chloroplasts types in one single cell (Freitag and Stichler, 2000; Voznesenskaya et al., 2001). One chloroplast type is positioned at the distal end and the other one at the proximal end of the chlorenchyma cell (Figure 2A). Both chloroplast types have similar structures as the different chloroplast types in the bundle sheath and mesophyll cells in Kranz anatomy species (**Chapter 1.1**). Chloroplasts at the proximal end have grana and contain starch, whereas the chloroplasts at the distal end have less grana and do not store starch (Freitag and Stichler, 2000; Voznesenskaya et al., 2001). Mitochondria are only found at the proximal end (Voznesenskaya et al., 2001; Voznesenskaya et al., 2003). Most of the peroxisomes are located at the proximal end and a few peroxisomes are also found at the distal end (Voznesenskaya et al., 2004) (Figure 2A). *S. aralocaspica* shows a similar carbon isotope composition ($\delta^{13}C$) as C4 or CAM (crassulacean acid metabolism) species (e.g. $\delta^{13}C$ value in mature leaves of *Suaeda aralocaspica* (- 13.78 ‰), *Salsola chivensis* [C4] (- 13.9 ‰), *Kalanchoë tubiflora* [CAM] (- 14.2 ‰) and *Suaeda heterophylla* [C3] (- 25.3 ‰)) (Bender et al., 1973; Freitag and Stichler, 2000; Voznesenskaya et al., 2001; Voznesenskaya et al., 2002). However, the main characteristic of CAM species is the acidification of photosynthetic tissue during the night, which was not observed in *Suaeda aralocaspica* (Voznesenskaya et al., 2002). These results and the missing Kranz anatomy was the first evidence that *S. aralocaspica* could perform C4 photosynthesis in one single cell (single-cell C4 or SCC4 photosynthesis) (Freitag and Stichler, 2000; Voznesenskaya et al., 2001; Voznesenskaya et al., 2002). While the succulent water storage cells also contain chloroplasts and labelling experiments have shown the existence of RuBisCO, it was excluded

that these cells perform C4 or CAM photosynthesis because of the absence of C4 related proteins (Voznesenskaya et al., 1999; Voznesenskaya et al., 2001).

Later, three other SCC4 species from the tribe Bienertieae, *Bienertia cycloptera* [Central Asian semi-deserts] (Voznesenskaya et al., 2002; Freitag and Stichler, 2002), *Bienertia sinuspersici* [Persian Gulf and Gulf of Oman] (Akhani et al., 2005) and *Bienertia kavirense* [Iranian salt deserts] (Akhani et al., 2012) were discovered. These species show a related structure of the chlorenchyma cells with two different chloroplast types but the chloroplast position differs in comparison to *S. aralocaspica* (**Chapter 1.1.1**) (Figure 2B). All four species are succulent halophytes and their habitats are desert or semi-desert regions. *Bienertia sinuspersici* (hereafter referred to as Bienertia) is considered a model organism for SCC4 photosynthesis and was used for the experiments in this thesis. Therefore, the following general introduction focuses mainly on this species.

1.2.1 Cell biology and development

Bienertia has a unique cell structure with two different cell compartments termed central (CC) and peripheral compartment (PC). Both compartments contain two different chloroplast types, the chloroplasts of the central compartment (C-chloroplasts) and the peripheral chloroplasts (P-chloroplasts). These chloroplasts have different functions in the C4 cycle and a different protein composition (**Chapter 1.2.2**). The P-chloroplasts have less grana and no starch grains compared to the C-chloroplasts (Voznesenskaya et al., 2002; Voznesenskaya et al., 2005). The P-chloroplasts are larger and have a doughnut-like shape whereas the C-chloroplasts are smaller and more round. The amount of chlorophyll in the two chloroplasts types and the number of chloroplasts per chlorenchyma cell were measured and have shown 6-times more C-chloroplasts and 4-times more chlorophyll in the C-chloroplasts over the P-chloroplasts (Offermann et al., 2011b). Experiments using cytoskeleton-disrupting drugs have shown that microtubules and actin filaments are necessary for the stability of both cell compartments and have an influence on the positioning of the chloroplasts (Chuong et al., 2006; Park et al., 2009).

The distribution of mitochondria and peroxisomes also show differences between the two cell compartments (Figure 2B). Early studies have found mitochondria exclusively in the CC and not in the PC (Voznesenskaya et al., 2002; Voznesenskaya et al., 2005). However, recent research methods like confocal microscopy of fluorescence stained mitochondria (Chuong et al., 2006; Park et al., 2009) or mitochondrial located GFP (green fluorescence protein)-fusion proteins in protoplasts (Lung et al., 2011) show the existence of a few mitochondria in the peripheral compartment. **Chapter 2.4** of this thesis introduces a new method for the visualization of mitochondria via GFP localization studies in chlorenchyma cells

by a transient *Agrobacterium*-mediated transformation protocol. Here, it is shown that the peripheral compartment contains more mitochondria than previously proven. Peroxisomes are predominantly located in the CC but also exist in the PC. This was also demonstrated by peroxisomal GFP localization studies in protoplasts (Lung et al., 2011), immunofluorescence studies (Chuong et al., 2006) and immunoblots with the peroxisomal marker antibody directed against hydroxypyruvate reductase (HPR1) (Offermann et al., 2011b). The existence of two different peroxisome types in one single cell was postulated by Choung et al. (2006) who observed static peroxisomes in the CC as well as mobile peroxisomes in the PC (Chuong et al., 2006).

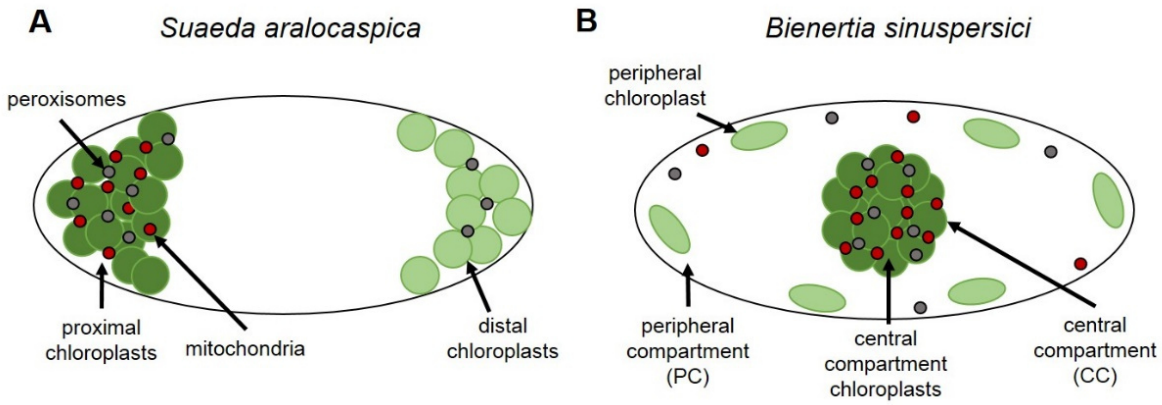

Figure 2: Schematic overview of the different chlorenchyma cell structures in the single-cell C4 species *Suaeda aralocaspica* and *Bienertia sinuspersici*.

A) Chlorenchyma cell of *Suaeda aralocaspica* with the two different chloroplasts at the proximal and distal end of the cell. Mitochondria and peroxisomes are located at the proximal end. Additionally, some peroxisomes exist at the distal end. **B)** The chlorenchyma cell of *Bienertia sinuspersici* consists of two different cell compartments (the peripheral [PC] and central compartment [CC]). These compartments contain the peripheral or central compartment chloroplasts. Mitochondria and peroxisomes are predominantly located in the CC but also detectable in the PC.

The chlorenchyma cells undergo a developmental process that can be divided into four stages (Figure 3) (Park et al., 2009; Koteyeva et al., 2016). In the youngest stage, only one chloroplast type exists in the chlorenchyma cell. mRNA *in situ* hybridization and immunolocalization studies have shown that C-specific proteins such as RuBisCO, accumulate in these chloroplasts, but C4 related proteins such as PPDK do not. The chloroplasts occupy most of the cytoplasmic space and the vacuole is very small. In the young stage, the vacuole expands and a pre-CC is formed. The chloroplasts still contain only C-specific proteins. In the intermediate stage, the cell expands and the two different chloroplast types begin to form. P-specific proteins are detectable in the P-chloroplasts. In the mature stage, the cells elongate and the two chloroplast types are fully developed. The C-chloroplasts and the nucleus form a

ball-like structure in the middle of the cell and the P-chloroplasts are located close to the plasma membrane. CBB cycle related proteins are more abundant in the C-chloroplasts whereas C4 related proteins are more abundant in the P-chloroplasts. Both compartments are connected by cytoplasmic channels and the vacuole completely surrounds the CC (Freitag and Stichler, 2002; Park et al., 2009; Koteyeva et al., 2016).

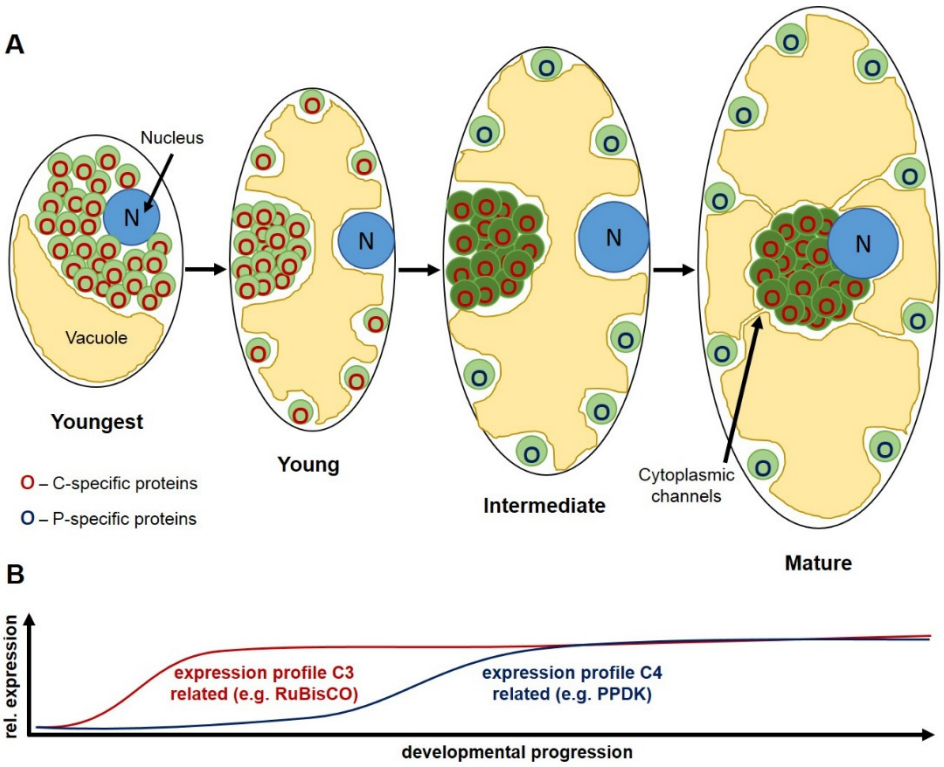

Figure 3: Development of chlorenchyma cells in the single-cell C4 species *Bienertia sinuspersici*. Adapted from (Park et al., 2009) and (Koteyeva et al., 2016), see **Chapter 2.3**

A) Four stages of cell development in Bienertia chlorenchyma cells. **B)** Relative expression profile of C3 and C4 related proteins during the developmental process. C-specific proteins - central compartment chloroplast-specific proteins; P-specific proteins - peripheral chloroplast-specific proteins; RuBisCO - Ribulose-1,5-bisphosphate-carboxylase/-oxygenase; PPDK - pyruvate, pi-dikinase

1.2.2 Biochemistry of single-cell C4 photosynthesis

The whole C4 pathway of the SSC4 species Bienertia takes place in one single cell and is dependent on the different protein composition in the two distinct chloroplasts types (P- and C-chloroplasts) (**Chapter 1.2.1**) (Figure 4). P-chloroplasts are mainly responsible for the regeneration of the primary CO_2 acceptor PEP (Offermann et al., 2011b). This thesis has shown that three enzymes that are involved in the regeneration of PEP, PPDK, adenylate kinase (AK) and the inorganic pyrophosphatase (PP) are specifically located in the P-chloroplasts (**Chapter 2.1**). PPDK catalyzes the phosphorylation of pyruvate to PEP under the consumption of ATP and inorganic phosphate (PP_i) (Edwards et al., 1985).

$$pyruvate + ATP + P_i \rightleftharpoons PEP + AMP + PP_i$$

However, the reaction favors the reverse direction at pH 7 and catalyzes the production of pyruvate instead of PEP. Therefore, AK and PP stabilize the reaction towards the direction of the phosphorylation of PA to PEP by the conversion of the end products adenosine monophosphate (AMP) and PP_i into adenosine diphosphate (ADP) and 2 P_i (Edwards et al., 1985). PEP is carboxylated by PEP-C in the cytoplasm to OAA and then transaminated to Asp by Asp-AT. Asp diffuses through the cytoplasmic channels into the mitochondria of the central compartment. There, Asp is transaminated back to OAA by mtAsp-AT. OAA is reduced by NAD-MDH (NAD malate dehydrogenase) to malate that is then decarboxylated by NAD-ME. The resulting CO_2 diffuses into the C-chloroplasts where it is fixed by the C-specific enzyme RuBisCO (**Chapter 2.1**).

This thesis also shows that most of the enzymes involved in the CBB cycle are more abundant in the C-chloroplasts except for the enzymes of the reductive phase (Figure 4) (**Chapter 2**). These proteins are either equally distributed in both chloroplast types (e.g. glyceraldehyde phosphate dehydrogenase (GAPDH)), or more abundant in the P-chloroplasts (e.g. phosphoglycerate kinase (PGK) and triose-phosphate isomerase (TPI)). Based on this result as well as Offermann et al. (2011b), it is postulated that a triose phosphate shuttle into the P-chloroplasts is necessary for the reduction of 3-PGA. There, 3-PGA is converted to 1,3-bisphosphoglycerate (1,3-BPGA) which is then reduced by GAPDH in the P-chloroplasts. The resulting dihydroxyacetone phosphate (DHAP) is transported back into the C-chloroplasts and regenerated in several steps to RuBP.

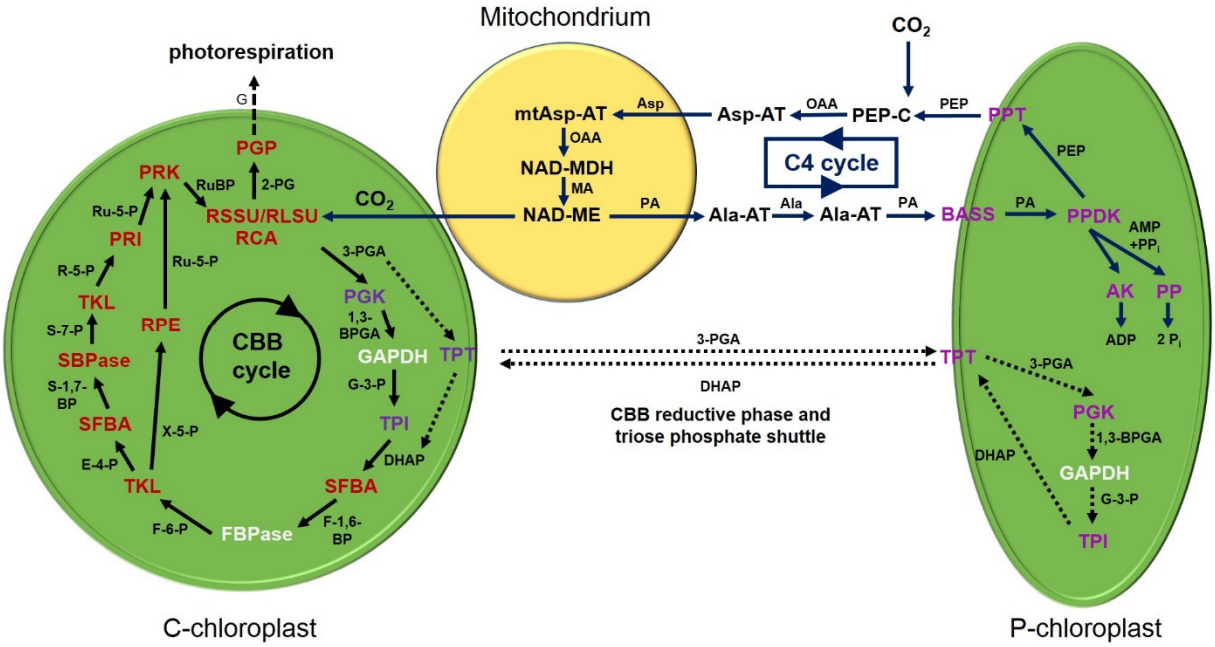

Figure 4: Overview about the single-cell C4 pathway. Adapted from **Chapter 2**

Red - C-specific enzymes; purple – P-specific enzymes; white equally contributed enzymes; blue arrows - C4 cycle; black arrows - Calvin-Benson-Bassham cycle (CBB cycle); dashed arrows - triose phosphate shuttle. **Abbreviations enzymes**: RSSU - RuBisCO small unit; RLSU - RuBisCO large subunit; RCA - rubisco activase; PGK - phosphoglycerate kinase; GAPDH - glyceraldehyde phosphate dehydrogenase; TPT - triose phosphate translocator; TPI – triose phoshate isomerase; SFBA - fructose bisphosphate aldolase; FBPase - 1,6-fructose bisphosphatase; TKL - transketolase; SBPase - sedoheptulose-1,7-bisphosphatase; RPE – ribulose phosphate epimerase; PRI - phosphoribose isomerase; PGP - phosphoglycolate phosphatase; mtAsp-AT - mitochondrial aspartate aminotransferase; NAD-MDH - NAD malate dehydrogenase; NAD-ME - NAD malic enzyme; Asp-AT - aspartate aminotransferase; PEP-C - phospho*enol*pyruvate carboxylase; Ala-AT - alanine aminotransferase; PPT - phosphoenolpyruvate phosphate translocator; BASS - bile-acid sodium symporter; PPDK - pyruvate, Pi-dikinase; AK - adenylate kinase; PP – pyrophosphatase. **Abbreviations metabolites**: 3-PGA - 3-phosphoglycerate; 1,3-BPGA – 1,3-bisphosphoglycerate; G-3-P - glyceraldehyde-3-phosphate; DHAP - dihydroxyacetone phosphate; F-1,6-BP - fructose-1,6-bisphosphate; F-6-P - fructose-6-phosphate; E-4-P - erythrose-4-phosphate; X-5-P - xylulose-5-phosphate; S-1,7-BP - sedoheptulose-1,7-bisphosphate; S-7-P - sedoheptulose-7-phosphate; R-5-P - ribose-5-phosphate; Ru-5-P - ribulose-5-phosphate; 2-PG - 2-phosphoglycolate; G – glycolate; OAA - oxaloacetate; MA - malate; Asp - aspartate; Ala - alanine; PA - pyruvate; PEP - phospho*enol*pyruvate; AMP - adenosine monophosphate; ADP - adenosine diphosphate.

1.3 How does differential accumulation of nuclear encoded proteins in the two different chloroplast types work?

M- and BSC-chloroplasts in Kranz C4 species and P- and C-chloroplasts in Bienertia, respectively, have a different composition of nuclear encoded proteins (**Chapter 1.1**, **Chapter 1.2 and Chapter 2.1**). For instance, M-chloroplasts as well as P-chloroplasts contain PPDK for the regeneration of PEP, whereas BSC-chloroplasts and C-chloroplasts are mainly responsible for the refixation of CO_2 and contain RuBisCO and other proteins from the CBB

cycle. These proteins are transcribed in the nucleus and translated in the cytoplasm. Thus, a regulation or sorting system for the transport and import into the chloroplast is necessary (**Chapter 1.5**). In Kranz C4 species, the two chloroplast types are separated in different cell types and a variety of mechanisms have been identified that contribute to the cell-specific accumulation of nuclear encoded chloroplast proteins including epigenetic (Heimann et al., 2013), transcriptional (Gowik et al., 2004; Brown et al., 2011; Nomura et al., 2005; John et al., 2014; Wang et al., 2013; Williams et al., 2016), post-transcriptional (Wang et al., 1992; Boinski et al., 1993; Patel et al., 2006; Patel et al., 2004; Fankhauser and Aubry, 2016), translational (Roth et al., 1996) and post-translational mechanisms (Feiz et al., 2002). In comparison to the spatial separation of the two chloroplast types in different cell types in Kranz C4 species, the unique cell morphology of Bienertia leads to the question how the cell distinguishes between the import of proteins in one chloroplast type, when the cell is controlled by only one nucleus (Offermann et al., 2011b). Mechanisms on the DNA level, e.g. epigenetic or transcriptional regulation, cannot explain the differential accumulation of nuclear encoded chloroplast targeted proteins. Thus, only posttranscriptional or (post-)translational mechanisms are possible.

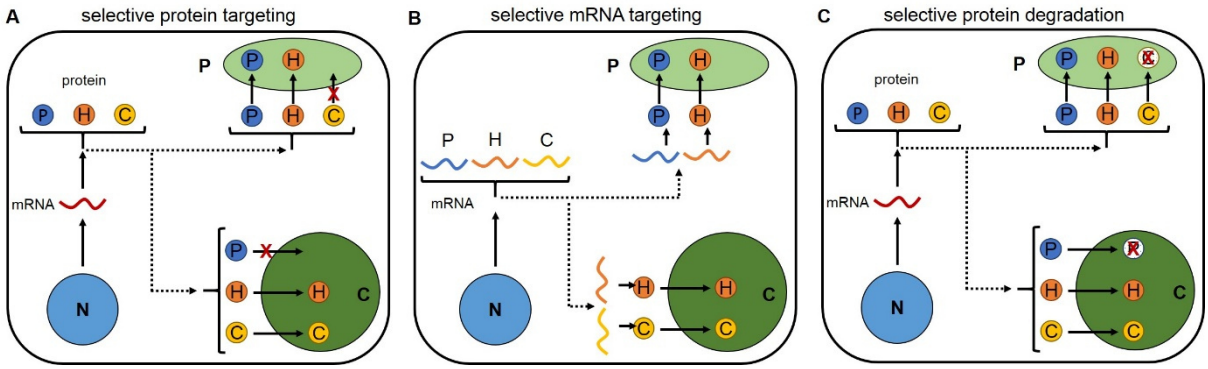

Figure 5: Three different hypotheses for differential localization of nuclear encoded chloroplast proteins in the two chloroplast types *of Bienertia sinuspersici*. Adapted from (Offermann et al., 2011a)

A) Selective protein targeting via different import mechanisms in both chloroplast types; **B)** Selective mRNA targeting to the two different chloroplasts and translation close to the chloroplast envelope; **C)** Selective protein degradation by differential located proteases. N – nucleus; P – peripheral chloroplast; C – central compartment chloroplast; P (blue) - P-specific protein/mRNA; H (orange) – housekeeper protein/mRNA; C (yellow) – C-specific protein (mRNA)

Offermann et al. (2011a) proposed three different hypotheses on how differential accumulation of nuclear encoded chloroplast proteins could function in Bienertia (Figure 5):

selective protein import, mRNA targeting or protein degradation (Offermann et al., 2011a). The first hypothesis describes selective import, where mRNA is translated in the cytoplasm and the resulting protein is transported alone or, under the utilization of chaperones, into one of the two chloroplast types. Different selective import mechanisms could exist, e.g. different translocon of the outer (TOC) and inner membrane (TIC) complexes or associated chaperones that block the import of improper located proteins (Figure 5A). In the second hypothesis, the mRNA is transported to the correct chloroplast type and translated close to the chloroplast surface. Thus, the probability for the import into the correct chloroplast type would be higher (Figure 5B). Selective protein degradation is a third hypothetical scenario that could explain selectivity. All proteins are transported into both chloroplast types. A selective protease could exist that degrades the incorrectly targeted proteins (Figure 5C).

This thesis examines potential protein targeting mechanisms including the selective protein as well as the selective mRNA targeting.

1.4 Chloroplast import of nuclear encoded proteins

During evolution, chloroplasts have evolved from photosynthetically active cyanobacteria which were hosted by eukaryotic cells to form a symbiosis. Over time, these bacteria were converted into semiautonomous plastids which take over the functions of the light-harvesting and carbon fixation reaction. During this process, most bacterial genes were transferred into the nucleus of the eukaryotic cell. Although not yet fully proven, it is commonly accepted as the endosymbiotic theory (Mereschkowsky, 1905). The transferred genes are translated into a precursor protein by cytoplasmic ribosomes and imported into the chloroplasts (overview Figure 6). Approximately 2000-3000 chloroplast proteins use this so called cytosolic pathway, whereas the plastid genome encodes only for about 100-200 proteins (Martin and Herrmann, 1998; Bruce, 2000).

The cell has developed different mechanisms for the import of nuclear encoded proteins into the chloroplast. The vast majority of these proteins use a protein import complex in the chloroplast envelope to enter into the chloroplasts. These are referred to as the translocon of the outer (TOC) and inner membrane (TIC) complex. Proteins entering through these complexes have a specific amino acid (aa) sequence at the N-terminus termed transit peptide (TP). These transit peptides are responsible for the recognition of the precursor proteins at the TOC-TIC complex. Additionally, cytoplasmic chaperones that interact with the transit peptides might be involved in the targeting to the chloroplasts (**Chapter 1.4.1**). In some cases, it has been shown that that mRNAs are transported to the vicinity of the chloroplast where then translation into the protein takes place. Afterwards, the protein is imported into the

chloroplast directly (**Chapter 1.4.3**). Approximately 12 % of the chloroplast proteins contain no TP and are imported by a transit peptide independent pathway (Armbruster et al., 2009). Outer envelope proteins typically do not have a transit peptide at the N-terminus. However, the transmembrane domain (TMD) at the N- or C-terminus is responsible for the targeting and integration in the chloroplast outer membrane (Li and Chen, 1996; Lee et al., 2014). A special form of this import mechanism is the recently discovered chaperone-like ankyrin repeat-containing protein 2 (AKR2) that binds to the TMD and supports the integration of membrane proteins into the envelope (Kim et al., 2014) (**Chapter 1.4.2**). Additionally, an alternative route was discovered that uses the secretory pathway by the endoplasmic reticulum (ER) and the Golgi apparatus (Villarejo et al., 2005) (**Chapter 1.4.4**).

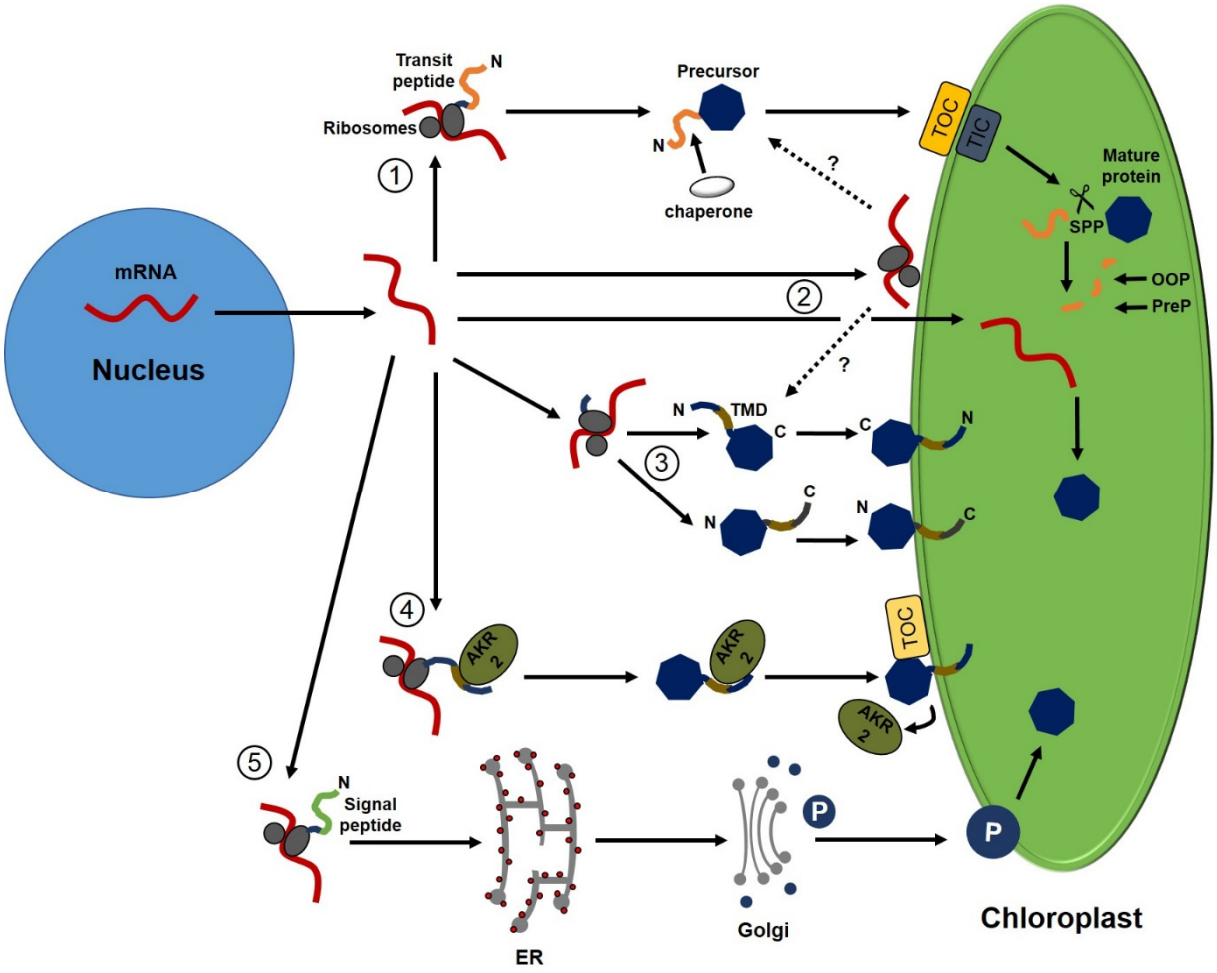

Figure 6: Overview of different chloroplast import pathways of nuclear encoded proteins. Modified from (Tian and Okita, 2014)

Five different pathways for the import of proteins in the chloroplasts. Option 1: mRNA is translated in the cytoplasm into a precursor protein with a N-terminal (N) transit peptide (TP). The precursor is transported to the chloroplast envelope supported by chaperones. The TP is recognized by the translocon of the outer (TOC) and inner membrane (TIC) complex and imported into the stroma where a stromal processing peptidase (SPP) cleaves off the TP. Then, the TP is degraded by the presequence protease (PreP) and the organellar oligopeptidase (OOP). Option 2: mRNA

is targeted to the chloroplast envelope and translated there into a protein that could use the import pathways of option 1 or 3. Alternatively, the mRNA could be imported directly into the chloroplast and translated there by chloroplast ribosomes. Option 3: outer envelope proteins are integrated spontaneously into the chloroplast membrane by a transmembrane domain (TMD) at the N- or C-terminus. Option 4: the ankyrin repeat protein 2 (AKR2) binds during translation to the TMD and transports the protein to the outer envelope. There, TOC75 initiates the insertion of the protein into the outer envelope membrane. Option 5: the protein contains an ER specific signal peptide at the N-terminus that initiates the import in the ER during translation. The protein is transported in vesicles to the Golgi apparatus and further to the chloroplast. There, the vesicle releases the protein into the stroma.

1.4.1 Transit peptide-mediated protein import through the TOC-TIC complex

Most chloroplast targeted proteins contain a short amino sequence at the N-terminus called transit peptide (TP) that is necessary for the chloroplast import by the TOC-TIC complex. Early studies have shown that these TPs vary in length (20 aa to > 100 aa) and in the most cases, have a high content of hydroxylated amino acids (serine in particular) and alanines but rarely acidic amino acids. Additionally, the N-terminus of the TPs contains only uncharged amino acids (Heijne et al., 1989; Ling et al., 2013). After import into the stroma, the TP is cleaved off by a stromal processing peptidase (SPP) (Richter and Lamppa, 1998; Trösch and Jarvis, 2011) and degraded by the presequence protease (PreP) and the organellar oligopeptidase (OOP) (Richter and Lamppa, 2002; Bhushan et al., 2005; Kmiec et al., 2014; Kmiec et al., 2013) (Figure 6 option 1). Previous studies have shown that TPs are rather unstructured in aqueous environments, whereas in hydrophobic environments the TPs form an α-helical structure. As no similarities between the different TPs were found, it was concluded that they do not have general sequence motifs (Bruce, 1998; Bruce, 2001). However, recent studies contradict these results and show that TPs are more structured. The bimodal model by Chotewutmontri et al. (2012) postulates that TPs contain different recognition sites for chaperones and TOC proteins which are separated by a linker sequence (Chotewutmontri et al., 2012). Later, the multi-selection and multi-order (M&M) model was published, which extends the bimodal model with the hypothesis that the order of motifs can vary among TPs (Li and Teng, 2013). Alanine substitution mutants in Arabidopsis supported these models and found multiple sequence subgroups for distinct chloroplast-targeting (Lee et al., 2008) as well as sequence motifs for the binding of different recognition proteins in the TOC complex (Lee et al., 2006; Lee et al., 2009), age-dependent import (Teng et al., 2012), and the binding of different chaperones (Ivey et al., 2000; Chotewutmontri and Bruce, 2015; Huang et al., 2016). Further studies have shown that motifs in the TPs act independently and can be transferred to a new sequence content (Lee et al., 2015). Additionally, it was shown that not only the primary sequence motif but also physiochemical properties are responsible for the interaction with the TOC complex (Chotewutmontri et al., 2012; Holbrook et al., 2016). Furthermore, the phosphorylation state of

the TP could regulate the protein import. Three protein kinases were discovered which phosphorylate the amino acids threonine and serine in the TP. The chaperone 14-3-3 binds to this phosphorylate amino acids and builds a complex with the chaperone heat shock protein 70 (HSP70). This cytoplasmic guidance complex transports the precursor protein to the TOC complex (TOC34) where an unknown phosphatase dephosphorylates the TP and removes the 14-3-3 chaperone (Su et al., 2001; Martin et al., 2006; Lamberti et al., 2011b; Lamberti et al., 2011a; Schwenkert et al., 2011). However, these results are controversially discussed because other evidence showed that phosphorylation of the TP has no influence on the transport and import into the chloroplasts (Nakrieko et al., 2004). This thesis analyzes the TPs of P-specific proteins in Bienertia and shows that the TPs of TPI and PPDK have a short sequence motif of four aa in the TP that is necessary for the different localization in the peripheral chloroplasts (**Chapter 2.3**).

The large GTPases TOC159 or TOC132/120 (Bauer et al., 2000) as well as the small GTPases TOC33 or TOC34 (Gutensohn et al., 2000) act as first receptors for precursor proteins. The import through the outer membrane occurs by the channel protein TOC75. Analyses of knockout mutants in Arabidopsis as well as protein binding assays and expression studies showed that these proteins build two distinct substrate-specific TOC-TIC import complexes. Photosynthetic precursors use TOC159 containing complexes, whereas non-photosynthetic housekeeping precursors prefer complexes containing TOC132 (Jarvis et al., 1998; Bauer et al., 2000; Ivanova et al., 2004; Yan et al., 2014). These differences in the import pathways are mediated by TPs that have recognition sites for the different TOC complexes (Lee et al., 2009). Additionally, the composition of the distinct TOC complexes within the chloroplast can vary during the developmental process. However, studies with yeast two-hybrid experiments and quantitative proteomic and transcriptomic analyses in Arabidopsis showed no evidence for the separated import of photosynthetic and non-photosynthetic proteins (Bischof et al., 2011; Dutta et al., 2014).

Especially TOC159 and TOC34 were analyzed regarding to their binding ability to TPs. Both TOC proteins can interact with precursor proteins but TOC34 is responsible for the first contact with the transit peptide whereas TOC159 initiates mainly the import through the TOC75 channel (Oreb et al., 2011). TOC34 exists as a homodimer in the inactive GDP (guanosine diphosphate)-loading state when no contact to the precursor protein exists (Sun et al., 2002). However, TOC34 is activated by the binding of the precursor protein which triggers the exchange of the intrinsic GDP (guanosine diphosphate) to GTP (guanosine triphosphate). Thus, TOC34 and TOC159 build a heterodimer and initiate the import process through the following GTP hydrolysis (Paila et al., 2015). The factors that are responsible for the activation of GTP hydrolysis are unknown. Most GTPases are activated by GTPase-activating proteins (GAPs) (Bos et al., 2007). In the case of TOC34, it was hypothesized that the dimerization

itself activates the GTPase but it has been shown that the hydrolysis rate of the dimerized TOC34 is lower than the hydrolysis rate of TOC34 in the absence of the precursor protein (Sun et al., 2002). Therefore, it was concluded that the precursor or only the TP act as GAP. Furthermore, phosphate release assays to test the GTP hydrolysis show a high stimulation of TOC34 by transit peptides (Reddick et al., 2007; Chotewutmontri et al., 2012). Holbrock et al. (2016) postulated that the aa motif FGLK, previously identified in some TPs (Lee et al., 2006; Chotewutmontri et al., 2012), acts as TOC34-binding element. After the removal of a proline close to the FGLK motif of the RSSU transit peptide, the interaction of the TP and TOC34 was impaired. This indicates that a secondary structure influences the binding capacity of the TPs. Holbrock et al. (2016) also hypothesize that this motif forms an arginine finger that directly interacts with the catalytic center of TOC34 and activates the GTP hydrolysis. However, it is also possible that changes in the secondary structure lead to problems in the transport of the precursor through the TOC75 channel or the binding of ATP-dependent molecular motor proteins in the stroma (Holbrook et al., 2016).

In summary, transit peptides contain more information than previously expected. Sequence motifs in the TPs act as binding site for chaperones or TOC proteins. Furthermore, the probability that TPs form secondary structures that initiate the import into the chloroplasts is very high.

1.4.2 Integration of outer envelope proteins

Signal-anchored (SA) as well as tail-anchored (TA) proteins of the outer envelope membrane (OEM) of chloroplasts are integrated into the membrane without a cleavable transit peptide (Figure 6 option 3). Most of these membrane proteins are responsible for the recognition and import of stromal and thylakoid proteins. Prominent examples for SA proteins are the outer envelope protein 7 (OEP7) and TOC64 as well as TOC33/34 and TOC159 for TA proteins (Lee et al., 2014). Instead of TPs, these proteins have a hydrophobic transmembrane domain at the N-terminus of SA proteins or the C-terminus of TA proteins, respectively. These proteins can either interact spontaneously with the OEM and anchor in the membrane, or cytosolic factors can assist the import process (Li and Chen, 1996; Lee et al., 2014). Previous studies have shown that the AKR2 is important for chloroplast targeting of SA as well as TA proteins, like OEP7, TOC64, and TOC33/34 (Figure 6 option 4) (Bae et al., 2008; Kim et al., 2014; Kim et al., 2015). AKR2 binds directly during the translation to their proteins on the TMDs and acts as a chaperone thereby avoiding the formation of secondary structures of the TMDs (Kim et al., 2015). Afterwards, AKR2 binds with the ankyrin-repeat domain (ARD) at the OEM and initiates the insertion of the proteins assisted by TOC75 (Lee et al., 2014).

The main import receptor TOC159 lacks a TMD. However, deletion experiments have shown that the C-terminal located M-domain is responsible for the insertion into the OEM (Lee et al., 2003). Interestingly, bioinformatical analysis of Bienertia BsTOC159 shows physiochemical similarities to N-terminal TPs. Localization studies showed that the C-terminus is essential for the insertion of BsTOC159 into the OEM. Furthermore, it acts as conventional TP when it is fused in front of the N-terminus of GFP (Lung and Chuong, 2012; Lung et al., 2014).

1.4.3 mRNA targeting

In some cases, it has been shown that mRNA can either be targeted close to the OEM and translation is initiated, or is directly imported into the chloroplasts (Figure 6 option 2) (Tian and Okita, 2014). The signal for mRNA targeting is mostly located in the coding region and/or the untranslated region (UTR) of the mRNA (Garcia et al., 2010; Gadir et al., 2011). The import of mRNA into the chloroplast was first observed for the eukaryotic translation initiation factor 4E (eIF4E) in four different species (*Arabidopsis thaliana*, *Nicotiana tabacum*, *Lactuca sativa*, *Spinacia oleracea*). Furthermore, the eIF4E mRNA transports the exogenous GFP mRNA into the chloroplast (Nicolaï et al., 2007). In *Nicotiana benthamiana*, a viroid non-coding mRNA (ncRNA) mediates the transport and accumulation of an exogenous mRNA into the chloroplast when it is fused at the 5'UTR end (Gomez and Pallas, 2010a; Gomez and Pallas, 2010b). In *Chlamydomonas reinhardtii*, the light-harvesting complex II (LHCII) mRNA was concentrated along the cytoplasmic border of the chloroplast basal region (Uniacke and Zerges, 2009). mRNA targeting is also observed in mitochondria that mainly use a similar peptide-mediated import mechanism as chloroplasts. Transcript analyses have shown that mRNAs of mitochondrial located proteins could be targeted to the mitochondria (Michaud et al., 2010). Furthermore, radioactively labelled *in vitro* transcripts could be detected at the surface of isolated mitochondria (Michaud et al., 2014a). Michaud et al. (2014b) also isolated a sequence on the 3'UTR of the voltage-dependent anion channel (VDAC) that is necessary for the transport of the mRNA to the mitochondria. This sequence can also target a reporter transcript close to the mitochondria (Michaud et al., 2014b).

1.4.4 Alternative protein import through the secretory pathway

Chloroplast located proteins can also use a TOC-TIC-independent import system along the secretory pathway that is specialized in the transport of glycoproteins to the chloroplasts (Villarejo et al., 2005). Recent examples for this alternative import pathway include α-amylase I-1 (AmyI-1) (Asatsuma et al., 2005; Kitajima et al., 2009), the manganese superoxide dismutase 1 (MSD1) (Shiraya et al., 2015) and an α-type carbonic anhydrase 1 (CAH1) (Buren et al., 2011). These proteins have an ER specific signal peptide at the N-terminus that initiates the import into the ER during translation at the ribosomes. Once within the ER lumen, these proteins can then be modified post-translationally (e.g. N-glycosylation) and transported in vesicles towards the Golgi apparatus. From there, the modified proteins are transported in Golgi vesicles to the chloroplast envelope (Figure 6 option 5). Baslam et al. (2016) postulates three hypotheses how the following import of the proteins could take place (Baslam et al., 2016). In the fusing/budding model, the Golgi vesicle fuses with the outer chloroplast envelope and releases the protein into the intermembrane space. From there, the protein can use the TIC complex or an unknown transporter for the further import into the stroma. In the invagination model, the Golgi vesicle is engulfed by the chloroplast outer and inner membrane and buds off after being absorbed into the stroma. After that, the vesicles break up and release the proteins. In the pass-through model, the vesicles are transported through pores or unknown unspecific transporters into the stroma. However, the exact pathway for the import through the secretory pathway is so far unknown.

1.5 Objectives of this thesis

The aim of this thesis was to resolve the regulatory mechanism involved in the selective accumulation of nuclear encoded chloroplast proteins in Bienertia. Special emphasis was put on the three hypotheses of differential accumulation of these proteins (see **Chapter 1.3**). Selective protein as well as mRNA targeting were analyzed by GFP fusion proteins in transfected protoplasts or in transient *Agrobacterium*-mediated transformed Bienertia cuttings.

i) The localization of P- and C-specific proteins was to be analyzed by large-scale proteomics. The results were then summarized in a model for carbon fixation in Bienertia (**Chapter 2.1**).

ii) New aspects in the recent literature on the development of chlorenchyma cells, subcellular positioning of both chloroplast types and the selective protein accumulation *in Bienertia sinuspersici* were to be collected and summarized (**Chapter 2.2**).

iii) The influence of the protein sequence on the differential targeting of the nuclear encoded chloroplast proteins PPDK, TPI, AK and RSSU was to be tested with GFP fusion proteins in Bienertia transfected protoplasts. Furthermore, a new protocol for the isolation of young protoplasts was to be developed to test age-dependent differences in the selective accumulation of proteins. Putative regulatory sequence elements were to be tested by mutation analysis (**Chapter 2.3**).

iv) A new protocol for transient *Agrobacterium*-mediated transformation in Bienertia was to be developed and verified by localization studies with established marker GFP-fusion proteins. The functionality of the protocol was also to be tested by the analysis of the endogenous genes (**Chapter 2.4**).

1.6 References

Akhani H, Chatrenoor T, Dehghani M, Khoshravesh R, Mahdavi P, Matinzadeh Z (2012)
A new species of Bienertia (Chenopodiaceae) from Iranian salt deserts. A third species of the genus and discovery of a fourth terrestrial C 4 plant without Kranz anatomy. *Plant Biosystems - An International Journal Dealing with all Aspects of Plant Biology* **146**: 550-559.

Akhani H, Barroca J, Koteeva N, Voznesenskaya E, Franceschi V, Edwards GE, Ghaffari SM, Ziegler H (2005)
Bienertia sinuspersici (Chenopodiaceae): a new species from Southwest Asia and discovery of a third terrestrial C_4 plant without Kranz anatomy. *Systematic Botany* **30:** 290–301.

Andersen KS, Bain JM, Bishop DG, Smillie R (1972)
Photosystem II activity in agranal bundle sheath chloroplasts from *Zea mays*. *Plant Physiology* **49:** 461–466.

Armbruster U, Hertle A, Makarenko E, Zühlke J, Pribil M, Dietzmann A, Schliebner I, Aseeva E, Fenino E, Scharfenberg M, Voigt C, Leister D (2009)
Chloroplast proteins without cleavable transit peptides: rare exceptions or a major constituent of the chloroplast proteome? *Molecular Plant* **2:** 1325–1335.

Asatsuma S, Sawada C, Itoh K, Okito M, Kitajima A, Mitsui T (2005)
Involvement of alpha-amylase I-1 in starch degradation in rice chloroplasts. *Plant & Cell Physiology* **46:** 858–869.

Bae W, Lee YJ, Kim DH, Lee J, Kim S, Sohn EJ, Hwang (2008)
AKR2A-mediated import of chloroplast outer membrane proteins is essential for chloroplast biogenesis. *Nature Cell Biology* **10:** 220–227.

Baslam M, Oikawa K, Kitajima-Koga A, Kaneko K, Mitsui T (2016)
Golgi-to-plastid trafficking of proteins through secretory pathway: Insights into vesicle-mediated import toward the plastids. *Plant Signaling & Behavior* **11:** e1221558.

Bauer J, Chen K, Hiltbunner A, Wehrli E, Eugster M, Schnell D, Kessler F (2000)
The major protein import receptor of plastids is essential for chloroplast biogenesis. *Nature* **403:** 203–207.

Bauwe H, Hagemann M, Fernie A (2010)
Photorespiration: players, partners and origin. *Trends in Plant Science* **15:** 330–336.

Bender MM, Rouhani I, Vines HM, Black CC (1973)
13C/12C ratio changes in Crassulacean acid metabolism plants. *Plant Physiology* **52:** 427-430.

Berry JA, Downton WJS, Tregunna EB (1970)
The photosynthetic carbon metabolism of *Zea mays* and *Gomphrena globosa*. The location of the CO_2 fixation and the carboxyl transfer reactions. *Canadian Journal of Botany* **48:** 777–786.

Bhushan S, Stahl A, Nilsson S, Lefebvre B, Seki M, Roth C, McWilliam D, Wright SJ, Liberles DA, Shinozaki K, Bruce BD, Boutry M, Glaser E (2005)
Catalysis, subcellular localization, expression and evolution of the targeting peptides degrading protease, AtPreP2. *Plant and Cell Physiology* **46:** 985–996.

Bischof S, Baerenfaller K, Wildhaber T, Troesch R, Vidi PA, Roschitzki B, Hirsch-Hoffmann M, Hennig L, Kessler F, Gruissem W, Baginsky S (2011)
Plastid proteome assembly without Toc159: photosynthetic protein import and accumulation of N-acetylated plastid precursor proteins. *The Plant Cell* **23:** 3911–3928.

Boinski JJ, Wang JL, Xu P, Hotchkiss T, Berry JO (1993)
Post-transcriptional control of cell type-specific gene expression in bundle sheath and mesophyll chloroplasts of *Amaranthus hypochondriacus*. *Plant Molecular Biology* **22**: 397

Bos JL, Rehmann H, Wittinghofer A (2007)
GEFs and GAPs: critical elements in the control of small G proteins. *Cell* **129:** 865–877.

Bowes G, Ogren WL, Hageman RH (1971)
Phosphoglycolate production catalyzed by ribulose diphosphate carboxylase. *Biochemical and Biophysical Research Communications* **45:** 716–722.

Brown NJ, Newell CA, Stanley S, Chen JE, Perrin AJ, Kajala K, Hibberd JM (2011)
Independent and parallel recruitment of preexisting mechanisms underlying C4 photosynthesis. *Science* **331:** 1436–1439.

Bruce BD (1998)
The role of lipids in plastid protein transport. *Plant Molecular Biology* **38:** 223–246.

Bruce BD (2000)
Chloroplast transit peptides: structure, function and evolution. *Trends in Cell Biology* **10:** 440–447.

Bruce BD (2001)
The paradox of plastid transit peptides: conservation of function despite divergence in primary structure. *Biochimica et Biophysica Acta* **1541:** 2–21.

Buren S, Ortega-Villasante C, Blanco-Rivero A, Martinez-Bernardini A, Shutova T, Shevela D, Messinger J, Bako L, Villarejo A, Samuelsson G (2011)
Importance of post-translational modifications for functionality of a chloroplast-localized carbonic anhydrase (CAH1) in *Arabidopsis thaliana*. *Public Library of Science ONE* **6:** e21021.

Chaves MM, Flexas J, Pinheiro C (2009)
Photosynthesis under drought and salt stress: regulation mechanisms from whole plant to cell. *Annals of Botany* **103:** 551–560.

Chotewutmontri P, Bruce BD (2015)
Non-native, N-terminal Hsp70 molecular motor recognition elements in transit peptides support plastid protein translocation. *The Journal of Biological Chemistry* **290:** 7602–7621.

Chotewutmontri P, Reddick LE, McWilliams DR, Campbell IM, Bruce BD (2012)
Differential transit peptide recognition during preprotein binding and translocation into flowering plant plastids. *The Plant Cell* **24:** 3040–3059.

Chuong SD, Franceschi VR, Edwards GE (2006)
The cytoskeleton maintains organelle partitioning required for single-cell C4 photosynthesis in Chenopodiaceae species. *The Plant Cell* **18:** 2207–2223.

Dutta S, Teresinski HJ, Smith MD (2014)
A split-ubiquitin yeast two-hybrid screen to examine the substrate specificity of atToc159 and atToc132, two Arabidopsis chloroplast preprotein import receptors. *Public Library of Science ONE* **9:** e95026.

Edwards GE, Kanai R, Black CC (1971)
Phosphoenolpyruvate carboxykinase in leaves of certain plants which fix CO_2 by the C4 dicarboxylic acid cycle of photosynthesis. *Biochemical and Biophysical Research Communications* **45:** 278–285.

Edwards GE, Lee SS, Chen TM, Black CC (1970)
Carboxylation reactions and photosynthesis of carbon compounds in isolated mesophyll and bundle sheath cells of *Digitaria sanguinalis* (L.) Scop. *Biochemical and Biophysical Research Communications* **39:** 389–395.

Edwards GE, Nakamoto H, Burnell JN, Hatch MD (1985)
Pyruvate,Pi dikinase and NADP-malate dehydrogenase in C4 photosynthesis. Properties and mechanism of light/dark regulation. *Annual Review of Plant Physiology* **36:** 255–286.

Fankhauser N, Aubry S (2016)
Post-transcriptional regulation of photosynthetic genes is a key driver of C4 leaf ontogeny. *Journal of Experimental Botany* **68**: 137-146.

Feiz L, Williams-Carrier R, Wostrikoff K, Belcher S, Barkan A, Stern DB (2002)
Ribulose-1,5-bis-phosphate carboxylase/oxygenase accumulation factor1 is required for holoenzyme assembly in maize. *The Plant Cell* **24:** 3435–3446.

Freitag H, Stichler W (2000)
A remarkable new leaf type with unusual photosynthetic tissue in a Central Asiatic genus of Chenopodiaceae. *Plant Biology* **2:** 154–160.

Freitag H, Stichler W (2002)
Bienertia cycloptera Bunge ex Boiss., Chenopodiaceae, another C4 plant without Kranz tissues. *Plant Biology* **4:** 121–132.

Gadir N, Haim-Vilmovsky L, Kraut-Cohen J, Gerst JE (2011)
Localization of mRNAs coding for mitochondrial proteins in the yeast *Saccharomyces cerevisiae*. *RNA* **17:** 1551–1565.

Garcia M, Delaveau T, Goussard S, Jacq C (2010)
Mitochondrial presequence and open reading frame mediate asymmetric localization of messenger RNA. *EMBO Reports* **11:** 285–291.

Gomez G, Pallas V (2010)
Can the import of mRNA into chloroplasts be mediated by a secondary structure of a small noncoding RNA? *Plant Signaling & Behavior* **5:** 1517–1519.

Gomez G, Pallas V (2010)
Noncoding RNA mediated traffic of foreign mRNA into chloroplasts reveals a novel signaling mechanism in plants. *Public Library of Science ONE* **5:** e12269.

Gowik U, Burscheidt J, Akyildiz M, Schlue U, Koczor M, Streubel M, Westhoff P (2004)
cis-regulatory elements for mesophyll-specific gene expression in the C4 plant *Flaveria trinervia*, the promoter of the C4 phosphoenolpyruvate carboxylase gene. *The Plant Cell* **16:** 1077–1090.

Gutensohn M, Schulz B, Nicolay P, Flügge U (2000)
Functional analysis of the two Arabidopsis homologues of Toc34, a component of the chloroplast protein import apparatus. *The Plant Journal* **23:** 771–783.

Haberlandt G (1904)
Physiologische Pflanzenanatomie. W. Engelmann, Leipzig

Hatch MD, Kagawa T (1976)
Photosynthetic activities of isolated bundle sheath cells in relation to differing mechanisms of C4 pathway photosynthesis. *Archives of Biochemistry and Biophysics* **175:** 39–53.

Hatch MD, Kagawa T, Craig S (1975)
Subdivision of C4-pathway species based on differing C4 acid decarboxylating systems and ultrastructural features. *Functional Plant Biology* **2:** 111–128.

Hatch MD, Slack CR (1966)
Photosynthesis by sugar-cane leaves. A new carboxylation reaction and the pathway of sugar formation. *The Biochemical Journal* **101:** 103–111.

Hattersley PW, Browning AJ (1981)
Occurrence of the suberized lamella in leaves of grasses of different photosynthetic types. In parenchymatous bundle sheaths and PCR (“Kranz”) sheaths. *Protoplasma* **109:** 371–401.

Heijne G von, **Steppuhn J, Herrmann RG** (1989)
Domain structure of mitochondrial and chloroplast targeting peptides. *European Journal of Biochemistry* **180:** 535–545.

Heimann L, Horst I, Perduns R, Dreesen B, Offermann S, Peterhansel C (2013)
A common histone modification code on C4 genes in maize and its conservation in Sorghum and *Setaria italica*. *Plant Physiology* **162:** 456–469.

Holbrook K, Subramanian C, Chotewutmontri P, Reddick LE, Wright S, Zhang H, Moncrief L, Bruce BD (2016)
Functional analysis of semi-conserved transit peptide motifs and mechanistic implications in precursor targeting and recognition. *Molecular Plant* **9:** 1286–1301.

Huang PK, Chan PT, Su PH, Chen LJ, Li H (2016)
Chloroplast Hsp93 directly binds to transit peptides at an early stage of the preprotein import process. *Plant Physiology* **170:** 857–866.

Ivanova Y, Smith MD, Chen K, Schnell DJ (2004)
Members of the Toc159 import receptor family represent distinct pathways for protein targeting to plastids. *Molecular Biology of the Cell* **15:** 3379–3392.

Ivey RA, Subramanian C, Bruce BD (2000)
Identification of a Hsp70 recognition domain within the Rubisco Small Subunit transit peptide. *Plant Physiology* **122:** 1289–1300.

Jarvis P, Chen LJ, Li HM, Peto CA, Fankhauser C, Chory J (1998)
An Arabidopsis mutant defective in the plastid general protein import apparatus. *Science* **282:** 100–103.

John CR, Smith-Unna RD, Woodfield H, Covshoff S, Hibberd JM (2014)
Evolutionary convergence of cell-specific gene expression in independent lineages of C4 grasses. *Plant Physiology* **165:** 62–75.

Kadereit G, Borsch T, Weising K, Freitag H (2003)
Phylogeny of Amaranthaceae and Chenopodiaceae and the evolution of C4 photosynthesis. *International Journal of Plant Sciences* **164:** 959–986.

Kellogg EA (1999)
Phylogenetic aspects of the evolution of C4 photosynthesis. *C4 Plant Biology* **12:** 411–444.

Kim DH, Lee JE, Xu ZY, Geem KR, Kwon Y, Park JW, Hwang I (2015)
Cytosolic targeting factor AKR2A captures chloroplast outer membrane-localized client proteins at the ribosome during translation. *Nature Communications* **6:** 6843.

Kim DH, Park MJ, Gwon GH, Silkov A, Xu ZY, Yang EC, Song S, Song K, Kim Y, Yoon HS, Honig B, Cho W, Cho Y, Hwang I (2014)
An ankyrin repeat domain of AKR2 drives chloroplast targeting through coincident binding of two chloroplast lipids. *Developmental Cell* **30:** 598–609.

Kitajima A, Asatsuma S, Okada H, Hamada Y, Kaneko K, Nanjo Y, Kawagoe Y, Toyooka K, Matsuoka K, Takeuchi M, Nakano A, Mitsui T (2009)
The rice alpha-amylase glycoprotein is targeted from the Golgi apparatus through the secretory pathway to the plastids. *The Plant Cell* **21:** 2844–2858.

Kmiec B, Teixeira PF, Berntsson RP, Murcha MW, Branca RM, Radomiljac JD, Regberg J, Svensson LM, Bakali A, Langel U, Lehtio J, Whelan J, Stenmark P, Glaser E (2013)
Organellar oligopeptidase (OOP) provides a complementary pathway for targeting peptide degradation in mitochondria and chloroplasts. *Proceedings of the National Academy of Sciences of the United States of America* **110:** E3761-9.

Kmiec B, Teixeira PF, Glaser E (2014)
Shredding the signal: targeting peptide degradation in mitochondria and chloroplasts. *Trends in Plant Science* **19:** 771–778.

Koteyeva NK, Voznesenskaya EV, Berry JO, Cousins AB, Edwards GE (2016)
The unique structural and biochemical development of single cell C4 photosynthesis along longitudinal leaf gradients in *Bienertia sinuspersici* and *Suaeda aralocaspica* (Chenopodiaceae). *Journal of Experimental Botany* **67:** 2587–2601.

Lamberti G, Gugel IL, Meurer J, Soll J, Schwenkert S (2011)
The cytosolic kinases STY8, STY17, and STY46 are involved in chloroplast differentiation in Arabidopsis. *Plant Physiology* **157:** 70–85.

Lamberti G, Drurey C, Soll J, Schwenkert S (2011)
The phosphorylation state of chloroplast transit peptides regulates preprotein import. *Plant Signaling & Behavior* **6:** 1918–1920.

Lee DW, Kim JK, Lee S, Choi S, Kim S, Hwang I (2008)
Arabidopsis nuclear-encoded plastid transit peptides contain multiple sequence subgroups with distinctive chloroplast-targeting sequence motifs. *The Plant Cell* **20:** 1603–1622.

Lee DW, Lee S, Lee G, Lee KH, Kim S, Cheong GW, Hwang I (2006)
Functional characterization of sequence motifs in the transit peptide of Arabidopsis small subunit of Rubisco. *Plant Physiology* **140:** 466–483.

Lee DW, Lee S, Oh YJ, Hwang I (2009)
Multiple sequence motifs in the Rubisco small subunit transit peptide independently contribute to Toc159-dependent import of proteins into chloroplasts. *Plant Physiology* **151:** 129–141.

Lee DW, Woo S, Geem KR, Hwang I (2015)
Sequence motifs in transit peptides act as independent functional units and can be transferred to new sequence contexts. *Plant Physiology* **169:** 471–484.

Lee J, Kim DH, Hwang I (2014)
Specific targeting of proteins to outer envelope membranes of endosymbiotic organelles, chloroplasts, and mitochondria. *Frontiers in Plant Science* **5:** 173.

Lee KH, Kim SJ, Lee YJ, Jin JB, Hwang I (2003)
The M domain of atToc159 plays an essential role in the import of proteins into chloroplasts and chloroplast biogenesis. *Journal of Biological Chemistry* **278:** 36794–36805.

Li HM, Chen LJ (1996)
Protein targeting and integration signal for the chloroplastic outer envelope membrane. *The Plant Cell* **8:** 2117–2126.

Li HM, Teng YS (2013)
Transit peptide design and plastid import regulation. *Trends in Plant Science* **18:** 360–366.

Ling Q, Trösch R, Jarvis P (2013)
The ins and outs of chloroplast protein transport. In plastid development in leaves during growth and senescence, Vol 36. Springer, Dordrecht, pp. 239–280.

Ludwig M (2016)
The roles of organic acids in C4 photosynthesis. *Frontiers in Plant Science* **7:** 647.

Lung SC, Yanagisawa M, Chuong SD (2011)
Protoplast isolation and transient gene expression in the single-cell C4 species, *Bienertia sinuspersici*. *Plant Cell Reports* **30:** 473–484.

Lung SC, Chuong SD (2012)
A transit peptide–like sorting signal at the C-terminus directs the *Bienertia sinuspersici* preprotein receptor Toc159 to the chloroplast outer membrane. *The Plant Cell* **24:** 1560–1578.

Lung SC, Smith MD, Weston JK, Gwynne W, Secord N, Chuong SD (2014)
The C-terminus of *Bienertia sinuspersici* Toc159 contains essential elements for its targeting and anchorage to the chloroplast outer membrane. *Frontiers in Plant Science* **5:** 722.

Maai E, Miyake H, Taniguchi M (2011)
Differential positioning of chloroplasts in C4 mesophyll and bundle sheath cells. *Plant Signaling & Behavior* **6:** 1111–1113.

Majeran W, Cai Y, Sun Q, van Wijk KJ (2005)
Functional differentiation of bundle sheath and mesophyll maize chloroplasts determined by comparative proteomics. *The Plant Cell* **17:** 3111–3140.

Martin T, Sharma R, Sippel C, Waegemann K, Soll J, Vothknecht UC (2006)
A protein kinase family in Arabidopsis phosphorylates chloroplast precursor proteins. *Journal of Biological Chemistry* **281:** 40216–40223.

Martin W, Herrmann RG (1998)
Gene transfer from organelles to the nucleus: how much, what happens, and why? *Plant Physiology* **118:** 9–17.

Mereschkowsky C (1905)
Über Natur und Ursprung der Chromatophoren im Pflanzenreiche. *Biologisches Centralblatt* **25:** 593-604

.

Michaud M, Marechal-Drouard L, Duchene AM (2014)
Targeting of cytosolic mRNA to mitochondria: naked RNA can bind to the mitochondrial surface. *Biochimie* **100:** 159–166.

Michaud M, Ubrig E, Filleur S, Erhardt M, Ephritikhine G, Marechal-Drouard L, Duchene AM (2014)
Differential targeting of VDAC3 mRNA isoforms influences mitochondria morphology. *Proceedings of the National Academy of Sciences of the United States of America* **111:** 8991–8996.

Michaud M, Marechal-Drouard L, Duchene AM (2010)
RNA trafficking in plant cells: targeting of cytosolic mRNAs to the mitochondrial surface. *Plant Molecular Biology* **73:** 697–704.

Nakrieko K, Mould RM, Smith AG (2004)
Fidelity of targeting to chloroplasts is not affected by removal of the phosphorylation site from the transit peptide. *The FEBS Journal* **271:** 509–516.

Nicolaï M, Duprat A, Sormani R, Rodriguez C, Roncato M-A, Rolland N, Robaglia C (2007)
Higher plant chloroplasts import the mRNA coding for the eucaryotic translation initiation factor 4E. *FEBS Letters* **581:** 3921–3926

Nomura M, Higuchi T, Katayama K, Taniguchi M, Miyao-Tokutomi M, Matsuoka M, Tajima S (2005)
The promoter for C4-type mitochondrial aspartate aminotransferase does not direct bundle sheath-specific expression in transgenic rice plants. *Plant & Cell Physiology* **46:** 743–753.

Offermann S, Okita TW, Edwards GE (2011)
How do single cell C4 species form dimorphic chloroplasts? *Plant Signaling & Behavior* **6:** 762–765.

Offermann S, Okita TW, Edwards GE (2011)
Resolving the compartmentation and function of C4 photosynthesis in the single-cell C4 species *Bienertia sinuspersici*. *Plant Physiology* **155:** 1612–1628.

Oreb M, Hofle A, Koenig P, Sommer MS, Sinning I, Wang F, Tews I, Schnell DJ, Schleiff E (2011)
Substrate binding disrupts dimerization and induces nucleotide exchange of the chloroplast GTPase Toc33. *The Biochemical Journal* **436:** 313–319.

Paila YD, Richardson LG, Schnell DJ (2015)
New insights into the mechanism of chloroplast protein import and its integration with protein quality control, organelle biogenesis and development. *Journal of Molecular Biology* **427:** 1038–1060.

Park J, Knoblauch M, Okita TW, Edwards GE (2009)
Structural changes in the vacuole and cytoskeleton are key to development of the two cytoplasmic domains supporting single-cell C4 photosynthesis in *Bienertia sinuspersici*. *Planta* **229:** 369–382.

Patel M, Corey AC, Yin LP, Ali S, Taylor WC, Berry JO (2004)
Untranslated regions from C4 amaranth AhRbcS1 mRNAs confer translational enhancement and preferential bundle sheath cell expression in transgenic C4 *Flaveria bidentis*. *Plant Physiology* **136:** 3550–3561.

Patel M, Siegel AJ, Berry JO (2006)
Untranslated regions of FbRbcS1 mRNA mediate bundle sheath cell-specific gene expression in leaves of a C4 Plant. *Journal of Biological Chemistry* **281:** 25485–25491.

Reddick LE, Vaughn MD, Wright SJ, Campbell lM, Bruce BD (2007)
In vitro comparative kinetic analysis of the chloroplast Toc GTPases. *Journal of Biological Chemistry* **282:** 11410–11426.

Rhoades MM, Carvalho A (1944)
The function and structure of the parenchyma sheath plastids of the maize leaf. *Bulletin of the Torrey Botanical Club* **71:** 335.

Richter S, Lamppa GK (1998)
A chloroplast processing enzyme functions as the general stromal processing peptidase. *Proceedings of the National Academy of Sciences of the United States of America* **95:** 7463–7468.

Richter S, Lamppa GK (2002)
Determinants for removal and degradation of transit peptides of chloroplast precursor proteins. *Journal of Biological Chemistry* **277:** 43888–43894.

Roth R, Hall LN, Brutnell TP, Langdale JA (1996)
Bundle sheath defective2, a mutation that disrupts the coordinated development of bundle sheath and mesophyll cells in the maize leaf. *The Plant Cell* **8:** 915–927.

Sage RF (2004)
The evolution of C4 photosynthesis. *New Phytologist* **161:** 341–370.

Sage RF (2016)
A portrait of the C4 photosynthetic family on the 50th anniversary of its discovery: species number, evolutionary lineages, and hall of fame. *Journal of Experimental Botany* **67**: 4039-4056

Schwenkert S, Soll J, Bolter B (2011)
Protein import into chloroplasts - how chaperones feature into the game. *Biochimica et Biophysica Acta* **1808:** 901–911.

Shiraya T, Mori T, Maruyama T, Sasaki M, Takamatsu T, Oikawa K, Itoh K, Kaneko K, Ichikawa H, Mitsui T (2015)
Golgi/plastid-type manganese superoxide dismutase involved in heat-stress tolerance during grain filling of rice. *Plant Biotechnology Journal* **13:** 1251–1263.

Su Q, Schmid K, Schild C, Boschetti A (2001)
Effect of precursor protein phosphorylation on import into isolated chloroplasts from Chlamydomonas. *FEBS Letters* **508:** 165–169.

Sun YJ, Forouhar F, Li HM, Tu SL, Yeh YH, Kao S, Shr HL, Chou CC, Chen C, Hsiao CD (2002)
Crystal structure of pea Toc34, a novel GTPase of the chloroplast protein translocon. *Nature Structural Biology* **9:** 95–100.

Teng YS, Chan PT, Li HM (2012)
Differential age-dependent import regulation by signal peptides. *Public Library of Science Biology* **10:** e1001416.

Tian L, Okita TW (2014)
mRNA-based protein targeting to the endoplasmic reticulum and chloroplasts in plant cells. *Cell Biology* **22:** 77–85.

Trösch R, Jarvis P (2011)
The stromal processing peptidase of chloroplasts is essential in Arabidopsis, with knockout mutations causing embryo arrest after the 16-cell stage. *Public Library of Science ONE* **6:** e23039.

Uniacke J, Zerges W (2009)
Chloroplast protein targeting involves localized translation in Chlamydomonas *Proceedings of the National Academy of Sciences of the United States of America* **106:** 1439–1444.

Villarejo A, Buren S, Larsson S, Dejardin A, Monne M, Rudhe C, Karlsson J, Jansson S, Lerouge P, Rolland N, Heijne G von, Grebe M, Bako L, Samuelsson G (2005)
Evidence for a protein transported through the secretory pathway en route to the higher plant chloroplast. *Nature Cell Biology* **7:** 1224–1231.

Voznesenskaya EV, Franceschi VR, Kiirats O, Artyusheva EG, Freitag H, Edwards GE (2002)
Proof of C4 photosynthesis without Kranz anatomy in *Bienertia cycloptera* (Chenopodiaceae). *The Plant journal* **31:** 649–662.

Voznesenskaya EV, Franceschi VR, Kiirats O, Freitag H, Edwards GE (2001)
Kranz anatomy is not essential for terrestrial C4 plant photosynthesis. *Nature* **414:** 543–546.

Voznesenskaya EV, Franceschi VR, Pyankov VI, Edwards GE (1999)
Anatomy, chloroplast structure and compartmentation of enzymes relative to photosynthetic mechanisms in leaves and cotyledons of species in the tribe Salsoleae (Chenopodiaceae). *Journal of Experimental Botany* **50:** 1779–1795.

Voznesenskaya EV, Koteyeva NK, Chuong SD, Akhani H, Edwards GE, Franceschi VR (2005)
Differentiation of cellular and biochemical features of the single-cell C4 syndrome during leaf development in *Bienertia cycloptera* (Chenopodiaceae). *American Journal of Botany* **92:** 1784–1795.

Voznesenskaya EV, Edwards GE, Kiirats O, Artyusheva EG, Franceschi VR (2003)
Development of biochemical specialization and organelle partitioning in the single-cell C4 system in leaves of *Borszczowia aralocaspica* (Chenopodiaceae). *American Journal of Botany* **90:** 1669–1680.

Voznesenskaya EV, Franceschi VR, Edwards GE (2004)
Light-dependent development of single cell C4 photosynthesis in cotyledons of *Borszczowia aralocaspica* (Chenopodiaceae) during transformation from a storage to a photosynthetic organ. *Annals of Botany* **93:** 177–187.

Wang J, Klessig D, Berry J (1992)
Regulation of C4 gene expression in developing amaranth leaves. *The Plant Cell* **4:** 173–184.

Wang P, Fouracre J, Kelly S, Karki S, Gowik U, Aubry S, Shaw MK, Westhoff P, Slamet-Loedin IH, Quick WP, Hibberd JM, Langdale JA (2013)
Evolution of GOLDEN2-LIKE gene function in C3 and C4 plants. *Planta* **237:** 481–495.

Williams BP, Burgess SJ, Reyna-Llorens I, Knerova J, Aubry S, Stanley S, Hibberd JM (2016)
An untranslated cis-element regulates the accumulation of multiple C4 enzymes in *Gynandropsis gynandra* mesophyll cells. *The Plant Cell* **28:** 454–465.

Yamada M, Kawasaki M, Sugiyama T, Miyake H, Taniguchi M (2009)
Differential positioning of C4 mesophyll and bundle sheath chloroplasts: aggregative movement of C4 mesophyll chloroplasts in response to environmental stresses. Plant & Cell Physiology **50:** 1736–1749.

Yan J, Campbell JH, Glick BR, Smith MD, Liang Y (2014)
Molecular characterization and expression analysis of chloroplast protein import components in tomato (*Solanum lycopersicum*). *Public Library of Science ONE* **9:** e95088.

Zhang YG, Pagani M, Liu Z, Bohaty SM, Deconto R (2013)
A 40-million-year history of atmospheric CO_2. *Philosophical Transactions of the Royal Society* **371:** 20130096.

Section 2 - Analysis of subcellular protein targeting mechanisms in the single-cell C4 species *Bienertia sinuspersici*: Publications

2.1 Publication I

Developmental and subcellular organization of single-cell C4 photosynthesis in *Bienertia sinuspersici* determined by large-scale proteomics and cDNA assembly from 454 DNA sequencing

Sascha Offermann[1], Giulia Friso[2], Kelly A. Doroshenk[3], Qi Sun[4], Richard M. Sharpe[5], Thomas W. Okita[3], Diana Wimmer[1], Gerald E. Edwards[5], and Klaas J. van Wijk[2]

[1] Institute of Botany, Leibniz University, Herrenhaeuser Strasse 2, Hannover 30419, Germany

[2] Department of Plant Biology, Cornell University, 332 Emerson Hall, Ithaca, New York 14853, United States

[3] Institute of Biological Chemistry, Washington State University, 299 Clark Hall, Pullman, Washington 99164, United States

[4] Computational Biology Service Unit, Cornell University, 618 Rhodes Hall, Ithaca, New York 14853, United States

[5] School of Biological Science, Washington State University, 303 Heald Hall, Pullman, Washington 99164, United States

Type of authorship:	Co-author
Type of article:	Research article
Share of the work:	10 %
Contribution to the publication:	data analysis and assisted in writing parts of the paper
Journal:	Journal of Proteome Research
5-year impact factor:	4.173
Date of publication:	March 16th, 2015
Number of citations (google scholar on May 19th, 2017):	8
DOI:	10.1021/pr5011907
PubMed-ID:	25772754

Journal of proteome research

Article

pubs.acs.org/jpr

Developmental and Subcellular Organization of Single-Cell C_4 Photosynthesis in *Bienertia sinuspersici* Determined by Large-Scale Proteomics and cDNA Assembly from 454 DNA Sequencing

Sascha Offermann,*[,†] Giulia Friso,[‡] Kelly A. Doroshenk,[§] Qi Sun,[∥] Richard M. Sharpe,[⊥] Thomas W. Okita,[§] Diana Wimmer,[†] Gerald E. Edwards,[⊥] and Klaas J. van Wijk[‡]

[†]Institute of Botany, Leibniz University, Herrenhaeuser Strasse 2, Hannover 30419, Germany

[‡]Department of Plant Biology, Cornell University, 332 Emerson Hall, Ithaca, New York 14853, United States

[§]Institute of Biological Chemistry, Washington State University, 299 Clark Hall, Pullman, Washington 99164, United States

[∥]Computational Biology Service Unit, Cornell University, 618 Rhodes Hall, Ithaca, New York 14853, United States

[⊥]School of Biological Science, Washington State University, 303 Heald Hall, Pullman, Washington 99164, United States

Supporting Information

ABSTRACT: Kranz C_4 species strictly depend on separation of primary and secondary carbon fixation reactions in different cell types. In contrast, the single-cell C_4 (SCC_4) species *Bienertia sinuspersici* utilizes intracellular compartmentation including two physiologically and biochemically different chloroplast types; however, information on identity, localization, and induction of proteins required for this SCC_4 system is currently very limited. In this study, we determined the distribution of photosynthesis-related proteins and the induction of the C_4 system during development by label-free proteomics of subcellular fractions and leaves of different developmental stages. This was enabled by inferring a protein sequence database from 454 sequencing of *Bienertia* cDNAs. Large-scale proteome rearrangements were observed as C_4 photosynthesis developed during leaf maturation. The proteomes of the two chloroplasts are different with differential accumulation of linear and cyclic electron transport components, primary and secondary carbon fixation reactions, and a triose-phosphate shuttle that is shared between the two chloroplast types. This differential protein distribution pattern suggests the presence of a mRNA or protein-sorting mechanism for nuclear-encoded, chloroplast-targeted proteins in SCC_4 species. The combined information was used to provide a comprehensive model for NAD-ME type carbon fixation in SCC_4 species.

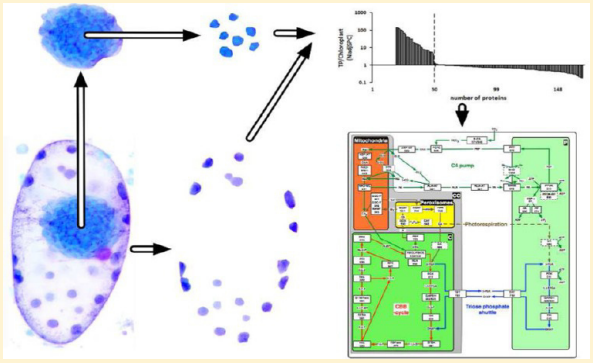

KEYWORDS: *single-cell C_4, photosynthesis, Bienertia sinuspersici, carbon-concentrating mechanism, proteomics, spectral counting, protein targeting, chloroplast development*

INTRODUCTION

The majority of plants performing C_4 photosynthesis utilize a CO_2 concentration mechanism that strictly depends on the close collaboration of two photosynthetic cell types (called Kranz anatomy). In the mesophyll cells (M) of these Kranz C_4 plants, a C_4 cycle captures atmospheric CO_2 with the formation of C_4 acids that are then decarboxylated in the adjacent bundle sheath (BS) cells. The released CO_2 is donated to the Calvin−Benson−Bassham (CBB) cycle, which leads to the synthesis of carbohydrates. Biochemically, C_4 plants are distinguished as belonging to the NAD-malic enzyme (NAD-ME), the NADP-malic enzyme (NADP-ME), or the phosphoenolpyruvate carboxykinase (PEP-CK) subtype based on the main type of decarboxylase utilized for the release of CO_2 in the BS. Species that have acquired a C_4 cycle have increased capacity for photosynthesis under conditions where CO_2 is most limiting (warm climates or limited availability of water).[1,2]

The discovery of terrestrial species performing C_4 photosynthesis within individual cells and without the need for the dual-cell, Kranz-type anatomy changed the view on the structural and biochemical requirements for C_4 photosynthesis. Single-cell C_4 (SCC_4) photosynthesis was first discovered in *Suaeda aralocaspica*,[3,4] and since then three more SCC_4 species in the genus *Bienertia* have been described in the Chenopodiaceae.[5−7] Independent evidence of a CO_2 concentrating mechanism (CCM) in these species was derived from ^{14}C-labeling experiments,[8,9] measurements of CO_2 compensation points and sensitivity of photosynthesis to O_2,[4,8,10] as well as analysis of carbon isotope composition of plant biomass.[3−7]

In contrast with Kranz-type C_4 photosynthesis, there is some evidence that SCC_4 photosynthesis uses internal subcellular

Received: November 18, 2014
Published: March 16, 2015

DOI: 10.1021/pr5011907
J. Proteome Res. 2015, 14, 2090−2108

compartmentalization to separate primary and secondary carbon fixation reactions. In the SCC_4 species *Bienertia cycloptera* and *B. sinuspersici* two different chloroplast types are located in a peripheral and a central compartment (CC) in chlorenchyma cells (illustrated in Figure 1A). Electron microscopy, immunolocalization studies, fluorescent probes specific for mitochondria, as well as in vivo localization studies indicate that mitochondria are restricted exclusively to the CC.[11−14] The central and peripheral compartments are connected by cytoplasmic channels (CPCs) (Figure 1A) that intersect the prominent central vacuole; it was proposed that this enables efficient metabolite exchange between the two compartments.[14] From immunolocalization studies of a few photosynthetic enzymes and assays on subcellular fractions from protoplasts, the following partial framework for SCC_4 carbon fixation has been developed. Atmospheric CO_2 is fixed into C_4 acids via phosphoenolpyruvate carboxylase (PEPC) in the peripheral compartment. C_4 acids produced in the peripheral compartment are believed to diffuse into the CC, where they can be decarboxylated by mitochondrial NAD-ME with the donation of CO_2 to Rubisco in the C chloroplasts. This is supported by studies showing selective localization of pyruvate, P_i dikinase (PPDK) that generates the substrate phosphoenolpyruvate (PEP) for PEPC in the peripheral chloroplasts (P), Rubisco in the central chloroplasts (C), and NAD-ME in mitochondria in the CC.[8] Additional evidence that these chloroplasts are specialized for function in C_4 photosynthesis came from studies with isolated intact P and C chloroplasts from *B. sinuspersici* (further referred to as *Bienertia* in the current study). The P chloroplasts show light-dependent conversion of pyruvate and inorganic phosphate (P_i) to PEP, indicating the function of PPDK, while only the C chloroplasts perform carbon fixation when provided inorganic carbon, indicating they have the CBB pathway.[15]

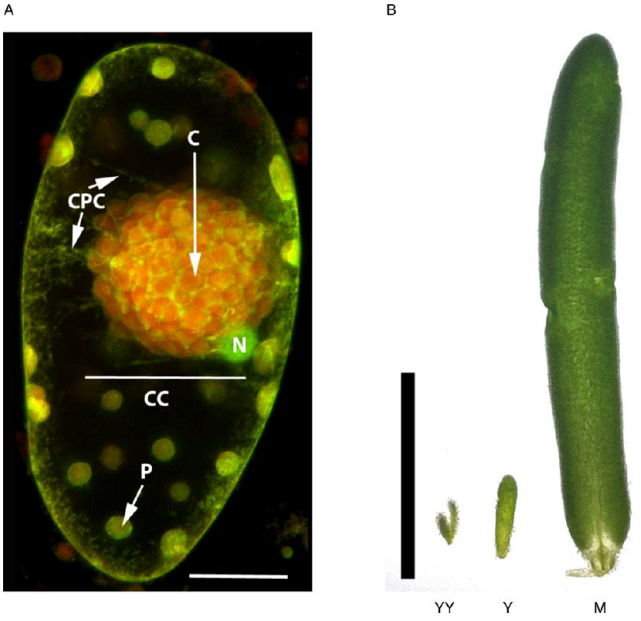

Figure 1. *Bienertia sinuspersici* cell and leaf morphology. (A) Confocal laser scanning micrograph of an acridine-orange-stained chlorenchyma cell. Peripheral chloroplasts (P) are embedded in a thin layer of cytosol and connected through cytoplasmic channels (CPCs) with the central compartment (CC) that hosts the central compartment chloroplasts (C). Acridine orange also stains the nucleus (N) green, which is typically localized close to the CC. Scale bar = 10 μm. (B) Size comparison of *Bienertia* leaves of the different developmental stages used for proteomic analysis. Youngest (YY, left), young (Y, middle), and mature (M, right) leaves. Scale bar = 1 cm.

As young leaves of *Bienertia* mature they develop a C_4 system through structural and biochemical changes. Chlorenchyma cells from very young *Bienertia* leaves (illustrated in Figure 1B) have not developed the two cytoplasmic domains;[13,14] the chloroplasts appear monomorphic and initially are thought to be in a C_3-like state.[8,14] As the cells mature, the two cytoplasmic domains develop with subcellular compartmentation of organelles and dimorphic chloroplasts for C_4 function.[13,16]

Questions about the development of C_4 photosynthesis and the proteins that are required for it to function can be addressed with systems biology approaches.[17] Large-scale proteome analysis of development of C_4 photosynthesis during leaf ontogeny and the functional differentiation of mesophyll and bundle sheath chloroplasts in mature leaves of a Kranz type C_4 have only been performed with maize, a NADP-malic enzyme type C_4 grass.[18−20] Analogous studies have not been made on NAD-ME-type grasses or eudicots.

Currently, the specific genes/proteins (enzymes and transporters) that were recruited for function of SCC_4 are not known. The objective of this study was therefore to identify specific proteins that support C_4 photosynthesis in this system by performing a proteomic analysis on subcellular fractions of mature cells. Additionally, the progression that occurs from young to mature leaves in the regulation of expression of proteins associated with the C_4 cycle, Calvin−Benson cycle, and photorespiration was analyzed. This study demonstrates that induction of the SCC_4 system involves large-scale proteome remodeling with an intricate pattern of differential protein distribution between the two chloroplast types. On the basis of proteome analysis, a scheme for intracellular function of C_4 photosynthesis in *Bienertia* is presented and includes light reactions, primary and secondary carbon fixation, as well as photorespiration.

MATERIALS AND METHODS

Plant Material and Growth Conditions

Bienertia sinuspersici plants were propagated and grown as described.[15]

2D-DIGE Analysis

For the 2D-DIGE analysis, mature *Bienertia* leaves were harvested and the two chloroplast types were prepared from protoplasts as previously described[15] in three independent biological replicates. (Each replicate consisted of sampling different individual plants on different days, followed by independent protein extraction and proteome analysis.) Chloroplasts were lysed in extraction buffer (0.1 M Tris-Cl pH 7.5, 0.1 M KCl, 1 mM EDTA, 10 μM leupeptin, 1 μM pepstatin, 1 mM PMSF, 1 mM DTT) and briefly sonicated (eight pulses with 30% power) with a model 300 V/T ultrasonicator equipped with a microtip horn (Biologics) under constant cooling on ice. Samples were centrifuged for 2 h at 4 °C at 16 000*g* to remove insoluble material. Proteins were extracted with phenol and precipitated overnight with three parts acetone at −20 °C. The protein pellet was resuspended in 2D lysis buffer (30 mM Tris-Cl pH 8.5, 7 M urea, 2 M thiourea, 4% (w/v) CHAPS) by vortexing and sonication (four times eight pulses with 30% power and cooling for 5 min between each cycle). Protein samples were centrifuged for 30 min at

DOI: 10.1021/pr5011907
J. Proteome Res. 2015, 14, 2090−2108

16 000*g*, and the concentration was measured using the RCDC assay (Biorad). A total of 50 μg protein from each of the two different chloroplast types was adjusted to 10 μL with lysis buffer and labeled with 100 pmol Cy3 or Cy5 CyDye minimal dyes (GE Healthcare) according to the manufacturer's instructions. The labeling reaction was terminated by the addition of an equal volume of 2× 2D lysis buffer and incubation for 10 min on ice. Differentially labeled protein samples were combined and carrier ampholytes (GE Healthcare; pH 6−11 and pH 3−10) were added to a final concentration of 0.5% each. The final volume was adjusted to 425 μL with sample buffer (8 M urea, 65 mM DTT, 4% (w/v) CHAPS). Insoluble material was removed by centrifugation (10 min, 16 000*g*). pH 3−10 nonlinear immobilized pH gradient (IPG) strips (24 cm, GE Healthcare) were reswelled overnight with DeStreak rehydration solution (GE Healthcare) according to the manufacturer's instructions, with appropriate carrier ampholytes added to 1%. Samples were focused on an Ettan IPGphor 3 System (GE Healthcare) using the following parameters: 500 V for 66 min; gradient to 1000 V for 66 min; gradient to 10 kV for 3.3 h; 10 kV until 50 000 Vh were reached. IPG strips were then run on 10−18% polyacrylamide (PAA) gradient gels as previously described.[21] 2D-DIGE gels were scanned using a FLA-5100 dual laser scanner with a Cy3/Cy5 dual emission filter (FUJI Medical, Stamford, CT) at 100 μm resolution. Cy3/Cy5 overlaid images were visualized using MultiGauge software (FUJI Medical). Spot density was analyzed using ImageJ,[22] and selected spots were excised and in-gel trypsin-digested (15 ng/μL Promega Trypsin Gold). Extracted tryptic peptides (5 μL) were loaded onto a Symmetry C18 trap column (180 μm × 20 mm, Waters Corporation) in a mixture of 0.1% formic acid in water (solvent A), followed by reverse-phase liquid chromatography (Waters nanoAcquity ultraperformance liquid chromatograph) using a BEH 130 C18 nanoAcquity column (75 μm × 200 mm, Waters Corporation). Solvents were changed according to the following sequence: 95% solvent A and 5% solvent B (0.1% formic acid in acetonitrile) for 1 min; increase in solvent B to 50% over the next 44 min; increase in solvent B to 90% over the next 5 min; held at 90% solvent B for 5 min, and return to 5% solvent B over the next 5 min. The flow rate was 400 nL/min. Peptides were sequenced using a Waters Q-Tof Premier quadrupole-time-of-flight mass spectrometer equipped with a nanospray ionization inlet in data-directed analysis (DDA) MS mode utilizing the following settings: 3.8 kV capillary voltage, 25 V cone voltage, 120 °C source temperature, 0.5 bar sheath gas pressure, 5 V collision energy, and 2150 V detector voltage. A mass range between 300 and 2000 Da and a scan time of 1s/scan were set for the MS survey. MS/MS spectra (limited to multiple positively charged ions producing a signal over 20 counts per second) were recorded over the range of 50−2000 Da at 2s/scan. Collision voltages were ramped between 15 and 55 V during the MS/MS scan. Peak list (pkl) files were generated using Protein Lynx Global Server (PLGS, Waters). Proteins were identified by searching the *Bienertia* transcriptome database generated by 454-sequencing (see the next section) containing 74 126 ESTs using the search engine Mascot (version 2.4, www.matrixscience.com) with the following settings: 1 missed cleavage allowed; fixed modification of cysteine carbamidomethylation; variable modification of methionine oxidation; 10 ppm peptide tolerance; and 0.1 Da MS/MS tolerance. Protein identifications were considered to be unambiguous if they had at least two peptide matches that meet or exceed the threshold values for the 95% confidence level.

Generation of Reference *Bienertia* Protein Sequence Database for Label-Free Mass-Spectroscopy-Based Identification and Quantification of the *Bienertia* Proteome

For generation of the *Bienertia* transcriptome, total RNA was isolated from 40 randomly pooled mature and young leaves using the TRIzol method (Invitrogen). Purified RNA was mixed in the ratio 1:3 (young/mature) and precipitated before shipping. mRNA isolation from total RNA and preparation of normalized cDNA was conducted by commercial service from Bio S&T (Montreal, Canada). The normalized cDNA was sequenced using a full run on a Roche 454 (FLX/titanium) instrument. Sequencing adaptors were removed using gsAssembler (Roche Life Sciences), followed by cleaning by LUCY[23] and SeqClean (http://sourceforge.net/projects/seqclean/) software, respectively. The resulting 149 835 reads (available under the accession number SRX85092 at the Sequence Read Archive (SRA), http://trace.ncbi.nlm.nih.gov) with more than 100 bp were assembled using iAssembler,[24] resulting in 74 126 ESTs. This transcriptome shotgun assembly project has been deposited at DDBJ/EMBL/GenBank under the accession GCEP00000000. The version described in this paper is the first version, GCEP01000000. A protein sequence database was created to search the mass spectral data. *Bienertia* ESTs were compared (using the basic local alignment search tool (BLAST)) to all predicted *Arabidopsis thaliana* (from here on *Arabidopsis*) proteins to obtain a training set to determine the codon usage matrix model. The most likely reading frames were determined using this codon usage model with the help of ESTscan.[25] These sequences were used to search the predicted proteomes of *Arabidopsis*, maize, and rice, and the best hits were used for annotation of the corresponding proteins. This resulted in 40 018 protein sequences of at least 50 amino acids in length. A contaminant set (Keratin, BSA, etc.) and a decoy database with the randomized protein sequences was added, resulting in a database named Bienertia_ProteinDB (80 411 sequences; 19 978 532 residues).

Sample Preparation for Quantification via Spectral Counting

For the developmental samples, 20 leaves of each developmental stage (youngest 0.3−1 mm, young 1−3 mm, and mature ∼2 cm long) were harvested for each replicate from different mature *Bienertia* plants. Leaves of the same developmental stage were pooled (separately for each biological replicate) and ground to a fine powder in liquid nitrogen. The frozen plant material was resuspended in extraction buffer (2% (w/v) SDS, 10% (w/v) glycerol, 62.5 mM Tris-HCl, pH 6.8, and 0.715 M 2-mercaptoethanol) and immediately boiled for 5 min. Insoluble material was removed by centrifugation (10 min, 16 000*g*) in a benchtop centrifuge. Protein concentration was determined with RCDC protein quantification kit (Bio-Rad), which tolerates detergents and reducing agents. For the localization samples, aliquots of protein extracts from the two chloroplast types, the central cytoplasmic compartment, and total protoplasts (TPs) that were prepared and characterized in a previous study were used. Tests with antibodies directed against chloroplast and nonchloroplast proteins showed that contamination of the isolated chloroplast preparations with cytosolic, mitochondrial, peroxisomal, and nuclear contaminations was very low (<3−5%) or even undetectable in most cases.[15] Total protein extracts (50 μg each) from the four

DOI: 10.1021/pr5011907
J. Proteome Res. 2015, 14, 2090−2108

different localization samples and the three different developmental samples were separated on Novex Tricine 10−20% PAA gels (Invitrogen). Individual gel lanes were cut into 10 (localization series) or 8 (developmental series) slices, and proteins were digested with trypsin. Extracted peptides were analyzed by nano LC−LTQ−Orbitrap MS using data-dependent acquisition and dynamic exclusion, essentially as previously described.[26] Peptide extracts were loaded on a guard column (LC Packings; MGU-30-C18PM), followed by separation on a PepMap C18 reverse-phase nano column (LC Packings nan75-15-03-C18PM), using 120 min gradients with 95% water, 5% acetonitrile (ACN), and 0.1% FA (solvent A) and 95% ACN, 5% water, and 0.1% FA (solvent B) at a flow rate of 200 nL/min. Each sample injection and analysis was followed by two blank injections to prevent carry over. The acquisition cycle consisted of a survey FTMS scan at the highest resolving power (100 000), followed by five data-dependent MS/MS scans acquired in the LTQ. Dynamic exclusion was used with the following parameters: exclusion size, 500; repeat count, 2; repeat duration, 30 s; exclusion time, 180 s; exclusion window, ±6 ppm. Target values were set at 5×10^5 and 3×10^4 for the survey and tandem MS scans, respectively, and the maximum ion accumulation times were set at 200 ms in both cases. Experiments were performed in two biological replicates with independent material sampling, protein and peptide extraction, and mass spectroscopy.

Processing of the MS Data, Database Searches, and Public Access

Peak lists (.mgf format) were generated using DTA supercharge (version 1.19) software (http://msquant.sourceforge.net/) and searched with Mascot version 2.2 (Matrix Science) against the generated Bienertia_ProteinDB (see above) database. For off-line calibration, first a preliminary search was conducted with the precursor tolerance window set at 30 ppm. Peptides with ion scores above 40 (this minimum threshold ensures that only matched spectra with low false-positive rate ($p < 0.01$) are used) were chosen as benchmarks to determine the offset for each LC−MS/MS run. This offset was then applied to adjust precursor masses in the peak lists of the respective .mgf file for recalibration (Friso et al. 2011).[27] The recalibrated peak lists were searched against the Bienertia_ProteinDB. Each of the peak lists were searched using Mascot version 2.2 (protein significance $p < 0.01$) for full tryptic peptides using a precursor ion tolerance window set at 6 ppm, variable Met oxidation, fixed Cys carbamidomethylation, and 1 miss cleavage allowed and for semitryptic peptides using a precursor ion tolerance window set at 3 ppm, variable Met oxidation, fixed Cys carbamidomethylation, glutamine to pyro-glutamic acid (N-term Q) modification, 1 miss cleavage allowed, and a minimal mascot ion score threshold of 30. This yielded a peptide false discovery rate below 1%, with peptide false-positive rate calculated as 2 (decoy_hits/total_hits). The false protein identification rate of protein identified with two or more peptides was zero. The Mascot search results were further filtered as follows to reduce the false protein identification rate of proteins identified by one peptide: ion score threshold was increased to 40 for one peptide identification, and mass accuracy on the precursor ion was required to be within 3 ppm. Precursor ion masses below 700 D were discarded. The mass spectrometry proteomics data have been deposited to the ProteomeXchange Consortium (http://www.proteomexchange.org/) via the PRIDE (http://www.ebi.ac.uk/pride/archive/) partner repository with the data set identifier PXD001910 and 10.6019/PXD001910.

Calculation of adjSPC, NadjSPC, Relative Abundance and Protein Ratios, and Grouping of Proteins with a High Percentage of Shared Matched Spectra

For protein quantification, spectral counts (SPC) were adjusted for the number of unique peptides versus shared peptides between similar proteins resulting in an adjusted spectral count (adjSPC), as described in detail in Friso et al.[18] Proteins that shared more than ∼80% of their matched adjusted peptides with other proteins were grouped using a similarity matrix, as described in Friso et al.[18] Normalized adjusted spectral counts (NadjSPC) used for the calculation of C/P as well as CC/TP ratios were calculated from adjSPC through division by the sum of all adjSPC in the corresponding sample, as defined in Friso et al.[27] To differentiate between nonchloroplast and bona fide chloroplast proteins as well as for identification of proteins that accumulate differentially between the C and P chloroplasts, we analyzed spectral count data using the beta-binomial test[28] in the statistical software package "R"[29] with the script provided by the authors. Tests were performed on adjSPC values because the beta-binomial test naturally normalized for the total number of spectral counts in each sample. The beta-binomial test accounts for within and between sample variation in a single statistical model.[30] To further increase the robustness of the statistical analysis, all p values from the beta-binomial test were corrected for multiple hypothesis testing using a graphically sharpened Benjamini and Hochberg procedure.[31] Adjusted p values (also known as q values) <0.1 were interpreted with indication for enrichment or significantly enriched (<0.05). Comparison of the quantitative results obtained by spectral counting to independent 2D-DIGE analysis as well as previous Western analysis on a few proteins[15] provided further confidence in the spectral count analysis for the SCC_4 system. For comparison of transit peptide features, we performed Student's t test either on the direct data or in the case of index data after transformation to the arcsine.

RESULTS

Because no comprehensive genome or transcriptome information for *Bienertia* or any closely related species was publicly available, a reference *Bienertia* transcriptome was generated using a mixture of RNA isolated from the youngest (representing the C_3-like stage) and mature (representing the fully developed C_4 stage) leaves to aid identification and quantification of proteins from leaves of different developmental stages. 454-cDNA sequencing yielded ∼600 000 reads, which were then assembled into 150 000 ESTs. From this, a total of 40 000 protein sequences with length of >50 amino acids were generated. (For details of the sequencing and assembly strategy, see the Materials and Methods.) This protein database was used to search tandem MS (MS/MS) data from proteomes of the four different localization samples (C, P, CC, and TP) ("localization series") and the total leaf extracts of the three different developmental stages (YY, Y, M) ("developmental series"). This resulted in 1497 identified proteins. Detailed information including assigned protein identification numbers, total adjusted spectral counts (adjSPC) as a measure of protein abundance, identified peptides, and information on the corresponding *Arabidopsis* (At) and *Zea mays* (Zm) homologues are available in Suppl. Table 1 in the SI.

DOI: 10.1021/pr5011907
J. Proteome Res. 2015, 14, 2090−2108

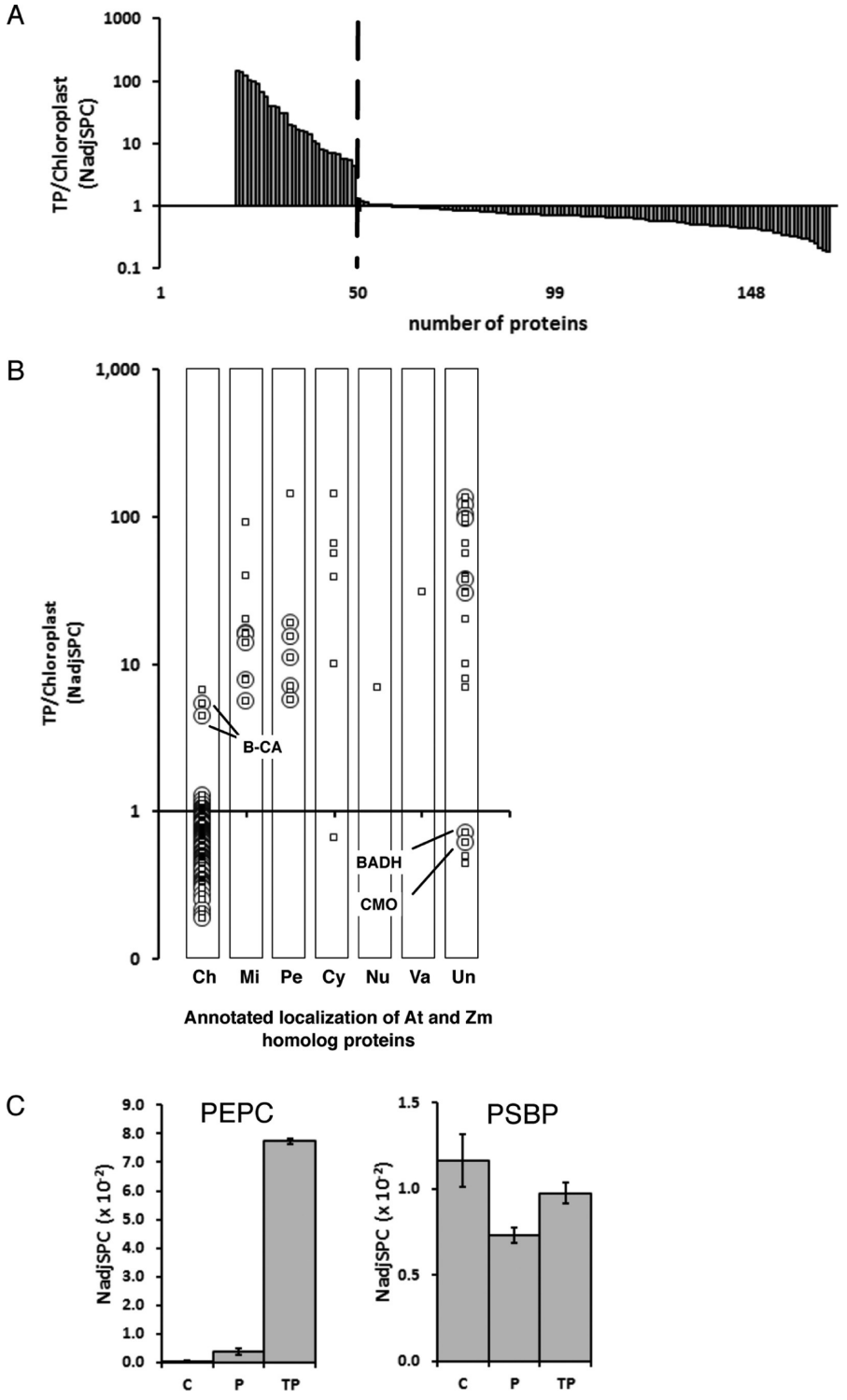

Figure 2. Determination of protein subcellular localization in *Bienertia* chlorenchyma cells. (A) Average TP/chloroplast ratios sorted by decreasing ratios. Proteins on the left from the dashed line are significantly enriched ($q < 0.05$) in TP over chloroplast fractions. (See also Suppl. Table 2 in the SI.) (B) Comparison of *Bienertia* TP/chloroplast ratios with subcellular localization in *Arabidopsis* (squares) and maize (circles). The horizontal line indicates a TP/chloroplast ratio of one. B-CA, beta-carbonic anhydrase; BADH, betaine aldehyde dehydrogenase; CMO, choline monoxygenase; Ch, chloroplast; Mi, mitochondria; Pe, peroxisomes; Cy, cytoplasm; Nu, nucleus; Va, vacuole; Un, unknown subcellular localization. (C) Example of a protein accumulation profile of a nonchloroplast protein (phosphoenolpyruvate carboxylase, PEPC) compared with a chloroplast localized protein (P-subunit of photosystem II, PSBP). Error bars indicate standard error of the mean (SEM) of two independent biological replicates.

To study abundances of individual proteins across subcellular fractions and leaf developmental stages, we applied a stringent minimum threshold of >14 adjSPC in each of the biological replicates of a localization or developmental sample. This resulted in 179 quantified proteins in the localization series and 163 quantified proteins in the developmental series; these represented the majority of the detected protein mass (77 and 63%, respectively), as calculated from normalized adjSPC

DOI: 10.1021/pr5011907
J. Proteome Res. 2015, 14, 2090−2108

ID	Name	protein abundance ratio Bs C/P	Bs q	Zm BS/M	relative mass distribution (%) per protein C	per protein P	total for BIN C	total for BIN P	total for category C	total for category P
Carbon fixation										
CBB-RBC		**2.5**		**3.9**						
558	RBCL	2.8	0.030	2.3	11.4	4.3				
451	RBCS-4/1	2.5	0.068	3.9	0.4	0.2				
559	RBCS-4/2	3.4	0.030	3.2	4.2	1.2	18.8	8.3		
562	RCA/1	1.8	0.066	4.3	2.0	1.2				
397	RCA/2	0.6	0.208	4.3	0.9	1.4				
CBB-regenerative		**1.5**		**3.9**						
771	FBPA	1.4	0.463	4.6	0.4	0.3				
561	SFBA2	4.9	0.003	3.9	3.0	0.6				
570	PRK2	1.4	0.084	4.2	0.7	0.5				
535	RPI	1.7	0.116		0.6	0.4	7.0	3.4		
567	RPE	2.0	0.066	4.3	0.3	0.2				
564	SBPase	1.6	0.030	3.0	0.7	0.5				
563	TKL1/1	1.4	0.281	3.0	0.6	0.4				
229	TKL1/3	1.5	0.156	3.0	0.7	0.5				
CBB-reductive		**0.8**		**1.0**						
560	GAPDH A	1.3	0.420	1.4	2.7	2.1				
651	GAPDH B	1.0	0.686	0.5	0.8	0.8	5.8	7.2		
511	PGK2	0.6	0.161	2.0	1.9	3.6				
515	TPI1	0.5	0.030	0.6	0.3	0.7				
Photorespiration										
773	PGP1	2.0	0.172	2.8	0.3	0.1	0.3	0.1		
Starch										
772	SS	2.3	0.068	4.4	0.4	0.2	0.4	0.2		
C4		**0.5**		**0.6**						
506	AK	0.5	0.030	0.2	0.4	0.7				
574	PP	0.6	0.109	0.7	0.3	0.5				
399	PPDK/1	0.3	0.067	0.6	0.3	1.1	8.6	19.3		
510	PPDK/2	0.3	0.003	0.6	4.4	13.2				
512	PPDK/3	0.9	0.068	0.6	3.3	3.9				
Envelope transporter		**0.6**		**0.1**						
505	MEP2	0.4	0.100	0.1	0.2	0.5				
676	PPT	0.6	0.381	0.1	0.2	0.4	0.8	1.7		
732	TPT	0.6	0.294	0.6	0.1	0.2				
526	BASS	0.4	0.030		0.2	0.6				
Metabolism/other										
OPP										
708	G6PI	0.1	0.025	1.7	0.0	0.2	0.0	0.2		
AA-meta.		**0.7**		**0.4**						
197	cysteine synthase	0.7	0.348	0.5	0.2	0.3	0.2	0.3		
30	ketol-acid reductoisomerase	0.7	0.313	0.4	0.1	0.2				
Lipids										
196	MOD1	0.4	0.034	0.4	0.1	0.2	0.1	0.2		
N-meta		**0.6**		**1.0**						
518	GS2	0.7	0.118	1.3	0.2	0.3				
519	NiR	0.6	0.100	0.2	0.2	0.4	1.2	2.0		
514	Fd-GOGAT 1/1	0.7	0.030	1.0	0.7	1.1				
699	Fd-GOGAT 1/2	0.3	0.100	1.0	0.1	0.2				
Secondary meta.		**1.1**								
527	BADH	1.2	0.569		0.4	0.4	0.7	0.6		
622	CMO	1.0	0.652		0.3	0.3				
Tetrapyrrole										
475	GSA 2	0.8	0.192	1.1	0.3	0.4	0.3	0.4		
Redox		**1.1**		**0.5**						
565	Prx A	0.9	0.274	0.7	0.5	0.6				
648	FSD2	1.4	0.281		0.2	0.2				
195	MDHAR	0.6	0.068	0.2	0.1	0.3	1.7	1.6		
29	PrxII E	0.8	0.307	0.8	0.2	0.2				
522	Prx Q	1.7	0.100	0.4	0.2	0.1				
612	TL29	2.1	0.030	0.5	0.5	0.3				
DNA, RNA, cell cycle and signalling		**1.2**		**1.6**						
484	CP31B	1.1	0.627		0.2	0.2				
499	FBN4	1.2	0.533	1.1	0.2	0.2				
566	HIP1.3	1.2	0.246	2.5	0.5	0.4	1.7	1.6		
496	CSP41A	1.0	0.579	2.1	0.3	0.3				
556	pTAC16	1.2	0.534	0.5	0.5	0.4				
Misc./Unknown		1.0		0.6						
516	ketone reductase (AOR)	0.8	0.156	3.2	0.3	0.4				
553	Flavin-reductase related 1	1.2	0.583	0.6	0.2	0.2				
613	thylakoid lumen 18.3 kDa	1.2	0.534	0.6	0.3	0.2	1.4	1.5		
605	unknown protein/1	0.7	0.118	1.3	0.2	0.3				
568	unknown protein/3	0.9	0.359	0.4	0.2	0.2				
824	unknown protein/2	1.2	0.381	0.5	0.2	0.2				
41.7	40.2									
7.3	8.3									

ID	Name	protein abundance ratio Bs C/P	Bs q	Zm BS/M	relative mass distribution (%) per protein C	per protein P	total for BIN C	total for BIN P	total for category C	total for category P
Light reactions										
PSII		**1.5**		**0.7**						
656	LHCII2.3	1.3	0.337	0.8	0.9	0.8				
595	LHCII3	1.6	0.284	0.8	0.2	0.1				
591	LHCII4.1	1.5	0.030	0.7	1.5	1.1				
833	LHCII4.2	1.1	0.418	0.7	0.5	0.4				
655	LHCII5	1.6	0.030	0.7	1.8	1.2				
658	LHCII6	1.1	0.499	0.8	0.3	0.3				
653	psbB	1.5	0.041	0.7	3.5	2.4				
590	psbC	1.4	0.046	0.9	4.9	3.7	20.2	14.5		
610	psbO	1.3	0.420	0.5	1.1	0.9				
609	psbP	1.6	0.084	0.5	1.5	1.0				
611	psbQ	1.2	0.281	0.4	0.6	0.5				
659	psbR	0.4	0.172	0.1	0.1	0.3				
593	psbS	1.5	0.299	0.3	0.5	0.4				
654	LHCII1.3/1	1.8	0.030	0.7	2.2	1.2				
657	LHCII1.3/2	1.9	0.264	0.7	0.5	0.3				
cytb6f		**1.2**		**0.9**						
601	petA	1.2	0.497	1.3	0.6	0.5	0.8	0.7		
489	petC	1.2	0.574	0.6	0.2	0.2				
PSI		**1.1**		**1.3**						
596	LHCI1.1	1.2	0.441	1.3	0.2	0.2				
594	LHCI2.1	3.5	0.067	1.5	0.3	0.1				
599	LHCI3	1.1	0.483	1.2	1.7	1.6				
592	LHCI4	1.2	0.499	1.1	0.6	0.5				
837	LHCI5	0.8	0.420	2.1	0.1	0.2				
836	psaA	1.0	0.621	1.5	0.3	0.3	7.6	7.4		
598	psaB	0.9	0.517	1.3	1.9	2.2				
615	psaD1	1.3	0.381	1.5	0.6	0.5				
600	psaF	0.9	0.517	1.2	1.0	1.1				
603	psaH	1.2	0.314	1.1	0.5	0.4				
604	psaL	1.0	0.655	1.3	0.4	0.4				
FNR										
616	FNR1	1.7	0.192	0.4	0.5	0.3	0.5	0.3		
ATPsynthase		**0.8**		**1.2**						
618	CF1a	0.8	0.067	1.2	4.5	5.8				
525	CF1b	0.6	0.030	1.1	5.8	9.7				
617	CF1d	1.2	0.299	1.3	0.4	0.4	11.4	16.6		
619	CF1y	0.8	0.246	1.5	0.4	0.5				
488	CFOII	0.9	0.625	1.0	0.2	0.2				
NDH		**0.7**		**2.4**						
508	NDF1	0.7	0.208	3.3	0.2	0.2				
507	NDF2	0.9	0.420	2.8	0.2	0.3				
584	NDH H	0.7	0.080	2.1	0.5	0.7				
614	NDH L	0.6	0.077	1.9	0.1	0.2	1.6	2.4		
586	NDH N	0.8	0.323	2.1	0.2	0.2				
456	NDH CRR31	1.0	0.621	3.9	0.3	0.3				
719	NDH CRRl	0.5	0.030	2.6	0.2	0.4				
722	PsbQ-like2	0.6	0.208	1.8	0.1	0.2				
Protein										
Protein assembly										
501	HCF136	1.0	0.621	0.7	0.3	0.3	0.3	0.3		
Protein degradation		**1.2**		**1.1**						
573	ClpC1	1.2	0.371	1.1	0.9	0.7				
452	ClpP4	1.2	0.441	1.4	0.2	0.2				
602	FtsH2	1.2	0.317	1.0	0.8	0.7	3.0	2.7		
500	FtsH5	1.0	0.696	1.1	0.7	0.7				
576	glycyl aminopeptidase	1.7	0.314	2.0	0.2	0.2				
28	LAP2	0.8	0.409	0.4	0.2	0.2				
Protein folding		**0.7**		**1.0**						
433	cpHSP90	1.4	0.308	1.6	0.3	0.2				
390	Cpn21	0.7	0.381	1.4	0.2	0.3				
454	Cpn60A1	0.7	0.280	0.7	0.8	1.1				
457	TLP21	0.7	0.121	1.4	0.2	0.3				
575	CYP20-3	1.1	0.686	0.1	0.2	0.2	3.4	4.5		
231	Cpn60B2/1	0.7	0.118	1.0	0.7	1.1				
389	cpHSP70-2/1	0.7	0.257	0.6	0.4	0.6				
434	Cpn60B2/2	0.9	0.470	1.0	0.2	0.2				
517	cpHSP70-2/2	1.0	0.534	0.6	0.4	0.5				
Protein synthesis		**0.8**		**0.7**						
513	EF-Tu-1	0.7	0.149	0.6	0.6	0.9				
485	EF-G	1.9	0.100	0.8	0.5	0.3	1.4	1.5		
504	PSRP7	0.8	0.483		0.3	0.3				
Protein targeting		**1.2**		**0.2**						
774	cpSecA	2.1	0.192	0.0	0.3	0.1				
679	TOC75-III	0.7	0.204		0.1	0.2	0.6	0.5		
554	TF1	1.2	0.509	0.3	0.2	0.2				
42.1	41.9									
8.7	9.5									

Figure 3. Differential protein accumulation in dimorphic chloroplasts of *Bienertia*. Abundance ratios and relative mass distribution of C and P enriched chloroplast proteins in *Bienertia sinuspersici* (Bs) determined from spectral counting and comparison with the bundle sheath/mesophyll (BS/M) ratios of the corresponding *Zea mays* (Zm) homologues (data taken from Friso, 2010).[18] Abundance ratios are color-coded with C and BS accumulating proteins shown in magenta and P and M accumulating proteins shown in cyan. *q* values correspond to *p* values from the beta-binomial test from two independent biological replicates, corrected for multiple hypothesis testing. Bold numbers indicate median values for individual BINs. Values for relative mass distribution are color-coded with highly abundant proteins shown in green and other proteins in yellow. See Suppl. Table 2 in the SI for full protein names.

DOI: 10.1021/pr5011907
J. Proteome Res. 2015, 14, 2090−2108

(NadjSPC). (See the Materials and Methods.) A full list of quantified proteins with associated information can be found in Suppl. Table 2 in the SI for the localization series and in Suppl. Table 6 in the SI for the developmental series.

Determination of Chloroplast Localized Proteins

For the analysis of differential protein accumulation between the two different chloroplast types, it is important to first distinguish between true chloroplast proteins and potential contamination of the chloroplast fractions from the cytoplasm or other subcellular locations. Chloroplast localization was determined based on the abundance ratio (calculated from NadjSPC) between proteins in the isolated chloroplasts and TP fractions (Figure 2A). Proteins with TP/chloroplast ratios below ~1 (120) were considered to be potential candidates for bona fide chloroplast proteins. Indeed, comparison with annotated subcellular localizations of the corresponding *Arabidopsis* and maize homologues (Figure 2B) indicated *Bienertia* proteins with low TP/chloroplast ratios corresponded to *Arabidopsis* and maize chloroplast-localized proteins. (See the Plant Proteome Database, PPDB, http://ppdb.tc.cornell.edu/.) In contrast, *Arabidopsis* and maize homologues of *Bienertia* proteins with high TP/chloroplast abundance ratios are located in mitochondria, peroxisomes, the cytoplasm, the nucleus, and the vacuole, or they had unknown subcellular localization. (Also see Supplemental Text 1 in the SI for the discussion of specific examples marked in the Figure.) Figure 2C shows an example of a typical cytosolic protein (PEPC) with a very high TP/chloroplast abundance ratio and in contrast the P-subunit of photosystem II (PSBP) as a bona fide chloroplast protein showing a much lower ratio.

Differential Protein Accumulation between Dimorphic Chloroplasts

We determined the functional distribution of the identified chloroplast proteins between the P and C chloroplasts in *Bienertia* and calculated C/P protein abundance ratios for each protein based on NadjSPC (Figure 3 and additional information in Suppl. Table 3 in the SI). Proteins were grouped into four major functional categories (carbon fixation, light reactions, metabolism, and protein processing) and further subdivided using an updated MapMan BIN system. (See ref 32.) The distribution of the proteins in these functional groups between the two types of chloroplasts in *Bienertia*, which has NAD-ME-type C_4, is compared with previously published data on bundle sheath (BS) versus mesophyll (M) cell protein distribution in the Kranz NADP-ME type plant maize (BS/M column in Figure 3 and Suppl. Table 3 in the SI) (data taken from Friso et al.).[18] Furthermore, to distinguish between low and high abundant proteins and to get a better understanding of the large-scale distribution of functions, we calculated the relative mass distribution per BIN and each of the four major functional categories (Figure 3).

In *Bienertia* almost all proteins of the carboxylation (CBB-RBC) and regenerative (CBB-regenerative) phase of the CBB cycle were more abundant in C chloroplasts. Rubisco activase (RCA) was an exception with one form being more abundant in C chloroplasts (ID562), whereas the other form (ID397) was more abundant in P chloroplasts. In contrast, proteins associated with the reductive phase of the CBB (CBB-reductive) were either about equally abundant in the two chloroplast types (α,β subunits of glyceraldehyde phosphate dehydrogenase (GAPDH, ID560, ID651)) or enriched in P chloroplasts (phosphoglycerate kinase (PGK), ID511; triose-phosphate isomerase (TPI), ID515). Besides CBB enzymes, the C chloroplasts had higher levels of starch synthase (SS, ID772) as well as phosphoglycolate phosphatase (PGP, ID773). The latter is one of the two chloroplast-localized proteins of the photorespiratory cycle (the second, glycerate kinase, was below the quantification threshold). Chloroplast enzymes involved in the C_4 cycle were generally more abundant in P chloroplasts. PPDK was quantified in three forms (ID399, ID510, ID512), and the most abundant one (ID510) was strongly associated with the P chloroplasts along with adenylate kinase (AK, ID506) and inorganic pyrophosphatase (PP, ID574), all of which are involved in regenerating PEP from pyruvate. Four chloroplast envelope transporters were quantified, and all were more abundant in P chloroplasts. The highest enrichment in the P chloroplasts was observed for the sodium-dependent pyruvate transporter (BASS,[33] ID526) and mesophyll envelope protein 2 (MEP2, ID505), a transporter with currently unknown substrate specificity. Also, the phosphate/PEP translocator (PPT, ID676) and the triose-phosphate translocator (TPT, ID732) were 67% enriched in P chloroplasts.

In comparing these results for *Bienertia* (C versus P) to maize (BS versus M), a similar distribution of proteins involved in carbon fixation in the CBB pathway was generally observed. They indicate preferential localization of proteins of the CBB-RBC and CBB-regenerative phase in the C chloroplasts of *Bienertia* and the BS chloroplasts of maize based on the high C/P and BS/M values, respectively. The median C/P values for CBB-RBC and CBB-regenerative phase were higher for the homologues in maize (BS/M ratio of 3.9 for both categories) than in *Bienertia* (2.5 and 1.5, respectively), although specific values for some homologues were similar or even higher in *Bienertia* (e.g., RBCL, RBCS, and SFBA2). The median values for the regenerative phase of the CBB-reductive phase were very similar for *Bienertia* and maize (0.8 and 1.0, respectively), indicating an equal distribution of this phase between the two types of chloroplasts. Proteins supporting the regeneration phase of the C_4 pathway (synthesis of PEP for PEPC) were more abundant in the P chloroplasts in *Bienertia* and M chloroplasts in maize.

Overall, in *Bienertia* the C chloroplasts invested more than 2 times more protein mass (~26% of the total quantified chloroplast protein mass) than P chloroplasts (~12%) in the carboxylation and the regenerative phase of the CBB, whereas protein investment in the reductive phase was ~24% higher in P chloroplasts. This was counterbalanced by an increased investment in C_4 cycle enzymes in P (~19%) over C chloroplasts (~9%). Interestingly, this reverse investment in CBB versus C_4 cycle proteins resulted in an almost equal overall investment of the two chloroplast types in carbon-fixation-related proteins (~42% in C versus ~40% in P).

Differences between C and P chloroplasts were also observed in the distribution of thylakoid proteins involved in the light reactions. Most photosystem II (PSII) proteins were more abundant in C than P chloroplasts, with a median C/P accumulation ratio of 1.5 for the 15 quantified subunits. In contrast, the two quantified subunits of the cytochrome *b6f* complex and the 11 subunits of photosystem I (PSI)-related proteins did not show a clear chloroplast-type-specific accumulation (median C/P 1.2 and 1.1, respectively). Four out of five subunits of the ATP synthase complex were slightly enriched in P chloroplasts (median C/P 0.8), similar to proteins associated with the NADH dehydrogenase (NDH) complex involved in cyclic electron flow (median C/P 0.7). C

DOI: 10.1021/pr5011907
J. Proteome Res. 2015, 14, 2090−2108

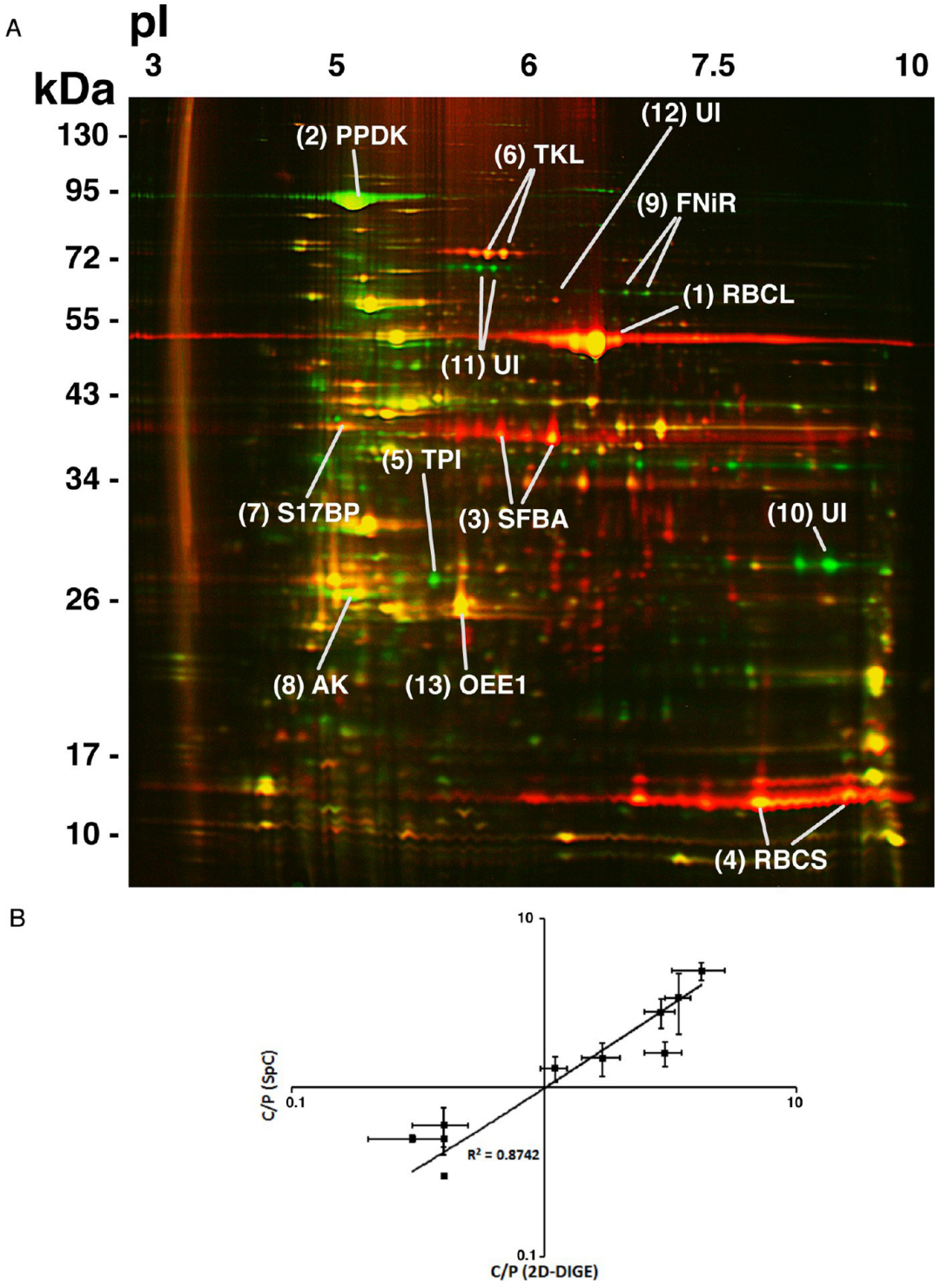

Figure 4. 2D-DIGE analysis of stromal chloroplast proteins in peripheral and central chloroplasts of *Bienertia*. (A) Proteins from C and P chloroplasts were isolated and differentially labeled with Cy3 and Cy5 dyes, respectively, and separated on broad range isoelectric gradient (pH 3–10) in the first dimension and by molecular weight in the second dimension. Differentially accumulating proteins are shown in red (C) or green (P), whereas equally abundant proteins are shown in yellow. AK, adenylate kinase; FNiR, ferredoxin nitrate reductase; OEE1, oxygen- evolving enhancer protein 1; PPDK, pyruvate P_i-dikinase; RBCL, ribulose bisphosphate carboxylase/oxygenase large subunit; RBCS, ribulose bisphosphate carboxylase/oxygenase small subunit; S17BP, sedoheptulose-1,7-bisphosphatase; SFBA, sedoheptulose/fructose bisphosphate aldolase; TKL, transketolase; TPI, triosephosphate isomerase; UI, unidentified. (B) Comparison of C/P ratios obtained from 2D-DIGE and spectral counting (SpC) experiments for 10 proteins. (For details see Supplemental Table 4 in the Supporting Information.) Error bars indicate standard error of the mean (SEM) of three (2D-DIGE) or two (spectral counting) biological replicates. *X* -and *Y*-axis intercept at the coordinates 1,1.

chloroplasts invested more protein mass in PSII proteins (~20%) than P chloroplasts (~15%), whereas P chloroplasts showed increased investment of ATP synthase and NDH complex proteins (combined ~19%) over C chloroplasts (combined ~13%). As observed for carbon fixation proteins, this resulted in similar overall investment in light reaction

DOI: 10.1021/pr5011907
J. Proteome Res. 2015, 14, 2090–2108

Table 1. List of CC Enriched Nonchloroplast Localized Proteins Determined from Spectral Counting and the Localization of Their Closest Arabidopsis and Maize Homologs[a]

ID	CC/C	CC/C q value	TP/CC	TP/CC q value	At annotation	loc. At	loc. Zm
738	only CC	0.002	0.17	0.045	mitochondrial ADP, ATP carrier protein (AAC3)	M	M
214	only CC	0.001	0.34	0.019	voltage-dependent ion channel VDAC1	M	M
481	only CC	0.001	0.35	0.065	glycine decarboxylase/glycine cleavage system P-protein (ATGLDP1)	M	M
213	only CC	0.001	0.40	0.046	heat shock protein mtHsc70−2 (Hsc70−5)	M	M
13	11.64	0.000	0.43	0.008	phosphate transporter (PHT3−1 or PIC1)	M	M
645	only CC	0.001	0.43	0.023	voltage-dependent ion channel VDAC1	M	M
394	only CC	0.001	0.46	0.066	Cpn60/HSP60	M	M
22	only CC	0.001	0.48	0.051	prohibitin, putative	M	n.Pl
623	40.64	0.001	0.49	0.046	dicarboxylate carrier (DIC1)	M	X
624	15.89	0.005	0.53	0.023	uncoupling mitochondrial protein (PUMP or UCP1)	M	X
546	only CC	0.002	0.55	0.107	glycine cleavage T-protein	X	n.Pl
543	23.44	0.001	0.56	0.030	malate dehydrogenase [NAD]	M	M
18	only CC	0.001	0.60	0.071	mitochondrial ADP, ATP carrier protein 2 (ACC2)	M	M
541	7.47	0.001	0.62	0.013	malate oxidoreductase, NAD-ME2	M	M
15	only CC	0.003	0.63	0.260	aldehyde dehydrogenase (ALDH2)	M	M
14	only CC	0.001	0.69	0.115	atp1 ATPase subunit 1	M	M
644	only CC	0.001	0.71	0.089	oxoglutarate/malate translocator (DTC)	M	M
212	20.99	0.002	0.74	0.227	H+-transporting ATP synthase beta chain	M	M
545	only CC	0.004	0.74	0.404	glycine/serine hydroxymethyltransferase; serine/threonine aldolase (SHM1)	M	n.Pl
542	17.00	0.001	0.77	0.214	putative aspartate aminotransferase Asp1	M	M
742	only CC	0.001	0.83	0.320	hydroxypyruvate reductase 1 (HPR1)	P	P
646	4.96	0.003	0.89	0.500	catalase 2 (CAT2)	P	P
551	3.43	0.004	1.03	0.404	alanine aminotransferase-2	P	P
741	11.51	0.011	1.09	0.320	alanine-glyoxylate aminotransferase (AGT1)	P	P
550	3.64	0.001	1.12	0.404	glycolate oxidase-1 (GOX-1)	P	P
445	4.75	0.006	1.16	0.231	malate dehydrogenase (PMDH2)	P	P
2	only CC	0.001	1.80	0.144	LOX1 lipoxygenase	X	X
529	only CC	0.001	3.42	0.009	ALAAT2 alanine transaminase	n.Pl	X
536	70.55	0.002	5.06	0.001	phosphoenolpyruvate carboxylase, putative (PPC2)	X	C
478	only CC	0.001	5.15	0.001	5-methyltetrahydropteroyltriglutamate S-methyltransferase (ATCIMS)	C	X
549	only CC	0.003	6.57	0.002	aspartate aminotransferase, cytoplasmic isozyme 1	C	P

[a] q values represent the p values from the beta-binomial test corrected for multiple hypothesis testing. M = mitochondria, P = peroxisomes, C = cytosol, n.Pl = not plastid, X = unknown localization.

proteins across the two chloroplast types (~42% each). Thus, the distribution of enzymes between the two chloroplast types for light reaction proteins was different for *Bienertia* and maize. Whereas PSII proteins and FNR were enriched in the C chloroplasts of *Bienertia*, they were enriched in the M chloroplasts of maize. NDH was enriched in P chloroplasts in *Bienertia*, while there was selective accumulation in the BS chloroplasts of maize.

As expected, the majority of the quantified protein mass in chloroplasts of *Bienertia* (82−84%) was attributed to photosynthesis-related processes; however, 50 proteins involved in other functions were quantified and some showed differential accumulation. For example, the median C/P ratio for four proteins associated with nitrogen assimilation (nitrite reductase, ID519; glutamate-ammonia ligase, ID518; and Fd-dependent glutamate synthase, ID514, ID699) was 0.6, indicating an enrichment in P chloroplasts. Also enriched in P chloroplasts were glucose-6-phosphate isomerase (G6PI, ID708) associated with the oxidative pentose phosphate pathway, enolyl-ACP reductase (MOD1, ID196) involved in fatty acid synthesis, and monodehydroascorbate reductase (MDHAR, ID195) involved in eliminating reactive oxygen species. In contrast, peroxiredoxin Q (PrxQ, ID522), which belongs to a group of ubiquitous thiol-dependent peroxidases capable of reducing a broad range of toxic peroxides and peroxinitrites, was enriched in C chloroplasts. Also, PSII-associated thylakoid lumen protein 29 (TL29,[34] ID612) as well as the plastid elongation factor G (EF-G) were enriched in C chloroplasts. This indicates that differences in the chloroplast protein accumulation patterns are not restricted to photochemistry and carbon fixation reactions.

To verify that the observed differential expression patterns by spectral counting could be reproduced by an independent method, we analyzed differential protein distribution between the two types of *Bienertia* chloroplasts via 2D differential gel electrophoresis (2D-DIGE) (Figure 4A). The two types of chloroplasts were isolated from chlorenchyma protoplasts, and the soluble stromal protein fractions were labeled differentially with fluorescing dyes (red/green) and separated by their isoelectric point and molecular weight. A small set of C- (red spots) and P- (green spots) enriched chloroplast proteins (ranging from very high to low abundance) was selected for identification by mass spectroscopy, and detailed information for 10 of the identified proteins is available in Suppl. Table 4 in the SI. Comparison of the 2D-DIGE results with the spectral counting data (Figure 4B) shows a high correlation (Pearson's R^2 = 0.87) of C/P chloroplast accumulation ratios between the two methods.

DOI: 10.1021/pr5011907
J. Proteome Res. 2015, 14, 2090−2108

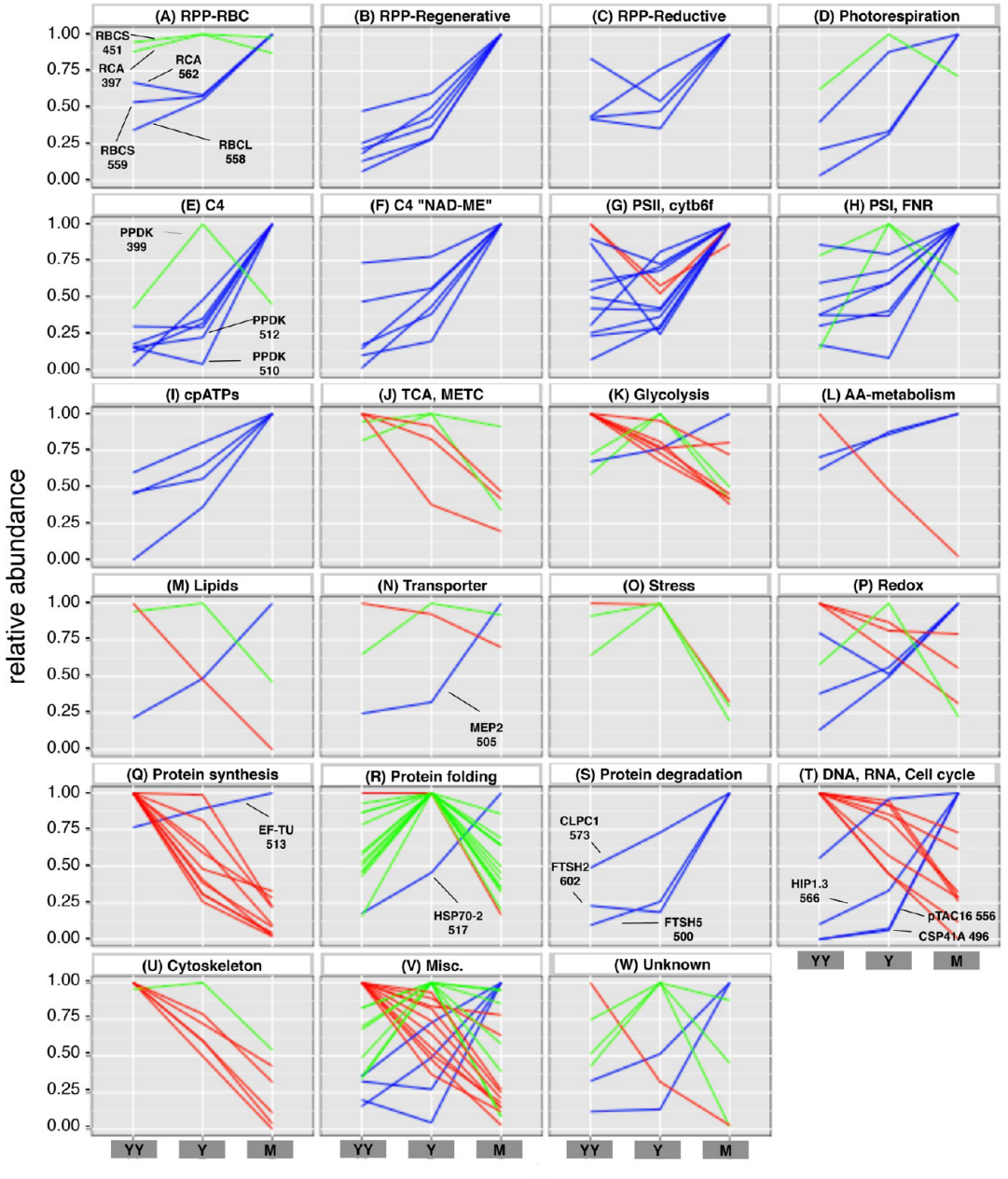

Figure 5. Protein accumulation in leaves of *Bienertia* over three different developmental stages, YY youngest; Y, young, and M, mature. Quantified proteins were normalized for the maximum expression and grouped according to biological functions following the BIN classification system. Color code indicates highest relative protein amount in mature (blue lines), young (green lines) or youngest leaves (red lines). Protein IDs and full protein names are accessible through Suppl. Table 6 in the SI.

Differentially Accumulating Proteins Do Not Share a Common Motif in Their Transit Peptides

The observed differential accumulation of many nuclear-encoded chloroplast-targeted proteins raises the question of how these proteins are targeted specifically to their respective chloroplast types. Differential chloroplast import, differential protein degradation within chloroplasts, and selective targeting of mRNAs have been hypothesized.[35] To investigate a potential role of transit peptides in differential protein accumulation, we compared the physicochemical features of the 35 nuclear-encoded proteins and their predicted chloroplast transit peptides (cTPs), which were found to be enriched in C or P ($q < 0.1$). Both groups of transit peptides displayed classical properties of cTPs observed for other species but no further obvious sequence motifs or special characteristics. (See Suppl. Figure 1 and Suppl. Table 5 in SI.)

Protein Composition of the Central Compartment

The above results indicate that C chloroplasts of *Bienertia* are enriched in certain enzymes of the CBB pathway, analogous to those in BS chloroplasts of Kranz type species. Because *Bienertia* is NAD-ME type C_4, its CC is proposed to functionally resemble the BS cell of Kranz type NAD-ME C_4 species because it harbors mitochondria, which are the site of C_4 acid decarboxylation via NAD-ME, along with peroxisomes and BS-like chloroplasts; however, there is no experimental information about the identity of proteins in the CC in relation to photosynthesis or additional functions of this compartment. Therefore, we compared protein abundance in the CC and C

DOI: 10.1021/pr5011907
J. Proteome Res. 2015, 14, 2090−2108

chloroplasts. Among the 179 quantified proteins of the localization series, 31 were either exclusively found or significantly enriched ($q < 0.05$) in the CC compared with the C (Table 1). This indicates they are CC proteins that are not localized to the chloroplasts of this compartment.

Among these nonchloroplast CC-enriched proteins were the highly abundant forms of mitochondrial aspartate aminotransferase (ASP-AT, ID542), NAD-ME (ID541), and NAD malate dehydrogenase (NAD-MDH, D543), making them likely candidates for the mitochondrial decarboxylation step in the SCC_4 cycle. Nonchloroplast proteins associated with the glycolate pathway and photorespiration were also identified in this compartment. This includes three of the CC-enriched proteins that could function in mitochondrial metabolism of glycine to serine in the glycolate pathway [glycine decarboxylase P protein (GDC-P, ID481), glycine cleavage T-protein (GDC-T, ID546), and serine hydroxymethyltransferase (SHM, ID545)]. Also, six proteins that were enriched in CC over C were annotated in *Arabidopsis* or maize as peroxisomal [hydroxypyruvate reductase (HPR, ID742), catalase (CAT, ID646), alanine aminotransferase (ALA-AT, ID551), alanine-glyoxylate aminotransferase (AGT, ID 741), glycolate oxidase (GOX, ID550), and malate dehydrogenase (PMDH, ID445)], which could function in the glycolate pathway. Identification of these enzymes in the CC supports a pathway for photorespiration in this compartment.

The enrichment in CC over C indicates the identified proteins are not located within chloroplasts within this compartment; however, it is also possible that CCs isolated from protoplasts are not completely pure and that some CC-enriched protein could constitute contamination. To test for this possibility, we further compared the TP/CC abundance ratios of the CC enriched proteins. (Proteins located outside of the CC are expected to have high TP/CC ratios.) The majority had low TP/CC ratios, and the corresponding *Arabidopsis* and maize proteins indicated mitochondrial localization in almost all cases; however, five proteins showed relatively high TP/CC ratios (>1.5) with four being significantly enriched in TP over CC ($q < 0.05$). Three represent highly abundant cytoplasmic components of the C_4 cycle (PEPC, ID536, and cytosolic isoforms of Ala-AT, ID529 and Asp-AT, ID 549). Additionally the methyltransferase ATCIMS (ID478), involved in amino acid metabolism, was also annotated as cytoplasmic in *Arabidopsis*. We therefore conclude that CC-enriched proteins with high TP/CC ratios most likely represent partial inclusion of high abundance cytoplasmic proteins within the CC. This could be caused during the isolation procedure when the CPCs that interconnect the peripheral cytoplasm with the cytoplasmic space in the CC seal and thereby trap cytoplasmic proteins in this compartment. Interestingly, the TP/CC ratio of peroxisomal proteins was in all cases close to one, which falls between the low ratio of the mitochondrial proteins and the high ratio of the cytoplasmic proteins. This indicates that peroxisomal proteins are not completely confined to the CC but also localize to the peripheral cytoplasm.

Developmental Changes

The structural features of chlorenchyma cells associated with the SCC_4 phenotype in *Bienertia* develop gradually from an undifferentiated state (no dimorphic chloroplasts or CC) in very young leaves, followed by development to an intermediate stage and full differentiation in mature leaves.[13,14] Using leaf tissue representing these three stages (Figure 1B), the relative protein abundances in this developmental series were compared. Out of the 163 quantified proteins, 56 proteins showed a significant ($q < 0.05$) increase, and 82 proteins showed a significant decrease in at least one of the developmental stages (Figure 5 and Suppl. Table 6 in the SI, which includes a list of proteins associated with the groups listed in the Figure).

The majority of the proteins involved in photosynthesis and photorespiration (Figure 5A–I) increased toward maturation (indicated by blue lines), with only a few exceptions peaking instead in the intermediate (green lines) or youngest leaves (red lines). The expression profiles also indicate isoform-specific differences. For example, RBCS and RCA were each identified in two different forms (panel A). Relative amounts of RCA ID397 and RBCS ID451 hardly changed throughout the three developmental stages, whereas abundance of RCA ID562 and RBCS ID559 increased toward maturation. Similarly, of the three quantified PPDK forms, PPDK ID510 and ID512 showed strong induction toward maturation, whereas PPDK ID399 peaked instead in intermediate leaves (panel E).

In contrast with photosynthesis-related proteins, proteins involved in mitochondrial respiration (panel J), glycolysis (panel K), protein synthesis (panel Q), DNA, RNA, cell cycle, and signaling-related proteins (panel T), as well as cytoskeleton-associated proteins (panel U) generally decreased toward maturation. Interestingly, proteins in the protein folding category (panel R) showed a different developmental pattern. Here all but one quantified protein had the highest relative amount in intermediate leaves in contrast with the protein synthesis category (panel Q) and the protein degradation category (panel S), which decreased and increased toward maturation instead. This indicates differences in the timing of protein synthesis, folding, and degradation in the developmental program.

Many of the categories were populated with too few members to allow for general conclusion about their developmental changes (e.g., AA-metabolism, panel K; lipids, panel L; stress, panel N; and others); however, in some of these nonphotosynthetic categories, individual proteins followed the expression pattern of photosynthetic proteins. For example, one of the quantified transporters (MEP2, ID505, panel N) strongly increased toward maturation, whereas the other two transporters changed very little between the different developmental stages. Similarly, chloroplastic elongation factor Ef-TU1 (ID513, panel P), cpHSP-70–2 (ID517, panel Q), proteases FtsH5 (ID500), FtsH2 (ID602), and ClpC1 (ID573) (panel R), and several plastid RNA-associated factors (HIP1.3, 566 and CSP41A, ID496, pTAC16, ID556, panel S) as well as two proteins with no *Arabidopsis* or maize homologues (panel U) followed the accumulation pattern of photosynthetic proteins. Their common expression pattern suggests these are candidates for involvement in developing SCC_4 photosynthesis.

DISCUSSION

C_4 photosynthesis is a complex metabolic trait that requires the coordinated expression of many proteins in several subcellular compartments. In Kranz-type NAD-ME C_4 species this includes coordination across two adjacent cell types, bundle sheath cells, and mesophyll cells and their specialized subcellular proteomes.[36] In terrestrial single-cell C_4 species such as *Bienertia*, the confinement of the complete NAD-ME C_4 pathway within a single cell requires specialized intracellular compartmentalization. Understanding subcellular protein localization is therefore

DOI: 10.1021/pr5011907
J. Proteome Res. 2015, 14, 2090–2108

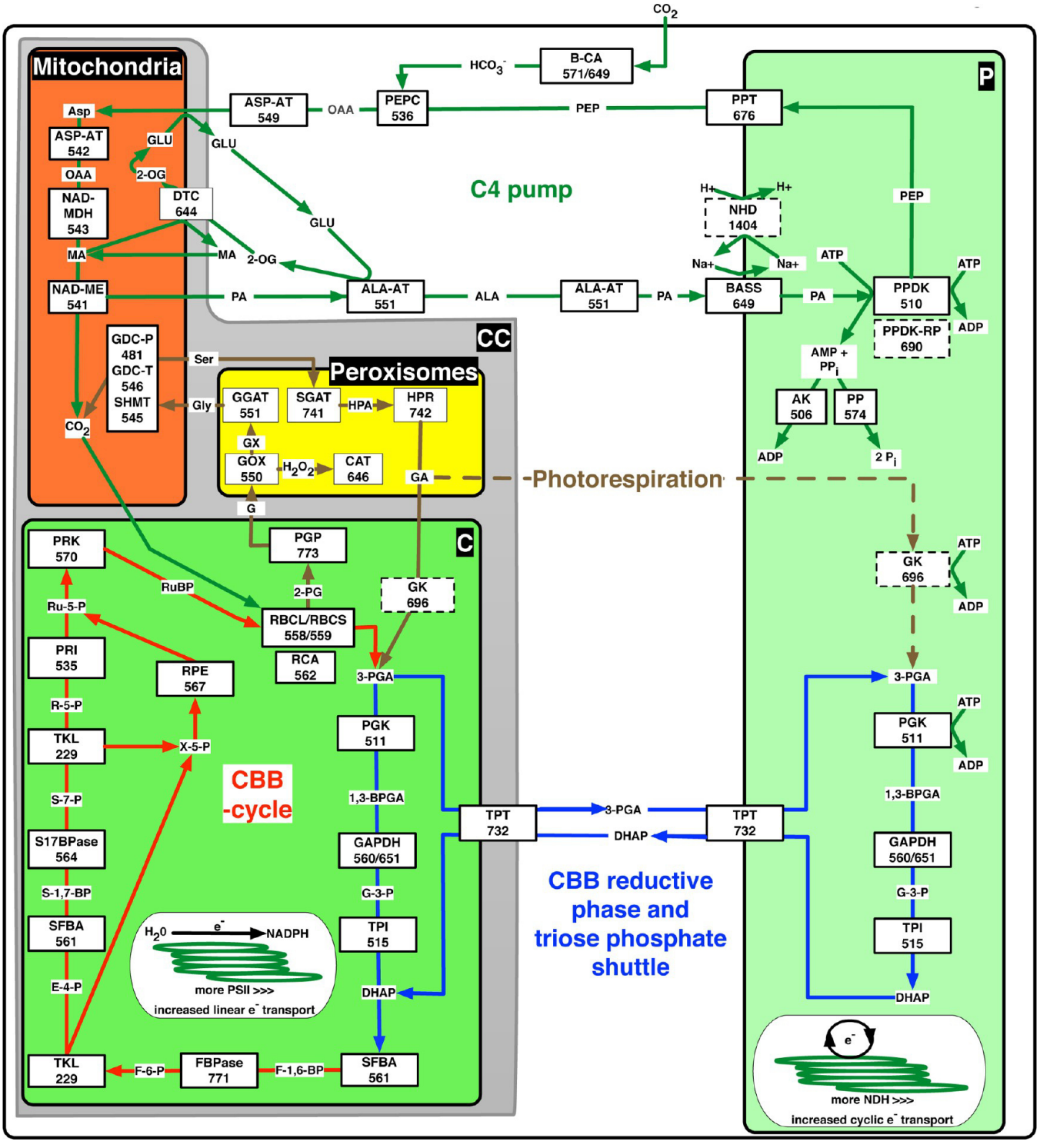

Figure 6. Model for carbon fixation in terrestrial SCC_4 species via an NAD-ME C_4 cycle. Subcellular localization was inferred from proteomics data and curated information on localization of closest protein homologues. Overall abundance, developmental expression profiles, and subcellular localization were used for selection of most probable isoforms involved in the specified processes. Arrows showing reactions of the main pathways are color coded in red (Calvin–Benson–Bassham cycle, CBB), blue (reductive phase of the CBB and the triose-phosphate shuttle, TPS), green (C_4 carbon concentrating mechanism, CCM), and brown (photorespiration). The central compartment (CC) is shaded in gray. Localization of proteins in boxes with dashed outlines is hypothetical. Numbers behind protein names can be used to identify the detailed localization and expression profiles in Figure 3 and Table 1 as well as full information in Supplemental Table 1 in Supporting Information. Abbreviations of enzymes: AK, adenylate kinase; ALA-AT, alanine aminotransferase; ASP-AT, aspartate aminotransferase; BASS, bile-acid sodium symporter; B-CA; beta carbonic anhydrase; CAT, catalase; DTC, di- and tricarboxylate carrier; FBPase, 1,6-fructose bisphosphatase; GAPDH, glyceraldehyde phosphate dehydrogenase; GDC-P/T, glycine decarboxylase P- and T subunits; GGAT, glutamate/glyoxylate aminotransferase; GK, glycerate kinase; GOX, glycolate oxidase; HPR, hydroxypyruvate reductase; NAD-MDH, NAD malate dehydrogenase; NAD-ME, NAD malic enzyme; PEPC, phosphoenolpyruvate carboxylase; PGK, phosphoglycerate kinase; PGP, phosphoglycolate phosphatase; PP, pyrophosphatase; PPDK, pyruvate, Pi-dikinase; PPT, phosphoenolpyruvate phosphate translocator; PRI, phosphoribose isomerase; PRK, phosphoribulokinase; RBCL/S, ribulose 1,5-bisphosphate carboxylase/oxygenase large

DOI: 10.1021/pr5011907
J. Proteome Res. 2015, 14, 2090−2108

Figure 6. continued

and small subunits; RCA, rubisco activase; RPE, ribulosephosphate epimerase; S17BPase, sedoheptulose-1,7-bisphosphatase; SFBA, sedoheptulose/fructose bisphosphate aldolase; SGAT, serine/glyoxylate aminotransferase; SHMT, serine hydroxymethyltransferase; TKL, transketolase; TPI, triose phosphate isomerase; TPT, triose phosphate translocator. Abbreviations of metabolites: ALA, alanine; ASP, aspartate; 1.3-BPGA, 1.3-bisphosphoglycerate; DHAP, dihydroxyacetone phosphate; E-4-P, erythrose-4-phosphate; F-1,6-BP, fructose-1,6-bisphosphate; F-6-P, fructose-6-phosphate; G, glycolate; GA, glycerate; G-3-P, glyceraldehyde-3-phosphate; GX, glyoxylate; GLU, glutamate; GLY, glycine; HPA, hydroxypyruvate; MA, malate; OAA, oxaloacetate; 2-OG, 2-oxoglutarate; PA, pyruvate; 2-PG, 2-phosphoglycolate; PEP, phosphoenolpyruvate; 3-PGA, 3-phosphoglycerate; R-5-P, ribose-5-phosphate; Ru-5-P, ribulose-5-phosphate; RuBP, ribulose bisphosphate; S-7-P, sedoheptulose-7-phosphate; S-1,7-BP, sedoheptulose-1,7-bisphosphate; SER, serine; X-5-P, xylulose-5-phosphate.

crucial to understand the mechanistic basis of this unusual type of C_4 photosynthesis. In this study on *Bienertia*, we collected detailed information on relative protein abundance in developing and fully mature leaves as well as subcellular localization of proteins in mature chlorenchyma cells that perform SCC_4 photosynthesis. On the basis of these qualitative and quantitative results, the developmental induction of C_4 photosynthesis and the subcellular compartmentation of proteins required to operate NAD-ME type C_4 photosynthesis were defined. This includes enzymes, putative transporters, and proteins involved in photochemistry.

Proteome Rearrangements Throughout Development of *Bienertia* Leaves

We used leaves of different developmental stages (YY, Y, and M) to track changes during development associated with the SCC_4 phenotype in *Bienertia* and to differentiate between C_4 and non-C_4 forms of photosynthetic proteins. C_4 isoforms were predicted to accumulate toward maturation, as observed in the analyses of RNA and protein accumulation patterns over a leaf developmental gradient of the Kranz C_4 species maize.[20,37,38] The *Bienertia* leaf material used in our study was similar to leaves utilized in a previous study.[16] There, it was shown that the morphology typical for the SCC_4 phenotype (formation of the CC, the peripheral compartment, and the connecting transvascular channels) had not yet been established in YY leaves. The Y leaves (~4 mm in length) represent an intermediate stage with limited development of the cytoplasmic domains, distinguished by indications of initial development of CC and P at the base of the leaf and further developed cytoplasmic domains toward the tip of the leaf, while complete development of the cytoplasmic domains has occurred in the chlorenchyma along the mature leaf. These three stages therefore represent a progression in the structural development of compartmentalization in the chlorenchyma cells.

We observed large-scale proteome rearrangements accompanying the individual developmental stages. Proteins involved in photosynthetic functions showed a strong increase toward maturation, whereas abundance of proteins involved in nearly all other biological functions was reduced in M compared with YY leaves (Figure 4). This suggests that the leaf undergoes a transition from a sink tissue toward a photosynthetic source tissue, which has also been observed in Kranz-type C_4 species.[20,39−42]

SCC_4 species such as *Bienertia* are suggested to undergo a C_3 or intermediate photosynthetic stage before the fully functional C_4 system is established. This hypothesis was derived from carbon isotope discrimination analysis throughout development, the occurrence of monomorphic chloroplasts with Rubisco early in development,[14] and the observation that transcripts and protein abundance of some C_4-related proteins were induced in later developmental stages compared with C_3-related proteins.[16] In some Kranz-type C_4 species, a C_3 default state also occurs with Rubisco appearing initially in both M and BS chloroplasts, while other Kranz types show biochemical specialization of chloroplasts very early in development. (See ref 41.)

Results from the current study indicate CBB carboxylation, and reductive phase proteins are induced very early in development in *Bienertia*, with most of them reaching 50% of the maximum amount in YY leaves (Figure 5); however, most proteins of the regenerative phase of the CBB (which were not previously identified) are of relatively low abundance in YY leaves, and they show a developmental induction very similar to many C_4-related proteins. Thus, early in development the regenerative phase may limit the expression of C_3 photosynthesis; furthermore, no clear indication for a C_3 stage (high expression of C_3-related proteins but low expression of C_4-related proteins) could be observed. This seems similar to the situation in the Kranz C4 species maize, where a default C_3 stage was also initially proposed for young tissues[43] and incomplete development of C_4 in young leaf tissues was suggested from sensitivity of photosynthesis to oxygen;[44] however, maize leaf proteome analysis did not support a default C_3 stage in very young leaf tissue,[20] and recent gas-exchange measurements detected no evidence of functional C_3 photosynthesis in young leaf tissue of maize.[38]

Selective Protein Accumulation in the Two Chloroplast Types

During the development of SCC4 photosynthesis, dimorphic chloroplasts are formed. This type of specialization, with two forms of an organelle within a cell, has not been reported for other plants. Here we show that proteins belonging to many different functional categories including the C_3 and C_4 carbon fixation pathway as well as certain proteins associated with light reactions, accumulate selectively in one of the two chloroplast types. The mechanism of selective accumulation of nuclear-encoded plastid targeted proteins in SCC_4 species is still not understood.

Several studies suggest plastids generally possess the ability for specific protein import. For example, pea root plastids fail to import photosynthetic proteins,[45] and specific differences in protein import have been observed between leucoplast and chloroplasts.[46] Also, chloroplasts seem to be capable of selective preprotein import dependent on the developmental stage,[47] and different import pathways have been suggested for low-abundance housekeeping proteins and highly abundant photosynthetic proteins.[48−50] Here we identified groups of proteins that accumulated in either the C or the P. Comparison of their transit peptides indicated no differences in their physicochemical properties such as amino acid composition, number of charged and uncharged amino acids, or hydrophobicity. Also, sequence alignment did not reveal any obvious similarities between members of C- and P-accumulating proteins. It is, of course, possible that potential selective targeting signals evaded

DOI: 10.1021/pr5011907
J. Proteome Res. 2015, 14, 2090−2108

our analysis because motifs as short as two consecutive charged amino acids have been shown to be important for the age-dependent import;[51] however, in vivo localization experiments using the transit peptides of PPDK and RBCS gave no indication for the control of selective import into the two chloroplast types in *Bienertia* as green fluorescent protein fusion constructs accumulated equally in both chloroplast types.[52] In conclusion, these results indicate that selective protein accumulation in SCC_4 species is most likely not controlled on the level of specific transit peptide recognition.

Integrative Model for Primary Carbon Fixation in SCC_4 Species

The combination of subcellular protein distribution in mature chlorenchyma cells, together with relative abundance information and developmental expression profiles, allowed us to select the likely candidates involved in carbon fixation and photosynthesis in the SCC_4 system. Results of the current study are shown by their ID numbers in the scheme shown in Figure 6, and the various steps of the CBB cycle, C_4 cycle, and photorespiration are discussed later.

Carboxylation Phase of the CBB Cycle. A key feature in Kranz-type C_4 species, regardless of the biochemical or structural subtype, is the confinement of final CO_2 fixation to the BS via the CBB pathway. Proteomic analysis shows the key phases of this pathway in *Bienertia* occur in chloroplasts in the CC. RBCL and RBCS selectively accumulate in the C chloroplasts (consistent with previous immunolocalization results)[8] and interestingly, two different isoforms of the small subunit were identified. In *Arabidopsis*, RBCS is encoded by a multigene family[53] and individual members are differentially regulated by light[54] and throughout development.[55] The two quantified forms in *Bienertia* showed different developmental patterns, with the more abundant form (ID559) increasing toward maturity and the less abundant form (ID451) peaking instead in YY leaves; however, both forms showed similar enrichment in the C prepared from mature leaves, suggesting that differential accumulation of RBCS is not limited to specific isoforms. This appears to be similar to the situation in maize, where two transcripts from different RbcS genes both showed a BS specific accumulation pattern.[56] RCA regulates the activity of Rubisco using energy from hydrolysis of ATP to uncouple inhibitory sugar phosphates from decarbamylated active sites, thereby releasing a dead-end complex.[57,58] Two isoforms of RCA differing in the C-terminal region have been identified in several species.[59,60] Both forms are catalytically active, but only the longer alpha form is redox-regulated.[61] Interestingly, in *Bienertia* the beta form (ID 562) is more abundant in the C chloroplasts, where it may function to regulate activation of Rubisco. The putative redox regulated alpha form (ID 397) is enriched in the P chloroplasts. The function of this protein is, however, uncertain.

Reductive Phase of the CBB Cycle and Integration of the Light Reactions. In contrast with the CBB-carboxylation phase and the CBB-regenerative phase, enzymes of the reductive phase of the CBB-cycle were enriched in P or about equally abundant in both chloroplast types. In addition, both types showed high amounts of the triose-phosphate transporter (TPT, ID732), which exchanges triose-phosphates for inorganic phosphate or phosphoglycerate (PGA).[62,63] This distribution can support the operation of a triose-phosphate shuttle (TPS) between the two chloroplast types in *Bienertia* (Figure 6). Such a TPS is considered to be an integral part of the C_4 cycle in NADP-ME species such as maize and sorghum because the agranal BS chloroplasts cannot produce sufficient reducing equivalents by linear electron transport to allow for reduction of all PGA synthesized by Rubisco. Instead, reductive power is shuttled from the M into the BS via malate and to varying extent also by the TPS.[19,64,65] Although the occurrence of the reductive phase of the CBB-cycle in the M of NAD-ME- and PEP-CK-type Kranz C_4 species has also been demonstrated,[66] the functional relevance is still unclear. In NADP-ME species BS chloroplasts have reduced grana development and capacity for the production of NADPH by linear electron transport and reduced evolution of O_2 by PSII, which was suggested to be advantageous in limiting photorespiratory activity due to a lower O_2/CO_2 ratio in BS cells;[67] however, in NAD-ME species, BS chloroplasts have well-developed grana[68] and the PSII/PSI ratio was found to be even higher in BS cells compared with M cells.[2,69,70] A higher granal index in C was also reported for *Bienertia*,[8,9] and our proteome data indicate enrichment of PSII components in the C. Furthermore, measurements of O_2 evolution with isolated C indicated a high capacity for linear electron transport in this chloroplast type.[15] Accordingly, there would seem to be little need to export PGA via the TPS to the P for reduction to triose-phosphates; however, the C are tightly packed within the CC (see Figure 1A), and self-shading of chloroplasts might reduce effective electron transport rates. Additionally, consumption of reducing power in the P might be low due to lack of CBB-cycle activity, with a primary function to provide ATP for PPDK in the carboxylation phase of the C_4 cycle during synthesis of aspartate (ASP);[15] therefore, operation of the TPS could provide an alternative sink for reducing power in the P. The TPS shuttle also could help balance the utilization of photochemically generated ATP between the two chloroplast types through phosphorylation of part of the PGA (by PGK) in the reductive phase in the P. In summary, the data presented here provide evidence that the TPS is also an integral part of C_4 metabolism in SCC_4 and may allow for flexibility in utilizing photochemically generated energy between the two types of chloroplasts. Further research is needed, however, to address the exact functional role of the TPS in *Bienertia* P chloroplasts as well as in other NAD-ME type species.

Cyclic electron transport balances the ATP/NADPH ratio in chloroplasts by using reducing power to drive ATP synthesis utilizing either NADPH or ferredoxin as a source.[71] In maize, the NDH complex (using NADPH as electron donor) is about 3 to 5 times enriched in BS.[18] In contrast, the quantified components of the NDH complex were either equally abundant in the two chloroplasts types or enriched in the P in *Bienertia*. This correlates with previous reports indicating higher NDH levels in the M of NAD-ME species.[72] The production of ATP by PSI-mediated cyclic electron transport may therefore contribute to the ATP requirement in the carboxylation phase of the cycle for synthesis of PEP in *Bienertia*.

Regenerative Phase of the CBB Cycle. Whereas BS-specific accumulation of Rubisco has been shown for numerous C_4 species, there is little information on the other CBB-cycle enzymes in Kranz-type C_4 species.[73−75] Only in the NADP-ME species maize has it been shown at the protein level that most of the regenerative phase enzymes at the protein level accumulate preferentially in BS chloroplasts.[18,20] In experiments with isolated chloroplasts of *Bienertia*, only the C were capable of CO_2-dependent oxygen evolution, which is indicative of the lack of a functional CBB-cycle in the P;[15]

DOI: 10.1021/pr5011907
J. Proteome Res. 2015, 14, 2090−2108

however, it was unclear if this is caused by reduced amounts of CBB-cycle enzymes or due to different mechanisms such as inactivation of CBB-cycle enzymes in the P. Here we quantified all of the enzymes required for the regenerative phase of the CBB cycle. (See candidate proteins for function in Figure 6.) Plastidic aldolase (SFBA), which is at the re-entry point of triose-phosphates into the regenerative phase of the CBB-cycle, showed the highest C/P ratio of all CBB-cycle enzymes measured, and this result was confirmed independently via 2D-DIGE. In contrast, the remaining enzymes of the regenerative phase showed less pronounced C-specific accumulation. The observed subcellular protein localization of a few selected enzymes would create a metabolic "drag" by limiting the occurrence of bottleneck enzymes to one of the two chloroplast types. Such bottlenecks have been identified in C_3 plants by down-regulation and overexpression of CBB-cycle enzymes. Perhaps surprisingly, it has been shown that it is usually the nonregulated steps of the CBB cycle (reversible reactions of aldolase and transketolase) that confer the highest metabolic control. In contrast, the thioredoxin-regulated irreversible steps catalyzed by GAPDH, fructose bisphosphatase (FBPase), and phosphoribulokinase (PRK) had little impact.[76,77] Thus, *Bienertia* seems to confine the regenerative phase of the CBB-cycle to C by selective targeting of only some of these bottleneck proteins.

Photorespiration. C_4 plants show reduced photorespiration compared with C_3 plants;[78,79] nevertheless, the pathway is indispensable in maize.[80] Here we quantified homologues to almost all known components of the photorespiratory pathway including the mitochondrial glycine decarboxylase complex (GDC), the peroxisomal GOX and aminotransferases, as well as chloroplast localized PGP enriched in C chloroplasts in *Bienertia*. (PGP accumulates specifically in the BS of maize.)[18] The tight metabolic and structural integration of mitochondria in the NAD-ME pathway enables efficient recapturing of CO_2 released by GDC, which would then face the same diffusive resistance and barriers as CO_2 resulting from the decarboxylation of C_4 acids (Figure 6).

The shortest route for photorespiratory derived glycerate to be fed back into the CBB cycle would be through a C chloroplast localized glycerate kinase (GK). Interestingly, previous research in Kranz C_4 NADP-ME and NAD-ME species indicated localization of GK in the M and not in the BS.[81] Here we did not assign a final subcellular localization for GK in *Bienertia* because it was just below the quantification threshold; however, the low C/P ratio (0.25) for GK in *Bienertia* suggests that part of the glycerate (GA) generated by photorespiration is further processed in the P (indicated by the dashed brown line in Figure 6). This would not only allow for utilization of P generated ATP; the 3-PGA produced could then also be utilized using the same enzymes and transporter as the 3-PGA in the triose-phosphate shuttle.

Primary Carbon Fixation in the CCM. The first two steps of the CCM are conserved in all Kranz-type C_4 plants investigated so far, independent of the biochemical subtype. First, atmospheric CO_2 is converted by carbonic anhydrase (CA) to bicarbonate, which is then used as the carbon donor for PEPC, and both reactions are catalyzed by cytoplasmic enzymes. In SCC_4 *Bienertia*, PEPC is also located in the cytoplasm, as shown in the present study and in previous work;[8,15] however, neither the exact identity nor the subcellular localization of CAs involved in SCC_4 was previously shown.[82] Activity assays indicated that the majority of CA activity in *Bienertia* is extraplastidial.[15] Here we identified two highly abundant beta-type CAs in *Bienertia*, and their *Arabidopsis* (a C_3 species) and maize (a C_4 species) homologues were both annotated as chloroplast-localized. In C_3 species, beta type CAs are mainly localized to chloroplasts, although their function is still poorly understood and they are most likely not directly involved in photosynthesis (reviewed in ref 83). Chloroplast beta-CAs have also been identified in C_4 *Flaveria* species and in maize,[18,84] and it has been hypothesized that expression of cytoplasmic and chloroplast CAs in M might help balance the pools of CO_2 and HCO_3^-;[85] however, the two most abundant forms quantified in this study were clearly localized outside of chloroplasts, most likely in the cytoplasm, where they are proposed to convert atmospheric CO_2 to bicarbonate, the substrate for PEPC (Figure 6).

C_4 Shuttle. The classical view of the NAD-ME C_4 pathway in Kranz-type C_4 species requires the operation of several aminotransferases, which act in combination with mitochondrial enzymes via a shuttle of aspartate and alanine to deliver CO_2 to the chloroplast. Kranz-type NAD-ME C_4 species are known to have high activities of aspartate and alanine aminotransferases.[86−88] In *Bienertia*, we quantified two highly abundant forms of ASP-AT, both showing an increase in abundance from YY to M leaves. ASP-AT2 (ID549) was localized to the cytosol and suggested to function in converting the product of PEPC, oxaloacetate to aspartate (Figure 6). ASP-AT1 (ID 542) is most likely located in mitochondria in the CC in the decarboxylation phase of the cycle. This identification and distribution of ASP-AT is in accordance with previous findings of cytosolic and mitochondrial forms from immunolocalization studies using antibodies on *Bienertia* leaves of different developmental stages and isolated subcellular compartments.[15,16] In contrast, only a single highly abundant form of cytosolic ALA-AT (ID551) was observed.

Following the transamination of aspartate to oxaloacetate in mitochondria in the CC, NAD-MDH converts oxaloacetate to malate, generating the substrate for NAD-ME. Interestingly, a prevalent mitochondrial form of NAD-MDH (ID543) in *Bienertia* was differentially regulated (no increase toward maturation), compared with all other potential C_4 enzymes in the developmental gradient. No differences in NAD-MDH activity and transcript abundance have been observed between C_3- and C_4-type Cleome species,[89,90] and it has been speculated that activity of the housekeeping C_3 form might be sufficient to support C_4 photosynthesis. The lack of increase in NAD-MDH during maturation observed in *Bienertia* indicates this could be a common feature of NAD-ME C_4 plants; therefore, NAD-MDH would be the first known example of a major enzyme involved in C_4 photosynthesis, which does not show altered regulation (i.e., increased expression levels) compared with its C_3 isoforms.

We identified a prevalent form of NAD-ME (ID541), and its compartmentation supports previous evidence of its mitochondrial localization.[8,15,91] In C_3 species, NAD-ME is believed to participate in respiration by providing an alternative source of pyruvate (PA) and other anaplerotic functions.[92,93] Subunit composition seems to vary significantly between species, as NAD-ME with either one or two subunits has been reported.[94] In *Arabidopsis*, alpha- and beta-type NAD-ME have been observed, and it has been suggested that they occur as homo- as well as heterodimers;[95] however, little is known about the characteristics of NAD-ME in the context of C_4 photosynthesis. In the C_4 species *Cleome gynandra*, alpha- and beta-type NAD-

DOI: 10.1021/pr5011907
J. Proteome Res. 2015, 14, 2090−2108

ME have been identified, and both show a BS-specific accumulation pattern.[96] In contrast, only a single highly expressed beta-type NAD-ME (homologue to NAD-ME2 from *Arabidopsis*) was observed in *Bienertia*. (The alpha form, NAD-ME1, was undetectable in the proteomics experiments, although a full-length sequence was present in the protein sequence database.) The expression of *Bienertia* NAD-ME2 follows the pattern of photosynthetic enzymes, not the pattern of respiratory enzymes, suggesting the major purpose of the identified NAD-ME form is to function in the C_4 cycle as opposed to respiration.

The NAD-ME C_4 pathway requires the import of ASP and export of PA by mitochondria at rates equal to the C_4 pump. Additionally, a 2-oxoglutarate/glutamate (2OG-GLU) shuttle and the associated transporter for these metabolites between the mitochondria and the cytosol are required to provide amino donors and acceptors for the transamination reactions of ASP and alanine (ALA) aminotransferases. With the exception of the 2-oxoglutarate/malate (2OG/MA) translocator,[97] none of these transporters have been identified for any NAD-ME C_4 species so far. Transporters involved in C_4 photosynthesis were predicted to be highly abundant due to the high fluxes associated with C_4 metabolism.[98] Among the most abundant transporter quantified in the CC of *Bienertia* was the di- and tricarboxylate carrier (DTC ID644), which most likely translocates 2OG for MA in the mitochondria (Figure 6). Also, the dicarboxylate carrier (DIC) was highly abundant; however, based on its transport characteristics in the C_3 plant *Arabidopsis*, it would not qualify as a good candidate for the ASP-GLU translocator because it has been shown to transport a variety of dicarboxylic acids including malate, oxaloacetate, and succinate but not aspartate.[99] Nevertheless, the substrate specificity, which has not been tested to date in C_4 plants, might be different.

Regeneration of PEP. The final step for completion of the C_4 CCM is the regeneration of the primary CO_2 acceptor PEP. For this, PA needs to be imported into the chloroplasts, followed by phosphorylation via PPDK using ATP generated by the light reactions. PEP can then leave the chloroplast and is available as a substrate for cytosolic PEPC for a new round of CO_2 fixation.

C_4 plants have generally been reported to either require or not require Na^+ for growth, and this has been shown to correlate with the presence of either a Na^+- or H^+-dependent uptake mechanism of PA into the M chloroplasts.[100] The responsible Na^+-dependent transporter has been recently characterized in C_4 *Flaveria* as BASS2 (bile-acid sodium symporter).[33] BASS2 was not detected in the proteome of maize,[26,98] which utilizes a Na^+-independent PA import mechanism instead.[101] In *Bienertia* we identified a BASS2 protein homologue that preferentially accumulates in the P chloroplasts (ID649) (Figure 6). Because BASS2 transport activity results in the net uptake of sodium, a second Na^+/H^+ proton antiporter (NHD) is required for balancing. Consistently we also identified this transporter (ID1404), but it was below the threshold for quantification and localization. These results suggest *Bienertia* uses the same mechanism for import of PA into chloroplasts, as described for *Flaveria*.

PA imported into the P can subsequently serve as a substrate for chloroplast PPDK. The P-specific accumulation of PPDK in *Bienertia* has been shown by immunolocalization,[8] and only the isolated P converts PA to PEP in a light-dependent manner;[15] however, the exact nature of the PPDK responsible for supporting C_4 photosynthesis had not been resolved. Here we identified several PPDK forms; the most abundant one (ID510) is suggested to function in the C_4 cycle as it exhibits typical characteristics of a C_4 form including an increase in abundance toward leaf maturation and P-specific accumulation. Energetics for the PPDK reaction under physiological conditions favors the dephosphorylation of PEP to PA rather than its synthesis. High levels of AK and PP are needed in leaves of C_4 plants to drive the reaction toward PEP synthesis by removing the end products adenosine monophosphate (AMP) and pyrophosphate (PPi).[102] Comparative transcriptomics showed upregulation of genes for AK and PP in C_4 species relative to C_3 species,[89] but C_4-specific forms of those enzymes have not yet been characterized at the protein level. Here we identified several forms of AK and PP, and we selected the most likely candidates by their localization and developmental accumulation patterns (Figure 6). Both are upregulated in M leaves and accumulate preferentially in the P. Finally, PEP generated by PPDK can be exported from the P to the cytosol by the PEP transporter (PPT, ID676).[103]

■ CONCLUSIONS

This proteomics study provides an integrated view of the quantitative subcellular distribution of proteins (across two chloroplast types, cytosol and mitochondria) supporting SSC_4 NAD-ME photosynthesis in *Bienertia*. Strong similarities to traditional Kranz-type NAD-ME C_4 species in terms of biochemical pathways are observed, where the central chloroplasts and peripheral chloroplasts in *Bienertia* probably function in a similar way as mesophyll and bundle sheath chloroplasts. With the detailed information on subcellular protein localization and sequence identity generated, it will now be possible to analyze the molecular mechanisms underlying the development of the SCC_4 system, including the mechanism responsible for differential protein accumulation in the two chloroplast types. Efforts are currently ongoing to engineer a C_4 pathway into C_3 plants such as rice.[104,105] Identifying proteins required for development of the very different mode in SCC_4 versus Kranz C_4 will be useful in efforts to introduce C_4 traits into C_3 crops.

■ ASSOCIATED CONTENT

Supporting Information

Supplemental text 1: Specific examples for determination of subcellular protein localization through TP/chloroplast ratios. Supplemental Figure 1: Features of *Bienertia* chloroplast transit peptides of differentially expressed proteins. Supplemental Table 1. List of all 1497 qualitatively identified *Bienertia* proteins. Supplemental Table 2. List of quantified proteins in chloroplasts and total protoplasts. Supplemental Table 3. Detailed information on the 120 quantified *Bienertia* chloroplast proteins. Supplemental Table 4. 2D-DIGE analyses of stromal proteins from the dimorphic chloroplasts. Supplemental Table 5. List of 39 C or P accumulating proteins. Supplemental Table 6. List of all quantified proteins in the developmental series. This material is available free of charge via the Internet at http://pubs.acs.org.

■ AUTHOR INFORMATION

Corresponding Author

*E-mail: s.offermann@botanik.uni-hannover.de. Phone: +49-511-7624452. Fax: +49-511-76219262.

DOI: 10.1021/pr5011907
J. Proteome Res. 2015, 14, 2090−2108

Notes

The authors declare no competing financial interest.

■ ACKNOWLEDGMENTS

Work in the S.O. lab was supported by the Deutsche Forschungsgemeinschaft under grant number OF106/1. The National Science Foundation supported work by T.W.O. and K.A.D. under grant number DBI 0605016, work by K.J.v.W. and Q.S. under grant number IOS-1127017, and work by G.E.E. under grant numbers IBN 0641232 and MCB 1146928, which includes international collaboration with S.O. sponsored by the Office of International Science and Engineering (OISE). We are grateful to Christoph Peterhansel for critical reading of the manuscript. Mass spectrometry analysis of 2D-DIGE derived samples was done by the University of Idaho Environmental Biotechnology Institute.

■ REFERENCES

(1) Edwards, G. E.; Walker, D. A. *C3, C4: Mechanisms, And Cellular and Environmental Regulation, Of Photosynthesis*; Blackwell Scientific Publications: Oxford, U.K., 1983.

(2) Hatch, M. D. C4 photosynthesis: a unique blend of modified biochemistry, anatomy and ultrastructure. *Biochim. Biophys. Acta* **1987**, *895*, 81−106.

(3) Freitag, H.; Stichler, W. A remarkable new leaf type with unusual photosynthetic tissue in a central asiatic genus of chenopodiaceae. *Plant Biol.* **2000**, *2*, 154−160.

(4) Voznesenskaya, E. V.; Franceschi, V. R.; Kiirats, O.; Freitag, H.; Edwards, G. E. Kranz anatomy is not essential for terrestrial C4 plant photosynthesis. *Nature* **2001**, *414*, 543−546.

(5) Akhani, H.; Barroca, J.; Koteeva, N.; Voznesenskaya, E.; Franceschi, V.; Edwards, G.; Ghaffari, S. M.; Ziegler, H. *Bienertia sinuspersici* (Chenopodiaceae): A new species from southwest Asia and discovery of a third terrestrial C4 plant without Kranz anatomy. *Syst. Bot.* **2005**, *30*, 290−301.

(6) Akhani, H.; Chatrenoor, T.; Dehghani, M.; Khoshravesh, R.; Mahdavi, P.; Matinzadeh, Z. A new species of *Bienertia* (Chenopodiaceae) from Iranian salt deserts: A third species of the genus and discovery of a fourth terrestrial C4 plant without Kranz anatomy. *Plant Biosyst.* **2012**, *146*, 1−10.

(7) Freitag, H.; Stichler, W. *Bienertia cycloptera* Bunge ex Boiss., Chenopodiaceae, another C4 plant without Kranz tissues. *Plant Biol.* **2002**, *4*, 121−132.

(8) Voznesenskaya, E. V.; Franceschi, V. R.; Kiirats, O.; Artyusheva, E. G.; Freitag, H.; Edwards, G. E. Proof of C4 photosynthesis without Kranz anatomy in *Bienertia cycloptera* (Chenopodiaceae). *Plant J.* **2002**, *31*, 649−662.

(9) Voznesenskaya, E. V.; Edwards, G. E.; Kiirats, O.; Artyusheva, E. G.; Franceschi, V. R. Development of biochemical specialization and organelle partitioning in the single-cell C4 system in leaves of *Borszczowia aralocaspica* (Chenopodiaceae). *Am. J. Bot* **2003**, *90*, 1669−1680.

(10) Smith, M. E.; Koteyeva, N. K.; Voznesenskaya, E. V.; Okita, T. W.; Edwards, G. E. Photosynthetic features of non-Kranz type C4 versus Kranz type C4 and C3 species in subfamily Suaedoideae (Chenopodiaceae). *Funct Plant Biol.* **2009**, *36*, 770−782.

(11) Chuong, S. D. X.; Franceschi, V. R.; Edwards, G. E. The cytoskeleton maintains organelle partitioning required for single-cell C4 photosynthesis in Chenopodiaceae species. *Plant Cell* **2006**, *18*, 2207−2223.

(12) Lung, S. C.; Chuong, S. D. X. A transit peptide-like sorting signal at the C terminus directs the *Bienertia sinuspersici* preprotein receptor Toc159 to the chloroplast outer membrane. *Plant Cell* **2012**, *24*, 1560−1578.

(13) Park, J.; Okita, T. W.; Edwards, G. E. Salt tolerant mechanisms in single-cell C4 species *Bienertia sinuspersici* and *Suaeda aralocaspica* (Chenopodiaceae). *Plant Sci.* **2009**, *176*, 616−626.

(14) Voznesenskaya, E. V.; Koteyeva, N. K.; Chuong, S. D. X.; Akhani, H.; Edwards, G. E.; Franceschi, V. R. Differentiation of cellular and biochemical features of the single-cell C4 syndrome during leaf development in *Bienertia cycloptera* (Chenopodiaceae). *Am. J. Bot* **2005**, *92*, 1784−1795.

(15) Offermann, S.; Okita, T. W.; Edwards, G. E. Resolving the compartmentation and function of C4 photosynthesis in the single-cell C4 species *Bienertia sinuspersici*. *Plant Phys.* **2011**, *155*, 1612−1628.

(16) Lara, M. V.; Offermann, S.; Smith, M.; Okita, T. W.; Andreo, C. S.; Edwards, G. E. Leaf development in the single-cell C4 system in *Bienertia sinuspersici*: Expression of genes and peptide levels for C4 metabolism in relation to chlorenchyma structure under different light conditions. *Plant Phys.* **2008**, *148*, 593−610.

(17) Fouracre, J. P.; Ando, S.; Langdale, J. A. Cracking the Kranz enigma with systems biology. *J. Exp. Bot.* **2014**, *65*, 3327−3339.

(18) Friso, G.; Majeran, W.; Huang, M.; Sun, Q.; van Wijk, K. J. Reconstruction of metabolic pathways, protein expression, and homeostasis machineries across maize bundle sheath and mesophyll chloroplasts: Large-scale quantitative proteomics using the first maize genome assembly. *Plant Phys.* **2010**, *152*, 1107−1108.

(19) Majeran, W.; Cai, Y.; Sun, Q.; van Wijk, K. J. Functional differentiation of bundle sheath and mesophyll maize chloroplasts determined by comparative proteomics. *Plant Cell* **2005**, *17*, 3111−3140.

(20) Majeran, W.; Friso, G.; Ponnala, L.; Connolly, B.; Huang, M.; Reidel, E.; Zhang, C.; Asakura, Y.; Bhuiyan, N. H.; Sun, Q.; et al. Structural and metabolic transitions of C4 leaf development and differentiation defined by microscopy and quantitative proteomics in maize. *Plant Cell* **2010**, *22*, 3509−3542.

(21) Doroshenk, K. A.; Crofts, A. J.; Morris, R. T.; Wyrick, J. J.; Okita, T. W. Proteomic analysis of cytoskeleton-associated RNA binding proteins in developing rice seed. *J. Proteome Res.* **2009**, *8*, 4641−4653.

(22) Schneider, C. A.; Rasband, W. S.; Eliceiri, K. W. NIH Image to ImageJ: 25 years of image analysis. *Nat. Methods* **2012**, *9*, 671−675.

(23) Chou, H. H.; Holmes, M. H. DNA sequence quality trimming and vector removal. *Bioinformatics* **2001**, *17*, 1093−1104.

(24) Zheng, Y.; Zhao, L.; Gao, J.; Fei, Z. iAssembler: a package for *de novo* assembly of Roche-454/Sanger transcriptome sequences. *BMC Bioinf.* **2011**, *12*, 453.

(25) Iseli, C.; Jongeneel, C. V.; Bucher, P. ESTScan: a program for detecting, evaluating, and reconstructing potential coding regions in EST sequences. *Proc. - Int. Conf. Intell. Syst. Mol. Biol.* **1999**, 138−148.

(26) Majeran, W.; Zybailov, B.; Ytterberg, A. J.; Dunsmore, J.; Sun, Q.; van Wijk, K. J. Consequences of C4 differentiation for chloroplast membrane proteomes in maize mesophyll and bundle sheath cells. *Mol. Cell. Proteomics* **2008**, *7*, 1609−1638.

(27) Friso, G.; Olinares, P. D. B.; Wijk, K. J. The Workflow for Quantitative Proteome Analysis of Chloroplast Development and Differentiation, Chloroplast Mutants, And Protein Interactions by Spectral Counting. In *Chloroplast Research in Arabidopsis: Methods and Protocols, Vol. II*; Jarvis, P., Ed.; Methods in Molecular Biology; Humana Press: Totowa, NJ, 2011; Vol. *775*, pp 265−282.

(28) Pham, T. V.; Piersma, S. R.; Warmoes, M.; Jimenez, C. R. On the beta-binomial model for analysis of spectral count data in label-free tandem mass spectrometry-based proteomics. *Bioinformatics* **2010**, *26*, 363−369.

(29) The R Development Core Team. *R: A Language and Environment for Statistical Computing*, 2013; R Foundation for Statistical Computing: Vienna, Austria; pp 1−1731. www.R-project.org.

(30) Albrethsen, J.; Knol, J. C.; Piersma, S. R.; Pham, T. V.; de Wit, M.; Mongera, S.; Carvalho, B.; Verheul, H. M. W.; Fijneman, R. J. A.; Meijer, G. A.; et al. Subnuclear proteomics in colorectal cancer: identification of proteins enriched in the nuclear matrix fraction and regulation in adenoma to carcinoma progression. *Mol. Cell. Proteomics* **2010**, *9*, 988−1005.

(31) Pike, N. Using false discovery rates for multiple comparisons in ecology and evolution. *Methods Ecol. Evol.* **2010**, *2*, 278−282.

DOI: 10.1021/pr5011907
J. Proteome Res. 2015, 14, 2090−2108

(32) Thimm, O.; Bläsing, O.; Gibon, Y.; Nagel, A.; Meyer, S.; Krüger, P.; Selbig, J.; Müller, L. A.; Rhee, S. Y.; Stitt, M. MAPMAN: a user-driven tool to display genomics data sets onto diagrams of metabolic pathways and other biological processes. *Plant J.* **2004**, *37*, 914−939.
(33) Furumoto, T.; Yamaguchi, T.; Ohshima-Ichie, Y.; Nakamura, M.; Tsuchida-Iwata, Y.; Shimamura, M.; Ohnishi, J.; Hata, S.; Gowik, U.; Westhoff, P.; et al. A plastidial sodium-dependent pyruvate transporter. *Nature* **2011**, *476*, 472−475.
(34) Granlund, I.; Storm, P.; Schubert, M.; Garcia-Cerdan, J. G.; Funk, C.; Schroder, W. P. The TL29 protein is lumen located, associated with PSII and not an ascorbate peroxidase. *Plant Cell Physiol.* **2009**, *50*, 1898−1910.
(35) Offermann, S.; Okita, T. W.; Edwards, G. E. How do single cell C4 species form dimorphic chloroplasts? *Plant Signaling Behav.* **2011**, *6*, 762−765.
(36) Sharpe, R. M.; Offermann, S. One decade after the discovery of single-cell C4 species in terrestrial plants: what did we learn about the minimal requirements of C4 photosynthesis? *Photosynth. Res.* **2014**, *119*, 169−180.
(37) Li, P.; Ponnala, L.; Gandotra, N.; Wang, L.; Si, Y.; Tausta, S. L.; Kebrom, T. H.; Provart, N.; Patel, R.; Myers, C. R.; et al. The developmental dynamics of the maize leaf transcriptome. *Nat. Genet.* **2010**, *42*, 1060−1067.
(38) Pick, T. R.; Bräutigam, A.; Schlüter, U.; Denton, A. K.; Colmsee, C.; Scholz, U.; Fahnenstich, H.; Pieruschka, R.; Rascher, U.; Sonnewald, U.; et al. Systems analysis of a maize leaf developmental gradient redefines the current C4 model and provides candidates for regulation. *Plant Cell* **2011**, *23*, 4208−4220.
(39) Wang, J. L.; Turgeon, R.; Carr, J. P.; Berry, J. O. Carbon Sink-to-Source Transition Is Coordinated with Establishment of Cell-Specific Gene Expression in a C4 Plant. *Plant Cell* **1993**, *5*, 289−296.
(40) Koteyeva, N. K.; Voznesenskaya, E. V.; Berry, J. O.; Chuong, S. D. X.; Franceschi, V. R.; Edwards, G. E. Development of structural and biochemical characteristics of C4 photosynthesis in two types of Kranz anatomy in genus Suaeda (family Chenopodiaceae). *J. Exp. Bot.* **2011**, *62*, 3197−3212.
(41) Koteyeva, N. K.; Voznesenskaya, E. V.; Cousins, A. B.; Edwards, G. E. Differentiation of C4 photosynthesis along a leaf developmental gradient in two Cleome species having different forms of Kranz anatomy. *J. Exp. Bot.* **2014**, *65*, 3525−3541.
(42) Aubry, S.; Kelly, S.; Kümpers, B. M. C.; Smith-Unna, R. D.; Hibberd, J. M. Deep evolutionary comparison of gene expression identifies parallel recruitment of trans-factors in two independent origins of C4 photosynthesis. *PLoS Genet.* **2014**, *10*, e1004365.
(43) Nelson, T.; Langdale, J. A. Developmental genetics of C4 photosynthesis. *Annu. Rev. Plant Biol.* **1992**, *43*, 25−47.
(44) Dai, Z.; Ku, M.; Edwards, G. E. C4 photosynthesis (The effects of leaf development on the CO2-concentrating mechanism and photorespiration in maize). *Plant Phys.* **1995**, *107*, 815−825.
(45) Yan, X. X.; Khan, S. S.; Hase, T. T.; Emes, M. J. M.; Bowsher, C. G. C. Differential uptake of photosynthetic and non-photosynthetic proteins by pea root plastids. *FEBS Lett.* **2006**, *580*, 6509−6512.
(46) Wan, J.; Blakeley, S. D.; Dennis, D. T.; Ko, K. Transit peptides play a major role in the preferential import of proteins into leucoplasts and chloroplasts. *J. Biol. Chem.* **1996**, *271*, 31227−31233.
(47) Teng, Y.-S. Y.; Chan, P.-T. P.; Li, H.-M. H. Differential age-dependent import regulation by signal peptides. *PLoS Biol.* **2012**, *10*, e1001416−e1001416.
(48) Ivanova, Y.; Smith, M. D.; Chen, K.; Schnell, D. J. Members of the Toc159 import receptor family represent distinct pathways for protein targeting to plastids. *Mol. Biol. Cell* **2004**, *15*, 3379−3392.
(49) Kubis, S.; Patel, R.; Combe, J.; Bédard, J.; Kovacheva, S.; Lilley, K.; Biehl, A.; Leister, D.; Ríos, G.; Koncz, C.; et al. Functional specialization amongst the Arabidopsis Toc159 family of chloroplast protein import receptors. *Plant Cell* **2004**, *16*, 2059−2077.
(50) Smith, M. D.; Rounds, C. M.; Wang, F.; Chen, K.; Afitlhile, M.; Schnell, D. J. atToc159 is a selective transit peptide receptor for the import of nucleus-encoded chloroplast proteins. *J. Cell Biol.* **2004**, *165*, 323−334.
(51) Teng, Y.-S.; Chan, P.-T.; Li, H.-M. Differential age-dependent import regulation by signal peptides. *PLoS Biol.* **2012**, *10*, e1001416.
(52) Rosnow, J.; Yerramsetty, P.; Berry, J. O.; Okita, T. W.; Edwards, G. E. Exploring mechanisms linked to differentiation and function of dimorphic chloroplasts in the single cell C4 species *Bienertia sinuspersici*. *BMC Plant Biol.* **2014**, *14*, 34.
(53) Krebbers, E.; Seurinck, J.; Herdies, L.; Cashmore, A. R.; Timko, M. P. Four genes in two diverged subfamilies encode the ribulose-1,5-bisphosphate carboxylase small subunit polypeptides of Arabidopsis thaliana. *Plant Mol. Biol.* **1988**, *11*, 745−759.
(54) Dedonder, A.; Rethy, R.; Fredericq, H.; Van Montagu, M.; Krebbers, E. Arabidopsis rbcS genes are differentially regulated by light. *Plant Phys.* **1993**, *101*, 801−808.
(55) Sawchuk, M. G.; Donner, T. J.; Head, P.; Scarpella, E. Unique and overlapping expression patterns among members of photosynthesis-associated nuclear gene families in arabidopsis. *Plant Phys.* **2008**, *148*, 1908−1924.
(56) Ewing, R. M.; Jenkins, G. I.; Langdale, J. A. Transcripts of maize RbcS genes accumulate differentially in C3 and C4 tissues. *Plant Mol. Biol.* **1998**, *36*, 593−599.
(57) Robinson, S. P.; Portis, A. R. Adenosine triphosphate hydrolysis by purified rubisco activase. *Arch. Biochem. Biophys.* **1989**, *268*, 93−99.
(58) Spreitzer, R. J.; Salvucci, M. E. Rubisco: structure, regulatory interactions, and possibilities for a better enzyme. *Annu. Rev. Plant Biol.* **2002**, *53*, 449−475.
(59) Rundle, S. J.; Zielinski, R. E. Organization and expression of two tandemly oriented genes encoding ribulosebisphosphate carboxylase/oxygenase activase in barley. *J. Biol. Chem.* **1991**, *266*, 4677−4685.
(60) Salvucci, M. E.; van de Loo, F. J.; Stecher, D. Two isoforms of Rubisco activase in cotton, the products of separate genes not alternative splicing. *Planta* **2003**, *216*, 736−744.
(61) Zhang, N.; Portis, A. R. Mechanism of light regulation of Rubisco: a specific role for the larger Rubisco activase isoform involving reductive activation by thioredoxin-f. *Proc. Natl. Acad. Sci. U. S. A.* **1999**, *96*, 9438−9443.
(62) Flugge, U. I.; Heldt, H. W. The phosphate-triose phosphate-phosphoglycerate translocator of the chloroplast. *Trends Biochem. Sci.* **1984**, *9*, 530−533.
(63) Heldt, H. W.; Flugge, U. I.; Borchert, S. Diversity of specificity and function of phosphate translocators in various plastids. *Plant Phys.* **1991**, *95*, 341−343.
(64) Edwards, G. E.; Voznesenskaya, E. V. C4 Photosynthesis: Kranz Forms and Single-Cell C4 in Terrestrial Plants. In *C4 Photosynthesis and Related CO_2 Concentrating Mechanisms*; Sage, R. F., Raghavendra, A. S., Eds.; Advances in Photosynthesis and Respiration; Springer: Dordrecht, The Netherlands, 2011; Vol. *32*, pp 29−61.
(65) Weiner, H.; Heldt, H. W. Inter-and intracellular distribution of amino acids and other metabolites in maize (*Zea mays* L.) leaves. *Planta* **1992**, *187*, 242−246.
(66) Ku, S. B.; Edwards, G. E. Photosynthesis in mesophyll protoplasts and bundle sheath cells of various types of C4 plants IV. Enzymes of respiratory metabolism and energy utilizing enzymes of photosynthetic pathways. *Z. Pflanzenphysiol.* **1975**, *77*, 16−32.
(67) Yoshimura, Y.; Kubota, F.; Ueno, O. Structural and biochemical bases of photorespiration in C4 plants: quantification of organelles and glycine decarboxylase. *Planta* **2004**, *220*, 307−317.
(68) Hattersley, P. W.; Watson, L. Diversification of photosynthesis. In *Grass Evolution and Domestication*; Chapman, G. P., Ed.; Cambridge University Press: Cambridge, U.K., 2009; pp 38−116.
(69) Edwards, G. E.; Walker, D. A. Three C4 subgroups: Biochemistry, Photochemistry and Taxonomy. In *C3,C4: Mechanisms, and Cellular and Environmental Regulation, of Photosynthesis*; Blackwell Scientific Publications: Oxford, U.K., 1983; pp 292−322.
(70) Pfundel, E.; Neubohn, B. Assessing photosystem I and II distribution in leaves from C4 plants using confocal laser scanning microscopy. *Plant, Cell Environ.* **2002**, *22*, 1569−1577.
(71) Shikanai, T. Cyclic electron transport around photosystem I: genetic approaches. *Annu. Rev. Plant Biol.* **2007**, *58*, 199−217.

DOI: 10.1021/pr5011907
J. Proteome Res. 2015, 14, 2090−2108

(72) Takabayashi, A.; Kishine, M.; Asada, K.; Endo, T.; Sato, F. Differential use of two cyclic electron flows around photosystem I for driving CO2-concentration mechanism in C4 photosynthesis. *Proc. Natl. Acad. Sci. U. S. A.* **2005**, *102*, 16898−16903.
(73) Kanai, R.; Edwards, G. E. Separation of mesophyll protoplasts and bundle sheath cells from maize leaves for photosynthetic studies. *Plant Phys.* **1973**, *51*, 1133−1137.
(74) Nelson, T.; Langdale, J. A. Patterns of leaf development in C4 plants. *Plant Cell* **1989**, *1*, 3−13.
(75) Sheen, J. Y.; Bogorad, L. Differential expression of the ribulose bisphosphate carboxylase large subunit gene in bundle sheath and mesophyll cells of developing maize leaves is influenced by light. *Plant Phys.* **1985**, *79*, 1072−1076.
(76) Raines, C. A. The Calvin cycle revisited. *Photosynth. Res.* **2003**, *75*, 1−10.
(77) Uematsu, K.; Suzuki, N.; Iwamae, T.; Inui, M.; Yukawa, H. Increased fructose 1,6-bisphosphate aldolase in plastids enhances growth and photosynthesis of tobacco plants. *J. Exp. Bot.* **2012**, *63*, 3001−3009.
(78) Dai, Z.; Ku, M.; Edwards, G. E. C4 photosynthesis (The CO2-concentrating mechanism and photorespiration). *Plant Phys.* **1993**, *103*, 83−90.
(79) Dai, Z.; Ku, M. S.; Edwards, G. E. Oxygen sensitivity of photosynthesis and photorespiration in different photosynthetic types in the genus Flaveria. *Planta* **1996**, *198*, 563−571.
(80) Zelitch, I.; Schultes, N. P.; Peterson, R. B.; Brown, P.; Brutnell, T. P. High glycolate oxidase activity is required for survival of maize in normal air. *Plant Phys.* **2009**, *149*, 195−204.
(81) Usuda, H.; Edwards, G. E. Localization of glycerate kinase and some enzymes for sucrose synthesis in C3 and C4 plants. *Plant Phys.* **1980**, *65*, 1017−1022.
(82) Park, J.; Okita, T. W.; Edwards, G. E. Expression profiling and proteomic analysis of isolated photosynthetic cells of the non-Kranz C4 species *Bienertia sinuspersici*. *Funct. Plant Biol.* **2010**, *37*, 1−13.
(83) Ludwig, M. Carbonic anhydrase and the molecular evolution of C4 photosynthesis. *Plant, Cell Environ.* **2012**, *35*, 22−37.
(84) Tetu, S. G.; Tanz, S. K.; Vella, N.; Burnell, J. N.; Ludwig, M. The Flaveria bidentis beta-carbonic anhydrase gene family encodes cytosolic and chloroplastic isoforms demonstrating distinct organ-specific expression patterns. *Plant Phys.* **2007**, *144*, 1316−1327.
(85) Majeran, W.; van Wijk, K. J. Cell-type-specific differentiation of chloroplasts in C4 plants. *Trends Plant Sci.* **2009**, *14*, 100−109.
(86) Hatch, M. D.; Kagawa, T.; Craig, S. Subdivision of C4-pathway species based on differing C4 acid decarboxylating systems and ultrastructural features. *Aust. J. Plant Physiol.* **1975**, *2*, 111.
(87) Hatch, M. D.; Kagawa, T. Photosynthetic activities of isolated bundle sheath cells in relation to differing mechanisms of C4 pathway photosynthesis. *Arch. Biochem. Biophys.* **1976**, *175*, 39−53.
(88) Kanai, R.; Edwards, G. E. Biochemistry of C4 Photosynthesis. In *C_4 Plant Biology*; Sage, R. F., Monson, R. K., Eds.; Academic Press: New York, 1999; pp 49−87.
(89) Bräutigam, A.; Kajala, K.; Wullenweber, J.; Sommer, M.; Gagneul, D.; Weber, K. L.; Carr, K. M.; Gowik, U.; Maß, J.; Lercher, M. J.; et al. An mRNA blueprint for C4 photosynthesis derived from comparative transcriptomics of closely related C3 and C4 species. *Plant Phys.* **2011**, *155*, 142−156.
(90) Sommer, M.; Brautigam, A.; Weber, A. P. M. The dicotyledonous NAD malic enzyme C4 plant *Cleome gynandra* displays age-dependent plasticity of C4 decarboxylation biochemistry. *Plant Biol.* **2012**, *14*, 621−629.
(91) Lung, S.-C.; Yanagisawa, M.; Chuong, S. D. X. Protoplast isolation and transient gene expression in the single-cell C4 species *Bienertia sinuspersici*. *Plant Cell Rep.* **2010**, *30*, 473−484.
(92) Long, J. J.; Berry, J. O. Tissue-specific and light-mediated expression of the C4 photosynthetic NAD-dependent malic enzyme of Amaranth mitochondria. *Plant Phys.* **1996**, *112*, 473−482.
(93) Wedding, R. T. Malic enzymes of higher plants: characteristics, regulation, and physiological function. *Plant Phys.* **1989**, *90*, 367−371.
(94) Maier, A.; Zell, M. B.; Maurino, V. G. Malate decarboxylases: evolution and roles of NAD(P)-ME isoforms in species performing C4 and C3 photosynthesis. *J. Exp. Bot.* **2011**, *62*, 3061−3069.
(95) Tronconi, M. A.; Fahnenstich, H.; Gerrard Weehler, M. C.; Andreo, C. S.; Flugge, U. I.; Drincovich, M. F.; Maurino, V. G. Arabidopsis NAD-Malic enzyme functions as a homodimer and heterodimer and has a major impact on nocturnal metabolism. *Plant Phys.* **2008**, *146*, 1540−1552.
(96) Brown, N. J.; Newell, C. A.; Stanley, S.; Chen, J. E.; Perrin, A. J.; Kajala, K.; Hibberd, J. M. Independent and parallel recruitment of preexisting mechanisms underlying C4 photosynthesis. *Science* **2011**, *331*, 1436−1439.
(97) Taniguchi, M.; Sugiyama, T. The expression of 2-oxoglutarate/malate translocator in the bundle-sheath mitochondria of *Panicum miliaceum*, a NAD-malic enzyme-type C4 plant, is regulated by light and development. *Plant Phys.* **1997**, *114*, 285−293.
(98) Bräutigam, A.; Hoffmann-Benning, S.; Hofmann-Benning, S.; Weber, A. P. M. Comparative proteomics of chloroplast envelopes from C3 and C4 plants reveals specific adaptations of the plastid envelope to C4 photosynthesis and candidate proteins required for maintaining C4 metabolite fluxes. *Plant Phys.* **2008**, *148*, 568−579.
(99) Palmieri, L.; Picault, N.; Arrigoni, R.; Besin, E.; Palmieri, F.; Hodges, M. Molecular identification of three *Arabidopsis thaliana* mitochondrial dicarboxylate carrier isoforms: organ distribution, bacterial expression, reconstitution into liposomes and functional characterization. *Biochem. J.* **2008**, *410*, 621−629.
(100) Aoki, N.; Ohnishi, J.-I.; Kanai, R. Two different mechanisms for transport of pyruvate into mesophyll chloroplasts of C4 plants—a comparative study. *Plant Cell Physiol.* **1992**, *33*, 805−809.
(101) Ohnishi, J.-I.; Flügge, U.-I.; Heldt, H. W.; Kanai, R. Involvement of Na+ in active uptake of pyruvate in mesophyll chloroplasts of some C4 plants. *Plant Phys.* **1990**, *94*, 950−959.
(102) Edwards, G. E.; Nakamoto, H.; Burnell, J. N. Pyruvate, Pi dikinase and NADP-malate dehydrogenase in C4 photosynthesis: properties and mechanism of light/dark regulation. *Annu. Rev. Plant Phys.* **1985**, *36*, 255−286.
(103) Fischer, K.; Kammerer, B.; Gutensohn, M.; Arbinger, B.; Weber, A.; Hausler, R. E.; Flugge, U. I. A new class of plastidic phosphate translocators: a putative link between primary and secondary metabolism by the phosphoenolpyruvate/phosphate antiporter. *Plant Cell* **1997**, *9*, 453−462.
(104) von Caemmerer, S.; Quick, W. P.; Furbank, R. T. The development of C4 rice: current progress and future challenges. *Science* **2012**, *336*, 1671−1672.
(105) Covshoff, S.; Hibberd, J. M. Integrating C4 photosynthesis into C3 crops to increase yield potential. *Curr. Opin. Biotechnol.* **2012**, *23*, 209−214.

DOI: 10.1021/pr5011907
J. Proteome Res. 2015, 14, 2090−2108

2.2 Publication II

Development, subcellular positioning and selective protein accumulation in the dimorphic chloroplasts of single-cell C4 species

Matthias Erlinghaeuser[1]*, Lisa Hagenau[1]*, Diana Wimmer[1]*, Sascha Offermann[1]

[1] Institute of Botany, Leibniz University, Herrenhaeuser Strasse 2, Hannover 30419, Germany

* equally contributed

Type of authorship:	First author
Type of article:	Review article
Share of the work:	30 %
Contribution to the publication:	prepared some figures and wrote parts of the paper
Journal:	Current Opinion in Plant Biology
5-year impact factor:	7.843
Date of publication:	April 11th, 2016
Number of citations (google scholar on May 19th, 2017):	2
DOI:	10.1016/j.pbi.2016.03.017
PubMed-ID:	27061048

Available online at www.sciencedirect.com

ScienceDirect

Current Opinion in Plant Biology

Development, subcellular positioning and selective protein accumulation in the dimorphic chloroplasts of single-cell C_4 species

Matthias Erlinghaeuser[1], Lisa Hagenau[1], Diana Wimmer[1] and Sascha Offermann

C_4 photosynthesis is typically associated with a carbon concentrating mechanism based on close collaboration between two photosynthetic cell types (Kranz C_4). Surprisingly, four species in the family Chenopodiaceae have been described, which perform all required steps for a functional and effective C_4 cycle within individual photosynthetic cells. These single-cell C_4 species utilize a unique subcellular compartmentation and two functionally different chloroplast types that mimic the functions of the two cell types of the Kranz C_4 system. In this review, we will summarize and discuss studies on chloroplast development, positioning and selective accumulation of nuclear encoded proteins, which ultimately allow the operation of a C_4 carbon concentrating mechanism within individual cells.

Address
Institute for Botany, Leibniz University Hannover, Germany

Corresponding author: Offermann, Sascha (s.offermann@botanik.uni-hannover.de)
[1] These authors contributed equally to the manuscript.

Current Opinion in Plant Biology 2016, **31**:76–82

This review comes from a themed issue on **Physiology and metabolism**

Edited by **Robert T Furbank** and **Rowan F Sage**

For a complete overview see the Issue and the Editorial

Available online 11th April 2016

http://dx.doi.org/10.1016/j.pbi.2016.03.017

Introduction

The majority of terrestrial C_4 plants utilize a carbon concentrating mechanism (CCM) that strictly relies on the cooperation of two different photosynthetic cell types that are arranged in a characteristic wreath-like pattern, commonly referred to as Kranz anatomy. An exciting exception from the C_4 equals Kranz rule was discovered within the family Chenopodiaceae, where a total of four species have been described to date that perform the CO_2 concentrating steps within individual photosynthetic cells [1–4]. These so-called single-cell C_4 species (SCC_4) separate the primary and secondary carbon fixation steps between distinct subcellular compartments. Currently, two structurally different types of SCC_4 are distinguished. In *Sueada aralocaspica*, the two distinct subcellular compartments are localized at opposing poles whereas in the Bienertia type one compartment is found internal to the other one. Most information currently available on SCC_4 comes from the model species *Bienertia sinuspersici* (from here on Bienertia). In Bienertia, one chloroplast type is located in a peripheral compartment (PC) and is specialized for the generation of the primary CO_2 acceptor phospho*enol*pyruvate (PEP) (Figure 1). The second chloroplast type is accompanied by mitochondria located in a central compartment (CC) and is specialized for final CO_2 fixation and the Calvin–Benson–Bassham (CBB) cycle. Such a biochemical and functional differentiation of two different chloroplasts within individual cells has not been observed so far outside of SCC_4 species and therefore represents a novum in plant cell biology.

The general biochemistry, physiology and gas exchange properties of SCC_4 photosynthesis have been studied in detail. In summary, the results show that the peripheral and central compartment of SCC_4 resemble the functions of mesophyll cells (MC) and bundle sheath cells (BSC) of Kranz C_4 species, respectively [5]. Also, the C_4 biochemistry seems conserved between single-cell and Kranz-type C_4 [6•], and SCC_4 species are as efficient in concentrating carbon as related Kranz C_4 species [7]. Because of these apparent similarities, the purpose of this review is not to give a comprehensive overview on available SCC_4 literature, which was also recently reviewed [8]. Instead, we want to focus on open questions and recent progress related to the unusual cell biology and the development, positioning and differentiation of the two chloroplast types, which ultimately allow SCC_4 species to perform a complete C_4 cycle within individual cells.

Biochemical differentiation of the two chloroplast types

In order to fulfill their specific roles in SCC_4, the PC and CC chloroplasts need to accumulate distinct sets of proteins, most of them encoded by the cell's nucleus. This includes thylakoid proteins involved in the light reactions (e.g. light harvesting complex proteins; LHCs), stromal proteins of the C_4 cycle (e.g. pyruvate, Pi dikinase; PPDK) and C_3 cycle (e.g. small subunit of Rubisco; RSSU) as well as envelope transporters for shuttling

Figure 1

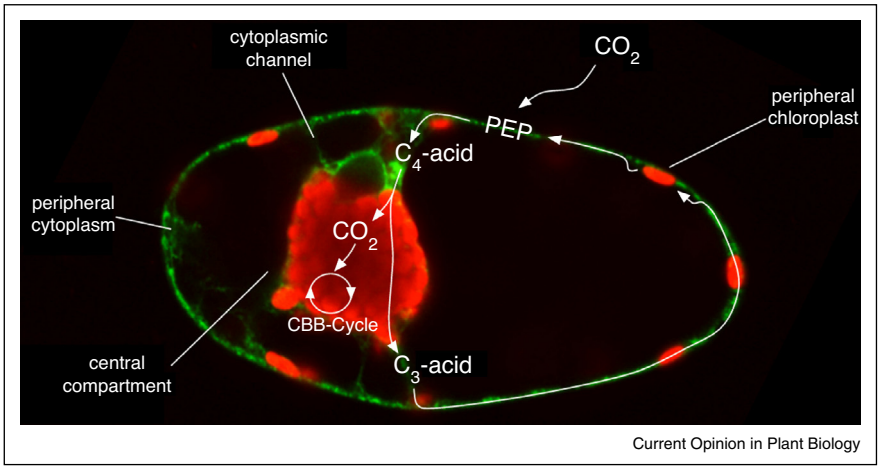

Bienertia cell morphology and carbon concentrating mechanism. Confocal laser scanning image of a Bienertia chlorenchyma cell expressing cytoplasmic localized green fluorescent protein. Chlorophyll autofluorescence is shown in red. CO_2 is fixed into C_4 acids utilizing phosphoenolpyruvate (PEP) generated by the peripheral chloroplasts. The resulting C_4 acids diffuse through cytoplasmic channels into the central compartment. Decarboxylation of C_4 acids occurs via mitochondria (not shown) within the central compartment and the released CO_2 is fixed through the Calvin–Benson–Bassham (CBB) cycle, which occurs exclusively in the CC chloroplasts. C_3 acids diffuse back into the peripheral compartment and are used by the peripheral chloroplasts to regenerate PEP.

metabolites in and out of chloroplasts (e.g. the pyruvate transporter; BASS) [2,5,6•,9]. At least three different scenarios can explain how such a mechanism could work in theory, including selective protein degradation, mRNA targeting and chloroplast type specific import [10] (Figure 2). Currently, very little is known about selective degradation of nuclear encoded chloroplast proteins. One example is the targeted degradation of chloroplast envelope components by the SP1 E3 ligase system. The system tags certain translocon components, which are subsequently degraded by the cytosolic 26S proteasome with ubiquitin and is required for correct chloroplast development [11••,12••]. In SCC_4 species, selective protein degradation has not yet been tested directly and comparative proteomics of isolated CC and PC chloroplasts did not identify any chloroplast type specific proteases [6•]. Therefore, an involvement of protein degradation in SCC_4 remains to be shown.

mRNA targeting has also been suggested as a potential mechanism for differential accumulation of nuclear encoded chloroplast proteins in the SCC_4 system. Typically, the signals for mRNA targeting reside either in the coding region and/or the untranslated region (UTR) of the mRNAs [13,14]. A direct mRNA targeting mechanism has yet to be described for higher plant chloroplasts but the 3′ untranslated region (UTR) of a voltage dependent anion carrier (VDAC) targets a reporter construct specifically for mitochondria in Arabidopsis [15]. This indicates that such a mechanism generally exists in plants. In Bienertia, the UTR of nuclear encoded Rubisco small subunit (rbcS) has been tested for its ability to deliver reporter constructs to either CC and PC chloroplasts, but no differential accumulation was observed [16••]. Therefore, the involvement of mRNA targeting in selective protein accumulation in SCC_4 is currently not supported.

Besides the discussed protein degradation and mRNA targeting pathways, more and more evidence emerges that chloroplasts in general can discriminate directly between different nuclear encoded precursors. The majority of nuclear encoded chloroplast targeted proteins are imported by the chloroplast TOC/TIC (translocon of the outer and inner chloroplast envelope) system. The main TOC complex consists of the central pore (TOC75) and receptor proteins of the TOC159 family (recently reviewed in [17,18]). The latter interact with transit peptides (TP) of precursor proteins. It has been demonstrated that distinct members of the TOC159 receptor family can mediate substrate-specific import [19–22]. For example, TOC159 containing complexes preferentially import photosynthetic precursors, whereas TOC complexes containing TOC132 import preferentially non-photosynthetic housekeeping precursors instead. Consequently, TOC159 family genes are differentially expressed in photosynthetic and non-photosynthetic organs [23–25] and several studies revealed that TPs have different TOC recognition elements according to the import pathway they use [26,27•]. Finally, TPs have also been shown to possess age-selective motifs that are distinguished by chloroplasts of different developmental stages [28]. Taken together, these data demonstrate that the chloroplast translocon

Figure 2

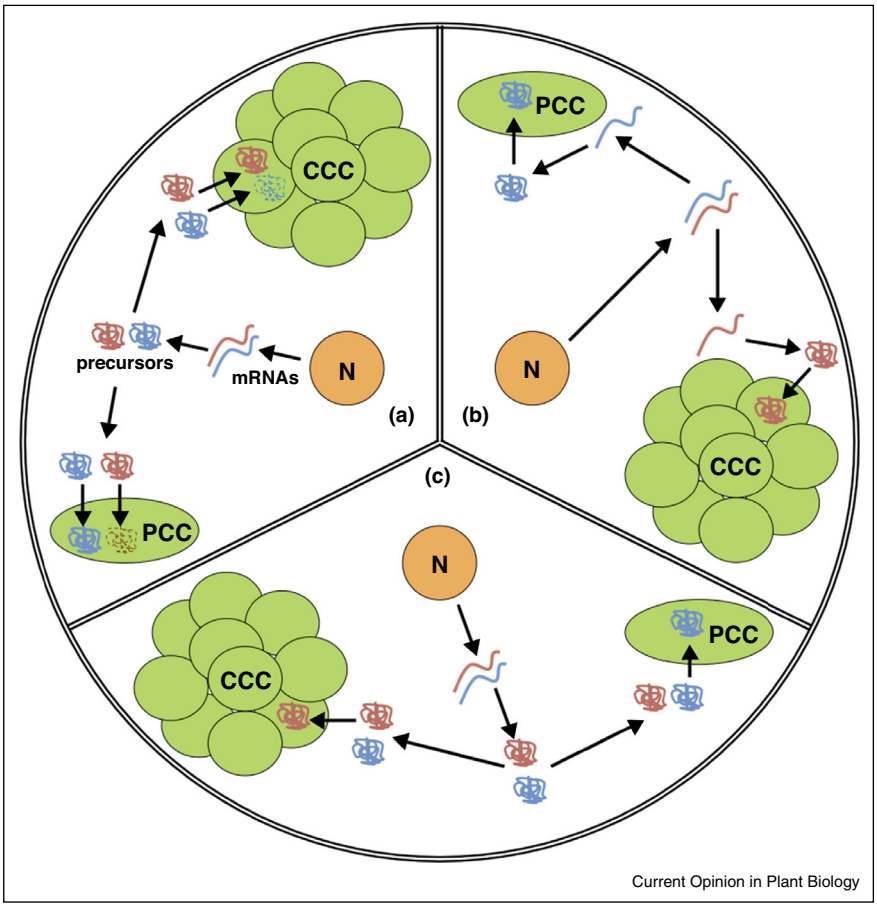

Three hypothetical models that could explain selective protein accumulation in the two chloroplast types of SCC_4 species. **(a)** Selective protein degradation: Nuclear (N) encoded mRNAs are translated into proteins in the cytoplasm that are in turn imported into both chloroplast types. After import, a degradation system removes unwanted proteins from either the central compartment chloroplasts (CCC) or the peripheral compartment chloroplasts (PCC). **(b)** mRNA targeting: mRNAs are targeted specifically to either the peripheral or central compartment and are then translated in close vicinity to the correct chloroplast type. Differential accumulation would not be controlled by the chloroplasts in this model. **(c)** Selective import: The CCC and PCC each have specific translocon receptors that interact with the precursors resulting in different protein uptake characteristics for the two types of chloroplasts.

system possesses enough flexibility that would allow for discrimination and sorting of proteins between the two different chloroplast types of SCC_4 species.

Expression of Bienertia TOC159/TOC132 at different developmental stages of leaves has been analyzed and seems to follow the pattern observed in other plants [29]. This confirms their role in substrate-specific import for photosynthetic and housekeeping proteins. However, Bienertia GFP-TOC fusions did not indicate differential accumulation in one or the other chloroplast type [29]. Furthermore, no evidence for selective TOC159 accumulation or related TOC/TIC components was discovered in a recent comparative proteomics study on the protein composition of the two chloroplast types in Bienertia [6•]. However, only the most abundant translocon components were quantified, so it is possible that less abundant factors were missed. Interestingly, the Bienertia TOC159 receptor itself was found to insert into the outer envelope by a transit peptide like C-terminal extension [29,30•]. In Arabidopsis, insertion of such outer envelope proteins is mediated by the cytoplasmic chaperone ARK2A [31]. If outer envelope receptors of the TOC family are indeed involved in selective protein uptake in the SCC_4 system, future analysis of chaperones can help to shed light on differential targeting of envelope proteins.

Although there is currently no indication for a specific TOC/TIC composition in the two chloroplast types, it is of course possible that TPs of differentially accumulating proteins could interact with unknown components. TPs

have been shown to contain certain sequence domains, for example, a non-charged stromal Hsp70 binding site on the N-terminus [32], a TOC receptor recognition site [26,27•,32] and a domain for the recognition of the stromal processing peptidase [32,33]. All of these domains can interact with different parts of the import apparatus. In Bienertia, bioinformatic comparison revealed no obvious sequence conservation between TPs of precursors that accumulate either in the CC or the PC chloroplasts [6•]. Furthermore, two studies tested experimentally if TPs can mediate differential protein accumulation in the two chloroplast types. In both studies, TP-GFP fusions localized in chloroplasts indicating that the conventional chloroplast import pathway is functional in the SCC_4 system, but no evidence for differential protein accumulation between the two chloroplast types was observed [16••,34]. This indicates that the TP is either not sufficient for differential protein accumulation or that the utilized test system (both studies used transient expression in protoplasts with GFP fusions) was not suitable for testing this question. In summary, no conclusive evidence has been presented so far for either of the three hypothesized mechanisms of selective protein accumulation in SCC_4 species.

Chloroplast development and subcellular positioning of the two chloroplast types

One of the most interesting features of SCC_4 is the development and coexistence of two chloroplast types and their unusual positioning within individual chlorenchyma cells. This specific positioning is believed to be crucial for functional SCC_4 photosynthesis [1,35,36]. In the mature stage, the two chloroplast types are fully differentiated with different biochemistry (C_4 and C_3 cycle related enzymes [2,5,6•,36], physiology (CO_2 fixation [5], PSII distribution [16••,6•] and redox state [16••]) and morphology (PC chloroplasts are bigger and have a characteristic donut-like shape [2,5]) (Figure 3). This differentiation goes along with the clear subcellular positioning in the peripheral and central compartment. In contrast, very young chlorenchyma cells have only one discernible chloroplast type that contains Rubisco but not the typical C_4 marker PPDK [9]. Microscopy of developing Bienertia tissues also revealed an intermediate stage where the CC and PC chloroplasts are clearly visible, but the cell has not yet reached its final size and thus complete separation of the subcellular compartments [9,36,37]. At this stage, the two chloroplast types are structurally (size and shape) indistinguishable. An early study found a lesser amount of Rubisco in the peripheral chloroplasts at the intermediate stage [9] which might indicate that chloroplast positioning and biochemical differentiation progress simultaneously. However, a recent immunolocalization study in Bienertia correlated the biochemical differentiation with structural adaption and chloroplast positioning in more detail. The results indicate clearly that in the SCC_4 system biochemical differentiation occurs only after final chloroplast positioning [38•].

In general, chloroplasts have the ability to change their subcellular position in response to high or low light [39,40]. However, Bienertia chloroplasts typically do not change their position within the cell under varying light conditions except for very prolonged low light treatment. Even then, only the central compartment moves towards the light source while the peripheral chloroplasts remain immobile [36,37]. Interestingly, this is in contrast to the situation in Kranz C_4 species. Here, the MSC chloroplasts show light-dependent movement while BSC chloroplast stay immobile. Moreover, the chloroplasts move individually and not as a unit as observed in Bienertia [41,42]. Overall, this suggests a different mechanism of light-dependent chloroplast movement operates in SCC_4 as opposed to Kranz C_4 species.

The cytoskeleton has been repeatedly implicated in chloroplast movement and positioning in plants [43–45]. There is somewhat conflicting data on the role of microtubules in maintaining chloroplast position and the integrity of the central compartment in Bienertia. Whereas one study showed disintegration of the central compartment after treatment with the microtubule disrupting drug oryzalin [46], another study observed changes in chloroplast distribution only after application of additional osmotic stress [37]. Accordingly, the authors theorized that the vacuole pressure could be responsible for keeping the chloroplasts in place even after disintegration of the cytoskeleton. Additionally, immunolocalization studies revealed that actin filaments wrap around the PC chloroplast and the central compartment in ring-like structures [46]. Interestingly, the actin filaments around the PC chloroplasts appear stronger under prolonged low light conditions which has been proposed to contribute to their immobility under changing light conditions [37]. However, treatment of Bienertia cells with actin-disrupting cytochalasin B showed no differences in chloroplast positioning [46,37]. Likewise, BS chloroplasts of the Kranz C_4 plant finger millet stay in place even after actin-disrupting drug treatment [41]. This is in contrast to chloroplasts of Arabidopsis where chloroplast positioning is sensitive to actin disruption [47] and could point to systematic differences in the chloroplast movement and positioning between C_3 and C_4 species. In Arabidopsis, chloroplast unusual positioning 1 (CHUP1) is located at the chloroplast outer membrane and has been identified together with kinesin-like protein for actin-based chloroplast movement 1 (KAC1) and KAC2 as essential for chloroplast anchoring [48,49•]. CHUP and KAC homologs have recently also been identified in the transcriptome of Bienertia, but their involvement in the positioning of the two chloroplasts types remains yet to be shown [6•].

Figure 3

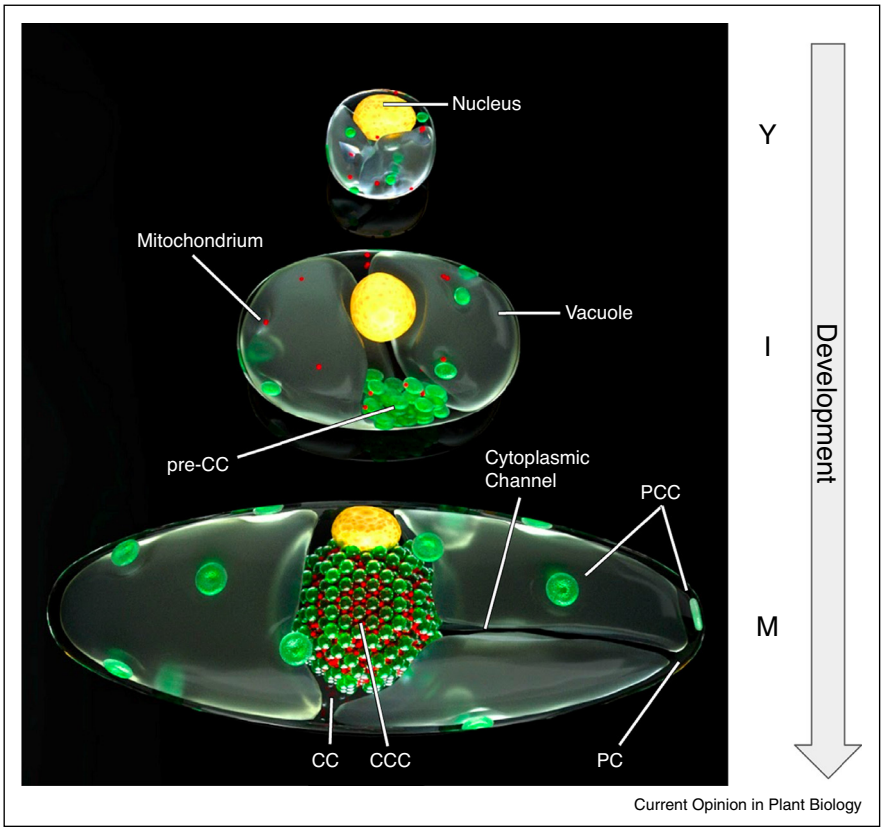

Chlorenchyma cell development in Bienertia. Young (Y) cells have only a single chloroplast type and show no indication for the SCC_4 typical subcellular compartmentation. Nucleus (yellow) and vacuole (opaque) occupy most of the cell's volume, and mitochondria (red) are scattered throughout the cell. In the intermediate (I) stage, chloroplasts are morphologically still indistinguishable but some start aggregating to form a pre-central compartment (pre-CC). In the mature (M) stage, the PC chloroplasts (PCC) and CC chloroplasts (CCC) are fully differentiated and all mitochondria are located within the CC. Cytoplasmic channels traverse the central vacuole and connect the PC with the CC. Note that the cytoplasmic channels make the vacuole appear to be compartmentalized although it has been demonstrated that mature chlorenchyma cells posses only a single central vacuole.
Source: Modified from Ref. [37].

Future perspectives

In conclusion, the mechanisms of chloroplast development and positioning in SCC_4 species are currently not well understood. This is not surprising, considering the complexity of chloroplast development in general. Several plant hormone signaling pathways, anterograde and retrograde signaling between the chloroplast and nucleus and the involvement of the ubiquitin-proteasome interact in chloroplast biogenesis. The situation is even more complicated in Kranz C_4 species in which two functionally specialized chloroplast types develop in two separate photosynthetic tissues and culminates in SCC_4 species where this differentiation occurs under the control of a single nucleus within individual cells. Clearly, further studies in SSC_4 as well as Kranz C_4 species are needed. For this, not only the hypotheses discussed here, but also alternative possibilities should be taken into consideration when designing future experiments.

Acknowledgments

We are very grateful to Hillary Cirka for the language editing of the manuscript. Work in the S.O. lab has been supported by the Deutsche Forschungsgemeinschaft under grant number OF106/1.

References and recommended reading

Papers of particular interest, published within the period of review, have been highlighted as:

- • of special interest
- •• of outstanding interest

1. Voznesenskaya EV, Franceschi VR, Kiirats O, Freitag H, Edwards GE: **Kranz anatomy is not essential for terrestrial C_4 plant photosynthesis**. *Nature* 2001, **414**:543-546.

2. Voznesenskaya EV, Franceschi VR, Kiirats O, Artyusheva EG, Freitag H, Edwards GE: **Proof of C_4 photosynthesis without Kranz anatomy in *Bienertia cycloptera* (Chenopodiaceae)**. *Plant J* 2002, **31**:649-662.

3. Akhani H, Barroca J, Koteeva N, Voznesenskaya E, Franceschi V, Edwards G, Ghaffari SM, Ziegler H: ***Bienertia sinuspersici* (Chenopodiaceae): a new species from Southwest Asia and**

discovery of a third terrestrial C_4 plant without Kranz anatomy. *Syst Bot* 2005, **30**:290-301.

4. Akhani H, Chatrenoor T, Dehghani M, Khoshravesh R, Mahdavi P, Matinzadeh Z: **A new species of *Bienertia* (Chenopodiaceae) from Iranian salt deserts: a third species of the genus and discovery of a fourth terrestrial C_4 plant without Kranz anatomy**. *Plant Biosyst* 2012, **146**:550-559.

5. Offermann S, Okita TW, Edwards GE: **Resolving the compartmentation and function of C_4 photosynthesis in the single-cell C_4 species *Bienertia sinuspersici***. *Plant Physiol* 2011, **155**:1612-1628.

6. • Offermann S, Friso G, Doroshenk KA, Sun Q, Sharpe RM, Okita TW, Wimmer D, Edwards GE, van Wijk KJ: **Developmental and subcellular organization of single-cell C_4 photosynthesis in *Bienertia sinuspersici* determined by large-scale proteomics and cDNA assembly from 454 DNA sequencing**. *J Proteome Res* 2015, **14**:2090-2108.

This study provides a comprehensive overview of the developmental induction of the SCC_4 system and the subcellular localization of the involved proteins by quantitative proteomics.

7. King JL, Edwards GE, Cousins AB: **The efficiency of the CO_2-concentrating mechanism during single-cell C_4 photosynthesis**. *Plant Cell Environ* 2012, **35**:513-523.

8. Sharpe RM, Offermann S: **One decade after the discovery of single-cell C_4 species in terrestrial plants: what did we learn about the minimal requirements of C_4 photosynthesis?** *Photosynth Res* 2014, **119**:169-180.

9. Voznesenskaya EV, Koteyeva NK, Chuong SD, Akhani H, Edwards GE, Franceschi VR: **Differentiation of cellular and biochemical features of the single-cell C_4 syndrome during leaf development in *Bienertia cycloptera* (Chenopodiaceae)**. *Am J Bot* 2005, **92**:1784-1795.

10. Offermann S, Okita TW, Edwards GE: **How do single cell C_4 species form dimorphic chloroplasts?** *Plant Signal Behav* 2011, **6**:762-765.

11. •• Ling Q, Huang W, Baldwin A, Jarvis P: **Chloroplast biogenesis is regulated by direct action of the ubiquitin–proteasome system**. *Science* 2012, **338**:655-659.

The authors discovered a new degradation mechanism for the regulation of the chloroplast protein import via the TOC/TIC complex. The described Ubiquitin E3 Ligase SP1 system is necessary for the biogenesis of chloroplasts as well as for stress tolerance in plants.

12. •• Ling Q, Jarvis P: **Regulation of chloroplast protein import by the ubiquitin E3 ligase SP1 is important for stress tolerance in plants**. *Curr Biol* 2015, **25**:2527-2534.

See annotation to Ref. [11••].

13. Garcia M, Delaveau T, Goussard S, Jacq C: **Mitochondrial presequence and open reading frame mediate asymmetric localization of messenger RNA**. *EMBO Rep* 2010, **11**:285-291.

14. Gadir N, Haim-Vilmovsky L, Kraut-Cohen J, Gerst JE: **Localization of mRNAs coding for mitochondrial proteins in the yeast *Saccharomyces cerevisiae***. *RNA* 2011, **17**:1551-1565.

15. Michaud M, Ubrig E, Filleur S, Erhardt M, Ephritikhine G, Maréchal-Drouard L, Duchêne AM: **Differential targeting of VDAC3 mRNA isoforms influences mitochondria morphology**. *Proc Natl Acad Sci U S A* 2014, **111**:8991-8996.

16. •• Rosnow J, Yerramsetty P, Berry JO, Okita TW, Edwards GE: **Exploring mechanisms linked to differentiation and function of dimorphic chloroplasts in the single cell C_4 species *Bienertia sinuspersici***. *BMC Plant Biol* 2014, **14**:34.

This paper tries to resolve the mechanism of differentiation and the function of the dimorphic chloroplasts in *Bienertia sinuspersici* and gives first hints for understanding the problem.

17. Demarsy E, Lakshmanan AM, Kessler F: **Border control: selectivity of chloroplast protein import and regulation at the TOC-complex**. *Front Plant Sci* 2014, **5**:483.

18. Paila YD, Richardson LG, Schnell DJ: **New insights into the mechanism of chloroplast protein import and its integration with protein quality control, organelle biogenesis and development**. *J Mol Biol* 2015, **427**:1038-1060.

19. Bauer J, Chen K, Hiltbunner A, Wehrli E, Eugster M, Schnell D, Kessler F: **The major protein import receptor of plastids is essential for chloroplast biogenesis**. *Nature* 2000, **403**:203-207.

20. Ivanova Y, Smith MD, Chen K, Schnell DJ: **Members of the Toc159 import receptor family represent distinct pathways for protein targeting to plastids**. *Mol Biol Cell* 2004, **15**:3379-3392.

21. Smith MD, Rounds CM, Wang F, Chen K, Afitlhile M, Schnell DJ: **atToc159 is a selective transit peptide receptor for the import of nucleus-encoded chloroplast proteins**. *J Cell Biol* 2004, **165**:323-334.

22. Inoue H, Rounds C, Schnell DJ: **The molecular basis for distinct pathways for protein import into *Arabidopsis* chloroplasts**. *Plant Cell* 2010, **22**:1947-1960.

23. Yu TS, Li HM: **Chloroplast protein translocon components atToc159 and atToc33 are not essential for chloroplast biogenesis in guard cells and root cells**. *Plant Physiol* 2001, **127**:90-96.

24. Kubis S, Patel R, Combe J, Bédard J, Kovacheva S, Lilley K, Biehl A, Leister D, Ríos G, Koncz C, Jarvis P: **Functional specialization amongst the *Arabidopsis* Toc159 family of chloroplast protein import receptors**. *Plant Cell* 2004, **16**:2059-2077.

25. Yan J, Campbell JH, Glick BR, Smith MD, Liang Y: **Molecular characterization and expression analysis of chloroplast protein import components in tomato (*Solanum lycopersicum*)**. *PLoS ONE* 2014, **9**:e95088.

26. Lee DW, Lee S, Oh YJ, Hwang I: **Multiple sequence motifs in the Rubisco small subunit transit peptide independently contribute to Toc159-dependent import of proteins into chloroplasts**. *Plant Physiol* 2009, **151**:129-141.

27. • Lee DW, Woo S, Geem KR, Hwang I: **Sequence motifs in transit peptides act as independent functional units and can be transferred to new sequence contexts**. *Plant Phys* 2015, **169**:471-484.

This work gives new insights into the organisation and structure of transit peptides. It shows that different sequence motifs in the transit peptide can interact independently with different translocon components during the chloroplast import process. Furthermore, these sequence motifs can be transferred to a new sequence context and keep their functionality.

28. Teng YS, Chan PT, Li Hm: **Differential age-dependent import regulation by signal peptides**. *PLoS Biol* 2012, **10**:e1001416.

29. Lung SC, Chuong SD: **A transit peptide-like sorting signal at the C terminus directs the *Bienertia sinuspersici* preprotein receptor Toc159 to the chloroplast outer membrane**. *Plant Cell* 2012, **24**:1560-1578.

30. • Lung SC, Smith MD, Weston JK, Gwynne W, Secord N, Chuong SD: **The C-terminus of *Bienertia sinuspersici* Toc159 contains essential elements for its targeting and anchorage to the chloroplast outer membrane**. *Front Plant Sci* 2014, **5**:722.

This paper describes the structure of the C-terminus of *Bienertia sinuspersici* TOC159 in detail and it shows for the first time the critical sequence elements for efficient targeting and anchorage in the outer envelope.

31. Kim DH, Lee JE, Xu ZY, Geem KR, Kwon Y, Park JW, Hwang I: **Cytosolic targeting factor AKR2A captures chloroplast outer membrane-localized client proteins at the ribosome during translation**. *Nat Commun* 2015, **6**:6843.

32. Chotewutmontri P, Reddick LE, McWilliams DR, Campbell IM, Bruce BD: **Differential transit peptide recognition during preprotein binding and translocation into flowering plant plastids**. *Plant Cell* 2012, **24**:3040-3059.

33. Richter S, Lamppa GK: **Determinants for removal and degradation of transit peptides of chloroplast precursor proteins**. *J Biol Chem* 2002, **277**:43888-43894.

34. Lung SC, Yanagisawa M, Chuong SD: **Protoplast isolation and transient gene expression in the single-cell C_4 species, *Bienertia sinuspersici***. *Plant Cell Rep* 2010, **30**:473-484.

35. Edwards GE, Franceschi VR, Voznesenskaya EV: **Single-cell C_4 photosynthesis versus the dual-cell (Kranz) paradigm**. *Annu Rev Plant Biol* 2004, **55**:173-196.

36. Lara MV, Offermann S, Smith M, Okita TW, Andreo CS, Edwards GE: **Leaf development in the single-cell C_4 system in *Bienertia sinuspersici*: expression of genes and peptide levels for C_4 metabolism in relation to chlorenchyma structure under different light conditions**. *Plant Physiol* 2008, **148**:593-610.

37. Park J, Knoblauch M, Okita TW, Edwards GE: **Structural changes in the vacuole and cytoskeleton are key to development of the two cytoplasmic domains supporting single-cell C_4 photosynthesis in *Bienertia sinuspersici***. *Planta* 2009, **229**: 369-382.

38. • Koteyeva NK, Voznesenskaya EV, Berry JO, Cousins AB, Edwards GE: **The unique structural and biochemical development of single cell C_4 photosynthesis along longitudinal leaf gradients in *Bienertia sinuspersici* and *Suaeda aralocaspica* (Chenopodiaceae)**. *J Exp Bot* 2016 http://dx.doi.org/10.1093/jxb/erw082.
This paper shows that chloroplast positioning precedes full biochemical differentiation in single-cell C4 species.

39. Wada M, Kagawa T, Sato Y: **Chloroplast movement**. *Annu Rev Plant Biol* 2003, **54**:455-468.

40. Königer M, Bollinger N: **Chloroplast movement behavior varies widely among species and does not correlate with high light stress tolerance**. *Planta* 2012, **236**:411-426.

41. Kobayashi H, Yamada M, Taniguchi M, Kawasaki M, Sugiyama T, Miyake H: **Differential positioning of C_4 mesophyll and bundle sheath chloroplasts: recovery of chloroplast positioning requires the actomyosin system**. *Plant Cell Physiol* 2009, **50**:129-140.

42. Yamada M, Kawasaki M, Sugiyama T, Miyake H, Taniguchi M: **Differential positioning of C_4 mesophyll and bundle sheath chloroplasts: aggregative movement of C_4 mesophyll chloroplasts in response to environmental stresses**. *Plant Cell Physiol* 2009, **50**:1736-1749.

43. Miyake H, Nakamura M: **Some factors concerning the centripetal disposition of bundle sheath chloroplasts during the leaf development of *Eleusine coracana***. *Ann Bot* 1993, **72**:205-211.

44. Kadota A, Yamada N, Suetsugu N, Hirose M, Saito C, Shoda K, Ichikawa S, Kagawa T, Nakano A, Wada M: **Short actin-based mechanism for light-directed chloroplast movement in *Arabidopsis***. *Proc Natl Acad Sci U S A* 2009, **106**:13106-13111.

45. Suetsugu N, Yamada N, Kagawa T, Yonekura H, Uyeda TQ, Kadota A, Wada M: **Two kinesin-like proteins mediate actin-based chloroplast movement in *Arabidopsis thaliana***. *Proc Natl Acad Sci U S A* 2010, **107**:8860-8865.

46. Chuong SD, Franceschi VR, Edwards GE: **The cytoskeleton maintains organelle partitioning required for single-cell C_4 photosynthesis in Chenopodiaceae species**. *Plant Cell* 2006, **18**:2207-2223.

47. Kandasamy MK, Meagher RB: **Actin–organelle interaction: association with chloroplast in *Arabidopsis* leaf mesophyll cells**. *Cell Motil Cytoskeleton* 1999, **44**:110-118.

48. Oikawa K, Yamasato A, Kong SG, Kasahara M, Nakai M, Takahashi F, Ogura Y, Kagawa T, Wada M: **Chloroplast outer envelope protein CHUP1 is essential for chloroplast anchorage to the plasma membrane and chloroplast movement**. *Plant Physiol* 2008, **148**:829-842.

49. • Suetsugu N, Sato Y, Tsuboi H, Kasahara M, Imaizumi T, Kagawa T, Hiwatashi Y, Hasebe M, Wada M: **The KAC family of kinesin-like proteins is essential for the association of chloroplasts with the plasma membrane in land plants**. *Plant Cell Physiol* 2012, **53**:1854-1865.
The authors show that KAC1 and 2 are essential for chloroplast movement as well as chloroplast anchoring to the plasma membrane. They also find that KACs along with CHUP are functionally conserved in land plants.

2.3 Publication III

Transit peptide elements mediate selective protein targeting to two different types of chloroplasts in the single-cell C4 species *Bienertia sinuspersici*

Diana Wimmer[1], Philipp Bohnhorst[1], Vinay Shekhar[2], Inhwan Hwang[3], Sascha Offermann[1]

[1] Institute of Botany, Leibniz University, Herrenhaeuser Strasse 2, Hannover 30419, Germany

[2] Faculty of Biology, Department Biology I – Botany, Ludwig-Maximilians-University Muenchen, Gross haderner Strasse 2-4, 82152 Planegg-Martinsried, Germany.

[3] Division of Integrative Biosciences and Biotechnology, Pohang University of Science and Technology, Pohang 790–784, Korea.

Type of authorship:	First author
Type of article:	Research article
Share of the work:	90 %
Contribution to the publication:	planned and performed all experiments, analyzed data, prepared all figures and wrote the paper
Journal:	Scientific Reports
5-year impact factor:	5.525
Date of publication:	January 23th, 2017
Number of citations (google scholar on May 19th, 2017):	0
DOI:	10.1038/srep41187
PubMed-ID:	28112241

SCIENTIFIC REPORTS

OPEN

Received: 12 October 2016
Accepted: 16 December 2016
Published: 23 January 2017

Transit peptide elements mediate selective protein targeting to two different types of chloroplasts in the single-cell C4 species *Bienertia sinuspersici*

Diana Wimmer[1], Philipp Bohnhorst[1], Vinay Shekhar[2], Inhwan Hwang[3] & Sascha Offermann[1]

Bienertia sinuspersici **is a terrestrial plant that performs C4 photosynthesis within individual cells through operating a carbon concentrating mechanism between different subcellular domains including two types of chloroplasts. It is currently unknown how differentiation of two highly specialized chloroplasts within the same cell occurs as no similar cases have been reported. Here we show that this differentiation in photosynthetic cells of *B. sinuspersici* is enabled by a transit peptide (TP) mediated selective protein targeting mechanism. Mutations in the TPs cause loss of selectivity but not general loss of chloroplast import, indicating the mechanism operates by specifically blocking protein accumulation in one chloroplast type. Hybrid studies indicate that this selectivity is transferable to transit peptides of plants which perform C4 by cooperative function of chloroplasts between two photosynthetic cells. Codon swap experiments as well as introducing an artificial bait mRNA show that RNA affects are not crucial for the sorting process. In summary, our analysis shows how the mechanism of subcellular targeting to form two types of chloroplast within the same cell can be achieved. This information is not only crucial for understanding single-cell C4 photosynthesis; it provides new insights in control of subcellular protein targeting in cell biology.**

Loss of carbon through photorespiration is common in C3 plants especially in warm or dry environments which results in significant decrease in growth and harvestable yields[1]. Photorespiration is initiated when the enzyme responsible for assimilation of carbon dioxide, ribulose 1,5-bisphosphate carboxylase/oxygenase (Rubisco) reacts with oxygen instead of CO_2. Rubisco's oxygenation versus its carboxylation activity increases when the intracellular CO_2 to O_2 ratio decreases as a result of stomatal closure in response to drought or heat stress[2], and because specificity of Rubisco for CO_2 declines with increasing temperature[3]. In order to overcome problems associated with photorespiration, in some plant families, CO_2 concentrating mechanisms evolved, including different forms of C4 photosynthesis. C4 photosynthesis can outperform C3 photosynthesis especially under photorespiratory conditions[4] and this created considerable interest in implementing a C4 cycle into C3 crops such as rice to improve yields and stress tolerance[5,6].

The C4 cycle functions to capture atmospheric CO_2 in one domain (by PEP carboxylase), and concentrate CO_2 in another domain (by decarboxylation of C4 acids) where the CO_2 is then assimilated by Rubisco in the Calvin-Benson-Bassham (CBB) cycle. The vast majority of all known C4 plants use a CO_2 concentrating mechanism based on a dual cell arrangement (Kranz anatomy) with spatial separation of primary and secondary CO_2 fixation reactions in two different cell types (mesophyll cells (MC) and bundle sheath cells (BSC)). However, a remarkable exception was discovered in the family Amaranthaceae. Here, a total of four species are known to perform a complete C4 cycle within individual photosynthetic cells (single-cell C4, SCC4)[7–10]. This is enabled by

[1]Institute for Botany, Leibniz University Hannover, Herrenhaeuser Strasse 2, Hannover 30419, Germany. [2]Faculty of Biology, Department Biology I – Botany, Ludwig-Maximilians-University Muenchen, Grosshaderner Strasse 2-4, 82152 Planegg-Martinsried, Germany. [3]Division of Integrative Biosciences and Biotechnology, Pohang University of Science and Technology, Pohang 790–784, Korea. Correspondence and requests for materials should be addressed to S.O. (email: s.offermann@botanik.uni-hannover.de)

a unique subcellular compartmentalization which to date has not been observed for other plants. Two structural variants of SCC4 exist: In *Suaeda aralocaspica*, two morphologically, biochemically and physiologically different types of chloroplast are located at opposing poles of the photosynthetic cells[9,11], whereas in the three other species (all members of the genus *Bienertia*), one chloroplast type (central (C) chloroplasts) is located in an internal compartment at the center of the cell and the other chloroplast type is located in the periphery close to the plasma membrane (peripheral (P) chloroplasts)[7,8,10,12]. Most information on single-cell C4 photosynthesis comes from the model species *Bienertia sinuspersici* (hereafter referred to as Bienertia). In Bienertia, it has been shown that the two chloroplast types are separated by a single large vacuole[13], which presumably serves as a diffusion barrier between the two reaction compartments. The peripheral and the central compartments are connected by numerous cytoplasmic channels for metabolite exchange[8,14]. The unique subcellular compartmentalization and the specialized biochemistry of the two chloroplast types observed in SCC4 species develop gradually during ontogenesis. In Bienertia, very young cells located at the base of young leaves show only a single chloroplast type that operates in a "default" C3 photosynthetic mode[14,15]. Towards maturation, the two chloroplast types and the peripheral and central domain develop through exposure to yet unknown signals. At the tip of young leaves, the two domains have completely separated, together with biochemical specialization and a fully functional C4 cycle within these cells[14].

Numerous studies have demonstrated that the two chloroplast types accumulate different sets of nuclear encoded proteins according to their specific functions in the C4 and C3 cycle respectively[8,9,15–18]. For example, nuclear encoded pyruvate, Pi-dikinase (PPDK), the key enzyme needed for generation of the primary CO_2 acceptor phospho*enol*pyruvate (PEP) is found specifically in the P-chloroplasts only. In contrast, P-chloroplasts lack Rubisco and a functional CBB cycle, which only operates in the C-chloroplasts. All currently known SCC4 species belong to the NAD-ME C4 subtype where decarboxylation of C4 acid occurs exclusively in mitochondria which in the case of Bienertia are restricted to the central compartment[15,19]. CO_2 released from mitochondrial decarboxylation can then be re-fixed by the adjacent C-chloroplasts. In summary, protein localization studies, gas exchange properties and physiological experiments indicated that the P- and C-chloroplasts of SCC4 species basically resemble the biochemistry and function of MC and BSC chloroplasts of Kranz C4 species[16,17,20,21].

In Kranz C4 species, it has been shown that many nuclear encoded proteins, either directly or indirectly related to their specific function in C4 photosynthesis, accumulate either in MC or BSC chloroplasts[22]. Large-scale expression data indicate that chloroplast type specific protein accumulation patterns can be explained mostly by cell type specific expression differences between MC and BSC[23]. Since the two chloroplasts of Bienertia develop and specialize within individual cells, tissue specific transcriptional control cannot account for the biochemical specialization of the two chloroplast types. Instead, a posttranscriptional mechanism must exist that ensures the correct targeting of proteins either to the P- or C-chloroplasts. It has been speculated that such a mechanism could work either by selective mRNA targeting, selective protein import into the chloroplasts or selective degradation within the two chloroplast types[24,25] but as of now, there is no experimental evidence on the nature of this mechanism.

Here we provide a detailed analysis of the targeting characteristics of recombinant fusion proteins in the SCC4 species *Bienertia sinuspersici*. We show that selective targeting to the peripheral chloroplasts is mediated by specific sequence elements within the transit peptide which are distinct from elements required for general chloroplast import. We provide the first experimental evidence on how subcellular targeting to specialized chloroplasts works and on how SCC4 species can use this to perform C4 photosynthesis within individual cells.

Results

Chloroplast type specific targeting can be replicated *in vivo* in young but not in mature protoplasts. Rubisco small subunit (RSSU) and PPDK are key enzymes operating in the CBB- and the C4 cycle, respectively. Their preferential accumulation in the P- and C-chloroplasts has been demonstrated previously by *in situ* localization studies[8,15] as well as western blot analysis[17] and proteomics[16]. Thus, we used these two markers as a starting point to analyze the mechanism behind selective protein accumulation in Bienertia. A full length precursor of RSSU (RSSU::GFP) and a precursor consisting of the first 224 out of 951 amino acids (AA) of PPDK ($PPDK_{224}$::GFP) were fused to GFP and tested in protoplasts isolated from mature Bienertia chlorenchyma cells. Neither construct showed chloroplast type specific accumulation. Instead, GFP appeared in a speckled pattern, presumably localized in the cytoplasm in the case of $PPDK_{224}$::GFP or accumulated in both chloroplast types in the case of full length RSSU::GFP (Fig. 1A). To test whether the utilization of a non-full length construct in the case of PPDK interfered with general chloroplast import, the same construct was used to transfect *Arabidopsis thaliana* protoplasts (Fig. S1). Here, $PPDK_{224}$::GFP was imported correctly into chloroplasts indicating that the observed mistargeting in mature Bienertia protoplasts is a Bienertia specific effect.

We also tested the influence of different light intensities, temperatures and buffer conditions during the transient expression procedure, as well as inclusion of the 5′UTR regions and testing of different RSSU isoforms. None of it resulted in a noticeable difference in the protein accumulation pattern compared to those observed in Fig. 1A. However, when the same constructs were tested side-by-side in protoplasts prepared from an earlier developmental stage (young chlorenchyma cells Fig. 1B) we observed strikingly different results for $PPDK_{224}$::GFP, since it was now localized predominantly in the P-chloroplasts (Fig. 1C). A similar localization pattern was observed for adenylate kinase (AK) which together with PPDK is involved in regeneration of PEP (Fig. 1D). We also tested localization of chloroplastic triose-phosphate isomerase (TPI). TPI is typically associated with the CBB-cycle and as such, it might not be expected in P-chloroplasts. However, C4 plants are able to export part of the 3-phosphoglycerate produced by the CBB-cycle to the mesophyll chloroplasts (in case of Kranz C4) or to the P-chloroplasts (in case of Bienertia) where it is reduced to glyceraldehyde 3-phosphate (G3P). After conversion by TPI to dihydroxyacetone phosphate (DHAP), triose-phosphates can then shuttle back to the bundle sheath (in case of Kranz C4) or the C-chloroplasts (in case of Bienertia) as part of the triose-phosphate

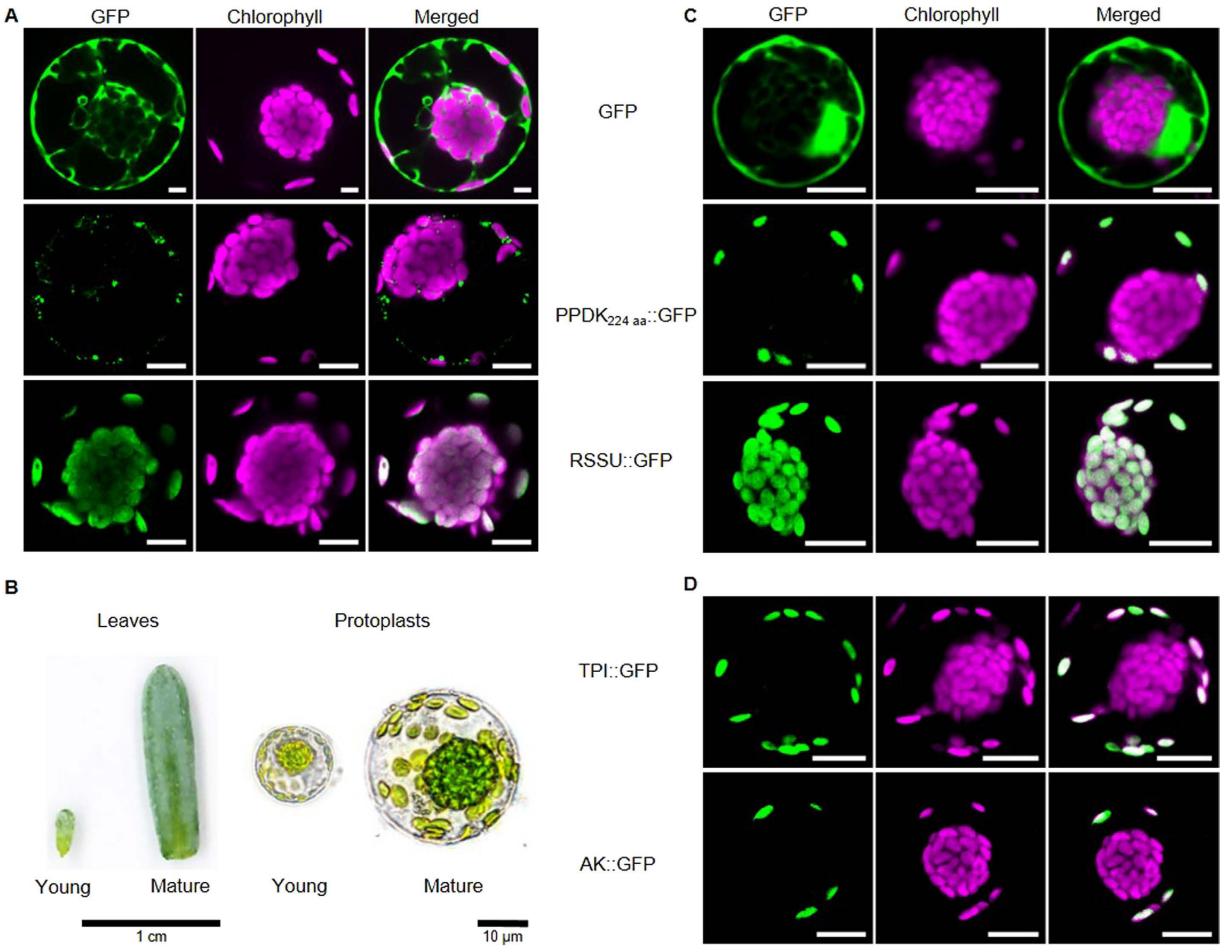

Figure 1. Subcellular localization of chloroplast targeted proteins in different developmental stages of *Bienertia sinuspersici*. (**A**,**C**,**D**) Confocal images of various transiently expressed GFP-fusion proteins in *B. sinuspersici* chlorenchyma protoplasts. All fluorescence images are shown in the GFP channel (green - excitation 488 nm/emission 509/525 nm) and chlorophyll autofluorescence (red - excitation 408 nm/emission 620/700 nm). Additionally, the merged channels are shown. All images are representative from $n \geq 5$ independent experiments. All scale bars = 10 μm. (**A**) Transient expression of GFP, $PPDK_{224}$-GFP and full length RSSU-GFP in mature protoplasts. (**B**) Size comparison between young (Y) and mature (M) leaves and protoplasts. Scale bar leaves = 1 cm; Scale bar protoplasts = 10 μm. (**C** + **D**) Transient expression of GFP, $PPDK_{224}$-GFP, RSSU-GFP, TPI-GFP and AK-GFP in young protoplasts. GFP – green fluorescent protein; PPDK – Pyruvate, Pi dikinase; RSSU – Rubisco small subunit; TPI – triosephosphate isomerase; AK – adenylate kinase.

shuttle (also called "open Calvin cycle"). In Bienertia, the most abundant isoform of TPI was shown to be strongly enriched in the P-chloroplasts[16] and its GFP fusion showed a localization pattern similar to that of PPDK and AK (Fig. 1D). In contrast, full length RSSU::GFP showed no indication for C-specific accumulation even in young protoplasts (Fig. 1C). Accordingly, correct localization of at least the P-targeted proteins in *in vivo* localization studies is dependent on the developmental stage or age of the utilized protoplasts, since correct targeting was observed in young but not mature protoplasts.

The transit peptide contains all information required for P-specificity. To further narrow down the elements necessary for P-specific protein accumulation, we tested if transit peptide (TP)::GFP-fusions of PPDK, AK and TPI (referred to below as TP_PPDK, TP_AK and TP_TPI) are sufficient for P-specific targeting (Fig. 2). In all cases tested, the efficiency in delivering GFP specifically to the P-chloroplasts was similar to the previously tested full length constructs (see Fig. 1C and D). This indicates that the TP already contains all the necessary information.

Discrete elements in the TP control either general import or P-specific import. Next, we analyzed whether discrete elements within the TPs can be identified that control P-specificity. Therefore, we constructed mutant TPI TP sequences where clusters of eight amino acids were sequentially substituted with alanines (Fig. 3A) under the assumption that this substitution would interfere with the inherent function of the underlying AA sequence. Mutations in cluster I generally resulted in no observable GFP expression, probably through interference of the induced mutations with translation. Compared to the wild type transit peptide TPI sequence

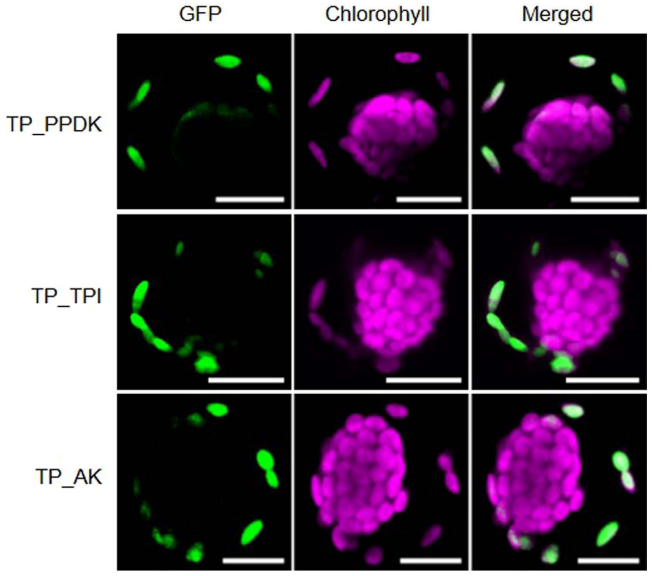

Figure 2. Subcellular localization of transit peptide GFP-fusions in young *Bienertia sinuspersici* protoplasts. Representative confocal images for all tested GFP-fusion constructs ($n > 5$) of GFP-fusion proteins of the P-specific proteins PPDK, TPI and AK in chlorenchyma protoplasts (TP_PPDK, TP_TPI, TP_AK). Transit peptides length was predicted by ChloroP[55] (Table S5). Protoplasts were analyzed as described in Fig. 1. Scale bars = 10 μm. GFP - green fluorescent protein; PPDK – Pyruvate, Pi dikinase; TPI – triosephosphate isomerase; AK – adenylate kinase.

(WT_TPI), we observed a strong reduction in P-specificity when the clusters II, IV, VII and VIII were mutated (Fig. 3B for a quantitative analysis and Fig. 3C for a representation of the observed phenotype). However, we also observed that in clusters II and IV the general import efficiency (that is import in either P- or C-chloroplasts) was severely reduced (by more than 50 and 80 percent in clusters II and IV, respectively) as the majority of GFP signal was found in the cytoplasm (Fig. 3C panels II and IV). Accordingly, the two elements located in clusters II and IV are required for general import and the two elements located in clusters VII and VIII are required for P-specificity.

The primary sequence for the P-specific elements is not conserved between different P-targeted transit peptides. To test, whether transit peptides of other P-targeted proteins contain similar elements as observed for the WT_TPI we repeated the analysis with the transit peptide of PPDK (Fig. 4). Similarly, we observed elements that when mutated reduced the overall import efficiency (for example clusters II and III). Mutations in two other clusters (V and VI) reduced P-specific import significantly but did not affect general import efficiency much, indicating a generally similar setup for the two TPs analyzed. However, comparing the AA sequences of the P-specific clusters VII and VIII from the WT_TPI (Fig. 3) with the P-specific clusters V and VI from this experiment revealed no obvious conservation of the primary AA sequence.

Targeting specificity is insensitive to changes in the mRNA sequence coding for the transit peptide. Since the alanine substitution experiments did not only affect the amino acid sequence but also the nucleotide sequence of the underlying mRNA coding for the TPs (through substituting all codons to codons for alanine), we cannot formally exclude that the observed effects are mRNA effects rather than TP effects. We therefore designed two experiments to distinguish between these two possibilities. Firstly, we created mutant sequences that contained as many nucleotide changes as possible within the mutated clusters (through wobbling of the third base and usage of alternative codons whenever possible) without affecting the amino acid sequence. Compared to the WT sequences, these mutations showed only between 25% to 50% sequence homology in the clusters VII and VIII for the WT_TPI and the cluster VI of the WT_PPDK, respectively (Fig. 5A). Compared to the alanine substitutions, these mRNA mutations had no effect on the P-targeting specificity for either the WT_TPI or the WT_PPDK sequence (Fig. 5B and C).

Additionally, we created a chimeric construct, consisting of an out-of-frame (OOF) nucleotide sequence for the TP of TPI fused to the (in-frame) full length RSSU including the TP (Fig. 5D). The frame-shifted leader from the P-specific TPI is almost identical (except for a 2 nucleotide insertion as shown in Fig. 5D) to the mRNA nucleotide sequence of the wild-type TPI transit peptide. This construct therefore comprises nearly the identical mRNA nucleotide sequence as the P-specific WT_TPI followed by a non-P-specific but functional full length RSSU (WT_TPI_OOF). Comparison with RSSU shows that the mRNA frame-shifted nucleotide sequence of the WT_TPI is not able to restore the P-specificity (Fig. 5E). In contrast, when the TP of TPI is fused in-frame in front of the TP of RSSU (Fig. S2A) or when the TP of RSSU is placed in-frame in front of the TP of TPI (Fig. S2B), P-specificity is restored.

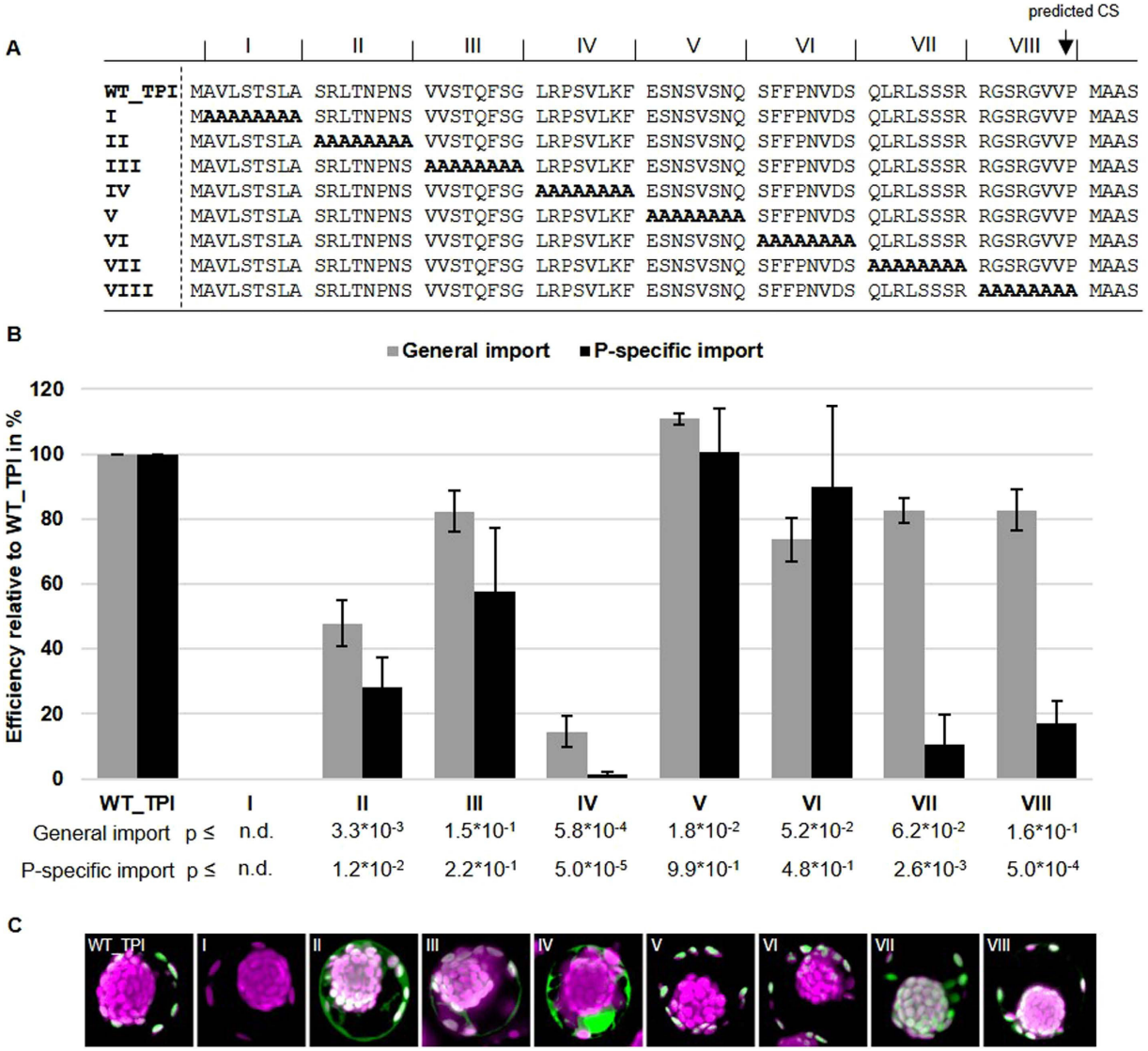

Figure 3. Distinct sequence elements in the transit peptide of TPI correlate with either general or P-specific chloroplasts import. (**A**) Sequences of WT_TPI and corresponding alanine substitution mutants. CS – cleavage site; TPI – triosephosphate isomerase. (**B**) Quantification of GFP signals in transfected protoplasts (WT_TPI; I – VIII mutant GFP-fusion constructs). Transfected protoplasts were counted and the expression pattern of GFP was categorized in general or P-specific import into the chloroplasts and shown as import efficiency relative to WT_TPI in percent. Quantification was performed as a blind study to reduce subjective bias as explained in Material and Methods. The means of four independent biological replicates are shown relative to WT_TPI. Error bars indicate standard error of the mean. Numbers indicate p-values from Student's t-test. (**C**) Representative confocal images for all tested GFP-fusion constructs in young protoplasts ($n > 5$).

In conclusion, both the wobble/codon swap experiment as well as the out-of-frame fusions did not indicate an involvement of mRNA effects in the specific targeting of the TPs to the P-chloroplasts. Instead, the amino acid sequence is the determining factor.

Detailed analysis of the P-specific elements. To determine the minimum sequence requirements for P-specificity, contribution of individual amino acids in clusters VII and VIII of WT_TPI and cluster V and VI of WT_PPDK were analyzed in detail (Fig. 6).

The AA sequences "QLRL" and "SSS" in Cluster VII as well as "RGSR" and "GVVP" in the clusters VIII of the WT_TPI were separately substituted with alanines (Fig. 6B for quantitative data and Fig. 6C for representative phenotypes). P-specificity of the triple S substitution was very similar to the wild type TP. In contrast, substitution of QLRL (Fig. 6C) almost completely abolished P-specificity. For Cluster VIII only the GVVP substitution showed a slight reduction in P-specificity but the effect was much smaller compared to the substitution of the whole cluster VIII. Breaking the QLRL motif further down showed only a moderate and somewhat additive effect

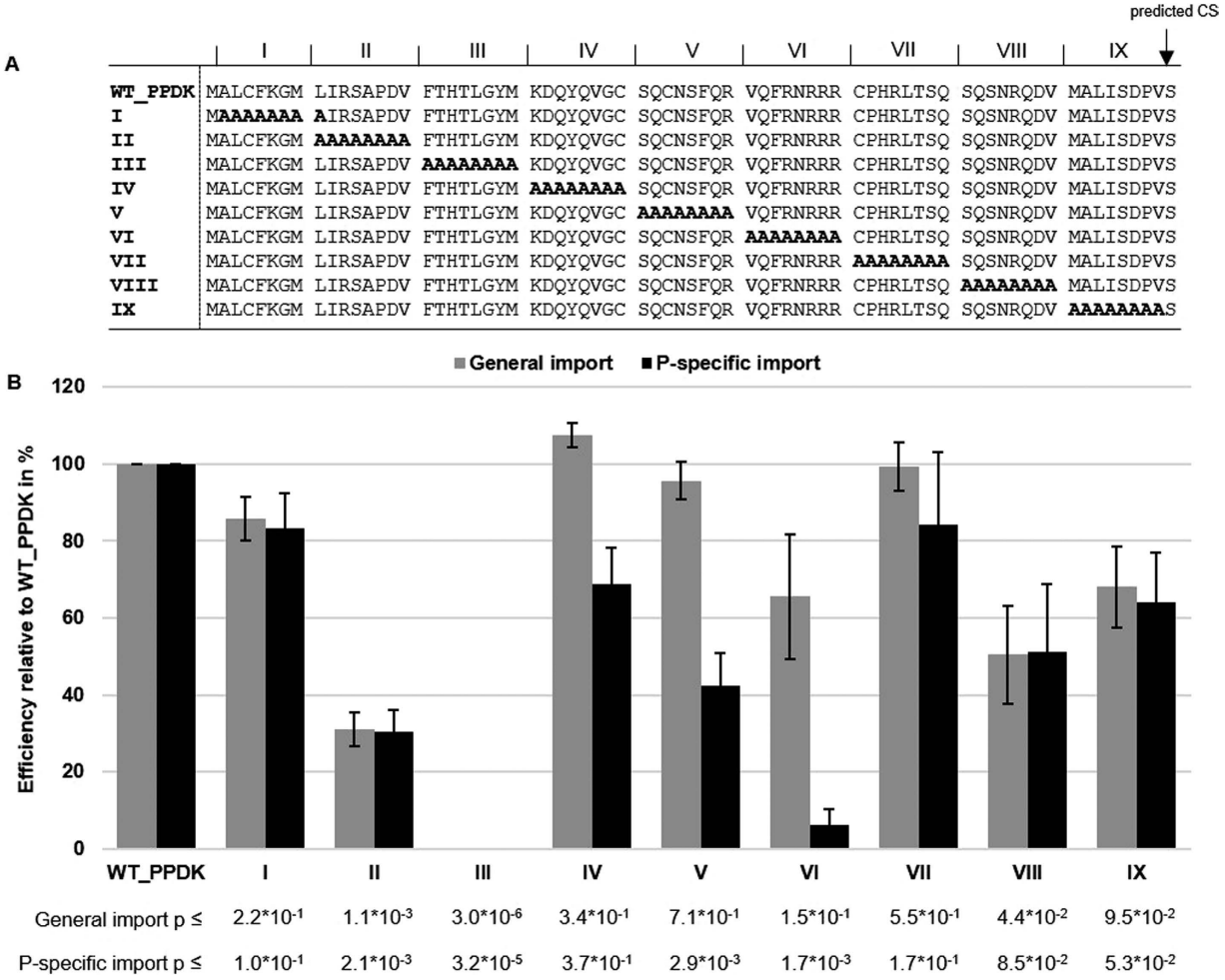

Figure 4. Distinct sequence elements in the transit peptide of PPDK correlate with either general or P-specific chloroplasts import. (**A**) Sequences of WT_PPDK and corresponding alanine substitution mutants. CS – cleavage site; PPDK – Pyruvate, Pi dikinase. (**B**) Quantification of GFP signals in transfected protoplasts (WT_PPDK; I – IX mutant GFP-fusion constructs) by fluorescence microscopy. Expression patterns were categorized and analyzed as described in Fig. 3 (n = 3). p-values are indicated in the figure.

in reduction of P-specificity for the QL, RL and R substitutions (Fig. 6D and E). In summary, for the TP of TPI a core element in cluster VII (QLRL) and the whole cluster VIII seem to be essential for P-specificity.

A similar analysis was performed on clusters V and VI on the TP of WT_PPDK (Fig. 6F–H). Because alanine substitution of cluster V also showed a slight reduction in P-specificity (see Fig. 4), a combined substitution with the amino acids "NSFQRVQF" spanning the clusters V and VI was performed. Also, the amino acids "VQFR" and "NRRR" of cluster VI were separately tested. Substitutions of the clusters VI, V_VI and of the "VQFR" sequence showed a significant reduction in P-specificity whereas substitution of the NRRR sequence showed the same P-specificity as the transit peptide of wild type PPDK.

Therefore, both the TP of TPI as well as the TP of PPDK carry short sequences of four amino acids (QLRL and VQFR) in their transit peptide which are essential for P-specificity.

The identified elements are necessary but not sufficient for P-specificity. The previous experiments demonstrated that the identified elements (QLRL of motif VII and the whole motif VIII) in the TP of TPI are necessary for P-specificity. We further tested if these elements are also sufficient to transfer P-specificity to an unrelated (non P-specific) TP from another species. Therefore, hybrid TPs with the N-terminus of the WT_TPI of the closely related C3 species *Suaeda heterophylla* (from here on Suaeda) and the C-terminus of varying length from the Bienertia WT_TPI (termed BsTPI) were constructed (Fig. 7A). Although the AA sequences of the wild type TPI transit peptides of Suaeda and Bienertia are 80.6% identical, the transit peptide of Suaeda TPI (from here on ShTPI) does not target GFP specifically to the P-chloroplasts when heterologously expressed in Bienertia protoplasts (Fig. 7B and C). Restoring the "QLRL" AA sequence at position 53 and 55 (construct 1) and the AA "P" at position 68 (predicted cleavage site) is not sufficient for restoring P-specificity (construct 2) although this reverts the motifs VII and VIII back to the state as found in WT_TPI from Bienertia. Only when three more AAs at the positions 45, 48 and 49 are converted to the same sequence as in the Bienertia WT_TPI transit peptide

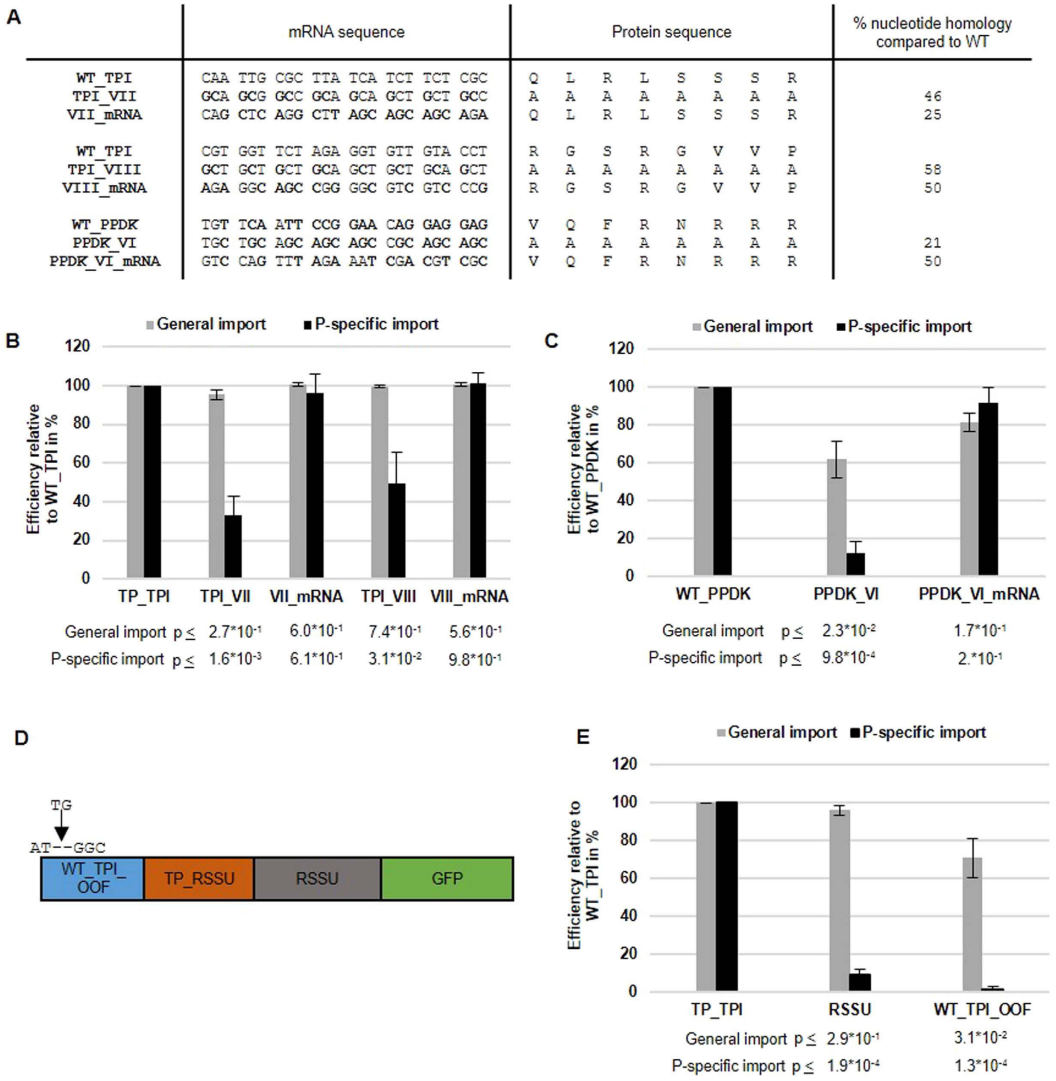

Figure 5. Mutations affecting the mRNA sequence but not the amino acid sequence of the transit peptides of TPI or PPDK do not affect P-specificity. (**A**) Partial mRNA sequences and corresponding amino acid sequences from wild type TPs (WT_TPI, WT_PPDK), their alanine substitutions (TPI_VII, TPI_VIII, PPDK_VI) and the wobbled/codon switched mRNA (VII_mRNA, VIII_mRNA, VI_mRNA). Numerals indicate homology compared to WT in percent. (**B**,**C**,**E**) Quantification of GFP signals in transfected protoplasts by fluorescence microscopy. Expression pattern of GFP was categorized in general or P-specific import. Protoplasts were analyzed and statistics were performed as described in Fig. 3. p-values are indicated in the figure. Efficiency of P-specific and general import of TPI (n = 4) (**B**) or PPDK (n = 3) (**C**) in comparison to the alanine substitution mutants and mRNA mutations. Error bars indicate standard error of the mean. (**D**) Chimeric construct of the nucleotide sequence of the TP of TPI fused in front of the coding region of full length RSSU-GFP. The nucleotide sequence of the TPI transit peptide contains a two nucleotide insertion at the start codon to produce an out of frame (OOF) shift resulting in a non-translatable mRNA sequence for the TPI TP followed by a translatable mRNA sequence for the full length RSSU. (**E**) Efficiency of P-specific and general import of the chimeric construct (n = 3).

P-specificity is fully restored (construct 3). The remaining differences in the N-terminus of the TP are however not important (construct 4), indicating that the P-specific region is clearly confined towards the C-terminus of the TP but specificity seems also to require several additional AAs which are located at some distance from each other.

Discussion

The C4 carbon concentrating mechanism in Bienertia requires elaborate subcellular compartmentation and accordingly, a protein sorting mechanism for nuclear encoded proteins to the two different chloroplast types. No comparable system is known from either plants or animals for chloroplasts or mitochondria. Therefore, no information on the mechanistic basis of the underlying sorting mechanism was available at the beginning of this study.

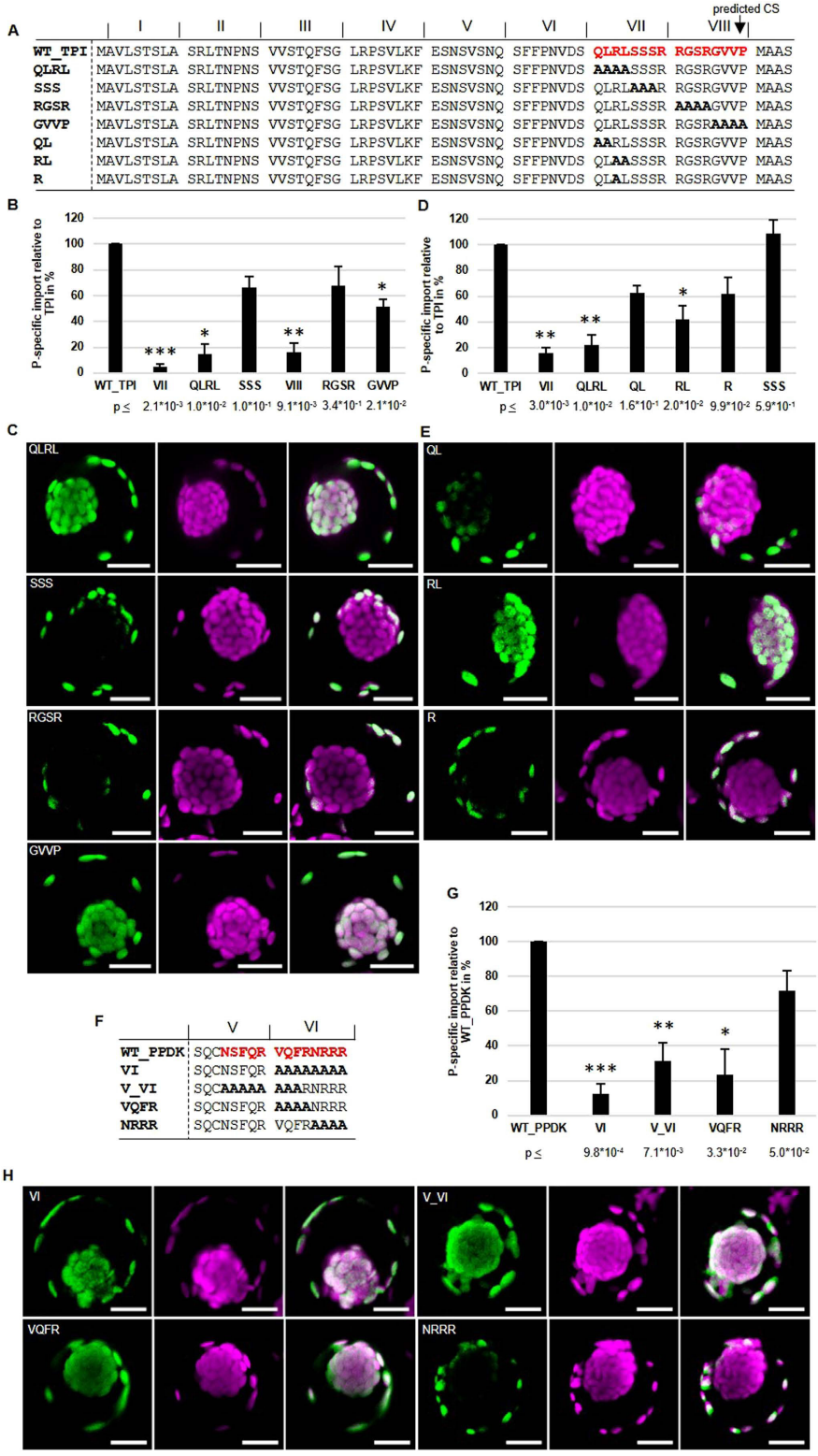

Figure 6. Four amino acids in the transit peptides of TPI and PPDK are necessary for P-specificity. (**A**–**E**) Sequences, quantification and representative images for TPI. (**F**–**H**) Sequences, quantification and representative images for PPDK. (**A**,**F**) Sequences of the wild type TPI and PPDK transit peptide sequences and the corresponding alanine substitution mutants. (**B**,**D**,**G**) Quantification of GFP signals in transfected protoplasts by fluorescence microscopy. Protoplasts were analyzed (n = 3) and statistics were performed as described in Fig. 3. Asterisks indicate significant differences from the corresponding control experiment (WT_TPI or WT_PPDK) by Student's t-test (*$p < 0.05$; **$p < 0.01$; ***$p < 0.001$). (**C**,**E**,**H**) Representative confocal images of observed phenotypes. For representative images of the phenotypes of WT_TPI and WT_PPDK see Fig. 2. For representative images of the phenotypes of motifs VII and VIII of TPI see Fig. 3).

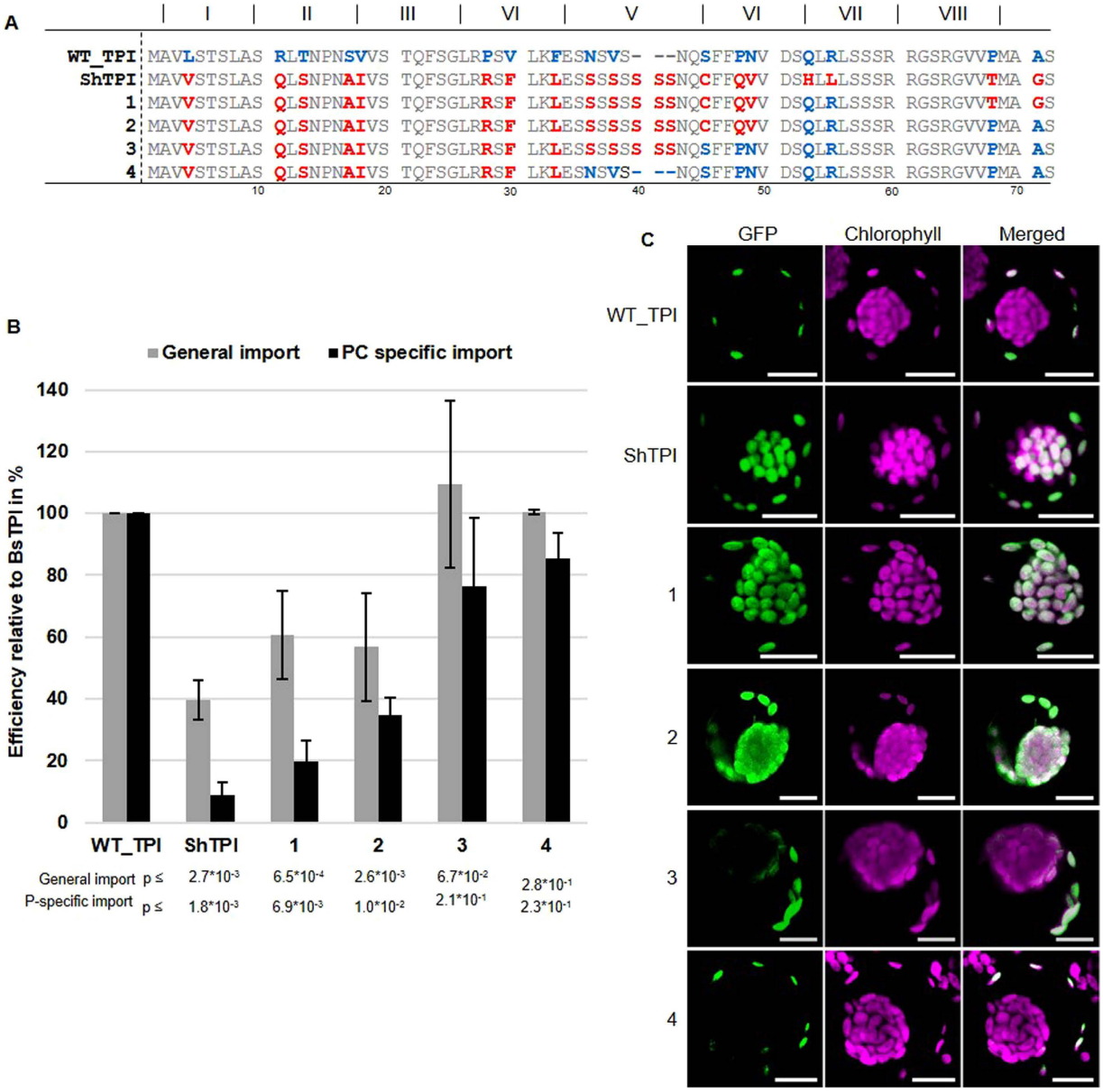

Figure 7. P-specificity from the SCC4 Bienertia TPI transit peptide can be transferred to the TP of the C3 species *Suaeda heterophylla*. (**A**) Sequences of the chimeric TPI TP fusions between Bienertia and *Suaeda heterophylla*. Blue and red letters indicate sequence differences between Bienertia and *S. heterophylla*, respectively. 1–4 indicate different chimeric constructs with varying amounts of sequence information from Bienertia included in the sequence of *S. heterophylla*. (**B**) Quantification of GFP signals in transfected protoplasts by fluorescence microscopy. Expression patterns were categorized and analyzed as described in Fig. 3. p-values are shown in the figure (n = 3). (**C**) Representative confocal images for the GFP-fusion constructs.

For all P-specific proteins tested, we identified the TP as the determining factor for correct localization. In C3 species, TPs have not only been shown to be necessary for correct chloroplast import, but are also able to discriminate between various plastid types in different tissues, e.g. chloroplasts and leucoplasts. This is achieved by a differential TOC/TIC composition as well as different binding properties of TPs[26,27]. Furthermore, different substrate-specific import pathways have been identified in chloroplasts, with some precursors using the TOC159 complex whereas others seem to prefer complexes with TOC132[28–30]. These differences in the import pathways are mediated by TPs which prefer different TOC-complexes[31,32]. In Bienertia, subcellular localization of the main TOC receptors TOC159/132 and TOC34 has been tested previously by *in vivo* localization studies. However, no preferential accumulation of the fusion constructs in either P- or C-chloroplasts was observed[33]. Therefore, there is currently no evidence for the involvement of these major TOC complexes in the differential sorting process.

To characterize the specific import pathway in Bienertia, we used extensive alanine scanning, a method that has previously been utilized successfully to identify specific motifs in the TPs of Arabidopsis[34–37]. Interestingly,

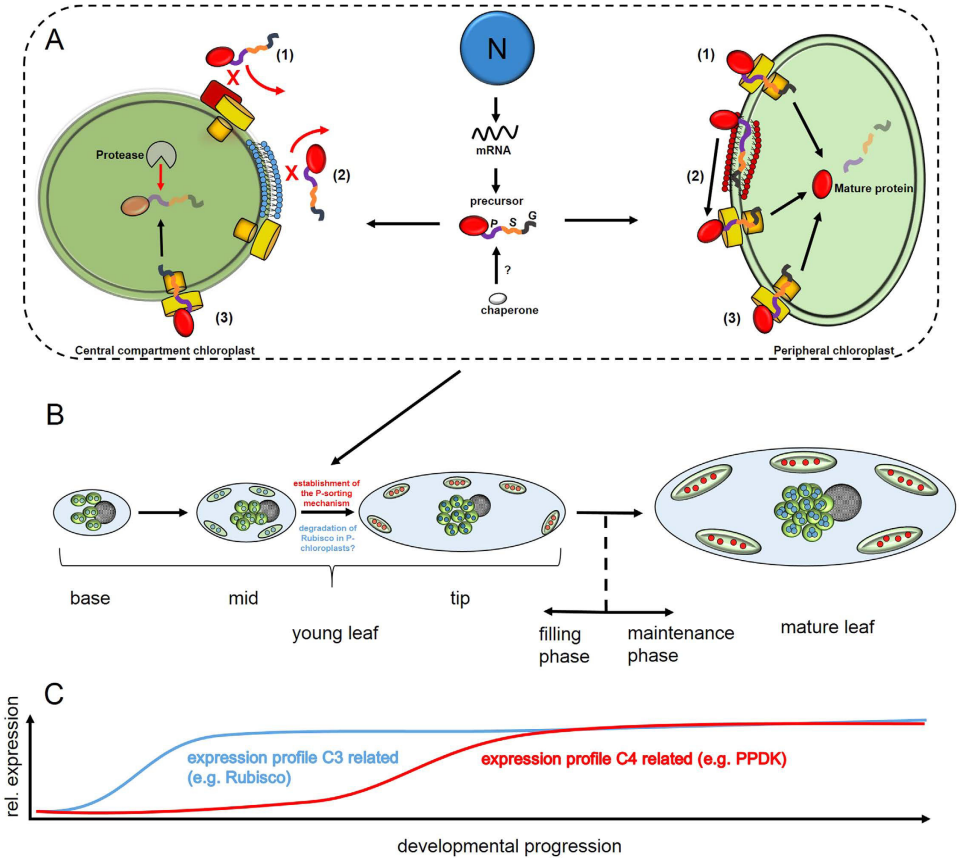

Figure 8. Summary and model for differential accumulation of nuclear encoded proteins within the two different chloroplast types of *Bienertia sinuspersici*. (**A**) Potential mechanisms for P-specific accumulation of nuclear encoded, plastid targeted proteins. Nuclear (N) encoded mRNAs for P-chloroplast specific proteins are translated without location preference. The TP precursors carry elements required for general chloroplast import (G) at the N-terminus and P-specific accumulation (P) at the C-terminus separated by spacers (S) and potentially can also interact with chaperones. Different scenarios could explain the TP mediated, P-specific accumulation: P-specific proteins could be blocked from import into the C-chloroplast via so far unknown components of the TOC-TIC complex (1); The P-element could block interaction with the C-chloroplast envelope (2); The P-element could refer degradation of P-specific proteins within the C-chloroplasts (3). (**B**) Developmental progression of Bienertia chlorenchyma cells. Young cells from the base of young leaves have only a single-chloroplast type that contains Rubisco (blue dots). In the midsections, chloroplasts have started positioning within the peripheral and the central compartment, but all still contain Rubisco along with raising levels of PPDK (modeled after[14]). Towards maturation, the P-specific sorting mechanism is initiated and Rubisco is removed (either by degradation or by preventing re-import) from the P-chloroplasts. In the tip of young leaves, chloroplast positioning and biochemical specialization is completed. (**C**) Simplified accumulation profiles of C3 and C4 related proteins during development (compiled from[8,15,16,18,43]. X-axis represents the same developmental stages (base, mid, tip and mature) as in (**B**).

our mutation experiments indicate that the identified elements on the TPs of P-specific precursors prevent import into the CC rather than facilitating the specific import into the P-chloroplasts (Fig. 8A). This can be concluded, since deactivation of these elements leads to import into both chloroplast types and not to a complete loss of import which would be expected if the elements are required for specific uptake into the P-chloroplasts. This mechanism might seem surprising, but it makes sense in the greater context: The general proteome of the two chloroplast types is similar in Bienertia[16] and accordingly, the vast majority of nuclear encoded plastid targeted proteins has to be imported into both chloroplast types. Therefore, information for both P- and C-targeting would be required for all those proteins to ensure equal distribution. Hence, it seems more economical to utilize the general chloroplast import pathway (also indicated by the fact that all tested Bienertia constructs were imported correctly when expressed in Arabidopsis protoplasts) and then prevent the few P-specific proteins from being imported into the C-chloroplasts. Accordingly, certain components that detect and subsequently block the passage of P-specific precursors could be connected to the TOC-TIC machinery of the C-chloroplasts (option 1 in Fig. 8A). The same might also be true for blocking C-specific proteins from import into P-chloroplasts although the latter case remains to be shown.

Historically, TPs have been regarded as being rather unstructured which was also connected to the high variability between different TPs as hardly any common motifs have been identified[38]. However, more recent studies

show that TPs are more structured than previously expected. The bimodal model postulates that TPs contain different recognition sites for stromal chaperones and TOC proteins which are coupled by a spacer element[39]. The multi-selection and multi-order (M&M) model extends the bimodal model with the hypothesis that the order of specific motifs can vary among TPs[40]. Comparable to these models, the N-terminus of the TP of P-specific precursors in Bienertia is responsible for general import into chloroplasts, followed by a spacer element (where the alanine substitutions had no effect on either the general or the P-specific import). The C-terminus is then responsible for P-selectivity. It is important to note that the P-specific element at the C-terminus overrides the general import element at the N-terminus. This probably indicates that the P-element was evolutionary acquired later "on top" of the already existing general import mechanism.

Although the identified QLRL and VQFR motifs are necessary for P-specificity, our experiments with Bienertia-*Suaeda heterophylla* hybrids indicate that they are not sufficient, since P-specificity was achieved only when the last 25 aa from the beginning of the C-terminus were restored (Fig. 7). In addition to the core P-element, the surrounding AA composition is of relevance, potentially indicating that this area acquires a structure. This could occur already in the cytosol, or as it has been speculated previously, upon contact with the chloroplast envelope[41]. It has been proposed that initial contact of TPs with the chloroplast envelope is mediated by the C-terminal part of the TP[42]. The C-terminus could then be integrated into the lipid-bilayer and diffuse along the chloroplast surface until the TP gets in contact with the TOC machinery[41] and the actual import process is initiated. Since our identified P-elements are located at the C-terminus we also consider this possibility as a means of discriminating between the two chloroplast types (option 2 in Fig. 8A). Of course this would require the envelopes of the two chloroplast types to be different, for example either in their lipid composition, or by the occurrence of additional receptors. This would then generate a contact surface that is either permissive for docking or in the case of P-specific precursors trying to dock to a C-chloroplast, prevent contact.

Lastly, it is possible that discrimination of the P-specific element does not occur prior to entry of the precursor into the chloroplasts. Instead, a chloroplast type specific protease that detects and subsequently degrades all precursors which are tagged with a P-specific element could be located specifically in the C-chloroplasts (option 3 in Fig. 8A). We can also not exclude that cytosolic or chloroplastic chaperones could be involved in transport, recognition and degradation of all three options discussed.

We consistently observed correct targeting for P- but not for C-localized proteins which could indicate different targeting mechanisms for the two protein classes. It has been demonstrated that the unique SCC4 related subcellular compartmentalization and the morphological and biochemical specialization of the two chloroplast types develop gradually from very young towards more mature cells[13–15,43] (Fig. 8B). For example, very young cells from the base of young leaves do not yet show a clear separation into P- and C-chloroplasts. Instead, chloroplasts appear monomorphic and mRNA *in situ* hybridization as well as immunolocalization studies indicate that all chloroplasts at this stage express and accumulate Rubisco large and small subunit, whereas at this stage there are very low levels of PPDK and other C4 cycle related proteins such as PEPC. In contrast, more developed cells from the midsection of young leaves already show the positioning of P- and C-chloroplasts although they still all contain Rubisco while at this stage leaves have low levels of PPDK[14]. Online isotope discrimination analysis furthermore showed that these young cells operate in a "default" C3 mode which is compatible with the lack of biochemical specialization observed in this stage[14]. Taken together this data indicate that subcellular positioning of P- and C-chloroplasts occurs during development before the actual biochemical specialization. This is also compatible with the expression patterns of C3 and C4 related proteins. Whereas expression and accumulation of C3 related proteins occurs early during development, previous *in situ* localization[14], expression[43] and proteome data[16] all indicate that C4 related transcripts and proteins accumulate much later during development (Fig. 8C). Accordingly, in the early stages, the sorting mechanism that keeps Rubisco out of the P-chloroplast is not yet developed. Once the subcellular development of chloroplasts in the C and P domains occurs, Rubisco is localized in both chloroplast types. Thus, it needs either to be degraded specifically in the P-chloroplasts at this stage or alternatively, import of new proteins needs to be prevented and the "normal" protein turnover (half-life time of Rubisco from other species has been estimated between a few days and a week[44,45]) would then remove Rubisco from the P-chloroplasts over time. Development of the blockage of entry of P-selective peptides by the central chloroplasts might occur before or immediately after initiation of the development of the two compartments. Finally at the tip of young leaves, complete partitioning of C3 and C4 related proteins in the P- and C-chloroplasts is achieved. In summary, the different timings in expression of C3 and C4 related proteins as well as the different accumulation characteristics observed previously and in this study suggest different mechanism may be responsible for targeting of P- and C-localized proteins.

It is tempting to speculate that correct C-specific RSSU targeting in young protoplasts could be achieved if levels and timing of expression would resemble the natural situation more closely. For example, it has been shown that correct targeting of different phosphate transporters in *Medicago truncatula* depends critically on the correct timing of expression which is achieved only under the control of their endogenous promoters but not under control of related promoters[46]. Accordingly, testing of *rbcS* fusions constructs under the control of their endogenous promoters in stably transformed plants would be needed to see if the sorting mechanism is also subject to temporal changes in the SCC4 system. However, neither stable transformation nor information on promoter sequences are currently available for Bienertia.

Numerous previous studies have reported the specific localization of PPDK and RSSU in the P- and C-chloroplasts, respectively[8,17,47]. In contrast, we observed in our experiments correct targeting (for the P-proteins) only when tested in protoplasts prepared from young but not from mature leaves. This is similar to a previous study, where also specific targeting was not observed for either P- or C-targeted GFP fusions in mature Bienertia protoplasts (young protoplasts were not tested)[48]. This discrepancy can probably be explained by the different analysis methods: Previous *in situ* localization and western/proteomics analysis captured a "snapshot" of the total protein accumulation in the chloroplasts, accumulated over the lifetime of the organelle. In contrast,

in vivo GFP localization studies also include the dynamics of the actual import reaction which might change throughout development. For example, it has been proposed that general import capacity is reduced in mature compared to younger chloroplasts[49] and this correlates with the overall expression levels of TOC components which are generally highest in young developing chloroplasts but reduced in mature organelles[29,31,50]. However, it was later shown that the situation is a little more complex in that different substrates are imported with different efficiencies in chloroplasts of different development stages[51]. Also in Bienertia, levels of TOC 159 and TOC132 decrease from a very high level in young developing cells to a basal level towards leaf maturation[33]. Accordingly, either TOC composition or the sorting/import capacity in mature Bienertia protoplasts might be inadequate, especially when fusion constructs are massively overexpressed under the control of the 35 S promoter. It is important to note however that transcript levels of both RSSU and PPDK are still high in mature leaves[43]. As a consequence, this would mean that either these transcripts are not efficiently translated to proteins in mature cells or that expression levels are still much lower compared to expression driven by the 35S promoter. Alternatively, it is also possible that the observed failure to correctly sort proteins is caused if mature protoplasts are more prone to stress compared to younger protoplasts. For example, mature protoplasts are much bigger and damage more easily during isolation. We observed frequently that the structural integrity in mature protoplasts was compromised, for example, the central compartment was often not located in the center but shifted towards the periphery of the cell, which might occur if the vacuole becomes damaged. In this case, the observed differences between young and mature protoplasts in the targeting behavior of P- and C-specific proteins would not truly reflect developmental effects but rather artifacts of the analysis method.

Conclusion

SCC4 species such as Bienertia represent not only a new way to perform a carbon concentrating cycle within individual cells in terrestrial plants; they are also an exciting puzzle for cell biologists. The occurrence of the same type of organelle in two specialized forms within individual cells suggests this requires novel mechanisms of intracellular protein sorting, as well as regulators of development and positioning of organelles. While we provide in this study the first step towards understanding this phenomenon, many questions remain unsolved. For example, the historical 'hen-egg' problem underlies all sorting mechanisms discussed here to some extent: If specific transporters, proteases or other unknown mechanism facilitate the selective accumulation in one or the other chloroplast types, how do these "determinants" reach their correct localization in the first place? Especially in plants, little is known about subcellular organization in the developmental context. The successful establishment of stable transformation technology together with detailed information on the genome of SCC4 species will be crucial to address this and other questions in the future.

Methods

Plant growth conditions. Seeds of *B. sinuspersici* were planted in soil and grown under controlled conditions in a GroBank Chamber (CLF Plant Climatics, Germany) at a day/night temperature of 25/20 °C. After germination for one day in the dark, seedlings were illuminated with a 16/8 h light/dark cycle at a photon flux intensity of 250 μmol $m^{-2} s^{-1}$. Plants were shifted after two weeks into a growth cabinet with a day/night temperature of 30/18 °C with 60% relative humidity and a photoperiod of 16/8 h light/dark at a photon flux intensity of 350 μmol $m^{-2} s^{-1}$. Plants were watered twice a week with 0.03 M NaCl and 0.001% (v/v) Wuxal fertilizer (Manna, Germany) and used after growing for 3 months for protoplast isolation.

Plasmid construction. Subcellular localization was visualized by GFP-fusion proteins. GFP-fusion constructs were generated utilizing the 35 S:puc18-spGFP6 expression vector[48]. Different sequences were fused at the 5′ end of GFP using *Xma*I/*Spe*I restriction sites (Table S1). For all experiments with endogenous Bienertia sequences, DNA fragments were amplified by PCR from cDNA, generated from Bienertia mRNA isolated by the GeneJET Plant RNA Purification Kit (Thermo Fisher Scientific, USA). Oligonucleotides (Metabion, Germany) used for amplification contained additional *Xma*I/*Spe*I restriction sites (Table S2). Vector and PCR fragments were digested with *Xma*I/*Spe*I and ligated into the backbone with T4 DNA Ligase (Thermo Fisher Scientific, USA). All constructs were verified by sequencing (Seqlab, Germany).

Mutagenesis. Alanine substitution mutants (Table S3) were generated by 'splicing by overlapping extension PCR' (SOE-PCR) as described[52] or with the QuickChange Lightning Site-Directed Mutagenesis Kit (Agilent Technologies, USA). Oligonucleotide sequences for mutagenesis are given in Table S2. For both mutagenesis techniques, the non mutated GFP-fusion constructs (TP_TPI, TP_PPDK) served as template. Complex mutagenesis constructs were generated by gene fragment synthesis service (Eurofins Genomic GmbH, Germany). Sequences are given in Table S4. All fragments contained a *Xma*I and *Spe*I restriction site on the 5′ or 3′ end for cloning into the expression vector 35 S:puc18-spGFP6[48].

Protoplast isolation and transient expression in protoplasts. Protoplasts of leaves from different developmental stages were utilized for localization experiments. Mature protoplasts were isolated from mature leaves (between 1.0–1.5 cm long) following an earlier protocol[17] with slight modifications: For isolation of chlorenchyma cells, the epidermis of several mature leaves was removed by gently squeezing and rolling with a round bottom tube. Leaves were then transferred into digest buffer (1.6% (w/v) Cellulase Onozuka R-10 (Duchefa, Netherlands), 0.25% (w/v) Macerozyme R-10 (Duchefa, Netherlands), 5 mM MES-NaOH, pH 5.7, 10 mM $CaCl_2$ and incubated for 1 h at 35 °C in a water bath. All buffers for protoplast isolation were supplemented with glycine-betaine in a concentration matching the internal osmolite concentration of Bienertia chlorenchyma cells as determined by a vapor pressure osmometer (Vapro 5520, Germany) to account for osmotic differences between buffer and isolated cells/protoplasts. Undigested remains of the leaves were removed with tweezers and protoplasts were centrifuged for 1 min at 51 xg in a swing-out rotor. Supernatant was discarded and the pellet was

resuspended in 20% (w/v) sucrose + glycine-betaine. Protoplasts were centrifuged for 5 min at 300 xg. Intact protoplasts floating on top of the sucrose cushion were transferred to a round bottom tube. Protoplasts were washed with glycine-betaine buffer (5 mM MES-NaOH, pH 5.7, 10 mM $CaCl_2$, glycine-betaine) and centrifuged for 1 min at 51 xg in a swing-out rotor. The supernatant was discarded and protoplasts were resuspended in glycine-betaine buffer.

For the isolation of young protoplasts, 0.3–0.5 cm long leaves served as source material. Leaves were cut once in longitudinal direction and transferred to a 35 mm petri dish with digestion buffer. Leaves were slowly shaken for 3 h and afterwards filtered through a 70 micron nylon mesh. Protoplasts were centrifuged for 5 min at 300 xg in a swing-out rotor and the supernatant was discarded. Protoplasts were washed with glycine-betaine buffer followed by centrifugation for 5 min at 300 xg in a swing-out rotor. The supernatant was discarded and protoplasts were resuspended in glycine-betaine buffer. Transfection of mature as well as young protoplasts was performed as described in ref. 47 but instead with 25 μg plasmid. *Arabidopsis thaliana* protoplast isolation and transfection was done as described in ref. 53.

Confocal microscopy. Confocal microscopy was performed using a Nikon Eclipse TE2000-E laser scanning confocal microscope (Nikon, Germany). Images were acquired through a Nikon Plan Apo, 60x/1,20 objective at a maximum digital resolution of 1024 × 1024 pixels. The fluorescence of GFP was analyzed by excitation at 488 nm and emission was detected between 509/26 nm. Chlorophyll autofluorescence was analyzed by excitation at 408 nm and emission was detected between 620/700 nm. Image processing was performed using Fiji[54].

Fluorescence microscopy. Fluorescence microscopy was performed using a Nikon Eclipse Ti fluorescence microscope (Nikon, Germany). Images were acquired through a Nikon Plan Apo, 40x/0.95 objective. The fluorescence of GFP was analyzed by excitation at 480/20 nm and emission was detected between 510/20 nm. Chlorophyll autofluorescence was analyzed by excitation of 550/75 nm and emission was detected between 590/675 nm. In order to quantify as many transformed protoplasts as possible, large composite pictures (0.4 mm × 0.4 mm at 400× magnification) of droplets containing protoplasts were acquired automatically (with an overlap of 2% between each individual picture) and saved for later quantification (see next section). Image processing was performed using NIS-Elements AR 4.40.00 (Nikon, Germany).

Quantification. For quantitative analysis, transformed protoplasts identified from automatically generated composite pictures were categorized into "P-specific", "general import" or "cytosolic". At least three completely independent biological replicates, conducted on different days with different batches of protoplasts for each construct tested, were analyzed. Differences for quantitative data were additionally tested statistically for significance to reduce noise from variability in the expression patterns of individual protoplasts. Therefore, count data was expressed relative to WT_TPI and WT_PPDK, respectively and ratios were then transformed to arcsine to achieve normal distribution, followed by a two-tailed Student's t-test. Generally, all situations to be compared were performed "blind" in order to avoid human bias from interpreting the microscopic results. Therefore, the experimenter performing the microscopic classifications was unaware of the nature of the construct he/she was observing. Only after quantification, the identity of the sample was revealed.

References

1. Walker, B. J., VanLoocke, A., Bernacchi, C. J. & Ort, D. R. The costs of photorespiration to food production now and in the future. *Annu Rev Plant Biol* **67,** 107–129 (2016).
2. Wingler, A., Lea, P. J., Quick, W. P. & Leegood, R. C. Photorespiration: metabolic pathways and their role in stress protection. *Philos Trans R Soc Lond B Biol Sci* **355,** 1517–1529 (2000).
3. Brooks, A. & Farquhar, G. D. Effect of temperature on the CO_2/O_2 specificity of ribulose-1,5-bisphosphate carboxylase/oxygenase and the rate of respiration in the light. Estimates from gas-exchange measurements on spinach. *Planta* **165,** 397–406 (1985).
4. Sage, R. F. The evolution of C4 photosynthesis. *New Phytol* **161,** 341–370 (2004).
5. Hibberd, J. M., Sheehy, J. E. & Langdale, J. A. Using C4 photosynthesis to increase the yield of rice-rationale and feasibility. *Curr Opin Plant Biol* **11,** 228–231 (2008).
6. von Caemmerer, S., Quick, W. P. & Furbank, R. T. The development of C4 rice: current progress and future challenges. *Science* **336,** 1671–1672 (2012).
7. Akhani H. *et al.* A new species of Bienertia (Chenopodiaceae) from Iranian salt deserts. A third species of the genus and discovery of a fourth terrestrial C4 plant without Kranz anatomy. *Syst Botany* **146,** 1–10 (2012).
8. Voznesenskaya, E. V. *et al.* Proof of C4 photosynthesis without Kranz anatomy in *Bienertia cycloptera* (Chenopodiaceae). *Plant J* **31,** 649–662 (2002).
9. Voznesenskaya, E. V., Franceschi, V. R., Kiirats, O., Freitag, H. & Edwards, G. E. Kranz anatomy is not essential for terrestrial C4 plant photosynthesis. *Nature* **414,** 543–546 (2001).
10. Akhani, H. *et al. Bienertia sinuspersici* (Chenopodiaceae): a new species from Southwest Asia and discovery of a third terrestrial C4 plant without Kranz anatomy. *Syst Botany* **30,** 290–301 (2005).
11. Freitag, H. & Stichler, W. A remarkable new leaf type with unusual photosynthetic tissue in a central asiatic genus of Chenopodiaceae. *Plant Biol* **2,** 154–160 (2000).
12. Freitag, H. & Stichler, W. *Bienertia cycloptera* Bunge ex Boiss., Chenopodiaceae, another C4 plant without Kranz tissues. *Plant Biol* **4,** 121–132 (2002).
13. Park, J., Knoblauch, M., Okita, T. W. & Edwards, G. E. Structural changes in the vacuole and cytoskeleton are key to development of the two cytoplasmic domains supporting single-cell C4 photosynthesis in *Bienertia sinuspersici*. *Planta* **229,** 369–382 (2009).
14. Koteyeva, N. K., Voznesenskaya E. V., Berry J. O., Cousins A. B. & Edwards G. E. The unique structural and biochemical development of single cell C4 photosynthesis along longitudinal leaf gradients in *Bienertia sinuspersici* and *Suaeda aralocaspica* (Chenopodiaceae). *J Exp Bot* **67,** 2587–2601 (2016).
15. Voznesenskaya, E. V. *et al.* Differentiation of cellular and biochemical features of the single-cell C4 syndrome during leaf development in *Bienertia cycloptera* (Chenopodiaceae). *Am J Bot* **92,** 1784–1795 (2005).
16. Offermann, S. *et al.* Developmental and subcellular organization of single-cell C4 photosynthesis in *Bienertia sinuspersici* determined by large-scale proteomics and cDNA assembly from 454 DNA Sequencing. *J Proteome Res* **14,** 2090–2108 (2015).

17. Offermann, S., Okita, T. W. & Edwards, G. E. Resolving the compartmentation and function of C4 photosynthesis in the single-cell C4 species *Bienertia sinuspersici*. *Plant Physiol* **155,** 1612–1628 (2011).
18. Voznesenskaya, E. V., Edwards, G. E., Kiirats, O., Artyusheva, E. G. & Franceschi, V. R. Development of biochemical specialization and organelle partitioning in the single-cell C4 system in leaves of *Borszczowia aralocaspica* (Chenopodiaceae). *Am J Bot* **90,** 1669–1680 (2003).
19. Chuong, S. D. X., Franceschi, V. R. & Edwards, G. E. The cytoskeleton maintains organelle partitioning required for single-cell C4 photosynthesis in Chenopodiaceae species. *Plant Cell* **18,** 2207–2223 (2006).
20. King, J. L., Edwards, G. E. & Cousins, A. B. The efficiency of the CO_2-concentrating mechanism during single-cell C4 photosynthesis. *Plant Cell Environ* **35,** 513–523 (2012).
21. Sharpe, R. M. & Offermann, S. One decade after the discovery of single-cell C4 species in terrestrial plants: what did we learn about the minimal requirements of C4 photosynthesis? *Photosynth Res* **119,** 169–180 (2014).
22. Friso, G., Majeran, W., Huang, M., Sun, Q. & van Wijk, K. J. Reconstruction of metabolic pathways, protein expression, and homeostasis machineries across maize bundle sheath and mesophyll chloroplasts: large-scale quantitative proteomics using the first maize genome assembly. *Plant Physiol* **152,** 1219–1250 (2010).
23. Chang, Y.-M. *et al.* Characterizing regulatory and functional differentiation between maize mesophyll and bundle sheath cells by transcriptomic analysis. *Plant Physiol* **160,** 165–177 (2012).
24. Offermann, S., Okita, T. W. & Edwards, G. E. How do single cell C4 species form dimorphic chloroplasts? *Plant Signal Behav* **6,** 762–765 (2011).
25. Erlinghaeuser, M., Hagenau, L., Wimmer, D. & Offermann, S. Development, subcellular positioning and selective protein accumulation in the dimorphic chloroplasts of single-cell C4 species. *Curr Opin Plant Biol* **31,** 76–82 (2016).
26. Chu, C. C. & Li, H. Protein import into isolated pea root leucoplasts. *Frontiers Plant Sci* **6,** 690 (2015).
27. Yan, X., Khan, S., Hase, T., Emes, M. J. & Bowsher, C. G. Differential uptake of photosynthetic and non-photosynthetic proteins by pea root plastids. *FEBS Lett* **580,** 6509–6512 (2006).
28. Inoue, H., Rounds C. & Schnell D. J. The molecular basis for distinct pathways for protein import into Arabidopsis chloroplasts. *Plant Cell* **22,** 1947–1960 (2010).
29. Jarvis, P. *et al.* An Arabidopsis mutant defective in the plastid general protein import apparatus. *Science* **282,** 100–103 (1998).
30. Bauer, J. *et al.* The major protein import receptor of plastids is essential for chloroplast biogenesis. *Nature* **403,** 203–207 (2000).
31. Ivanova, Y., Smith M. D., Chen, K. & Schnell, D. J. Members of the Toc159 import receptor family represent distinct pathways for protein targeting to plastids. *Mol Biol Cell* **15,** 3379–3392 (2004).
32. Smith, M. D. *et al.* atToc159 is a selective transit peptide receptor for the import of nucleus-encoded chloroplast proteins. *J Cell Biol* **165,** 323–334 (2004).
33. Lung, S. C. & Chuong, S. D. A transit peptide-like sorting signal at the C terminus directs the *Bienertia sinuspersici* preprotein receptor Toc159 to the chloroplast outer membrane. *Plant Cell* **24,** 1560–1578 (2012).
34. Lee, D. W. *et al.* Arabidopsis nuclear-encoded plastid transit peptides contain multiple sequence subgroups with distinctive chloroplast-targeting sequence motifs. *Plant Cell* **20,** 1603–1622 (2008).
35. Lee, D. W. *et al.* Functional characterization of sequence motifs in the transit peptide of Arabidopsis small subunit of rubisco. *Plant Physiol* **140,** 466–483 (2006).
36. Lee, D. W., Lee, S., Oh, Y. J. & Hwang, I. Multiple sequence motifs in the rubisco small subunit transit peptide independently contribute to Toc159-dependent import of proteins into chloroplasts. *Plant Physiol* **151,** 129–141 (2009).
37. Lee, D. W., Woo, S., Geem, K. R. & Hwang, I. Sequence motifs in transit peptides act as independent functional units and can be transferred to new sequence contexts. *Plant Physiol* **169,** 471–484 (2015).
38. Bruce B. D. The paradox of plastid transit peptides: conservation of function despite divergence in primary structure. *Biochim Biophys Acta* **1541,** 2–21 (2001).
39. Chotewutmontri, P., Reddick L. E., McWilliams D. R., Campbell I. M. & Bruce B. D. Differential transit peptide recognition during preprotein binding and translocation into flowering plant plastids. *Plant Cell* **24,** 3040–3059 (2012).
40. Li, H.-M. & Teng, Y.-S. Transit peptide design and plastid import regulation. *Trends Plant Sci* **18,** 360–366 (2013).
41. Elkehal, R., Becker T., Sommer M. S., Königer M. & Schleiff E. Specific lipids influence the import capacity of the chloroplast outer envelope precursor protein translocon. *Biochim Biophys Acta* **1823,** 1033–1040 (2012).
42. Pinnaduwage, P. & Bruce, B. D. *In vitro* interaction between a chloroplast transit peptide and chloroplast outer envelope lipids is sequence-specific and lipid class-dependent. *J Biol Chem* **271,** 32907–32915 (1996).
43. Lara, M. V. *et al.* Leaf development in the single-cell C4 system in *Bienertia sinuspersici*: expression of genes and peptide levels for C4 metabolism in relation to chlorenchyma structure under different light conditions. *Plant Physiol* **148,** 593–610 (2008).
44. Webber, A. N., Nie, G.-Y. & Long, S. P. Acclimation of photosynthetic proteins to rising atmospheric CO_2. *Photosynth Res* **39,** 413–425 (1994).
45. Simpson, E., Cooke, R. J. & Davies, D. D. Measurement of protein degradation in leaves of *Zea mays* using ^{3}[H]Acetic anhydride and tritiated water. *Plant Physiol* **67,** 1214–1219 (1981).
46. Pumplin, N., Zhang, X., Noar, R. D. & Harrison, M. J. Polar localization of a symbiosis-specific phosphate transporter is mediated by a transient reorientation of secretion. *PNAS* **109,** E665–E672 (2012).
47. Lung, S.-C., Yanagisawa, M. & Chuong, S. D. X. Protoplast isolation and transient gene expression in the single-cell C4 species, *Bienertia sinuspersici*. *Plant Cell Rep* **30,** 473–484 (2012).
48. Rosnow, J., Yerramsetty, P., Berry, J. O., Okita, T. W. & Edwards, G. E. Exploring mechanisms linked to differentiation and function of dimorphic chloroplasts in the single cell C4 species *Bienertia sinuspersici*. *BMC Plant Biol* **14,** 1 (2014).
49. Dahlin, C. & Cline, K. Developmental regulation of the plastid protein import apparatus. *Plant Cell* **3,** 1131–1140 (1991).
50. Yan, J. *et al.* Molecular characterization and expression analysis of chloroplast protein import components in tomato (*Solanum lycopersicum*). *PLoS ONE* **9,** e95088 (2014).
51. Teng, Y.-S., Chan, P.-T. & Li, H.-M. Differential age-dependent import regulation by signal peptides. *PLoS Biol* **10,** e1001416 (2012).
52. Heckman, K. L. & Pease, L. R. Gene splicing and mutagenesis by PCR-driven overlap extension. *Nature Protoc* **2,** 924–932 (2007).
53. Yoo, S. D., Cho, Y. H. & Sheen, J. Arabidopsis mesophyll protoplasts: a versatile cell system for transient gene expression analysis. *Nature Protoc* **2,** 1565–1572 (2007).
54. Schindelin, J. *et al.* Fiji: an open-source platform for biological-image analysis. *Nat Methods* **9,** 676–682 (2012).
55. Emanuelsson, O., Nielsen, H. & von Heijne, G. ChloroP, a neural network-based method for predicting chloroplast transit peptides and their cleavage sites. *Protein Sci* **8,** 978–984 (1999).

Acknowledgements

Work in the S.O. lab was supported by the Deutsche Forschungsgemeinschaft (OF 106/1-1) and S.O. and I.H were funded by the "Cooperative Research Program for Agriculture Science & Technology Development (Project No. 0109532016) "Rural Development Administration, Republic of Korea".

Author Contributions

D.W., I.H. and S.O. designed research; D.W., P.B. and V.S. performed research; D.W. analyzed data and prepared the figures; and D.W., I.H. and S.O. wrote the paper.

Additional Information

Supplementary information accompanies this paper at http://www.nature.com/srep

Competing financial interests: The authors declare no competing financial interests.

How to cite this article: Wimmer, D. *et al.* Transit peptide elements mediate selective protein targeting to two different types of chloroplasts in the single-cell C4 species *Bienertia sinuspersici*. *Sci. Rep.* **7**, 41187; doi: 10.1038/srep41187 (2017).

Publisher's note: Springer Nature remains neutral with regard to jurisdictional claims in published maps and institutional affiliations.

Tab. S1. DNA sequences used for localization studies with GFP-fusion constructs

All gene fragments used for localization studies were cloned to the 5' end of GFP. ppdk – pyruvate; Pi-dikinase; rbcS – Rubisco small subunit; tpi – triosephosphate isomerase; ak – adenylate kinase, TP_ppdk – transit peptide of pyruvate; Pi-dikinase; TP_tpi – transit peptide of triosephosphate isomerase; TP_ak – transit peptide of adenylate kinase

ppdk224aa
gctacccggg**ATG**GCATTATGTTTCAAAGGAATGCTAATCAGATCTGCTCCAGATGTATTTACACATACACTTGGTTATATGAAGGACCAATATCAAGTTGGTTGTAGCCAATGCAATAGTTTTCAGCGTGTTCAATTCCGGAACAGGAGGAGATGCCCACATCGATTAACTAGCCAGAGCCAGTCCAACAGAC
AAGATGTCATGGCTTTGATCTCAGACCCAGTTTCAACCACCACACAGCAGCGAGTATTTACCTTTGGTAAAGGAAGAAGTGACGGGGACAAGAGCATGAAGTCCTTGTTGGGAGGTAAAGGAGCAAATCTTGCAGAAATGGCAAGCATAGGTTTATCTGTTCCTCCTGGGTTGACCATTTCTACAGAAGCATGC
CAAGAGTATCAGGACAGTGGCAAAATGCTTCCTGAAAGTCTGTGGGAGGAAATCCTTGAGGGCTTGAGGGTTATAGAGAGTGACATGGGAGCATACCTTGGAGACTCCTCTACACCTCTTCTACTTTCAGTTCGTTCTGGTGCTGCGATTTCTATGCCAGGGATGATGGACACTATCCTTAATCTTGGACTTAA
TGATGAAGTAGTTTCAGGGCTCGCCGCAAAGAGTGGAGAACGCTTTGCCTATGATTCATTTAGGCGCTTCTTGGACATGTTTGGTTGTGTAGTCATGGGTactagttgc

rbcS
atacccgggg**ATG**GCTTCCAGTTTGATGTCCAGCGCTGCCACTGCTGCCGTTGCTACCGCCGCTAGTGCTCAGGCAAGCATGGTGGCATCATTCAACGGGTTGAAGTCCACTTCAGCTTTCCCTGTTACCAGGAAATCCGACAATGACATTACTTCTCTTCCTAGCAACGGTGGAAAAGTCCAATGCATGCAGGTG
TGGCCACCAATTGGCAAGAAGAAGTTCGAGACTCTTTCTTACCTTCCACCTCTATCTACAGAATCCTTGTTGCGTGAGATCCAATACCTTCTTAACAAAGGTTGGGTACCCTGCTTAGAATTCGAGCCAGAACACGGATTTGTGTACCGTGAGAACCACAGGTCACCAGGGTACTATGATGGACGCTACTGGACC
ATGTGGAAGCTCCCCATGTTCGGATGCACTGACCCAGCTCAGGTTGTGAATGAGCTCGAGGAGGCCAAGAAGGCTTACCCACAAGCCTTCATCCGGATCATTGGGTTCGACAACGTGCGTCAAGTCCAGTGCATCAGTTTCATTGCCTACAAGCCCCCAGGCTACataactagt

tpi
atacccgggg**ATG**GCGGTTCTCTCAACTTCATTAGCGTCGCGGTTGACTAACCCTAACTCTGTTGTTTCTACTCAGTTTTCTGGTCTACGACCGTCGGTTCTTAAGTTTGAAAGTAATTCTGTTTCGAATCAGAGCTTTTTCCCGAATGTTGATTCTCAATTGCGCTTATCATCTTCTCGCCGTGGTTCTAGAGGT
GTTGTACCTATGGCTGCTTCTGGAAAGTTTTCTGGTATTCGACCATCGTTTCATAAGTTTGAAAGTAGTTCTGTTTCGAATCAAAGCTTTTTCCAGAATGTCGACTCTCATTTGCGCTTATCATCTTCTCGCCGTGGTTCTAGAGATGTTGCAGCTATGGCTGCTTCTGGAAAGTTCTTCGTTGGCGGTAATTGG
AAGTGTAATGGGACCAAAGAATCAATCACTAAGCTTGTTTCAGACTTGAACAGTGCAACATTGGAGGCTGATGTTGATGTTGTTGTCGCACCTCCGTTTGTTTACATTGATCAAGTTAAGAATTCTCTGACCAGTCGAGTAGAGATGTCAGCACAAAACTGTTGGATTGGGAAAGGTGGGGCTTTTACGGGAGAA
ATCTGTGCTGAACAATTGAAGGATCTTGGGTGCCAGTGGGTTATTCTTGGGCATTCTGAGCGAAGACATGTTATTGGGGAAAATGATGAGTTTATAGGGAAAAAGGCTGCATATGCTTTGAACCAAGGTCTTGGAGTAATAGCATGTATTGGAGAGCTGTTAGAAGAAAGAGAAGCAGGAAAAACCTTTGATGTA
TGCTACCAACAATTGAAGGCTTTTGCAGATGCCGTTCCTAGCTGGGATAAGGTTGTCATTGCTTATGAACCTGTATGGGCTATTGGTACTGGCAAAGTAGCTACCCCAGAGCAGGCTCAAGAAGTGCATGTTGCTGTTCGGAATTGGCTTAAAAAGAATGTTTCTGAAGAAGTTGCTTCTAAGATGCGCATCATT
TATGGAGGGTCTGTTAATGGAGGCAACTGTGCAGAGCTTGCGAAACAAGAAGATATAGATGGATTTCTTGTGGGAGGTGCTTCTTTGAAGGGCCCTGAGTTCGCCACCATTGCTAATTCTGTGACAGCAAAGAAAGTTGCTGCCactagttat

Ak
aacccgggg**ATG**AATTCCTCTACCATTTATGGAAAGCCTAATTCCGCCATTCTCTCACCCCCTTCTCCTTTTTCCCGCACTTCCTCTCCTAAATTCTCTTCAGTCTCCTTCAATTCTCATCCCTCCCTCTCCTTTCGCTTCGATCAATTAGCAACTTCACATAAGTCACGCATTCATCATCGTCATCGTCATCGTC
ATCGTCGTTCCAATTTTGTGGCTATGGCATCTACTGATAACTCAAACCCACTGGGGATTATGATATCGGGTGCTCCAGCATCTGGCAAAGGGACTCAATGTGAGCTCATAACTGAGAAATATGGTTTGGTGCATATTGCTGCTGGAGATTTGCTTCGGACAGAGATCAAATCTGGTAGTGAAAATGGAAAACAAG
CCAAGGAATACATGGACAAAGGACAGTTGGTTCCAGATGAAATAGTTGTAAAGATGGTTAAAGACCGTTTGCTGCAATCAGATTCACAAGAGAACGGCTGGCTTTTGGATGGATACCCAAGAAGCTTATCTCAAGCAATTGCTCTCAAGGACTTTGGGCTCCAACCTGACCTTTTCATTCTTTTGGAAGTCCCTG
AAGAATTACTTGTTGAGAGGGTTGTTGGACGAAGGTTAGATCCTGATACTGGAAAAATATACCACATGAAGTATTCCCCTCCTGAGAATGATGAAGTTGCTTCCAGGCTCACTCAGCGGTTTGATGATACCGAGGAAAAGGTAAAATTGCGTCTGCAAACTTACCATCAAAATGTGGAGGCAGTGCTTTCCATGT
ATGAAGACATAATTTTTAAGGTTGATGGAAGTGTTAAAAAAGATGATGTATTTGCTCAGATCGACAAGGCACTCTCCAAGCTTGTGGAACAAAAAACTGCTTCAAAATCGGCGGCAGCCactagttt

TP_ppdk
gctacccgggg**ATG**GCATTATGTTTCAAAGGAATGCTAATCAGATCTGCTCCAGATGTATTTACACATACACTTGGTTATATGAAGGACCAATATCAAGTTGGTTGTAGCCAATGCAATAGTTTTCAGCGTGTTCAATTCCGGAACAGGAGGAGATGCCCACATCGATTAACTAGCCAGAGCCAGTCCAACAGACA
AGATGTCATGGCTTTGATCTCAGACCCAGTTTCAactagttcg

TP_tpi
gctacccgggg**ATG**GCATTATGTTTCAAAGGAATGCTAATCAGATCTGCTCCAGATGTATTTACACATACACTTGGTTATATGAAGGACCAATATCAAGTTGGTTGTAGCCAATGCAATAGTTTTCAGCGTGTTCAATTCCGGAACAGGAGGAGATGCCCACATCGATTAACTAGCCAGAGCCAGTCCAACAGACA
AGATGTCATGGCTTTGATCTCAGACCCAGTTTCAactagttcg

TP_ak
aacccgggg**ATG**AATTCCTCTACCATTTATGGAAAGCCTAATTCCGCCATTCTCTCACCCCCTTCTCCTTTTTCCCGCACTTCCTCTCCTAAATTCTCTTCAGTCTCCTTCAATTCTCATCCCTCCCTCTCCTTTCGCTTCGATCAATTAGCAACTTCACATAAGTCACGCATTCATCATCGTCATCGTCATCGTC
ATCGTCGTTCCAATTTTGTGGCTATGaaactagt

Tab. S2. Oligonucleotide sequences

Oligonucleotides for the amplification of endogenous genes and mutagenesis via SOE-PCR, QuickChange mutagenesis and PCR based mutagenesis.

SOE-PCR

Oligo name	Sequence (5' to 3')
TPI_II_fw	TCAACTTCATTAGCGGCGGCGGCTGCCGCTGCCGCTGTTGTTTCTACT
TPI_II_rv	AGTAGAAACAACAGCGGCAGCGGCAGCCGCCGCCGCCGCTAATGAAGTTGA
TPI_III_fw	AACTCTGTTGTTGCTGCTGCGGCTGCTGCTGCAGCACCGTCGGTTCTT
TPI_III_rv	AAGAACCGACGGTGCTGCAGCAGCAGCCGCAGCAGCAACAACAGAGTT
TPI_IV_fw	CAGTTTTCTGGTGCAGCAGCGGCGGCTGCTGCGGCTGAAAGTAATTCT
TPI_IV_rv	AGAATTACTTTCAGCCGCAGCAGCCGCCGCTGCTGCACCAGAAAACTG
TPI_V_fw	GTTCTTAAGTTTGCAGCTGCTGCTGCTGCGGCTGCGAGCTTTTTCCCG
TPI_V_rv	CGGGAAAAAGCTCGCAGCCGCAGCAGCAGCAGCTGCAAACTTAAGAAC
TPI_VI_fw	GTTTCGAATCAGGCCGCTGCCGCGGCTGCTGCTGCTCAATTGCGCTTA
TPI_VI_rv	TAAGCGCAATTGAGCAGCAGCAGCCGCGGCAGCGGCCTGATTCGAAAC
TPI_VII_fw	AATGTTGATTCTGCAGCGGCCGCAGCAGCTGCTGCCCGTGGTTCTAGA
TPI_VII_rv	TCTAGAACCACGGGCAGCAGCTGCTGCGGCCGCTGCAGAATCAACATT
TPI_QLRL_fw	AATGTTGATTCTGCAGCAGCAGCATCATCTTCTCGC
TPI_QLRL_rv	GCGAGAAGATGATGCTGCTGCTGCAGAATCAACATT
TPI_SSS_fw	GATTCTCAATTGCGCTTAGCAGCTGCTCGCCGTGGTTCTAGAGG
TPI_SSS_rv	CCTCTAGAACCACGGCGAGCAGCTGCTAAGCGCAATTGAGAATC
PPDK_II_fw	TTCAAAGGAATGGCTGCCGCTGCTGCTGCTGCTGCATTTACACATACA
PPDK_II_rv	TGTATGTGTAAATGCAGCAGCAGCAGCAGCGGCAGCCATTCCTTTGAA
PPDK_III_fw	GCTCCAGATGTAGCAGCTGCTGCAGCTGCTGCTGCGAAGGACCAATAT
PPDK_III_rv	ATATTGGTCCTTCGCAGCAGCAGCTGCAGCAGCAGCTACATCTGGAGC
PPDK_IV_fw	ACACTTGGTTATATGGCTGCTGCTGCTGCAGCTGCTGCTAGCCAATGCAAT
PPDK_IV_rv	ATTGCATTGGCTAGCAGCAGCTGCAGCAGCAGCAGCCATATAACCAAGTGT
PPDK_V_fw	CAAGTTGGTTGTGCCGCTGCTGCTGCTGCTGCGGCTGTTCAATTCCGG
PPDK_V_rv	CCGGAATTGAACAGCCGCAGCAGCAGCAGCAGCGGCACAACCAACTTG
PPDK_VI_fw	AGTTTTCAGCGTGCTGCAGCAGCAGCCGCAGCAGCATGCCCACATCGA
PPDK_VI_rv	TCGATGTGGGCATGCTGCTGCGGCTGCTGCTGCAGCACGCTGAAAACT
PPDK_VII_fw	AACAGGAGGAGAGCCGCAGCTGCAGCAGCTGCCGCGAGCCAGTCCAAC
PPDK_VII_rv	GTTGGACTGGCTCGCGGCAGCTGCTGCAGCTGCGGCTCTCCTCCTGTT
PPDK_VIII_fw	TTAACTAGCCAGGCAGCAGCAGCCGCAGCAGCTGCCATGGCTTTGATC
PPDK_VIII_rv	GATCAAAGCCATGGCAGCTGCTGCGGCTGCTGCTGCCTGGCTAGTTAA
PPDK_VQFR_fw	AGTTTTCAGCGTGCTGCAGCCGCGAACAGGAGGAGA
PPDK_VQFR_rv	TCTCCTCCTGTTCGCGGCTGCAGCACGCTGAAAACT
PPDK_NRRR_fw	GTTCAATTCCGGGCCGCAGCAGCATGCCCACATCGA
PPDK_NRRR_rv	TCGATGTGGGCATGCTGCTGCGGCCCGGAATTGAAC

QuickChange Mutagenesis

Oligo name	Sequence (5' to 3')
TPI_RL_fw	GATTCTCAATTGGCCGCATCATCTTCTCGCCGTGGT
TPI_RL_rv	ACCACGGCGAGAAGATGATGCGGCCAATTGAGAATC
TPI_QL_fw	AATGTTGATTCTGCAGCGCGCTTATCATCTTCTCGCCGT
TPI_QL_rv	ACGGCGAGAAGATGATAAGCGCGCTGCAGAATCAACATT
TPI_R_fw	CCCGAATGTTGATTCTCAATTGGCCTTATCATCTTCTC
TPI_R_rv	GAGAAGATGATAAGGCCAATTGAGAATCAACATTCGGG

PCR-based mutagenesis

Oligo name	Sequence (5' to 3')
TPI_I_fw	atacccgggATGGCGGCTGCCGCAGCTGCAGCAGCGTCG
TPI_VIII_rv	ataactagtAGAAGCAGCCATAGCTGCAGCAGCTGCAGCAGCAGCGCG
PPDK_I_fw	atacccgggATGGCAGCAGCAGCAGCAGCAGCGGCAATCAGATCTGCT
PPDK_IX_rv	aaaactagtTGAAGCTGCGGCTGCGGCCGCTGCCGCGACATCTTGTCT
TPI_RGSR_rv	ataactagtAGAAGCAGCCATAGCTGCAGCAGCTCTAGAACC
TPI_GVVP_rv	ataactagtAGAAGCAGCCATAGGTACAACACCTGCAGCAGCAGCGCGAGA

PCR endogenous sequences

Oligo name	Sequence (5' to 3')
35S_fw	ACAATCCCACTATCCTTCGCA
GFP_rv	TCACCTTCACCCTCTCCACT
TPI_fw	atacccgggATGGCGGTTCTCTCAACTTCA
TPI_rv	ataactagtGGCAGCAACTTTCTTTGCTGT
TP_TPI_rv	ataactagtAGAAGCAGCCATAGGTACAACACC
AK_fw	aacccgggATGAATTCCTCTACCATTTA
AK_rv	aaactagtGGCTGCCGCCGATT
TP_AK_rv	aaactagtCATAGCCACAAAATTGGAACGACG
PPDK_fw	gctacccgggATGGCATTATGTTTCAAAGGAATGCTAATCAG
PPDK_rv	gcaactagtACCCATGACTACACAACCAAAC
TP_PPDK_rv	cgaactagtTGAAACTGGGTCTGAGATCAAAGC
rbcS_fw	atacccgggATGGCTTCCAGTTTGATGTCC
rbcS_rv	ataactagtGTAGCCTGGGGGCTTGTAGGC
TP_rbcS_rv	ataactagtCATGCATTGGACTTTTCCACCGTTGC

Tab. S3. Sequences of mutated gene fragments generated by SOE-PCR or QuickChange mutagenesis
All mutated gene fragments used for localization studies were cloned to the 5'end of GFP. Small letters – restriction sites; ATG is marked in bold

Method SOE-PCR:

tpi_II
atacccggg**ATG**GCGGTTCTCTCAACTTCATTAGCGGCGGCGGCGGCTGCCGCTGCCGCTGTTGTTTCTACTCAGTTTTCTGGTCTACGACCGTCGGTTCTTAAGTTTGAAAGTAATTCTGTTTCGAATCAGAGCTTTTTCCCGAATGTTGATTCTCAATTGCGCTTATCATCTTCTCGCCGTGGTTCTAGAGG
TGTTGTACCTATGGCTGCTTCTactagttat

tpi_III
Atacccggg**ATG**GCGGTTCTCTCAACTTCATTAGCGTCGCGGTTGACTAACCCTAACTCTGTTGTTGCTGCTGCGGCTGCTGCTGCAGCACCGTCGGTTCTTAAGTTTGAAAGTAATTCTGTTTCGAATCAGAGCTTTTTCCCGAATGTTGATTCTCAATTGCGCTTATCATCTTCTCGCCGTGGTTCTAGAGG
TGTTGTACCTATGGCTGCTTCTactagttat

tpi_V
atacccggg**ATG**GCGGTTCTCTCAACTTCATTAGCGTCGCGGTTGACTAACCCTAACTCTGTTGTTTCTACTCAGTTTTCTGGTCTACGACCGTCGGTTCTTAAGTTTGCAGCTGCTGCTGCTGCGGCTGCGAGCTTTTTCCCGAATGTTGATTCTCAATTGCGCTTATCATCTTCTCGCCGTGGTTCTAGAGG
TGTTGTACCTATGGCTGCTTCTactagttat

tpi_VI
atacccggg**ATG**GCGGTTCTCTCAACTTCATTAGCGTCGCGGTTGACTAACCCTAACTCTGTTGTTTCTACTCAGTTTTCTGGTCTACGACCGTCGGTTCTTAAGTTTGAAAGTAATTCTGTTTCGAATCAGGCCGCTGCCGCGGCTGCTGCTGCTCAATTGCGCTTATCATCTTCTCGCCGTGGTTCTAGAGG
TGTTGTACCTATGGCTGCTTCTactagttat

tpi_VII
atacccggg**ATG**GCGGTTCTCTCAACTTCATTAGCGTCGCGGTTGACTAACCCTAACTCTGTTGTTTCTACTCAGTTTTCTGGTCTACGACCGTCGGTTCTTAAGTTTGAAAGTAATTCTGTTTCGAATCAGAGCTTTTTCCCGAATGTTGATTCTGCAGCGGCCGCAGCAGCTGCTGCCCGTGGTTCTAGAGG
TGTTGTACCTATGGCTGCTTCTactagttat

ppdk_II
gctacccggg**ATG**GCATTATGTTTCAAAGGAATGGCTGCCGCTGCTGCTGCTGCTGCATTTACACATACACTTGGTTATATGAAGGACCAATATCAAGTTGGTTGTAGCCAATGCAATAGTTTTCAGCGTGTTCAATTCCGGAACAGGAGGAGATGCCCACATCGATTAACTAGCCAGAGCCAGTCCAACAGAC
AAGATGTCATGGCTTTGATCTCAGACCCAGTTTCAactagttcg

ppdk_III
gctacccggg**ATG**GCATTATGTTTCAAAGGAATGCTAATCAGATCTGCTCCAGATGTAGCTGCTGCTGCAGCTGCTGCTGCGAAGGACCAATATCAAGTTGGTTGTAGCCAATGCAATAGTTTTCAGCGTGTTCAATTCCGGAACAGGAGGAGATGCCCACATCGATTAACTAGCCAGAGCCAGTCCAACAGAC
AAGATGTCATGGCTTTGATCTCAGACCCAGTTTCAactagttcg

ppdk_IV
gctacccggg**ATG**GCATTATGTTTCAAAGGAATGCTAATCAGATCTGCTCCAGATGTATTTACACATACACTTGGTTATATGGCTGCTGCTGCTGCAGCTGCTGCTAGCCAATGCAATAGTTTTCAGCGTGTTCAATTCCGGAACAGGAGGAGATGCCCACATCGATTAACTAGCCAGAGCCAGTCCAACAGAC
AAGATGTCATGGCTTTGATCTCAGACCCAGTTTCAactagttcg

ppdk_V
gctacccggg**ATG**GCATTATGTTTCAAAGGAATGCTAATCAGATCTGCTCCAGATGTATTTACACATACACTTGGTTATATGAAGGACCAATATCAAGTTGGTTGTGCCGCTGCTGCTGCTGCTGCGGCTGTTCAATTCCGGAACAGGAGGAGATGCCCACATCGATTAACTAGCCAGAGCCAGTCCAACAGAC
AAGATGTCATGGCTTTGATCTCAGACCCAGTTTCAactagttcg

ppdk_VI
Gctacccggg**ATG**GCATTATGTTTCAAAGGAATGCTAATCAGATCTGCTCCAGATGTATTTACACATACACTTGGTTATATGAAGGACCAATATCAAGTTGGTTGTAGCCAATGCAATAGTTTTCAGCGTGCTGCAGCAGCAGCCGCAGCAGCATGCCCACATCGATTAACTAGCCAGAGCCAGTCCAACAGAC
AAGATGTCATGGCTTTGATCTCAGACCCAGTTTCAactagttcg

ppdk_VII
Gctacccggg**ATG**GCATTATGTTTCAAAGGAATGCTAATCAGATCTGCTCCAGATGTATTTACACATACACTTGGTTATATGAAGGACCAATATCAAGTTGGTTGTAGCCAATGCAATAGTTTTCAGCGTGTTCAATTCCGGAACAGGAGGAGAGCCGCAGCTGCAGCAGCTGCCGCGAGCCAGTCCAACAGAC
AAGATGTCATGGCTTTGATCTCAGACCCAGTTTCAactagttcg

Tab. S3. Sequences of mutated gene fragments generated by SOE-PCR or QuickChange mutagenesis
All mutated gene fragments used for localization studies were cloned to the 5'end of GFP. small letters – restriction sites; ATG is marked in bold

Method SOE-PCR

tpi_SSS
atacccggg**ATG**GCGGTTCTCTCAACTTCATTAGCGTCGCGGTTGACTAACCCTAACTCTGTTGTTTCTACTCAGTTTTCTGGTCTACGACCGTCGGTTCTTAAGTTTGAAAGTAATTCTGTTTCGAATCAGAGCTTTTTCCCGAATGTTGATTCTCAATTGCGCTTAGCAGCTGCTCGCCGTGGTTCTAGAGG
TGTTGTACCTATGGCTGCTTCTactagttat

tpi_I
tacccggg**ATG**GCGGCTGCCGCAGCTGCAGCGGCGTCGCGGTTGACTAACCCTAACTCTGTTGTTTCTACTCAGTTTTCTGGTCTACGACCGTCGGTTCTTAAGTTTGAAAGTAATTCTGTTTCGAATCAGAGCTTTTTCCCGAATGTTGATTCTCAATTGCGCTTATCATCTTCTCGCCGTGGTTCTAGAGGT
GTTGTACCTATGGCTGCTTCTactagttat

ppdk_I
aatacccggg**ATG**GCAGCAGCAGCAGCAGCAGCGGCAATCAGATCTGCTCCAGATGTATTTACACATACACTTGGTTATATGAAGGACCAATATCAAGTTGGTTGTAGCCAATGCAATAGTTTTCAGCGTGTTCAATTCCGGAACAGGAGGAGATGCCCACATCGATTAACTAGCCAGAGCCAGTCCAACAGAC
AAGATGTCATGGCTTTGATCTCAGACCCAGTTTCAactagttcg

ppdk_IX
gctacccggg**ATG**GCATTATGTTTCAAAGGAATGCTAATCAGATCTGCTCCAGATGTATTTACACATACACTTGGTTATATGAAGGACCAATATCAAGTTGGTTGTAGCCAATGCAATAGTTTTCAGCGTGTTCAATTCCGGAACAGGAGGAGATGCCCACATCGATTAACTAGCCAGAGCCAGTCCAACAGAC
AAGATGTCGCGGCAGCGGCCGCAGCCGCAGCTTCAactagtttt

tpi_RGSR
atacccggg**ATG**GCGGTTCTCTCAACTTCATTAGCGTCGCGGTTGACTAACCCTAACTCTGTTGTTTCTACTCAGTTTTCTGGTCTACGACCGTCGGTTCTTAAGTTTGAAAGTAATTCTGTTTCGAATCAGAGCTTTTTCCCGAATGTTGATTCTCAATTGCGCTTATCATCTTCTCGCCGTGGTTCTAGAGC
TGCTGCAGCTATGGCTGCTTCTactagttat

tpi_GVVP
atacccggg**ATG**GCGGTTCTCTCAACTTCATTAGCGTCGCGGTTGACTAACCCTAACTCTGTTGTTTCTACTCAGTTTTCTGGTCTACGACCGTCGGTTCTTAAGTTTGAAAGTAATTCTGTTTCGAATCAGAGCTTTTTCCCGAATGTTGATTCTCAATTGCGCTTATCATCTTCTCGCGCTGCTGCTGCAGG
TGTTGTACCTATGGCTGCTTCTactagttat

tpi_QLRL
atacccggg**ATG**GCGGTTCTCTCAACTTCATTAGCGTCGCGGTTGACTAACCCTAACTCTGTTGTTTCTACTCAGTTTTCTGGTCTACGACCGTCGGTTCTTAAGTTTGAAAGTAATTCTGTTTCGAATCAGAGCTTTTTCCCGAATGTTGATTCTGCAGCGGCCGCATCATCTTCTCGCCGTGGTTCTAGAGG
TGTTGTACCTATGGCTGCTTCTactagttat

QuickChange Mutagenesis

tpi_QL
atacccggg**ATG**GCGGTTCTCTCAACTTCATTAGCGTCGCGGTTGACTAACCCTAACTCTGTTGTTTCTACTCAGTTTTCTGGTCTACGACCGTCGGTTCTTAAGTTTGAAAGTAATTCTGTTTCGAATCAGAGCTTTTTCCCGAATGTTGATTCTGCAGCGCGCTTATCATCTTCTCGCCGTGGTTCTAGAGG
TGTTGTACCTATGGCTGCTTCTactagttat

tpi_RL
atacccggg**ATG**GCGGTTCTCTCAACTTCATTAGCGTCGCGGTTGACTAACCCTAACTCTGTTGTTTCTACTCAGTTTTCTGGTCTACGACCGTCGGTTCTTAAGTTTGAAAGTAATTCTGTTTCGAATCAGAGCTTTTTCCCGAATGTTGATTCTCAATTGGCCGCATCATCTTCTCGCCGTGGTTCTAGAGG
TGTTGTACCTATGGCTGCTTCTactagttat

tpi_R
atacccggg**ATG**GCGGTTCTCTCAACTTCATTAGCGTCGCGGTTGACTAACCCTAACTCTGTTGTTTCTACTCAGTTTTCTGGTCTACGACCGTCGGTTCTTAAGTTTGAAAGTAATTCTGTTTCGAATCAGAGCTTTTTCCCGAATGTTGATTCTCAATTGGCCGCATCATCTTCTCGCCGTGGTTCTAGAGG
TGTTGTACCTATGGCTGCTTCTactagttat

Tab. S4

Sequences of mutated gene fragments generated by gene synthesis

All mutated gene fragments used for localization studies were cloned to the 5' end of GFP. small letters – restriction sites; ATG is marked in bold. Italic letters in WT_TP_OOF marked the sequence of the 'out of frame transit peptide' of TPI.

Method gene synthesis

tpi_VII_mRNA
ataccc**ATG**GCGGTTCTCTCAACTTCATTAGCGTCGCGGTTGACTAACCCTAACTCTGTTGTTTCTACTCAGTTTTCTGGTCTACGACCGTCGGTTCTTAAGTTTGAAAGTAATTCTGTTTCGAATCAGAGCTTTTTCCCGAATGTTGATTCTCAGCTCAGGCTTAGCAGCAGCAGACGTGGTTCTAGAGGT
GTTGTACCTATGGCTGCTTCTataactagt

tpi_VIII_mRNA
ataccc**ATG**GCGGTTCTCTCAACTTCATTAGCGTCGCGGTTGACTAACCCTAACTCTGTTGTTTCTACTCAGTTTTCTGGTCTACGACCGTCGGTTCTTAAGTTTGAAAGTAATTCTGTTTCGAATCAGAGCTTTTTCCCGAATGTTGATTCTCAATTGCGCTTATCATCTTCTCGCAGAGGCAGCCGGGGC
GTCGTCCCGATGGCTGCTTCTactagttat

ppdk_VI_mRNA
gctaccc**ATG**GCATTATGTTTCAAAGGAATGCTAATCAGATCTGCTCCAGATGTATTTACACATACACTTGGTTATATGAAGGACCAATATCAAGTTGGTTGTAGCCAATGCAATAGTTTTCAGCGTGTCCAGTTTAGAAATCGACGTCGCTGCCCACATCGATTAACTAGCCAGAGCCAGTCCAACAGAC
AAGATGTCATGGCTTTGATCTCAGACCCAGTTTCAactagttcg

WT_tpi_OOF
ataccc**ATG***ATACGGCGGTTCTCTCAACTTCATTAGCGTCGCGGTTGACTAACCCTAACTCTGTTGTTTCTACTCAGTTTTCTGGTCTACGACCGTCGGTTCTTAAGTTTGAAAGTAATTCTGTTTCGAATCAGAGCTTTTTCCCGAATGTTGATTCTCAATTGCGCTTATCATCTTCTCGCCGTGGTTCTAGAG*
*GTGTTGTACCT***ATG**GCTGCTTCTATGGCTTCCAGTTTGATGTCCAGCGCTGCCACTGCTGCCGTTGCTACCGCCGCTAGTGCTCAGGCAAGCATGGTGGCATCATTCAACGGGTTGAAGTCCACTTCAGCTTTCCCTGTTACCAGGAAATCCGACAATGACATTACTTCTCTTCCTAGCAACGGTGGAAAAGTCC
AATGCATGCAGGTGTGGCCACCAATTGGCAAGAAGAAGTTCGAGACTCTTTCTTACCTTCCACCTCTATCTACAGAATCCTTGTTGCGTGAGATCCAATACCTTCTTAACAAAGGTTGGGTACCCTGCTTAGAATTCGAGCCAGAACACGGATTTGTGTACCGTGAGAACCACAGGTCACCAGGGTACTATGATG
GACGCTACTGGACCATGTGGAAGCTCCCCATGTTCGGATGCACTGACCCAGCTCAGGTTGTGAATGAGCTCGAGGAGGCCAAGAAGGCTTACCCACAAGCCTTCATCCGGATCATTGGGTTCGACAACGTGCGTCAAGTCCAGTGCATCAGTTTCATTGCCTACAAGCCCCCAGGCTACcgaactagt

ppdk_V_VI
gctaccc**ATG**GCATTATGTTTCAAAGGAATGCTAATCAGATCTGCTCCAGATGTATTTACACATACACTTGGTTATATGAAGGACCAATATCAAGTTGGTTGTAGCCAATGCGCTGCTGCTGCGGCTGCTGCAGCCCGGAACAGGAGGAGATGCCCACATCGATTAACTAGCCAGAGCCAGTCCAACAGACA
AGATGTCATGGCTTTGATCTCAGACCCAGTTTCAactagttcg

ppdk_VQFR
gctaccc**ATG**GCATTATGTTTCAAAGGAATGCTAATCAGATCTGCTCCAGATGTATTTACACATACACTTGGTTATATGAAGGACCAATATCAAGTTGGTTGTAGCCAATGCAATAGTTTTCAGCGTGCTGCAGCCGCGAACAGGAGGAGATGCCCACATCGATTAACTAGCCAGAGCCAGTCCAACAGACA
AGATGTCATGGCTTTGATCTCAGACCCAGTTTCAactagttcg

ppdk_NRRR
gctaccc**ATG**GCATTATGTTTCAAAGGAATGCTAATCAGATCTGCTCCAGATGTATTTACACATACACTTGGTTATATGAAGGACCAATATCAAGTTGGTTGTAGCCAATGCAATAGTTTTCAGCGTGTTCAATTCCGGGCCGCAGCAGCATGCCCACATCGATTAACTAGCCAGAGCCAGTCCAACAGACA
AGATGTCATGGCTTTGATCTCAGACCCAGTTTCAactagttcg

ShTPI
aaaccc**ATG**GCGGTTGTATCAACTTCATTAGCGTCGCAACTAAGTAACCCTAACGCCATTGTTTCAACTCAGTTTTCTGGTCTTCGACGATCGTTTCTTAAGCTTGAAAGTAGTTCTTCTTCTTCTTCTTCAAATCAATGCTTTTTTCAAGTTGTTGATTCTCATTTGCTCTTATCGTCTTCTCGCCGTGGT
TCTAGAGGTGTTGTTACTATGGCTGGTTCTactagttaa

ShTPI_1
aaaccc**ATG**GCGGTTGTATCAACTTCATTAGCGTCGCAACTAAGTAACCCTAACGCCATTGTTTCAACTCAGTTTTCTGGTCTTCGACGATCGTTTCTTAAGCTTGAAAGTAGTTCTTCTTCTTCTTCTTCAAATCAATGCTTTTTTCAAGTTGTTGATTCTCAATTGCGCTTATCGTCTTCTCGCCGTGGT
TCTAGAGGTGTTGTTACTATGGCTGGTTCTactagttaa

ShTPI_2
aaaccc**ATG**GCGGTTGTATCAACTTCATTAGCGTCGCAACTAAGTAACCCTAACGCCATTGTTTCAACTCAGTTTTCTGGTCTTCGACGATCGTTTCTTAAGCTTGAAAGTAGTTCTTCTTCTTCTTCTTCAAATCAATGCTTTTTTCAAGTTGTTGATTCTCAATTGCGCTTATCGTCTTCTCGCCGTGGT
TCTAGAGGTGTTGTTCCTATGGCTGCTTCTactagttaa

ShTPI_3
aaaccc**ATG**GCGGTTGTATCAACTTCATTAGCGTCGCAACTAAGTAACCCTAACGCCATTGTTTCAACTCAGTTTTCTGGTCTTCGACGATCGTTTCTTAAGCTTGAAAGTAGTTCTTCTTCTTCTTCTTCAAATCAAAGCTTTTTTCCGAATGTTGATTCTCAATTGCGCTTATCGTCTTCTCGCCGTGGT
TCTAGAGGTGTTGTTCCTATGGCTGCTTCTactagttaa

ShTPI_4
aaaccc**ATG**GCGGTTGTATCAACTTCATTAGCGTCGCAACTAAGTAACCCTAACGCCATTGTTTCAACTCAGTTTTCTGGTCTTCGACGATCGTTTCTTAAGCTTGAAAGTAATTCTGTTTCTAATCAAAGCTTTTTTCCGAATGTTGATTCTCAATTGCGCTTATCGTCTTCTCGCCGTGGTTCTAGAGGT
GTTGTTCCTATGGCTGCTTCTactagttaa

Tab. S5. ChloroP predicted transit peptide sequences of P-chloroplast localized proteins
CS (cleavage site) score - is the MEME scoring matrix score for the suggested cleavage site (55), TP (transit peptide) length - predicted length of the precursor proteins PPDK – pyruvate; Pi-dikinase; TPI – triosephosphate isomerase; AK – adenylate kinase

Protein	CS-score	TP length
PPDK	0.519	72
TPI	0.583	64
AK	0.590	69

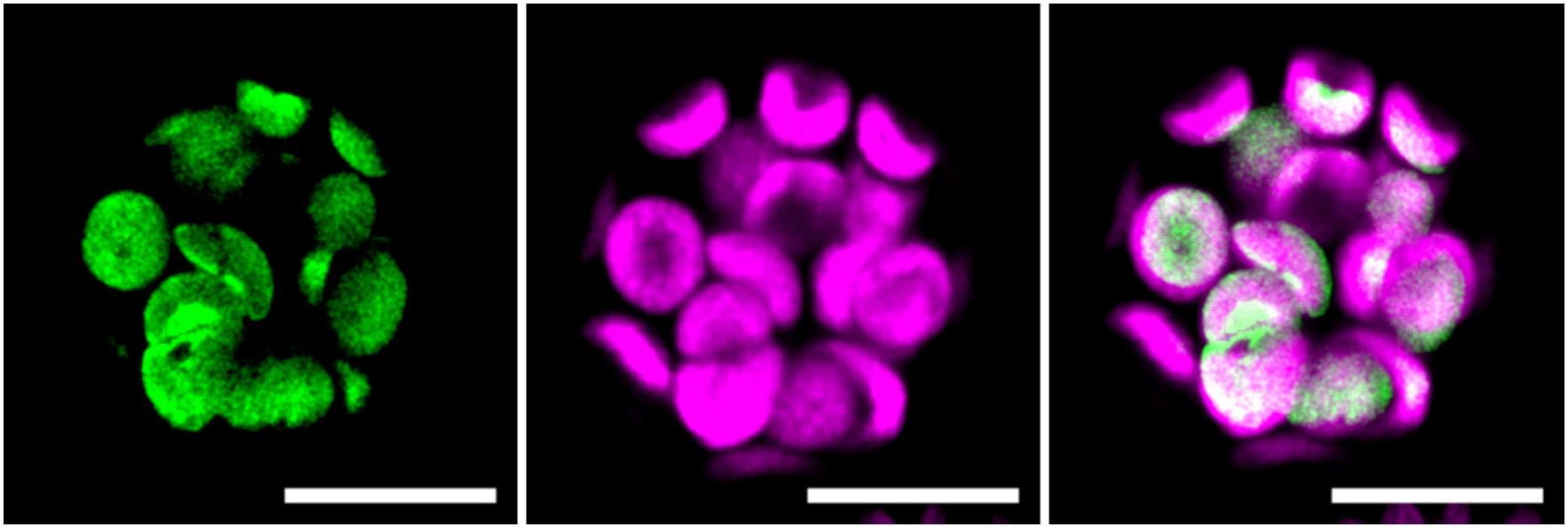

Fig. S1. Subcellular localization of PPDK in *Arabidopsis thaliana*
Confocal image of Bienertia sinuspersici PPDK224-GFP-fusion heterologously expressed in A. thaliana mesophyll protoplasts. The fluorescence image is shown in the GFP channel (excitation 488 nm/emission 509/525 nm) and the chlorophyll autofluorescence in the red channel (excitation 408 nm/emission 620/700 nm). Additionally, the merged channel is shown. The image is representative for n = 2 independent experiments. All scale bars = 10 µm

2.4 Publication IV

Development of an *Agrobacterium*-mediated transformation protocol for the single-cell C4 species *Bienertia sinuspersici* enables high resolution *in vivo* protein localization analysis of subcellular compartmentation

Diana Wimmer[1], Philipp Bohnhorst[1], Daniela Impe[2], Inhwan Hwang[3] and Sascha Offermann[1*]

[1] Institute for Botany, Leibniz University Hannover, Herrenhaeuser Strasse 2, D-30419, Hannover, Germany

[2] Leibniz Institute of Plant Genetics and Crop Plant Research (IPK-Gatersleben), Genebank Department, Cryo and Stress Biology Group, Corrensstrasse 3, D-06466 Stadt Seeland, Germany

[3] Division of Integrative Biosciences and Biotechnology, Pohang University of Science and Technology, Pohang 790–784, Korea

Type of authorship:	First author
Type of article:	Research article
Share of the work:	85 %
Contribution to the publication:	planned and performed all experiments, analyzed data, prepared all figures and wrote the paper
Journal:	BMC Plant Biology
5-year impact factor:	3.631
Date of publication:	Submitted on February 28th, 2017

Development of an *Agrobacterium*-mediated transformation protocol for the single-cell C4 species *Bienertia sinuspersici* enables high resolution *in vivo* protein localization analysis of subcellular compartmentation

Diana Wimmer[1], Philipp Bohnhorst[1], Daniela Impe[2], Inhwan Hwang[3] and Sascha Offermann[1*]

[1]Institute for Botany, Leibniz University Hannover, Herrenhaeuser Strasse 2, D-30419, Hannover, Germany

[2]Leibniz Institute of Plant Genetics and Crop Plant Research (IPK-Gatersleben), Genebank Department, Cryo and Stress Biology Group, Corrensstrasse 3, D-06466 Stadt Seeland, Germany

[3]Division of Integrative Biosciences and Biotechnology, Pohang University of Science and Technology, Pohang 790–784, Korea

*Correspondence and requests for materials should be addressed to SO (email: s.offermann@botanik.uni-hannover.de)

Keywords

Bienertia sinuspersici, single-cell C4, *Agrobacterium*-mediated transformation, organelle positioning, NAD-ME C4 type, C4 photosynthesis, callus transformation, subcellular compartmentalization, GFP localization studies

Abstract

Bienertia sinuspersici is one of four terrestrial plant species known to perform C4 photosynthesis within individual photosynthetic cells. This is achieved through a specialized subcellular compartmentalization of primary and final CO_2 fixation and collaboration of two different chloroplast types within individual cells. While recent progress has been made in understanding the biochemistry and cell biology of this unique species, major molecular tools for in-depth analysis are currently unavailable.

Here we report the successful establishment of an *Agrobacterium*-mediated transformation system for *Bienertia sinuspersici*. Our results show that detached but not attached branches or direct injection of bacteria into Bienertia leaves results in successful transformation, possibly indicating that the immune system of intact and unstressed plants can effectively suppress infection by agrobacteria. Transformation efficiency was increased more than two-fold when leaves were mechanical wounded prior to vacuum infiltration. Also, Bienertia callus derived from leaf, shoot and root explant material was amenable to agrobacteria transformation which should provide useful in further attempts to create stably transformed Bienertia plants.

The established *Agrobacterium*-mediated transformation protocol was then used to probe for subcellular localization of several membrane associated marker proteins all indicating conservation of the unique single-cell C4 cell morphology in transformed cells. Analysis of green fluorescence protein (GFP) fusions of peroxisomal and mitochondrial markers revealed large numbers of these organelles not only as expected in the central cytoplasmic compartment but also in the periphery. Time lapse microscopy further indicated that mitochondria in both compartments are rather static in contrast to peroxisomes which are highly dynamic especially in the peripheral compartment.

Background

The majority of terrestrial plant species tend to photorespire under CO_2 limiting conditions. Such conditions are typically induced by closure of stomata due to high temperature or low water availability [1]. During photorespiration, the central CO_2 fixing enzyme ribulose-1,5-bisphosphate (Rubisco) reacts with oxygen instead of CO_2 and the resulting fixation product 2-phosphoglycolate needs to be detoxified in an energy consuming process that also releases previously fixed carbon [2, 3].

C4 plants operate a biochemical CO_2 concentrating mechanism that effectively suppresses photorespiration [4]. It has evolved independently at least 61 times and is found in many diverse plant families [5]. The vast majority of known C4 species use a specialized arrangement of two different photosynthetic cell types (termed Kranz anatomy) [6]. In Kranz C4 species, CO_2 is initially prefixed in mesophyll cells and the resulting C4 acids diffuse into the neighboring bundle sheath cells. Here, C4 acids are decarboxylated and the released CO_2 is ultimately fixed by Rubisco [7]. Since the C4 cycle runs faster than the Calvin-Benson-Bassham (CBB) cycle, C4 plants can effectively concentrate CO_2 around Rubisco [8]. However, C4 photosynthesis requires additional energy to operate the CO_2 concentrating mechanism on top of the CBB cycle [8].

The requirement for two cooperating cells types as realized in Kranz C4 photosynthesis has been believed to be mandatory for C4 photosynthesis for many years. However, a unique form of C4 has been identified in the family Amaranthaceae. Here, a total of four species are known to perform a complete C4 carbon concentrating mechanism within individual photosynthetic cells [9–13]. Single-cell C4 (SCC4) photosynthesis requires a special subcellular compartmentalization which has been best studied in the model species *Bienertia sinuspersici*. The cytoplasm of the chlorenchyma cells is separated by a large vacuole into a peripheral compartment and a second compartment at the cell's center [14]. Small cytoplasmic strands intersect the vacuole and allow for metabolite exchange between the two compartments. The two compartments harbor chloroplasts which differ significantly in their biochemical, physiological and morphological properties [15, 16]. The peripheral

compartment chloroplasts (PC chloroplasts) are dispersed throughout the peripheral cytoplasm, have a characteristic donut-like shape and are much larger compared to the central compartment chloroplasts [17]. The central compartment chloroplasts (CC chloroplasts) aggregate together with mitochondria to a ball like structure in the center of the cell [15].

In order to operate a C4 cycle within individual cells, atmospheric CO_2 is initially captured in the peripheral cytoplasm by action of cytoplasmic phosphoenolpyruvate carboxylase (PEPC). The peripheral chloroplasts are specialized for production of the primary CO_2 acceptor phosphoenolpyruvate (PEP) required for this reaction but lack a functional CBB cycle. C4 acids produced by the primary carboxylation reaction are converted to aspartate and diffuse through the cytoplasmic strands into the mitochondria of the central compartment. Here, CO_2 is released by mitochondrial NAD dependent malic enzyme (NAD-ME) and is then finally fixed through the CBB cycle in the surrounding central chloroplasts. Pyruvate resulting from mitochondrial decarboxylation is converted to alanine which diffuses back into the peripheral chloroplasts to complete the cycle [17, 18].

The basic biochemical properties of single-cell C4 photosynthesis are reasonably well understood. Also, we were recently able to demonstrate that targeting of nuclear encoded proteins specifically to the peripheral chloroplasts is controlled by short amino acid motifs in the transit peptides of peripheral chloroplast specific proteins [19]. Nevertheless, it is still completely unknown how the two different chloroplast types can develop and co-exist within individual cells and how the unique formation of the two subcellular compartments is regulated. Also, little information is available on the subcellular distribution of other organelles and the overall organization of these highly unusual cells. More detailed analysis has been hampered by the fact that many tools such as mutant collections, a sequenced genome or the ability to produce stably transformed plants are currently not available for any of the single-cell C4 species. As a first step, we therefore attempted to establish a protocol for *Agrobacterium*-mediated transformation. Our results indicate that Bienertia chlorenchyma cells as well as callus can indeed be transformed by agrobacteria. The developed protocol was further used to demonstrate the subcellular localization of several cellular membrane

systems and gave new insights into the distribution of mitochondria between the peripheral and central compartment.

Material & Methods

Plant material

Seeds of *Bienertia sinuspersici* were planted in soil and grown under controlled conditions in a GroBank Chamber (CLF Plant Climatics) at a day/night temperature of 25/20 °C. After germination for one day in the dark, seedlings were illuminated with a 16 h/8 h light/dark cycle at a photon flux intensity of 250 µmol m^{-2} s^{-1}. Plants were shifted after two weeks into a growth cabinet with a day/night temperature of 30/18 °C with 50 % relative humidity and a photoperiod of 16/8 h light/dark at a photon flux intensity of 350 µmol m^{-2} s^{-1}. Plants were watered twice a week with 0.03 M NaCl and 0.001 % (v/v) Wuxal fertilizer (Manna) and used after growing for 3-4 months for the *Agrobacterium*-mediated transformation.

Nicotiana tabacum L. cv. Petit Havana SR1 were grown in the greenhouse at long day conditions (16 h light/8 h dark). Six weeks old plants were transiently transformed with *Agrobacterium tumefaciens* [20].

Plasmid construction

Subcellular protein localization was visualized by GFP fusion constructs. *Bienertia sinuspersici nad-me (nad dependent malic-enzyme)* (102 nucleotide (nt) length) and *nad-mdh (nad-malate dehydrogenase)* (1038 nt length) gene fragments (Additional file 1) were amplified by polymerase chain reaction with *pfu* polymerase (Thermo Scientific) from cDNA, generated from Bienertia mRNA isolated by the GeneJET Plant RNA Purification Kit (Thermo Fisher Scientific). Oligonucleotides (Eurofins Genomics) for amplification are listed in Additional file 2.

Amplified gene fragments were cloned into the pENTR/D-TOPO vector (Invitrogen) and sequences were verified by sequencing (Seqlab). These constructs were used as entry vectors for the recombination with the Gateway LR clonase II (Invitrogen) in the binary

destination vector pEarley103 [21]. Constructs were verified by sequencing. Generated constructs as well as the different organelle markers (endoplasmic reticulum (ER), vacuole, plasma membrane, peroxisomes, mitochondria [22] and GUS vectors (cGUS and 35S GUS [23]) were transformed in agrobacteria (GV3101::pMP90RK) by electroporation.

Preparation of callus culture

Seeds were sterilized for 30 s in 70 % ethanol followed by an incubation for 5 min in household bleach Danklorix (CP GABA) and were washed three times with distilled water. Seeds were then germinated on PGR (plant growth regulators)-free plant culture medium (4.4 g/l Murashige & Skoog (MS) medium (Duchefa), 2 % (w/v) household sugar, 0.01 M NaCl, 0.2 % (v/v) plant preservative mixture (PPM) (Plant Cell Technology), 0.3 % (w/v) Gelrite (Duchefa), 0.1 M 2-(N-morpholino)ethanesulfonic acid (MES) (Sigma-Aldrich), 0.1 % (v/v) 1000xMS vitamin mixture (Duchefa)) for 4-7 days in the dark at room temperature. 1-3 cm long seedlings were used for callus induction. Seedlings were separated into cotyledons, hypocotyls and roots and transferred on callus induction medium (4.4 g/l MS medium 2 % (w/v) household sugar, 0.1 M NaCl, 0.2 % (v/v) PPM, 0.3 % (w/v) Gelrite, 10 µM 2,4-D (Duchefa) and 4 µM BAP [6-Benzylaminopurine] (Sigma-Aldrich), 0.1 M MES, 0.1 % (v/v) 1000xMS vitamin mixture). Explants were cultivated in low light conditions (4-10 µmol m^{-2} s^{-1}) in a 16 h/8 h light/dark cycle and at a temperature of 22 °C. After 4 weeks, explants were transplanted onto fresh callus induction medium. After another 2-4 weeks, callus was used for *Agrobacterium*-mediated transformation.

***Agrobacterium*-mediated transformation**

For callus as well as transient leaf transformation, agrobacteria (GV3101::pMP90RK) were grown overnight at 28 °C to an OD_{600} of 1.0-1.5 and centrifuged to harvest the bacteria. The pellet was resuspended in 2x infiltration buffer (8.86 g/l MS medium, 10 % (w/v) household sugar, 20 mM MES, 0.2 mM acetosyringone (Sigma-Aldrich)) and diluted to an OD_{600} of 0.4. The bacterium solution was incubated for 60 min at room temperature without shaking.

Calli from cotyledons, hypocotyls and roots were co-cultivated with agrobacteria for transformation. Therefore, calli were first incubated for 1 h in the bacterium solution at room

temperature. Calli were then dried on a sterile filter paper and transferred on PGR-free plant culture medium. Co-cultivation took place in the dark at 28 °C for 3 days. After this, 20 µg/ml kanamycin was added and calli were cultivated for another 4 weeks. Transformation was verified by β-glucuronidase (GUS) assay.

Transient leaf transformation was performed by vacuum infiltration. Therefore, 3-4 cm long branches of 3-4 month old Bienertia plants were harvested and the oldest leaves were removed. Leaves were then pricked approximately 1 mm deep and between 8-14 times dependent on the length of the leaf with a cannula (BD Microlance3, 0.4x19 cm) to increase transformation efficiency. A 50 ml conical tube was filled to two-thirds with the bacteria solution and the cutting was placed upside down into the tube and pushed with a styrofoam piece into the bacteria solution until the whole cutting was covered. Vacuum infiltration was performed for 10 s at 28 in. Hg and was repeated twice or until the leaves changed their color from light to dark green. Afterwards, cuttings were dried on a paper towel and put into a Sterivent High Container 107x94x96 mm (Duchefa) with 200 ml PGR-free plant culture medium. Cuttings were incubated for 2 - 5 days under low light conditions (20 - 50 µmol m^{-2} s^{-1}).

GUS stain

GUS assays were performed with cuttings five days after transformation and with callus four weeks after transformation. Transformed cuttings were placed upside down in a 50 ml conical tube. Transformed calli were transferred into a 24 well plate. Cuttings and calli were treated with 96 % (v/v) GUS stain solution (1 M Tris-HCl, 50 mM NaCl, 100 mM ferricyanid (AppliChem), 100 mM ferrocyanid (Sigma-Aldrich), 2 % (v/v) x-gluc (Carl Roth), 0.01 % Triton X (Merck)). Cuttings and calli were vacuum infiltrated for 15 min at 28 in. Hg and incubated at 37 °C overnight. Samples were washed with water once and incubated in 96 % ethanol overnight at 37 °C followed by a rehydration step with water overnight at room temperature.

Confocal microscopy

Confocal microscopy was performed on an inverted Nikon Eclipse TE2000-E laser scanning confocal microscope (Nikon). Images were acquired through a Plan Apo, 60x/1.20 water

immersion objective (Nikon) at a maximum digital resolution of 2048 x 2048 pixels. The fluorescence of GFP was analyzed by excitation at 488 nm with an argon laser and emission was detected between 509/526 nm. Chlorophyll autofluorescence was analyzed by excitation at 408 nm with a diode laser and emission was detected between 605/676 nm. Image processing was performed using Fiji [24]. Pictures of the organelle markers were acquired as a z-stack with a step size of 0.65 µm and represented as z-projections (projection type: sum slices).

Fluorescence microscopy

Fluorescence microscopy was performed using a Nikon Eclipse Ti fluorescence microscope (Nikon). Images were acquired through a Plan Apo, 100x/1.40 Oil objective (Nikon). The fluorescence of GFP was analyzed by excitation at 480/520 nm and emission was detected between 510/520 nm. Chlorophyll autofluorescence was analyzed by excitation of 550/575 nm and emission was detected between 590/675 nm. Time lapse images were captured every 5 s and represented as z-projection (projection type: max slices). Image processing was performed using Fiji [24].

Results

***Development of a protocol for transgene expression in Bienertia sinuspersici chlorenchyma cells and callus by Agrobacterium*-mediated transformation**

In order to further analyze the unique cell morphology in Bienertia including the central (CC) and peripheral compartment (PC) (Fig. 1A-B) an *Agrobacterium*-mediated transformation protocol was established. Initially, procedures similar to published transformation protocols for *Arabidopsis thaliana* [25, 26] and *Nicotiana tabacum* [20] were evaluated. Therefore, tips of branches of 3-4 month old intact Bienertia plants (Fig. 1C) were submerged and vacuum infiltrated in a solution of agrobacterium transformed with a GUS expression construct under control of a 35S promoter. Transformation efficiency was tested several days after infiltration

but generally, no transformed tissue was detected as judged by the absence of blue staining (data not shown). Also, addition of different surfactants such as Triton X, Tween-20, Silwet-L-77, and even direct injection of bacteria into Bienertia leaves with a syringe did not result in any positive transformants. However, when detached branches instead of attached branches (Fig. 1D-G) were used for vacuum infiltration, a weak but clearly detectable blue staining indicative for successful transformation was observed in transformation solutions containing the GUS construct (35S GUS) but not in branches infiltrated with a control construct lacking the 35S promoter (cGUS) (Fig. 1H).

Next, the influence of leaf wounding on transformation efficiency was tested. Leaves were pricked repeatedly with a needle before infiltration and transformation efficiency was determined again by GUS assay. Intensity of the GUS staining was markedly increased and also was much more homogenous in pricked vs. non-pricked leaves (Fig. 1I). Especially younger leaves at the tip of the branch benefited from the pricking treatment. The pricked cGUS control showed only very weak GUS staining. Quantitatively, the pricking treatment increased the transformation efficiency by more than two-fold (Fig. 1J).

Since Bienertia is obviously compatible with *Agrobacterium*-mediated transformation, it was further tested if callus can also be transformed. This might provide a useful tool for further attempts in creating stably transformed Bienertia plants. Callus was induced from different explant materials (hypocotyls, cotyledons and roots of seedlings) on media containing 10 µm 2-4-D and 4 µM BAP. Calli were subsequently grown for 4 weeks and then subjected to *Agrobacterium*-mediated transformation. Calli from all explant material tested showed blue GUS staining indicative for successful transformation with agrobacteria (Fig 2A-C). In contrast no blue stain was detectable in the control vectors without the 35S promoter (Fig. 2D).

In summary, the results indicate that Bienertia is generally amenable to *Agrobacterium*-mediated transformation. Transformation of chlorenchyma cells is efficient in detached but not attached branches and furthermore in callus. Mechanical wounding greatly increases transformation efficiency and homogeneity.

Organelle distribution and subcellular compartmentalization probed by transient marker expression

Next, the *Agrobacterium*-mediated transformation protocol was used to probe the distribution of several organelles using organelle specific marker-GFP fusions. Due to the specialized cell morphology in Bienertia, a single optical section cannot accurately reflect the signal in the two compartments. Therefore, the optical layers of the peripheral and the central compartment were separately analyzed (Fig. 3A).

The marker for the ER revealed a dense reticulate network in the layer of the PC as well as in the layer of the CC between the individual CC chloroplasts (Fig. 3B). The depth projection (Z-projection) of multiple optical slices indicated no obvious association of the ER with either the PC or CC chloroplasts or specific compartmentalization. Comparison with the localization of the marker in tobacco epidermal cells indicated a similar overall appearance and distribution.

For the tonoplast marker, the GFP pattern in the layer of the PC appeared less reticulate and in the CC layer, cytoplasmic strands which connect the CC to the PC were clearly visible (Fig. 3C). The Z-projection indicated no fragmentation or segmentation of the tonoplast membrane. Overall distribution of the tonoplast marker appeared also very similar to tobacco epidermal cells.

The plasma membrane marker showed in the PC layer a distribution similar to the tonoplast marker (Fig. 3D). However, there was no indication for association of this marker with the cytoplasmic strands, neither in the CC layer nor in the Z-projection. The Z-projections indicated that this marker was associated to some extend with the nuclear membrane (see arrow). This behavior was observed in both, Bienertia chlorenchyma as well as in tobacco epidermal cells.

In summary, the three membrane associated markers tested indicated no signs of cellular deterioration. Furthermore, overall distribution as well as the similarity to the localization pattern observed in tobacco indicate that *Agrobacterium*-mediated transformed Bienertia chlorenchyma cells are generally suitable for subcellular localization studies.

Next, we tested the subcellular distribution of peroxisomal and mitochondrial marker proteins. Peroxisomes were scattered in the peripheral compartment but no obvious association with the peripheral chloroplasts was observed (Fig. 4A). Peroxisomes in the central compartment appeared between individual central chloroplasts and were mostly confined to the outer region of the central compartment. In contrast, the central region of the central compartment appeared devoid of peroxisomes.

Mitochondria take a special role in NAD-ME type C4 species such as Bienertia since they are the site of C4 acid decarboxylation and thereby involved in the primary carbon assimilation reactions. Previous experiments with mitochondria specific fluorescent dyes indicated that they are mostly restricted to the CC [14, 27] in accordance to their proposed function in the C4 pathway. Probing subcellular distribution with a mitochondria specific marker indicated that indeed there is a very high density of mitochondria in the space between the chloroplasts of the CC (Fig. 4B). Interestingly, mitochondria were mostly confined to the central region of the central compartment whereas the outer region was relatively devoid of mitochondria thereby indicating an inverse localization compared to the peroxisomes in this compartment. Surprisingly, the mitochondrial marker also indicated a high density of mitochondria in the layer of the PC. Since this result was unexpected, the experiment was repeated with two additional endogenous Bienertia specific mitochondrial markers. Localization of GFP-fusions of the transit peptide of mitochondrial NAD-ME (Fig. 4C) and full length NAD-malate dehydrogenase (NAD-MDH, Fig. 4D) confirmed the presence of numerous mitochondria also in the PC.

Previous experiments using peroxisomal specific dyes indicated that peroxisomes in the peripheral compartment exhibit are high mobility [27]. We therefore used the *Agrobacterium*-mediated transformation system to compare the mobility of peroxisomes and mitochondria in the two compartments. Mobility of individual peroxisomes in the peripheral compartment appeared indeed very high. For example, the peroxisomes labeled "1" and "2" traveled more than 0.13 and 0.005 micrometer per second, respectively (Fig. 5A). In contrast, peroxisomes labeled "3" and "4" were rather immobile. Direct comparison shows that mitochondrial movement was much lower compared to peroxisomes over the time period analyzed (Fig. 5B and Additional file 3).

In summary, the results indicate that peroxisomes as well as mitochondria occur in both, the peripheral as well as the central compartment. Within the central compartment the distribution of mitochondria is different from the distribution of peroxisomes. Whereas individual peroxisomes appear to be highly mobile especially in the peripheral compartment, mitochondria show a much lower mobility.

Discussion

Plant cells can be genetically transformed by various methods. The most prominent examples include direct DNA delivery by chemical transfection of protoplasts, delivery of DNA into cells by particle bombardment and indirect delivery using vector systems such as viruses or plant infecting bacteria [28].

Successful transformation by particle transformation of Bienertia has been reported [27], however the method requires very specialized equipment. Furthermore, since DNA coated particles have to enter the leaf by passing through the epidermal layer, transformation events in chlorenchyma cells are rather rare as they depend critically on the pressure applied in relation to the thickness of each individual leaf.

Several studies reported the successful transformation of protoplasts isolated from Bienertia chlorenchyma cells [29–31] and we recently analyzed the mechanism of differential protein targeting to the two different chloroplast types using transfected protoplasts [19]. However, this method is rather time consuming and the handling is difficult for inexperienced scientist. Furthermore, we observed in many cases that the structural integrity in protoplasts can be compromised as judged by the dislocation of the central compartment or the general clumping of chloroplasts [19]. It is therefore highly desirable to have a more simple and efficient method that also better preserves the unique structural features of these highly unusual cells.

Agrobacterium-mediated transformation has become the method of choice for many plant species due to its speed and simplicity. However, many monocots such as maize and rice [32] as well as some eudicots [33, 34] are considered to be recalcitrant to *Agrobacterium*-

mediated transformation. The exact circumstances are not yet fully understood but may include mechanical barriers, genetic incompatibility as well as the plant's innate immune defense systems [32, 35–37] including the production of reactive oxygen species in response to the infection [38]. Some plants produce antibacterial substances that function against gram-negative bacteria such as agrobacteria [39–42]. For *Bienertia cycloptera* which is a sister species to *Bienertia sinuspersici* and also a SCC4 species it was reported that leave oils operate against gram-negative and gram-positive bacteria as well as some fungi [43]. Accordingly, it cannot be excluded that *Bienertia sinuspersici* has similar antimicrobial defense capabilities. Interestingly, we observed successful transformation exclusively in detached branches but never in attached branches or even when bacteria were directly delivered into the leaves by a syringe indicating that most likely the immune system in fully intact and unstressed plants effectively suppressed an agrobacteria infection.

Succulent halophytes such as Bienertia often exhibit thick cell walls and cuticles [44] which can complicate the entrance of agrobacteria into the leaf. Surfactants such as Silwet or Triton X have been used in many cases to increase the permeability of the epidermis [45]. However, in the case of Bienertia, we did not observe improved transformation. Instead, the use of surfactants resulted in necrosis of the leaf tissue. However, mechanical wounding induced by pricking the leaves with a needle before vacuum infiltration markedly increased transformation efficiency and homogeneity. Similar treatments have also been reported to increase transformation efficiency in other succulent species such as *Notocactus scopa* cv. *Soonjung*, *Kalanchoe blossfeldiana* and *Hylotelephium telephium* [46, 47] indicating that indeed the succulent nature of the Bienertia leaves might be partly responsible for the inability of agrobacteria to successfully infect intact and unstressed tissue.

Generation of stably transgenic plants often relies on regeneration from callus. For example, the closely related halophytic species *Suaeda salsa* and *Atriplex gmelini* [48, 49] as well as the more distantly related *Limonium bicolor* [50], *Leymus chinensis* [51], *Thellungiella halophila* [52] and *Mesembryanthemum crystallinum* [53, 54] have all been successfully transformed via callus transformation and subsequent regeneration. Here, we have demonstrated that also callus of Bienertia can be successfully transformed by agrobacteria. Previous reports show, that regeneration of plants from Bienertia callus is generally possible

[55, 56]. It can therefore be expected that a combination of the previous established regeneration protocols together with our *Agrobacterium*-mediated transformation protocol will allow for generation of stably transformed Bienertia plants in the future.

We used the established *Agrobacterium*-mediated transformation protocol to probe for subcellular localization of several organelle associated marker proteins. GFP-markers for proteins associated with the membrane systems of the ER, the tonoplast and the plasma membrane verified the structural integrity of the transformed cells. We also tested the subcellular distribution of peroxisomes and mitochondria. Localization of both organelles was previously analyzed in transformed protoplast using GFP fusions of peroxisomal and mitochondrial targeting sequences [29]. Furthermore, localization of peroxisomes was analyzed using *in situ* hybridization with antibodies directed against peroxisomal catalase [27], and distribution of mitochondria was probed using mitochondria specific dyes such as rhodamine 123 [27, 29] and mitotracker orange CMTMRos [14]. In all cases, results indicated that especially the mitochondria are located predominantly in the central compartment. In contrast, we observed in this study localization of numerous peroxisomes and mitochondria not only in the central but also in the peripheral compartment. Reasons for this discrepancy might include differences in microscopy (we specifically analyzed optical slides of the peripheral compartment layer as well as the central compartment layer whereas most previous studies focused on the layer of the central compartment only). Furthermore, mitochondria specific dyes such as rhodamine and mitotracker are sensitive for the mitochondrial membrane potential [57, 58]. Accordingly, it would be possible that mitochondria in the central and peripheral compartments have different membrane potentials and therefore stain with different efficiencies with the two dyes mentioned. Mitochondria are the primary site of C4 acid decarboxylation in NAD-ME C4 species such as Bienertia. Our observation that mitochondria are also abundant in the periphery raises the question how futile release of CO_2 from decarboxylation of C4 acids in the peripheral compartment is prevented. Theoretically, mitochondria in the periphery could either be impaired in the uptake of C4 acids (aspartate) or, alternatively, they could the lack decarboxylation enzymes. Our experiments indicate that peripheral mitochondria are at least able to import GFP tagged

NAD-MDH (tested as full length protein) and NAD-ME (tested as the transit peptide) which catalyze the two steps of the decarboxylation reaction of CO_2 from the C4 acid oxaloacetate. Therefore, there is currently no evidence for absence of these proteins from the peripheral mitochondria.

Alternatively, mitochondria might be able to dynamically move between the central and the peripheral compartment, thereby appearing either concentrated in the central compartment or as observed by us, distributed between both compartments. Generally, mitochondria and peroxisomes are considered to be highly mobile organelles and peak velocities of up to 10 μm s^{-1} have been recorded in plants for both organelle types [59–61]. For Bienertia, it has previously been noted that individual peroxisomes in the peripheral compartment exhibit a high mobility whereas peroxisomes in the central compartment are rather immobile and connected to the CC chloroplasts [27]. Our time lapse microscopy analysis confirmed the high mobility of peripheral peroxisomes and the rather static nature of the peroxisomes in the central compartment. However, there was no indication for mitochondrial movement in either compartment, instead mitochondria appeared rather static compared to peroxisomes.

Conclusion

We demonstrate that the single-cell C4 species *Bienertia sinuspersici* is amenable to *Agrobacterium*-mediated transformation. The developed protocol will provide a useful tool in further attempts to understand the unique cellular compartmentalization associated with single-cell C4 photosynthesis. Furthermore, when combined with previously published regeneration protocols it can be expected that stably transformed Bienertia plants and mutant studies finally become feasible.

List of abbreviations

BAP: 6-Benzylaminopurine; CBB cycle: Calvin-Benson-Bassham cycle; CC: central compartment; ER: endoplasmic reticulum; GFP: green fluorescent protein; MES: 2-(N-morpholino)ethanesulfonic acid; MS: Murashige & Skoog; NAD-MDH: NAD dependent malate dehydrogenase; NAD-ME: NAD dependent malic enzyme; nt: nucleotide; PC: peripheral compartment; PEP: phosphoenolpyruvate; PEPC: phosphoenolpyruvate carboxylase; PGR: plant growth regulators; PIP2A: plasma membrane intrinsic protein 2A; PPM: plant preservative mixture; PTS: peroxisomal targeting signal; Rubisco: ribulose-1,5-bisphosphate carboxylase; SCC4: single-cell C4; SOX: sulfite oxidase; WAK2: wall-associated receptor kinase 2; GUS: β-glucuronidase; **γ**-TIP: tonoplast intrinsic protein

Declarations

Ethics approval and consent to participate

This study does not contain any research requiring ethical consent or approval.

Consent for publication

Not applicable.

Availability of data and materials

The datasets used and/or analyzed during the current study are available from the corresponding author on reasonable request.

Competing interests

The authors declare that they have no competing interests.

Funding

Work in the SO lab was supported by the Deutsche Forschungsgemeinschaft (OF 106/1-1) and work in the IH and SO labs was funded by the "Cooperative Research Program for Agriculture Science & Technology Development (Project No.0109532016) "Rural Development Administration, Republic of Korea".

Authors' contributions

DW designed research; DW, PB and DI performed research; DW and PB analyzed data; DW prepared the figures; and DW, IH and SO wrote the paper. All of the authors have read and approved the final manuscript, and agreed to be accountable for all aspects of the work.

Acknowledgements

Not applicable.

Figure Legends

Fig. 1: *Agrobacterium*-mediated transformation of *Bienertia sinuspersici.*

(**A+B**) Brightfield and fluorescence image (excitation 550/575 nm and emission 590/675 nm) of Bienertia chlorenchyma cells; scale bar = 10 µm; CC – central compartment; PC – peripheral compartment. (**C**) 3 – 4 month old Bienertia plant. (**D+E**) Detached branches (**D**) before and (**E**) after vacuum infiltration; scale bar = 2 cm. (F) Cultivation of transformed branches in a container with plant cultivation medium. (**G**) Pricked Bienertia leaf. (**H+I**) GUS stain of pricked and non-pricked transformed leaves; 35S GUS – positive control; cGUS – negative control; scale bar = 1 cm (**J**) Transformation efficiency of pricked and non-pricked (control) leaves transformed with either the 35S GUS or cGUS construct; n = 7. Vertical bars represent standard error of the mean.

Fig. 2: *Agrobacterium*-mediated transformation of *Bienertia sinuspersici* callus.

Callus was grown on callus induction medium with 10 µM 2-4-D and 4 µM BAP. (**A-C**) *Agrobacterium*-mediated transformation with the GUS expression vector 35S GUS. Explant material of (**A**) hypocotyls (**B**) cotyledons and (**C**) roots of seedlings. (**D**) Non-transformed control.

Fig. 3: Subcellular localization of GFP-tagged marker proteins in *Bienertia sinuspersici* chlorenchyma cells after *Agrobacterium*-mediated transformation.

(**A**) Schematic of the optical layers analyzed by confocal microscopy; PC – peripheral compartment; CC – central compartment. (**B-D**) Confocal images of various transiently expressed GFP-fusion proteins in *Bienertia sinuspersici* chlorenchyma and tobacco epidermis cells after *Agrobacterium*-mediated transformation. All fluorescence images are shown in the GFP channel (green – excitation 488 nm/emission 509/525 nm) and the chlorophyll autofluorescence channel (magenta – excitation 408 nm/emission 620/700 nm). Additionally, the merged channels are shown. Each GFP-tagged marker protein is also shown as Z-projection made by a multi-image Z-stack. All images are representative from n ≥ 5 independent experiments. All scale bars = 10 µm. (**B**) Expression of the ER GFP-fusion

marker protein with a synthetic HDEL sequence at the C-terminus and the signal peptide of AtWAK2 (wall-associated receptor kinase 2) at the N-terminus of GFP. (**C**) Expression of the vacuole GFP-fusion marker protein with the aquaporin **γ**-TIP (tonoplast intrinsic protein). (**D**) Expression of the plasma membrane GFP-fusion marker protein with the aquaporin AtPIP2A (plasma membrane intrinsic protein 2A).

Fig. 4: Subcellular localization of peroxisomal and mitochondrial GFP-tagged markers in *Bienertia sinuspersici* chlorenchyma cells after *Agrobacterium*-mediated transformation.

(**A-D**) Confocal images of various transiently expressed GFP-fusion proteins in *Bienertia sinuspersici* after *Agrobacterium*-mediated transformation. All fluorescence images are shown in the GFP channel (green – excitation 488 nm and emission 509/525 nm) and the chlorophyll autofluorescence channel (magenta – excitation 408 nm and emission 620/700 nm). Additionally, the merged channels are shown. All images are representative from n ≥ 5 independent experiments. All scale bars = 10 µm. **(A)** Peroxisomal targeting signal (PTS2) fused at the C-terminus of GFP (**B**) Mitochondrial signal peptide of yeast sulfite oxidase (ScSOX4) fused to the N-terminus of GFP.

(**C**) *Bienertia sinuspersici* NAD-ME transit peptide fused to the N-terminus of GFP **(D)** *Bienertia sinuspersici* NAD-MDH fused to the N-terminus of GFP.

Fig. 5: Mobility of peroxisomes and mitochondria in *Bienertia sinuspersici* chlorenchyma cells (A+B) Z-projections of time lapse fluorescence images (5 s steps). All fluorescence images are shown in the GFP channel (green – excitation 480/520 nm and emission 510/520 nm) and the chlorophyll autofluorescence channel (magenta - excitation 550/575 nm and emission 590/675 nm). All scale bars = 10 µm; arrows show the beginning and the end of the organelle movement over the time period analyzed. (**A**) Peroxisome (PTS) and (**B**) mitochondria marker (ScSOX4) as described in Fig. 4.

Additional file 1

.ppt

DNA sequences used for localization studies with GFP-fusion constructs.

All gene fragments used for localization studies were fused to the 5' end of GFP. NAD-MDH - NAD malate dehydrogenase; TP_NAD-ME – transit peptide of NAD-malic enzyme

Additional file 2

.ppt

Oligonucleotide sequences

Oligonucleotides for the amplification of *Bienertia sinuspersici* genes for Gateway cloning.

Additional file 3

.mov

Video showing a side-by-side comparison of the mobility of *Bienertia sinuspersici* peroxisomes and mitochondria in the peripheral and central compartment.

File name: additionalFile03_video_peroxisome_and_mitochondria_movements

References

1. Chaves MM, Flexas J, Pinheiro C. Photosynthesis under drought and salt stress: regulation mechanisms from whole plant to cell. Ann Bot. 2009;103:551–60.
2. Bowes G, Ogren WL, Hageman RH. Phosphoglycolate production catalyzed by ribulose diphosphate carboxylase. Biochem Biophys Res Com. 1971;45:716–22.
3. Sage RF. The evolution of C4 photosynthesis. New Phytol. 2004;161:341–70.
4. Hatch MD, Slack CR. Photosynthesis by sugar-cane leaves. A new carboxylation reaction and the pathway of sugar formation. Biochem J. 1966;101:103–11.
5. Sage RF. A portrait of the C4 photosynthetic family on the 50th anniversary of its discovery: species number, evolutionary lineages, and hall of fame. J Exp Bot. 2016;67:4039–56.
6. Haberlandt G. Physiologische Pflanzenanatomie. 4th ed. W. Engelmann, Leipzig. 1904
7. Garner DMG, Mure CM, Yerramsetty P, Berry JO. Kranz Anatomy and the C4 pathway. John Wiley & Sons, Ltd. 2016
8. Hatch MD. Chemical energy costs for CO_2 fixation by plants with differing photosynthetic pathways. Prediction and measurement of photosynthetic productivity. Wageningen: Center of Agric. Publ. Doc. 1970;215-20
9. Freitag H, Stichler W. A remarkable new leaf type with unusual photosynthetic tissue in a Central Asiatic genus of Chenopodiaceae. Plant Biology. 2000;2:154–60.
10. Voznesenskaya EV, Franceschi VR, Kiirats O, Freitag H, Edwards GE. Kranz anatomy is not essential for terrestrial C4 plant photosynthesis. Nature. 2001;414:543–6.
11. Freitag H, Stichler W. *Bienertia cycloptera* Bunge ex Boiss., Chenopodiaceae, another C4 Plant without Kranz tissues. Plant Biology. 2002;4:121–32.
12. Akhani H, Chatrenoor T, Dehghani M, Khoshravesh R, Mahdavi P, Matinzadeh Z. A new species of Bienertia (Chenopodiaceae) from Iranian salt deserts: A third species of the genus and discovery of a fourth terrestrial C4 plant without Kranz anatomy. Plant Biosyst. 2012:1–10.

13. Akhani H, Barroca J, Koteeva N, Voznesenskaya E, Franceschi V, Edwards G, Ghaffari SM, Ziegler H. *Bienertia sinuspersici* (Chenopodiaceae): A new species from Southwest Asia and discovery of a third terrestrial C_4 plant without Kranz Anatomy. Syst Bot. 2005;30:290–301.
14. Park J, Knoblauch M, Okita TW, Edwards GE. Structural changes in the vacuole and cytoskeleton are key to development of the two cytoplasmic domains supporting single-cell C4 photosynthesis in *Bienertia sinuspersici*. Planta. 2009;229:369–82.
15. Voznesenskaya EV, Franceschi VR, Kiirats O, Artyusheva EG, Freitag H, Edwards GE. Proof of C4 photosynthesis without Kranz anatomy in *Bienertia cycloptera* (Chenopodiaceae). Plant J. 2002;31:649–62.
16. Voznesenskaya EV, Koteyeva NK, Chuong SDX, Akhani H, Edwards GE, Franceschi VR. Differentiation of cellular and biochemical features of the single-cell C4 syndrome during leaf development in *Bienertia cycloptera* (Chenopodiaceae). Am J Bot. 2005;92:1784–95.
17. Offermann S, Okita TW, Edwards GE. Resolving the compartmentation and function of C4 photosynthesis in the single-cell C4 species *Bienertia sinuspersici*. Plant Physiol. 2011;155:1612–28.
18. Offermann S, Friso G, Doroshenk KA, Sun Q, Sharpe RM, Okita TW, Wimmer D, Edwards GE, van Wijk KJ. Developmental and subcellular organization of single-cell C4 photosynthesis in *Bienertia sinuspersici* determined by large-scale proteomics and cDNA assembly from 454 DNA sequencing. J Proteome Res. 2015;14:2090–108.
19. Wimmer D, Bohnhorst P, Shekhar V, Hwang I, Offermann S. Transit peptide elements mediate selective protein targeting to two different types of chloroplasts in the single-cell C4 species *Bienertia sinuspersici*. Sci Rep. 2017;7:41187
20. Earley KW, Haag JR, Pontes O, Opper K, Juehne T, Song K, Pikaard CS. Gateway-compatible vectors for plant functional genomics and proteomics. Plant J. 2006;45:616–29.
21. Nelson BK, Cai X, Nebenfuhr A. A multicolored set of *in vivo* organelle markers for co-localization studies in Arabidopsis and other plants. Plant J. 2007;51:1126–36.

22. Laxa M, Müller K, Lange N, Doering L, Pruscha JT, Peterhänsel C. The 5′UTR intron of Arabidopsis GGT1 aminotransferase enhances promoter activity by recruiting RNA polymerase II. Plant Physiol. 2016;172:313–27.
23. Schindelin J, Arganda-Carreras I, Frise E, Kaynig V, Longair M, Pietzsch T, Preibisch S, Rueden C, Saalfeld S, Schmid B, Tinevez JY, White DJ, Hartenstein V, Eliceiri K, Tomancak P, Cardona A. Fiji: an open-source platform for biological-image analysis. Nat Methods. 2012;9:676–82.
24. Bechtold N, Pelletier G. In planta *Agrobacterium*-mediated transformation of adult *Arabidopsis thaliana* plants by vacuum infiltration. In: Martinez-Zapater JM, Salinas J, editors. Arabidopsis Protocols. Totowa, NJ: Humana Press; 1998. p. 259–266.
25. Martinez-Zapater JM, Salinas J, editors. Arabidopsis Protocols. Totowa, NJ: Humana Press; 1998.
26. Sparkes IA, Runions J, Kearns A, Hawes C. Rapid, transient expression of fluorescent fusion proteins in tobacco plants and generation of stably transformed plants. Nat Protoc. 2006;1:2019–25.
27. Chuong SD, Franceschi VR, Edwards GE. The cytoskeleton maintains organelle partitioning required for single-cell C4 photosynthesis in Chenopodiaceae species. Plant Cell. 2006;18:2207–23.
28. Barampuram S, Zhang ZJ. Recent advances in plant transformation. Methods Mol Biol. 2011;701:1–35.
29. Lung SC, Yanagisawa M, Chuong SD. Protoplast isolation and transient gene expression in the single-cell C4 species, *Bienertia sinuspersici*. Plant Cell Rep. 2011;30:473–84.
30. Lung SC, Chuong SD. A transit peptide–like sorting signal at the C-terminus directs the *Bienertia sinuspersici* preprotein receptor Toc159 to the chloroplast outer membrane. Plant Cell. 2012;24:1560–78.
31. Rosnow J, Yerramsetty P, Berry JO, Okita TW, Edwards GE. Exploring mechanisms linked to differentiation and function of dimorphic chloroplasts in the single-cell C4 species *Bienertia sinuspersici*. BMC Plant Biol. 2014;14:34.
32. Sood P, Bhattacharya A, Sood A. Problems and possibilities of monocot transformation. Biol Plantarum. 2011;55:1–15.

33. van Wordragen MF, Dons HJM. *Agrobacterium tumefaciens*-mediated transformation of recalcitrant crops. Plant Mol Biol Rep. 1992;10:12–36.
34. Atif RM, Patat-Ochatt EM, Svabova L, Ondrej V, Klenoticova H, Jacas L, Griga M, Ochatt SJ. Gene Transfer in Legumes. In: Lüttge U, Beyschlag W, Francis D, Cushman J, editors. Progress in Botany: Vol. 74. Berlin, Heidelberg: Springer; 2013. p. 37–100.
35. Sood P, Bhattacharya A, Joshi R, Gulati A, Chanda S, Sood A. A method to overcome the waxy surface, cell wall thickening and polyphenol induced necrosis at wound sites - the major deterrents to *Agrobacterium*-mediated transformation of bamboo, a woody monocot. J Plant Biochem Biot. 2014;23:69–80.
36. Zhu Y, Nam J, Humara JM, Mysore KS, Lee LY, Cao H, et al. Identification of Arabidopsis rat mutants. Plant Physiol. 2003;132:494–505.
37. Citovsky V, Kozlovsky SV, Lacroix B, Zaltsman A, Dafny-Yelin M, Vyas S, Tovkach A, Tzfira T. Biological systems of the host cell involved in *Agrobacterium* infection. Cell Microbiol. 2007;9:9–20.
38. Franklin G, Conceiçao LF, Kombrink E, Dias AC. *Hypericum perforatum* plant cells reduce *Agrobacterium* viability during co-cultivation. Planta. 2008;227:1401–8.
39. Ghanney N, Rhouma A. *Schinus terebinthifolius* Raddi (Anacardiaceae) leaf extracts: Antibacterial activity against two *Agrobacterium tumefaciens* strains. J Crop Prot. 2015;4:85–96.
40. Halima B, Abdellah F, Mouhcine F, Kawtar FB. Anti-bacterial activity of *Coriaria myrtifolia* against *Agrobacterium tumefaciens*: Plant pathogen responsible for crown gall. Afr J Microbiol Res. 2013;7:5529–32.
41. Franklin G, Conceicao LFR, Kombrink E, Dias ACP. Xanthone biosynthesis in *Hypericum perforatum* cells provides antioxidant and antimicrobial protection upon biotic stress. Phytochemistry. 2009;70:60–8.
42. Sheikh M, Malik AR, Meghavanshi MK, Mahmood I. Studies on some plant extracts for their antimicrobial potential against certain pathogenic microorganisms. AJPS. 2012;03:209–13.

43. Jahromi MAF, Etemadfard H, Zebarjad Z. Chemical characterization and antimicrobial activity of essential oil from the leaves of *Bienertia cycloptera*. Chem Nat Compd. 2016;52:936–8.

44. Hajibagheri MA, Hall JL, Flowers TJ. The structure of the cuticle in relation to cuticula transpiration in leaves of the halophyte *Suaeda maritima* (L.) Dum. New Phytol. 1983;94:125-31.

45. Curtis IS, Nam HG. Transgenic radish (*Raphanus sativus* L. longipinnatus Bailey) by floral-dip method – plant development and surfactant are important in optimizing transformation efficiency. Transgenic Res. 2001;10:363–71.

46. Jones RW. Application of succulent plant leaves for *Agrobacterium* infiltration-mediated protein production. J Microbiol Methods. 2016;120:65–7.

47. Seol E, Jung Y, Lee J, Cho C, Kim T, Rhee Y, Lee S. In planta transformation of *Notocactus scopa* cv. Soonjung by *Agrobacterium tumefaciens*. Plant Cell Rep. 2008;27:1197–206.

48. Zhao SZ, Ruan Y, Sun HZ, Wang BS. Highly efficient *Agrobacterium*-based transformation system for callus cells of the C3 halophyte *Suaeda salsa*. Acta Physiol Plant. 2008;30:729–36.

49. Uchida A, Nagamiya K, Takabe T. Transformation of *Atriplex gmelini* plants from callus lines using *Agrobacterium tumefaciens*. Plant Cell Tiss Org. 2003;75:151–7.

50. Yuan F, Chen M, Yang J, Leng B, Wang B. A system for the transformation and regeneration of the recretohalophyte *Limonium bicolor*. In Vitro Cell Dev Biol - Plant. 2014;50:610–7.

51. Sun YL, Hong SK. *Agrobacterium tumefaciens*-mediated transformation of the halophyte *Leymus chinensis* (Trin.). Plant Mol Biol Rep. 2012;30:1253–63.

52. Li HQ, Xu J, Chen L, Li MR. Establishment of an efficient *Agrobacterium tumefaciens*-mediated leaf disc transformation of *Thellungiella halophila*. Plant Cell Rep. 2007;26:1785–9.

53. Ishimaru K. Transformation of a CAM plant, the facultative halophyte *Mesembryanthemum crystallinum* by *Agrobacterium tumefaciens*. Plant Cell Tiss Org. 1999;57:61–3.

54. Konieczny R, Obert B, Bleho J, Novak O, Heym C, Tuleja M, Müller J, Strnad M, Menzel D. Samaj J. Stable transformation of *Mesembryanthemum crystallinum* (L.) with *Agrobacterium rhizogene*s harboring the green fluorescent protein targeted to the endoplasmic reticulum. J Plant Physiol. 2011;168:722–9.

55. Northmore JA, Zhou V, Chuong SDX. Multiple shoot induction and plant regeneration of the single-cell C4 species *Bienertia sinuspersici*. Plant Cell Tiss Organ Cult. 2012;108:101–9.

56. Northmore JA, Sigurdson D, Schoor S, Rustum A, Chuong SDX. Thidiazuron induces high-frequency indirect shoot organogenesis of *Bienertia sinuspersici*: A single-cell C4 species. Plant Cell Tiss Organ Cult. 2016;126:141–51.

57. Johnson LV, Walsh ML, Chen LB. Localization of mitochondria in living cells with rhodamine 123. Proc Natl Acad Sci USA. 1980;77:990–4.

58. Macho A, Decaudin D, Castedo M, Hirsch T, Susin SA, Zamzami N, Kroemer G. Chloromethyl-X-rosamine is an aldehyde-fixable potential-sensitive fluorochrome for the detection of early apoptosis. Cytometry. 1996;25:333–40.

59. Jedd G, Chua NH. Visualization of peroxisomes in living plant cells reveals acto-myosin-dependent cytoplasmic streaming and peroxisome budding. Plant Cell Physiol. 2002;43:384–92.

60. Zheng M, Beck M, Müller J, Chen T, Wang X, Wang F, Wang Q, Wang Y, Baluska F, Logan DC, Samaj J, Lin J. Actin turnover is required for myosin-dependent mitochondrial movements in Arabidopsis root hairs. PLOS ONE. 2009;4:e5961.

61. van Gestel K, Köhler RH, Verbelen J. Plant mitochondria move on F-actin, but their positioning in the cortical cytoplasm depends on both F-actin and microtubules. J Exp Bot. 2002;53:659–67.

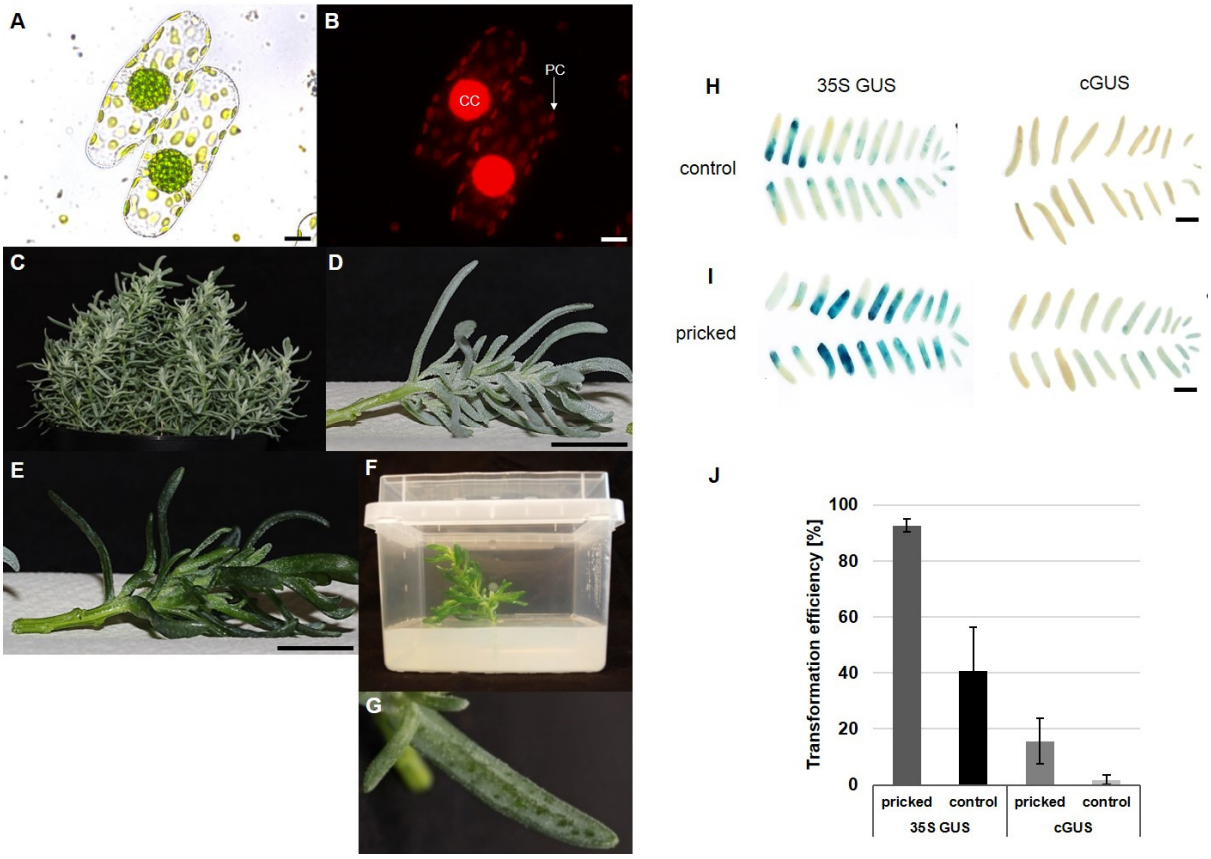
A
B
PC
CC
C
D
E
F
G
H
35S GUS
cGUS
control
I
pricked
J
Transformation efficiency [%]
100
80
60
40
20
0
pricked
control
pricked
control
35S GUS
cGUS

Figure 1

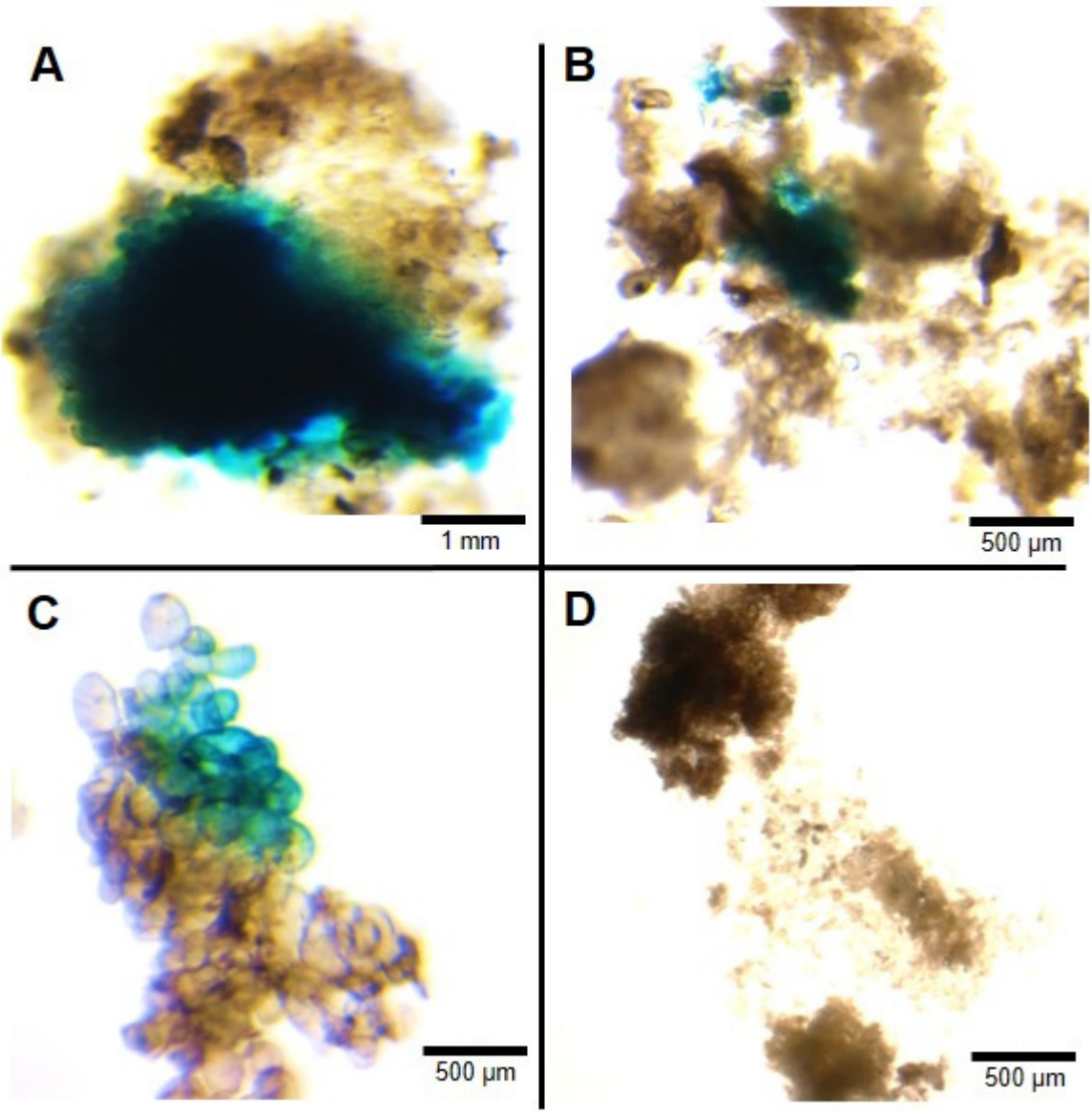

Figure 2

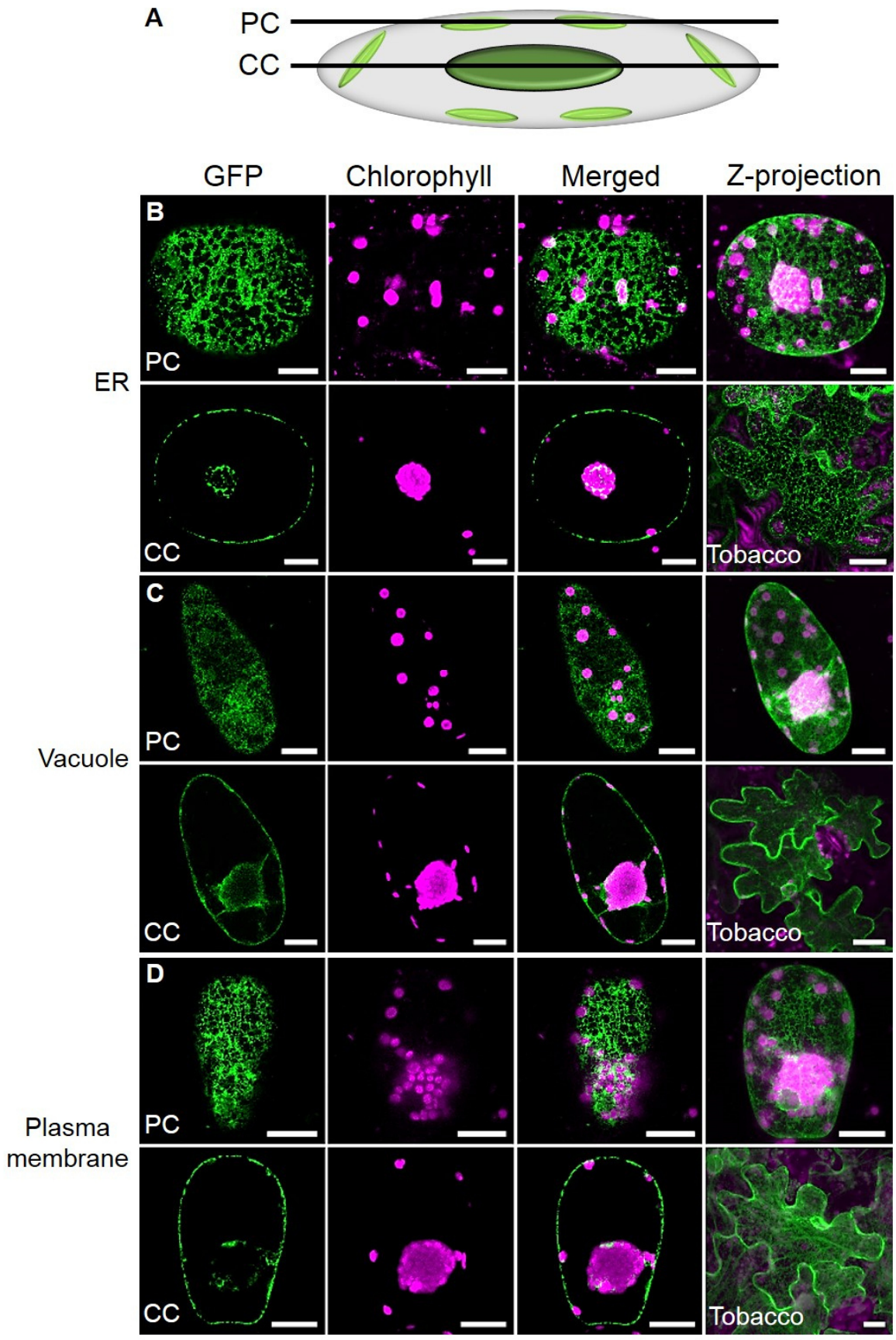
A
PC
CC
GFP
Chlorophyll
Merged
Z-projection
B
PC
ER
CC
Tobacco
C
PC
Vacuole
CC
Tobacco
D
PC
Plasma membrane
CC
Tobacco

Figure 3

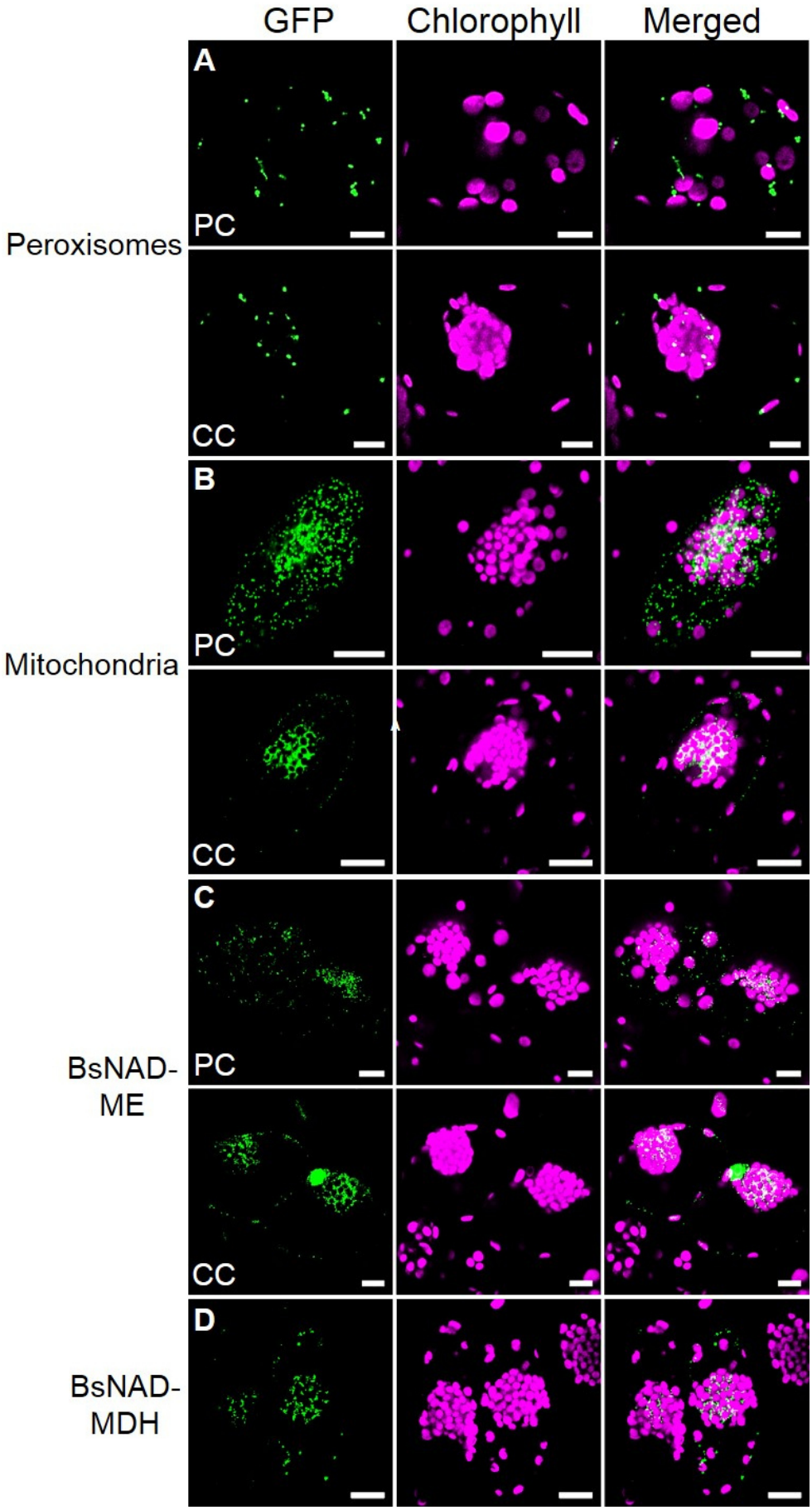
GFP
Chlorophyll
Merged
A
PC
Peroxisomes
CC
B
PC
Mitochondria
CC
C
PC
BsNAD-
ME
CC
D
BsNAD-
MDH

Figure 4

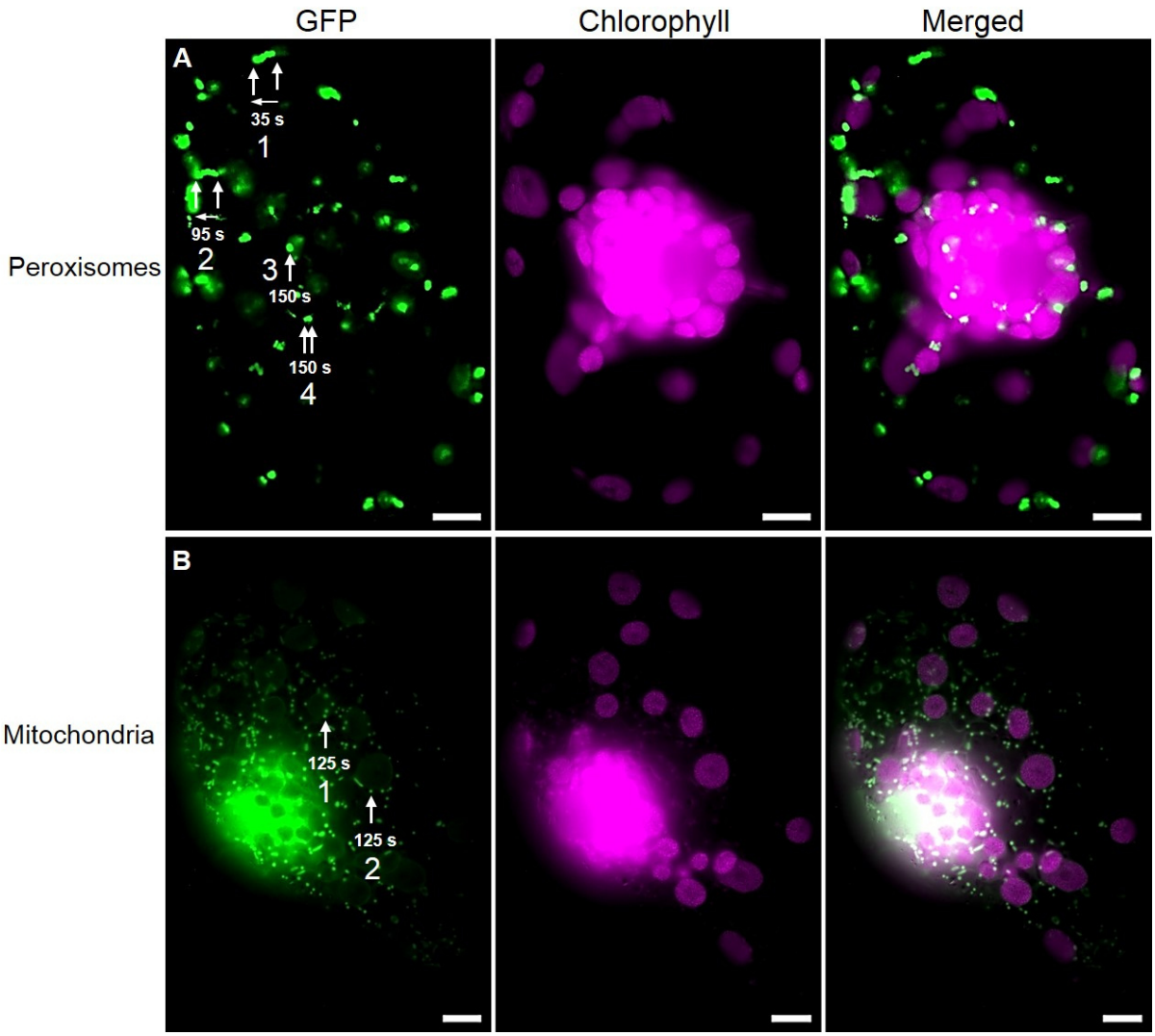
GFP
Chlorophyll
Merged
A
35 s
1
95 s
2
3
150 s
150 s
4
Peroxisomes
B
125 s
1
125 s
2
Mitochondria

Figure 5

Additional file 1. DNA sequences used for localization studies with GFP-fusion constructs.
All gene fragments used for localization studies were fused to the 5' end of GFP. NAD-MDH - NAD malate dehydrogenase; TP_NAD-ME – transit peptide of NAD-malic enzyme

NAD-MDH (1038 nt)

ATGAGGACTGAATTCCTAAGATCTGTTCAATCAGCAGTTAGAAGAAGCAATTATGCTTCATCAACTCGCAATTTCTCTTCTTCTGCTTCAAATCCTGAACGCAAAGTCACTGTTCTTGGTGCTGCTGGTGGTATTGGTCAACC
CCTTTCCATGTTAATGAAGCTTAATCCTCTTGTTTCTACTCTTTCTCTTTACGATCTTGCTGGTACCCCTGGTGTTGCTGCTGATTGTAGCCATATCAATACTAGAGCTCAGGTTTCTGGTTATATGGAGGACAAGGATCTGG
CAAAGGCACTTGAGGGATCAGATGTCGTAATTATTCCTGCCGGTGTGCCGAGGAAGCCGGGTATGACACGTGATGATCTCTTTAATATCAATGCCGGTATTGTGAAAAACCTCTGCCAGCATGTTGCCAAACACTGCCCTAAT
GCTCTTGTCAACATGATTAGCAACCCTGTAAACTCAACAGTGCCAATTGCCTCTGAGGTTTTCAAGGAAGCTGGTACCTATGATCCCAAGAGGTTGTTTGGTGTGACAACCTTGGATGTGGTTAGGGCTAAGACTTTCTATGC
AACAAAGACTGGCCTTTCAGTTGAAGAGGTTAACGTGCCTGTTGTTGGAGGACATGCTGGCATAACCATTCTGCCATTGTTTTCTCAAGCTTTCCCACAAGCCAATCTTGGAGAAGATGACATTGTAGCTCTTACAAAGAGAA
CACAAGATGGAGGAACAGAAGTTGTTGAGGCTAAGGCTGGAAAGGGTTCAGCAACATTGTCCATGGCTTACGCTGGAGCCATATTTGCTGATGCTTGCTTAAAGGGACTGAACGGTGTCCCAGATGTTGTCGAGTGTTCATTC
GTAGAGTCAAATGTCACTGAACTGCCCTTCTTTGCTTCTAAGGTGAGGTTGGGAGTGAACGGAGTAGAAGAAATCCATGGATTGGGCTCCATGTCGGACTACGAGAAAGAAGGTTTAGCAAAACTCATTCCCGAGCTCAAATC
TTCCATCCAAAAGGGGATTGACTTCGCCCACAAGAAT

TP_NAD-ME (102 nt)

ATGTGGAAGGTTTGCCTATCGACGGCGGCGAATCTCCGCCGTACGCGGCGGTTTTCCGCATTCGCAGCGTTTCCGGGACCTTCTATTGTTCGCAAGCGCGGT

Additional file 2. Oligonucleotide sequences
Oligonucleotides for the amplification of *Bienertia sinuspersici* genes for Gateway cloning.

Oligo name	Sequence (5‘ to 3‘)
NAD-ME_for	caccATGTGGAAGGTTTGCCTATCG
TP_NAD-ME_rev	ACCGCGCTTGCGAACAATAGA
NAD-MDH_for	caccATGAGGACTGAATTCCTAAGA
NAD-MDH_rev	ATTCTTGTGGGCGAAGTC

Appendix

Curriculum Vitae

Name:	Diana Wimmer
Date of Birth:	February 12th, 1986
Place of Birth:	Alfeld (Leine), Germany
Citizenship:	Citizen of Germany

School Education

2005 – 2007	"Berufsbildende Schule" Einbeck and KWS Saat AG, training as "Landwirtschaftlich-technische Assistentin"
1998 – 2005	Secondary school "Gymnasium Alfeld" in Alfeld (Leine) Qualification A-level
1997 – 1998	"Orientierungsschule" in Alfeld (Leine)
1992 – 1996	Primary School in Langenholzen

Academic Education

04/2012 – 04/2017	PhD student at the Leibniz Universität Hannover, Institute of Botany, Dr. Sascha Offermann
10/2010 – 03/2012	Student at the Leibniz Universität Hannover, M. Sc. Plant Biotechnology (grade: "very good") Thesis: "Wild beets as genetic resource for the uniparental genome elimination in sugar beets"
10/2007 – 09/2010	Student at the Leibniz Universität Hannover, B. Sc. Plant Biotechnology (grade: "good") Thesis: "Molecular characterization of the small GTPase MtRac1 in *Medicago truncatula* via RNA interference (RNAi) during pathogenic interaction with *Aphanomyces euteiches*"

List of Publications

Wimmer D, Bohnhorst P, Shekhar V, Hwang I, Offermann S (2017)

Transit peptide elements mediate selective protein targeting to two different types of chloroplasts in the single-cell C4 species *Bienertia sinuspersici*

Scientific Research **7**: 41187

Erlinghaeuser M[1], Hagenau L[1], Wimmer D[1], Offermann S (2016)

Development, subcellular positioning and selective protein accumulation in the dimorphic chloroplasts of single-cell C4 species.

Current Opinion in Plant Biology **31**: 76–82. [1]equally contributed

Offermann S, Friso G, Doroshenk KA, Sun Q, Sharpe RM, Okita TW, Wimmer D, Edwards GE, van Wijk KJ *(*2015)

Developmental and subcellular organization of single-cell C4 photosynthesis in *Bienertia sinuspersici* determined by large-scale proteomics and cDNA assembly from 454 DNA Sequencing.

Journal of Proteome Research **14**: 2090–2108.

Kiirika LM Bergmann HF, Schikowsky C, Wimmer D, Korte J, Schmitz U, Niehaus K Colditz F *(*2012)

Silencing of the Rac1 GTPase MtROP9 in *Medicago truncatula* stimulates early mycorrhizal and oomycete root colonizations but negatively affects rhizobial infection.

Plant Physiology **159**: 501–516.

Conference contributions

Satellite Workshop of the 17th International Congress on Photosynthesis Research (August 2016), Düsseldorf, Germany

Talk:

“Selective protein targeting in dimorphic chloroplasts of the single-cell C4 species *Bienertia sinuspersici*”

29. Meeting Molecular Biology of Plants (February 2016), Dabringhausen, Germany

Talk:

”Identification of novel regulatory elements involved in differential accumulation of nuclear encoded chloroplast proteins in the single-cell C4 *Bienertia sinuspersici*”

Gordon Research Seminar and Gordon Research Conference - CO_2 Assimilation in Plants: Genome to Biome, (June 2014), Waterville Valley, USA

Poster:

”Chloroplast dimorphism in the single-cell C_4 species *Bienertia sinuspersici* - Identification of regulatory elements involved in differential accumulation of nuclear encoded chloroplast proteins”

Danksagung

Ich bedanke mich bei Dr. Sascha Offermann für die Möglichkeit in seiner Arbeitsgruppe promovieren zu dürfen und für die lange Finanzierung meiner Arbeitsstelle. Ich bedanke mich auch für die Bereitstellung eines interessanten Themengebietes und die Möglichkeit mich darin frei entfalten zu können. Unsere wissenschaftlichen Diskussionen und deine Hilfestellungen während der Promotion waren sehr hilfreich für mich.

Ich danke Prof. Dr. Christoph Peterhänsel für die Aufnahme am Institut für Botanik und für seine hilfreichen Anmerkungen während meiner Versuche.

Ich danke Prof. Dr. Braun und Prof. Dr. Ngezahayo für die Übernahme des Korreferates beziehungsweise des Vorsitzes für meine Promotion.

Vielen Dank Steffi für unsere lange Freundschaft vom 1. Semester an. Wir haben uns immer unterstützt und konnten uns aufeinander verlassen. Du warst mir während dieser langen Zeit eine starke Stütze und mit dir zusammen fiel mir die Promotion wesentlich leichter.

Ich bedanke mich auch bei Lisa, Matthias, Philipp und Anna. Ihr wart die beste Arbeitsgruppe, die ich jemals hatte und ich bin froh, dass wir diese lange Zeit so harmonisch zusammen verbringen konnten. Auch unsere privaten Unternehmungen werden mir immer im Gedächtnis bleiben.

Julia danke ich für die Unterstützung bei der Isolierung der Bienertia Protoplasten. Ohne dich wäre ich nie fertig geworden.

Ich danke auch Miriam für die Hilfestellungen bei verschiedenen molekularbiologischen Fragen und der ganzen AG Peterhänsel für die Unterstützung der „kleinen Schwester“ AGSO.

Danke Leni für das Korrekturlesen meiner Arbeit.

Zu guter Letzt danke ich der wichtigsten Person in meinem Leben. Marcel, du warst und bist immer für mich da. Auch in schwierigen Lebenslagen hast du mich immer unterstützt.

Dankeschön!